CRS
Spanish Portuguese Local Chapter

XIV Spanish-Portuguese Conference on Controlled Drug Delivery

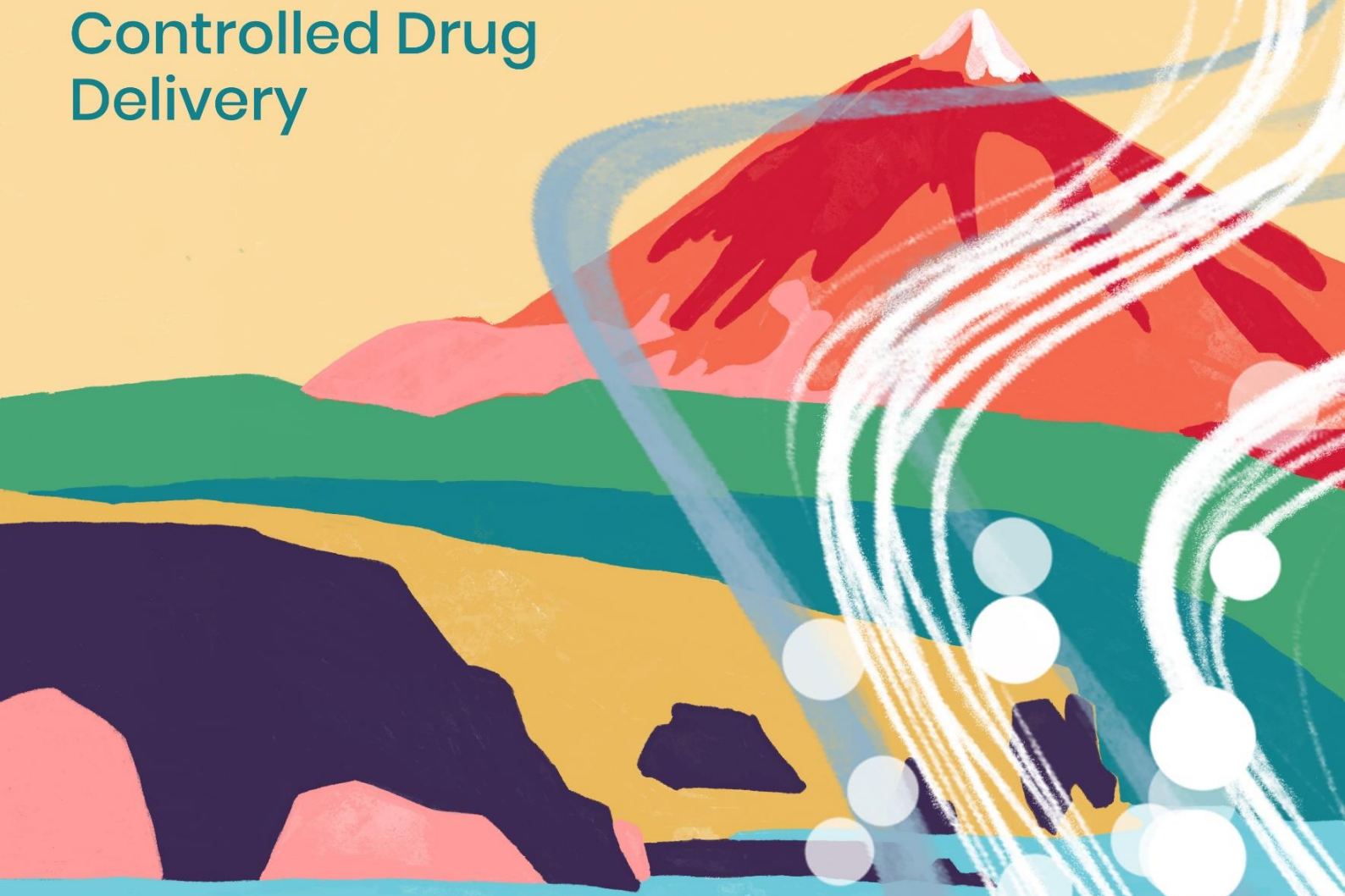

Designing
the way to the peak

Tenerife - Virtual Meeting
January 26-28th, 2022

Abstract Book

Index

SPLC-CRS Board

Carmen María Évora, President (University of La Laguna)

Araceli Delgado Hernández, Secretary, (University of La Laguna)

Bruno Sarmento, Vice-president; (University of Porto)

Helena Florindo, Vice-secretary, (University of Lisboa)

María Blanco Prieto, Govern, (University of Navarra)

Manuel Santander, Treasurer, (Universidad de Castilla La Mancha)

Scientific Committee

Rosa Mª Hernández (University of País Vasco)

Patricia Díaz-Rodríguez (University of Santiago de Compostela)

Carmen Alvarez-Lorenzo (University of Santiago de Compostela)

Rocío Herrero (University Complutense de Madrid)

Amparo Sánchez (University of Salamanca)

María Jesús Vicent (Príncipe Felipe Research Center, Valencia)

Manoli Igartua (University of País Vasco)

María Ángeles Solinís (University of País Vasco)

Edorta Santos (University of País Vasco)

Alicia Rodríguez-Gascón (University of País Vasco)

Elisa Garbayo (University of Navarra)

Victoria Lozano (University of Castilla-La Mancha)

Dolores Torres (University of Santiago de Compostela)

Ana Melero (University of Valencia)

José das Neves (i3S-University of Porto)

Bruno Silva (International Iberian Nanotechnology Laboratory, Braga)

Susana Simões (CIBB-University of Coimbra)

Luísa Corvo (University of Lisbon)

António Almeida (University of Lisbon)

João Nuno Moreira (University of Coimbra)

María José Alonso (University of Santiago de Compostela)

SPLC Young Scientist Committee

Souhaila El Moukhtari (University of Navarra)

Patricia García García (University of La Laguna)

Mireya López Borrajo (University of Santiago de Compostela)

Cláudia Martins (University of Porto)

Partners-Sponsors

CRS Controlled Release Society

Universidad de La Laguna

CAMPUS ATLÁNTICO TRICONTINENTAL CANARIAS 2010/2015
CAMPUS DE EXCELENCIA DE ÁMBITO REGIONAL

Gobierno de Canarias
Agencia Canaria de Investigación, Innovación y Sociedad de la Información

Bial
Keeping life in mind.

Lipoid

iesmat
Soluciones Tecnológicas Aplicadas

Welcome message

Dear participants,

On behalf of the Board of the Spanish-Portuguese Local Chapter of the Controlled Release Society (SPLC-CRS), we are glad to welcome you to the XIVth Conference of our chapter This year, at the last moment, due to the pandemic, we had to adapt the meeting to a virtual format. We have tried our best, we have extended the duration of the meeting to three days to include several sessions dedicated to the presentation of posters. We think that despite not being able to develop the meeting face to face we can enjoy an interesting scientific program, containing:

- 3 Plenary Lectures presented by distinguished experts in the area of Drug Delivery, Ben Boyd (President CRS, Monash University, Australia), Camilla Foged (University of Copenhagen. Denmark) and Alvaro Mata (University of Nottingham, UK).

- 6 scientific sessions that include 3 talks by invited speakers, Nuno Azevedo (University of Porto. Portugal), Pieter Vader (University Medical Center Utrecht. Netherlands) and Jesús Santamaría (University of Zaragoza, Spain) and oral communications or posters focusing on various areas of Drug Delivery, such as: Technological Tools in Advanced Drug Delivery Systems, Biomimetic Structures for Diagnosis and Therapy, Innovative Strategies for Drug Targeting and Hydrogels and 3D Models for Drug Delivery Systems. The fifth session is organized by the Young Scientific Committee. In addition, the young researchers will participate in an Interactive Session with Prof. Jesús Santamaría. The last session is structured as a discussion between Meritxell Teixidó (Chief Executive Officer / Chief Scientific Officer at Gate2Brain SL. Barcelona, Spain) and Jose Luis Lanciego (Head of department of Neuroscience at the Center for Applied

Medical Research. University of Navarra, Spain) on the positive vs negative aspects of brain targeted drug delivery systems.

Also, as is usual in our meeting, the best PhD thesis developed in the last two years will be awarded thanks to funding from the company Bial, keeping life in mind. The best oral communication and poster presented during the meeting will also be recognized thanks to the financial support of the international CRS. By last, we would like to thank all the sponsors for their financial support to help the organization of the Conference.

We also want to thank all the members of the organizing, scientific, Young Scientific Committee, and the thesis, poster and oral communications evaluation committees. Thanks also to the moderators of the different scientific sessions.

We look forward to welcoming you to this virtual meeting!

Carmen Évora

President of the SPLC-CRS

Araceli Delgado

Secretary of the SPLC-CRS

Scientific Program

Wednesday 26th January

Time: Western European Time (Canary Islands local time)

09.00 - 09.30	**Welcome Ceremony** Vice-rector of the University of La Laguna (ULL) Ben Boyd (CRS President) Carmen Évora (SPLC-CRS President) Bruno Sarmento (SPLC-CRS Vice president)
09.30 - 10.15	**PLENARY LECTURE 1** **Ben Boyd** University of Copenhagen, Denmark, and Monash University, Australia. ***"Metabolic labelling as a potential new approach to localised drug delivery"*** **Moderator**: María Jesús Vicent (Príncipe Felipe Research Center, Valencia)

SESSION 1. Technological Tools in Advanced Drug Delivery Systems

Moderator: Bruno Sarmento. University of Porto

10.15 - 10.45	**Invited speaker** **Nuno Azevedo** Laboratory for Process Engineering, Environment, Biotechnology and Energy (LEPABE). Faculty of Engineering. University of Porto. Portugal. ***"Delivery of nucleic acid mimics into bacteria"***
10.45 - 11.45	**Short talks** (10 min + 5 min questions) ***"Protamine nanoparticles as non-viral vectors for gene-delivery in the treatment of glioblastoma"*** S. Barrios-Esteban, R. Rahman, C. Alexander, M. Garcia-Fuentes and N. Csaba, Universidade de Santiago de Compostela. ***"Dexamethasone and melatonin co-loaded PLGA microspheres: potential chronic neuroprotective strategy for glaucoma"*** M. Brugnera; M. Vicario-de-la-Torre; V. Andrés-Guerrero; I. Bravo-Osuna; I.T. Molina-Martinez and R. Herrero-Vanrell, Complutense University of Madrid. ***"Peptide nano-vaccine against SARS-CoV-2 infection"***

	R.C. Acúrcio, R. Kleiner, B. Carreira, D. Vaskovich, Y. Liubomirski, E. Yeini, C. Araújo, C. Plama, A.S. Viana, J. Gonçalves, R. Satchi-Fainaro, H.F. Florindo. University of Lisbon ***"Smart targeted nanohybrids as dual-approach drug delivery systems against colorectal cáncer"*** J. Gonzalez-Valdivieso, R. Vallejo, A. Girotti, S. Rodriguez-Rojo, Mercedes Santos, F.J. Arias. University of Valladolid.
11.45 - 12:15	**Break**
12.15 - 13:30	**Posters Session** (2-3 min each + 10-15 min for questions) **Optimization of PLGA/PEI nanoparticles covered with poly(I:C) for cáncer immunotherapy.** L. Gonzalez-Melero, R.M. Hernandez, E. Santos-Vizcaino, M. Igartua. University of Basque Country **Amoebicidal Effect of Pitavastatin Nanoparticles in Acanthamoeba castellani Neff.** A. Oliva, I. Sifaoui, P. Díaz-Rodríguez, J. Lorenzo, J.E. Piñero. Universidad de La Laguna. **Cell-free synthesis of Ebola virus matrix protein VP40 Virus-like particles**. S. Gutiérrez-Gutiérrez, C. Rivas-Vázquez, A Vidal, M. García-Fuentes. Santiago de Compostela. **Chamomilla pollen microcapsules as multistep delivery systems.** L. Valverde-Fraga, J. M. Ageitos, S. Robla, N. Csaba. Universidade de Santiago de Compostela. **Gone with the Waste - Quantification of the exact composition of polymeric nanocapsules.** G. Berrecoso, J. Crecente-Campo, M.J. Alonso. Universidade de Santiago de Compostela. **Infliximab microencapsulation by Coaxial Ultrasonic Atomization preserves its biological activity: in vitro evaluation**. I. Lamela-Gómez, J. Blanco-Méndez, F.J. Otero-Espinar, A. Luzardo-Álvarez. Universidade de Santiago de Compostela. **Carvacrol-loaded microcapsules by a coaxial method for varroosis control. Effective parameters on their production**. A. Luzardo-Álvarez, I. Lamela-Gómez, X. Rodríguez-Maciñeiras, E. Fatira, A. Frías-Álvarez, A. Gracia Molina. Universidade de Santiago de Compostela. **Mucoadhesive buccal formulations based on lyophilized liposomes: application to sildenafil citrate**. A. Sánchez Navarro, P. Buján Costas, C. Maderuelo, A. Zarzuelo and M.J de Jesús Valle. Universidad de Salamanca **Catinonic liposomal formulation for cyclopirox nail administration.** F.J. Otero Espinar, V. De Monte VIdal, V. Díaz Tomé, V. Dominguez Arca, E. Vazquez Lage, M. Casas Parada, G. Prieto Estevez. Universidade de Santiago de Compostela. **Development of a liposomal formulation containing Cyclosporin A for the treatment of dry eye disease.** M.A. González-Cela Casamayor, M.A. Caballo González, M. Vicario de la Torre, M. Guzmán Navarro, J.M. Benítez del Castillo, E.M. González-Alonso Alegre, A. Rodríguez, B. de las Heras, R. Herrero Vanrell and I.T. Molina Martínez. Complutense University of Madrid. **Budesonide microparticles for ocular administration.** M. Guzmán-Navarro, I. González Criado, J. Rodriguez Villanueva. University of Alcalá. **Moderator**: Luísa Corvo. University of Lisbon.

13.30 - 15:00	**Time for Lunch**
15.00 - 16:25	**Posters Session** (2-3 min each + 10-15 min for questions) **New treatment for fungal keratitis: A combined eye drops of two antifungals.** V. Díaz-Tomé, X. García-Otero, R. Varela-Fernández, J. Llovo-Taboada, M. González-Barcia, A. Fernández-Ferreiro, F.J. Otero-Espinar. Universidade de Santiago de Compostela **Bevacizumab-loaded PLGA intravitreal implants prepared by supercritical fluid technology.** C. Bendicho-Lavilla; I. Seoane-Viaño; V. Santos-Rosales; A. Luzardo-Álvarez; C.A. García-Gonzalez; F.J. Otero-Espinar. Universidade de Santiago de Compostela. **Bevacizumab loaded lipidic lyotropic liquid crystals as a promising platform for ocular diseases.** G. Blanco-Fernández, B. Blanco-Fernández, A. Fernández-Ferreiro, F.J. Otero-Espinar. Universidade de Santiago de Compostela. **Development of surface-modified lipid-polymer hybrid nanoparticles: bulk formulation vs microfluidics.** E. Briffault, H. Rouco, P. Diaz-Rodriguez, P. Garcia-Garcia, D. Molina, A. Delgado and C. Evora. Universidad de La Laguna. **Microfluidics for precise tuning of cubosome nanoparticle size.** C.J.O. Ferreira, M. Barros, C. Botelho, M.E.C.D. Real Oliveira, B.F.B. Silva. University of Minho. **Characterization and in vivo evaluation of quercetin-loaded zein nanoparticles.** R. Campión, A.L. Martínez-López, C.J. González-Navarro, E. de Paz-Barragán, C. Matías-Sainz, J.M. Irache. University of Navarra. **A Nanotechnology-based Immunotherapeutic Strategy Against KRAS mutated Colorectal Adenocarcinoma**. F. Andrade, D. Rafael, S. Montero, V.Z. Diaz-Riascos, S. Schwartz, and I. Abasolo. Vall d'Hebron Institut de Recerca. **Self-Illuminating Biocompatible Nanosystems can Induce Apoptosis Via Photodynamic Therapy (PDT)**. M. Abal-Sanisidro, L. Ruiz-Cañas, M.G. Blanco, R. López-López, B. Jr Sainz, M. de la Fuente. Health Research Institute of Santiago de Compostela (IDIS). **Evaluation of Eudragit S100 Nanofibers as pH responsive antimicrobial release system.** L. Miranda-Calderón, C. Yus, G. Landa, M. Arruebo, G. Mendoza and S. Irusta. Universidad de Zaragoza. **Nucleic acid based medicinal products for Fabry disease: critical formulation factors to ensure effective delivery.** I. Gómez-Aguado, J. Rodríguez-Castejón, M. Beraza-Millor, A. Rodríguez-Gascón, A. del Pozo-Rodríguez and M.A. Solinís. University of Basque Country. **Fluorescence Cross-Correlation Spectroscopy reveals extent of association between liposomes and DNA and the number of DNA molecules per lipid nanoparticle.** R. Gaspar, J.L. Paris, P.A.A. De Beule, B.F.B. Silva. INL - International Iberian Nanotechnology Laboratory **DOSY as an Alternative Technique to Monitor the Degradation of Polypeptide-Based Drug Delivery Systems.** J.J. Arroyo-Crespo, I. Conejos-Sánchez, D. Morelló-Bolumar, S. Stifano, V.J. Nebot and M.J. Vicent. Centro de Investigación Príncipe Felipe **Moderator**: Rosa Mª Hernández. University of Basque Country.

16.25 - 17:00	**PhD Thesis Award sponsored by Bial** **Moderator**: Rocío Herrero. University Complutense de Madrid.
17.00 - 18:00	Interactive Session with **Prof. Jesús Santamaría**. University of Zaragoza. ***"A PhD degree and Beyond. Thoughts for early-career researchers"***

Thursday 27th January

Time: Western European Time (Canary Islands local time)

09.00 - 09.45	**PLENARY LECTURE 2** **Camilla Foged** Department of Pharmacy. Vaccine Design and Delivery Group. University of Copenhagen. Denmark ***"Opportunities and challenges in the delivery of mRNA vaccines"*** **Moderator:** María Blanco. University of Navarra

SESSION 2. Biomimetic Structures for Diagnosis and Therapy

Moderator: Susana Simões. Centre for Innovative Biomedicine and Biotechnology (CIBB). University of Coimbra

09.45 - 10.15	**Invited speaker** **Pieter Vader** CDL Research and Department of Experimental Cardiology. University Medical Center (UCM) Utrecht. Netherlands. ***"Extracellular vesicle-mediated RNA delivery: From mechanistic insights to therapeutic applications"***
10.15 - 11.15	**Short Talks** (10 min + 5 min questions) ***"Functionalization of a meniscus prosthesis with polymeric coatings for the sustained release of anti-inflammatory drugs"*** A. Fernandez Blanco, G. Lou, J. C. Campo, M. J. Alonso, Universidade de Santiago de Compostela. ***"Exosome-mediated MEK1 silencing is a promising approach against triple negative breast cancer regression"*** D. Ferreira, C. Santos-Pereira, M. Costa, J. Afonso, A. Longatto-Filho, F. Baltazar, R. Kalluri, J. Moreira and L.R. Rodrigues, University of Minho. ***"Etoposide and edelfosine lipid nanomedicines as a synergistic combination therapy for neuroblastoma"*** SH. El Moukhtari, G.M. Pelin, M.J. Blanco-Prieto, University of Navarra. ***"Pollen-based platforms for pulmonary delivery of nanoencapsulated rifabutin"*** S. Robla, J.M. Ageitos, R. Ambrus, N. Csaba, Universidade de Santiago de Compostela.
11.15 - 11:30	**Posters Session** (2-3 min each + 5 min for questions) **In vitro production, isolation and characterization of Ebola virus-like particles.**

	R. Mellid-Carballal, C. Rivas, M. Garcia-Fuentes. Universidade de Santiago de Compostela. **Self-assembling dendrimer for the delivery of antisense NAMs into bacteria.** M. Gomes, I. Resende, S. Pereira, L. Peng, R. S. Santos, N. F. Azevedo. University of Porto. **Transtympanic delivery of the pneumoccal endolysin MSlys via PEGylated liposomes.** M. D. Silva, K. Ray, F. M. Gama, A. K. Remenschneider, and S. Sillankorva. University of Minho.
11.30 - 12:00	**Break**

SESSION 3. Innovative Strategies for Drug Targeting

Moderator: Helena Florindo. University of Lisbon

12.00 - 12.30	**Invited speaker** **Jesús Santamaría** Department of Chemical and Environmental Engineering. Instituto de Nanociencia y Materiales de Aragon (INMA). University of Zaragoza ***"Extracellular vesicles as selective vectors for delivery of nanomaterials to tumors"***
12.30 - 13.45	**Short Talks** (10 min + 5 min questions) ***"Lipid-based non viral gene therapy for Fabry disease:Ex vivo and in vivo evaluation"*** J. Rodríguez-Castejón, I. Gómez-Aguado, M. Beraza-Millor, M.A. Solinís, A. del Pozo-Rodríguez and A. Rodríguez-Gascón, University of the Basque Country. ***"Treating Neurodegeneration with Synergistic Combinations of Polypeptide-Based Nanoconjugates Targeting Oxidative Stress and Inflammation"*** I. Conejos-Sánchez, E. Masiá, M.J. Vicent, Centro de Investigación Príncipe Felipe. ***"Combining glucose-responsive nanoparticles and iPSCs differentiation: an innovative strategy to treat diabetes"*** JM. Marques, A.M. Carvalho, R. Nunes, J. das Neves, H. Florindo, D. Ferreira, B. Sarmento, University of Porto. ***"Multifunctional nanoparticles as an anticancer approach for the intracellular delivery of monoclonal antibodies"*** A.M. López-Estévez, L. Sanjurjo, J. Pellico, R.T.M. de Rosales, D. Torres, and M.J. Alonso, Universidade de Santiago de Compostela. ***"Non-viral delivery of CRISPR/Cas9 DNA for gene editing via multivalent cationic liposome system"*** D.A. Sousa, R. Gaspar, J. O. Ferreira, F.Baltazar, B. Silva 2 and L.R. Rodrigues. University of Minho.

13.45 - 15:15	**Time for Lunch**
15.15 - 16:20	**Posters Session** (2-3 min each + 10-15 min for questions) **Ultraflexible lipid vesicles allow in vitro skin permeability of Cyanocobalamin: a potential treatment for Vitamin B12 deficiency.** A.J. Guillot, P. Merino, T.M. Garrigues, A. Melero. University of Valencia. **Targeted cathelicidin nanomedicines as novel glucoregulator for diabetes therapy.** C. Cristelo, F. M. Gama, B. Sarmento. University of Porto. **Preclinical basis of nanostructured lipid carriers (NLC) loaded with aflibercept: design, development and characterization.** X. García-Otero, V.F. R. Varela-Fernández, J. Blanco-Méndez, M. González-Barcia, P. Aguiar, A. Fernández-Ferreiro and F. J. Otero-Espinar. Universidade de Santiago de Compostela. **Infliximab-loaded PLGA nanoparticles: design, development, and physicochemical characterization.** R. Varela-Fernández, X. García-Otero, M.I. Lema-Gesto, M. González-Barcia, and F.J. Otero-Espinar. Universidade de Santiago de Compostela. **Inulin-PCL nanoparticles as an adjuvant delivery system for highly purified recombinant antigens**. S. Jesus, J. Panão Costa, H. Duarte, M. Colaço, O. Borges. University of Coimbra. **Novel polypeptide-based conjugates for mitochondrial targeting.** C. Pegoraro, I. Conejos-Sánchez, M.J. Vicent. Centro de Investigación Príncipe Felipe. **Receptor-targeted nanocarriers modulate cannabinoid anticancer activity through delayed cell internalization.** M. Durán-Lobato, J. Álvarez-Fuentes, M. Fernández-Arévalo, L. Martín-Banderas. Universidad de Sevilla. **3D printed tacrolimus suppositories for the treatment of ulcerative colitis.** I. Seoane-Viaño, J.J. Ong, A. Luzardo-Álvarez, M. González-Barcia, A. Basit, F.J. Otero-Espinar, A. Goyanes. Universidade de Santiago de Compostela. **Moderator**: Alicia Rodríguez-Gascón. University of Basque Country
16.20 - 17:25	**Posters Session** (2-3 min each + 10-15 min for questions) **Development of shear-responsive microaggregates based on PLGA nanoparticles for targeted delivery**. M.M. El-Hammadi; R. Otero-Candelera; L. Martín-Navarro; J. Álvarez-fuentes; L. Martin Banderas. Universidad de Sevilla. **Lipid-polymeric hybrid nanoparticles funcionalized with a specific aptamer: cellular uptake and citotocicity.** P. Díaz-Rodríguez, P García-García, C. Évora and A. Delgado. Universidad de La Laguna. **Organs toxicity of oligonucleotide aptamer-lipid-polymer nanoparticles for osteoporosis**. R. Reyes, P. García-García, P. Díaz-Rodríguez, M.R. Arnau, C. Évora, A. Delgado. Universidad de La Laguna. **Immunotoxicological properties of yeast-derived glucan particles.** J. Panão Costa, M. Colaço, S. Jesus, O. Borges. University of Coimbra.

	The influence of curcumin-encapsulated glucan nanoparticles on oxidative stress in liver cells. M. Colaço, O. Borges, T. Roquito, J. Panão Costa, S. Jesus. University of Coimbra. **Preparation, characterization and efficacy of polylactide glycolide-chitosan nanoparticles loaded with Curcuma**. J. Molpeceres, C. Tizón, G. Yagüe and M.R. Aberturas. University of Alcalá. **Polymeric nanoparticles loaded anti-viral peptide efficiently inhibits SARS-CoV-2**. A. Mali, C. Zannella, S. Anthiya, M. Galdiero, G. Franci, M.J. Alonso. University of Luigi Vanvitelli and University of Santiago de Compostela. **Novel Hybrid Nanosystem for Magnetically Targeted Antitumoral Activity Enhancement.** N. Cruz, J.O. Pinho, G. Soveral, N. Matela, C. Pinto Reis, M.M. Gaspar. University of Lisbon. **Moderator**: Bruno Silva. International Iberian Nanotechnology Laboratory, Braga.

Friday 28th January

Time: Western European Time (Canary Islands local time)

09.00 - 09.45	**PLENARY LECTURE 3** **Álvaro Mata** Chair in Biomedical Engineering and Biomaterials. School of Pharmacy. University of Nottingham. ***"Bioengineering biomimetic 3D environments and in vitro models through supramolecular self-assembly"*** **Moderator:** Carmen Álvarez (University of Santiago de Compostela)

SESSION 4. Hydrogels and 3D Models for Drug Delivery Systems

Moderator: Patricia Díaz-Rodríguez. University of Santiago de Compostela.

09.45 - 11.00	**Short Talks** (10 min + 5 min questions) ***"Biocompatible Injectable Smart Hydrogels-based Depot Systems: A Dual-Anticancer Drug Sustained Release Strategy"*** D. Rafael, F. Andrade, M.M. Roca-Melendres, D. Hide, I. Raurell, M. Martell, S. Schwartz, M. Oliva, E. Duran-Lara and I. Abasolo. Vall D'Hebron Institut de Recerca. ***"Modulating muchoadhesion and mucopenetration in multiresponsive nanogels"*** M. Calderón, S. Orellano, J. Udabe and A. Sonzogni. University of the Basque Country. ***"Does it GUT what it takes? A new 3D bioengineered in vitro intestinal model to predict permeability"*** M.H. Macedo, A.S. Barros, E. Martinez, C.C. Barrias, B. Sarmento, University of Porto. ***"Uterine leiomyoma 3D preclinical model for evaluating ganirelix delivery system"*** P. García-García, A. Salas, C. Évora, P. Díaz-Rodríguez, T.A. Almeida and A. Delgado, Universidad de La Laguna **"*Evaluation of lipid nanosystems for cancer treatment in static and non-static 3D models*"** M. Cascallar, A. Martins, M. Ferrero, E. Escorihuela, S. Calabuig-Fariñas, L. Diéguez, E. Jantus-Lewintre, M. de la Fuente. Health Research Institute of Santiago de Compostela (IDIS)/CIBERONC
11.00 - 11:30	**Break**

11.30 - 12:30	**Posters Session** (2-3 min each + 10-15 min for questions) **Carboxymethyl cellulose-based 3D scaffolds for wound healing.** C. Alvarez-Lorenzo, L. Díaz-Gómez, I. González-Prada, R. Millán and A. Concheiro. Universidade de Santiago de Compostela. **Gelatin hydrofilms with bioactive compounds Aloe vera and EGF for chronic wound healing applications**. I. Garcia-Orue, A. Etxabide, K. de la Caba, P. Guerrero, M. Igartua, E. Santos-Vizcaino, R. M. Hernandez. University of the Basque Country **A novel sumecton enriched gelatin-based scaffold for bone regeneration.** I. Lukin, I. Erezuma, G. Orive. University of Basque Country. **Extracellular vesicle-loaded hydrogel for stimulating cardiac repair after myocardial infarction.** E. Garbayo, L. Saludas, P. Gil-Cabrerizo, G. Abizanda, F. Prosper, M.J Blanco-Prieto. University of Navarra. **Novel injectable thermosensitive hydrogel containing chitosan-dextran sulphate nanoparticles for antigen delivery**. E. Giuliano, S. Anthiya, C. Alvarez-Lorenzo, D. Cosco and M.J. Alonso. University of Santiago de Compostela. **Functionalized hyaluronic acid-based hydrogel for ophthalmic application. Preliminary studies**. A. Aragón-Navas, M. Johnson, Sigen A, I. Bravo-Osuna, V. Andrés-Guerrero, H. Tai, W. Wang, R. Herrero-Vanrell. Complutense University of Madrid. **Mucoadhesive nanoparticles for ocular delivery of ketorolac.** M. Oliva, F. Andrade, D. González, and D. Rafael. Universitat de Barcelona. **Licensing hydrogels maintain the immunomodulatory phenotype of human mesenchymal stromal cells in a murine colitis model**. A. Gonzalez-Pujana, A. Beloqui, J.J. Aguirre, M. Igartua, E. Santos-Vizcaino, R.M. Hernandez. University of the Basque Country **Moderator**: Dolores Torres. University of Santiago de Compostela.

SESSION 5. Young Scientist Networking

Moderators: Cláudia Martins (Univ. Porto), Souhaila El Moukhtari (Univ. Navarra), Mireya L. Borrajo (Univ. Santiago de Compostela) and Patricia García-García (Univ. La Laguna).

12.30 - 13.30	**Short Talks** (7 min + 3 min questions) ***"Exploiting the chemotherapeutic and immunomodulatory effect of brain and glioblastoma dual-targeted nanoparticles – a nanomedicine, chemistry and tumor biology therapeutic recipe making use of a novel tumor niche-recapitulating 3D spheroid construct"*** C. Martins, C.M. Barbosa, M. Araújo, S. J. Smith, M. J. Oliveira, D. Lamprou, R. Rahman, J. W. Aylott, B. Sarmento. University of Porto. ***"Nanosystems for the development of mRNA vaccines"*** M.L. Borrajo, S. Anthiya, G. Lou, and MJ. Alonso. University of Santiago de Compostela

	"mRNA Reprograming Matrices for driving chondroblast differentiation in vitro and in vivo " H. Rilo-Alvarez, A. M. Ledo, M. Lopez-Peña, F. M. Muñoz, A. Vidal, M. Garcia-Fuentes. University of Santiago de Compostela ***"Nanoclay-incorporated HA/alginate scaffolds as SDF-1 smart delivery-platforms for bone tissue engineering"*** I. Erezuma, , I. Lukin, P. García-García, A. Delgado, R. Reyes , C. Evora and G. Orive. University of Basque Country. ***"Extracellular vesicles from hair follicle and adipose tissue-derived mesenchymal stem cells: Flow cytometry characterization and functional comparison for the treatment of diabetic ulcers"*** K. Las Heras, F. Royo, C. Garcia-Vallicrosa, M. Igartua, E. Santos-Vizcaino, J.M. Falcon-Perez, R Hernandez. University of Basque Country. **"*Direct powder extrusion 3D printing of polyhydroxybutyrate implants for prolonged drug release*"** S. Moroni, M. Tiboni, L. Casettari. University of Urbino
13.30 - 15:00	**Time for Lunch**

FINAL SESSION. Discussion: Positive-negative aspects of brain targeted drug delivery systems

15.00 - 16.00	**Jose Luis Lanciego vs Meritxell Teixidó** **Jose L. Lanciego** Head of department of Neuroscience at the Center for Applied Medical Research (CIMA). University of Navarra. **Meritxell Teixidó** Chief Executive Officer/Chief Scientific Officer at Gate2Brain SL. Barcelona. Spain. **Moderator**: M.J. Alonso (University of Santiago de Compostela)
16.00 - 16.30	***Awards for the best oral communication and poster.*** ***Closing ceremony***
16.30 - 17.30	***General Assembly of the SPLC-CRS***

Plenary Lecture

PL1: ***"Metabolic labelling as a potential new approach to localized drug delivery"***. Ben Boyd, University of Copenhagen, Denmark, and Monash University, Australia. (p.20)

PL2: ***"Opportunities and challenges in the delivery of mRNA vaccines"***. Camila Foged, Department of Pharmacy. Vaccine Design and Delivery Group. University of Copenhagen. Denmark. (p.21)

PL3: ***"Bioengineering biomimetic 3D environments and in vitro models through supramolecular self-assembly"***. Álvaro Mata, Chair in Biomedical Engineering and Biomaterials. School of Pharmacy. University of Nottingham. (p.22)

PL1: Metabolic labelling as a potential new approach to localised drug delivery

Ben Boyd

University of Copenhagen, Denmark, and Monash University, Australia

We have been concerned with the interaction of complex lipid particles with cells and trying to understand how on the one hand the underlying structure of the particle may influence their interaction with cells such as vascular endothelial cells, and on the other hand how they may be ‘forced’ to interact with cells using antibody-free 'cellular Velcro' approaches in the gut using metabolic labelling and click chemistry. For the former we have been using simple models to mimic arterial and vascular flow in formats that offer the opportunity for additional in situ analytical techniques. The latter approach is shaping as an interesting option for localizing particles or other delivery vectors to specific regions of the gut.

PL2: Opportunities and challenges in the delivery of mRNA vaccines

Camilla Foged

Department of Pharmacy. Vaccine Design and Delivery Group. University of Copenhagen. Denmark

PL3: Bioengineering biomimetic 3D environments and in vitro models through supramolecular self-assembly

Álvaro Mata

1Chair in Biomedical Engineering and Biomaterials. School of Pharmacy. University of Nottingham.

Living systems have evolved to grow and heal through self-assembling processes capable of organizing a wide variety of molecular and cellular building-blocks at multiple size scales. While advances in nanotechnology and biofabrication are enhancing our capacity to emulate features of some of these biological structures, it is increasingly evident that recreation of their complexity and adaptability will require new ways of fabricating. This talk will present our laboratory's efforts to combine supramolecular events found in nature such as self-assembly, disorder-to-order transitions, or diffusion-reaction processes with engineering and materials science to design environments with higher levels of biological relevance. I will describe methodologies to develop: a) hydrogels for 3D cell culture with tuneable physical and chemical properties[1], b) 3D materials that can mimic features of the tumour microenvironment of ovarian and pancreatic cancer[2,3], c) fluidic devices that can recreate key physiological features of native vasculature[4], d) mineralizing materials that can emulate the way tissues mineralize[5].

References

1. Derkus et al, Acta Biomaterialia 2019, 10.1016/j.actbio.2020.03.025.
2. Osuna de la Peña et al, Nature Communications 2021, 10.1038/s41467-021-25921-9.
3. Hedegaard et al, Science Advances 2020, 10.1126/sciadv.abb3298.
4. Wu et al, Nature Communications 2020, 10.1038/s41467-020-14716-z.
5. Elsharkawy et al, Nature Communications 2018, 10.1038/s41467-018-04319-0.

Invited speaker

IS1: "***Delivery of nucleic acid mimics into bacteria***" Nuno Azevedo, Laboratory for Process Engineering, Environment, Biotechnology and Energy (LEPABE). Faculty of Engineering. University of Porto. Portugal. (p.24)

IS2: "***Extracellular vesicle-mediated RNA delivery: From mechanistic insights to therapeutic applications***". Pieter Vader, CDL Research and Department of Experimental Cardiology. University Medical Center (UCM) Utrecht. Netherlands. (p.25)

IS3: "***Extracellular vesicles as selective vectors for delivery of nanomaterials to tumors***". Jesus Santamaría, Department of Chemical and Environmental Engineering. Instituto de Nanociencia y Materiales de Aragon (INMA). University of Zaragoza. (p.26)

IS1: Delivery of nucleic acid mimics into bacteria

Nuno F. Azevedo

LEPABE, Dep of Chemical Engineering, Faculty of Engineering of the University of Porto, Portugal

Delivery of nucleic acid mimics (NAMs) or nucleic acid analogues for therapeutic applications is now entering a golden age, and several oligonucleotides have recently been approved by regulatory authorities (1). Up until now these applications have been mainly targeting human cells, but strategies aimed at microorganisms, and more specifically bacteria, are starting to emerge (2). Like for human cells, NAMs can be engineered to hybridize with specific sequences in bacteria with high affinity and hence be used to inhibit the translation of essential genes. However, as the bacterial envelope barrier hinders NAMs internalization, suitable and bacteria-specific delivery vectors are in dire need. In here, I will discuss limitations and advantages on the application of liposomes, dendrimers, vitamin B12 and cell-penetrating peptides as carriers for NAMs in bacteria. Important aspects to discuss include a stable association between the NAMs and the carriers in the presence of biofluids, the type of interaction between the carriers and the cell envelope and also the accumulation of NAMs inside the cell that each carrier is able to achieve.

(1) Roberts et al (2020), Advances in oligonucleotide drug delivery, Nature Reviews Drug Discovery.

(2) Santos et al (2018), Nanomaterials and molecular transporters to overcome the bacterial envelope barrier: Towards advanced delivery of antibiotics, Advanced Drug Delivery Reviews.

IS2: Extracellular vesicle-mediated RNA delivery: from mechanistic insights towards therapeutic applications

Pieter Vader

CDL Research and Department of Experimental Cardiology. University Medical Center (UCM) Utrecht. Netherlands.

Extracellular vesicles (EVs) play a pivotal role in intercellular communication through functional transfer of bioactive cargo, including RNA molecules. Despite increasing interest in EV-mediated RNA transfer, understanding of the pathways and mechanisms regulating EV-mediated RNA delivery and processing is limited due to a lack of suitable readout systems. Here, we show a novel CRISPR/Cas9-based reporter system that allows the study of EV-mediated RNA transfer at single-cell resolution. We employed this system to compare the delivery efficiency of EVs to clinically approved state-of-the-art DLin-MC3-DMA lipid nanoparticles and several in vitro transfection reagents. We found that EVs delivered RNA several orders of magnitude more efficiently than these synthetic systems. This finding supports the continued research into EVs as potential RNA delivery vehicles. To overcome challenges related to the difficulty of RNA loading into EVs, we prepared EV-liposome hybrid nanoparticles and evaluated them as siRNA delivery systems in terms of cellular uptake, toxicity, and gene-silencing efficacy. We show that hybrids combine benefits of both synthetic and biological drug delivery systems and might serve as future therapeutic carriers of siRNA.

IS3: Extracellular vesicles as selective vectors for delivery of nanomaterials to tumors

M. Sancho-Albero, M. Encinas-Giménez, V. Sebastian, E. Perez, L. Lujan, M.P. Martín-Duque, J. Santamaria

Nanoscience and Materials Institute of Aragon (INMA), Department of Chemical Engineering, University of Zaragoza, Spain

CIBER-BBN, Instituto de Salud Carlos III, Madrid, Spain

Therapies against cancer include Chemotherapy, Radiotherapy, Surgery, Immunotherapy, Precision Medicine and Hormone Therapy, among others. In spite of this variety of techniques, cancer is still of the leading causes of death: By current estimates, by 2040 almost 30 million new cases will be diagnosed yearly, and cancer will cause around 15 million deaths worldwide. Nanomedicine, -the application of nanomaterials and, in general, of nanotechnology to medicine-, was heralded as the new alternative that could circumvent many of the obstacles that plagued more conventional approaches. However, recent studies have shown that selective delivery of nanoparticles to tumors in vivo remains an unsolved challenge. Currently, methods that rely on the EPR effect or even targeted delivery mediated by antibodies and other biomolecules, present a very low delivery efficiency, around 1%, (Wilhelm et al. Nat Rev. Mater. 2016).

It is clear that, unless nanomaterials can be delivered selectively (or at least preferentially) to the tumor, the exciting prospects of nanotechnology in cancer will fail to materialize. For this reason, a variety of alternative delivery methods are being investigated using. Among these, the so-called Trojan Horse strategies that use whole cells (mesenchimal stem cells, dendritic cells, etc) or cell-derived structures (exosomes, microvesicles) as vectors for selective delivery, are raising a strong interest. We, among others, have shown that extracellular vesicles such as exosomes exhibit exciting targeting capabilities, being able to selectively deliver nanoparticles in vitro to cells of the same origin (Sancho-Albero et al. J. Nanobiotechnol. 2019, Sancho-Albero et al. Nature Catalysis, 2019). Recently, we have gone a step further and also demonstrated a strong increase of targeting selectivity in vivo, not only for primary tumors, but also for multinodular (analogous to metastatic) tumors (Sancho-Albero et al. J. Extracell. Vesicles, 2022).

In summary, while still in need of strong development, the use of extracellullar vesicles as selective delivery vectors to tumors presents exciting possibilities that may help to finally realize the strong potential of nanomaterials in oncology.

Abstracts for Oral Presentation

Session 1: Technological Tools in Advanced Drug Delivery Systems

O1.1: "***Protamine nanoparticles as non-viral vectors for gene-delivery in the treatment of glioblastoma***". S. Barrios-Esteban, R. Rahman, C. Alexander, M. Garcia-Fuentes and N. Csaba, Universidade de Santiago de Compostela. (p.33)

O1.2: "***Dexamethasone and melatonin co-loaded PLGA microspheres: potential chronic neuroprotective strategy for glaucoma***". M. Brugnera; M. Vicario-de-la-Torre; V. Andrés-Guerrero; I. Bravo-Osuna; I.T. Molina-Martinez and R. Herrero-Vanrell, Complutense University of Madrid. (p.35)

O1.3: "***Peptide nano-vaccine against SARS-CoV-2 infection***" R.C. Acúrcio, R. Kleiner, B. Carreira, D. Vaskovich, Y. Liubomirski, E. Yeini, C. Araújo, C. Plama, A.S. Viana, J. Gonçalves, R. Satchi-Fainaro, H.F. Florindo. University of Lisbon. (p.37)

O1.4: "***Smart targeted nanohybrids as dual-approach drug delivery systems against colorectal cáncer***". J. Gonzalez-Valdivieso, R. Vallejo, A. Girotti, S. Rodriguez-Rojo, Mercedes Santos, F.J. Arias. University of Valladolid. (p.38)

O1.1: Protamine nanoparticles as non-viral vectors for gene-delivery in the treatment of glioblastoma

S. Barrios-Esteban[1;2;3]*, R. Rahman[2], C. Alexander[3], M. Garcia-Fuentes[1] and N. Csaba[1]

[1]*Center for Research in Molecular Medicine and Chronic Diseases, Dept. Pharmacology, Pharmacy and Pharmaceutical Technology, University of Santiago de Compostela, 15782, A Coruña, Spain*
[2]*Biodiscovery Institute, School of Medicine, University of Nottingham, NG7 2RD, Nottingham, United Kingdom*
[3]*Boots Science Building, School of Pharmacy, University of Nottingham, NG7 2TQ, Nottingham, United Kingdom*

*e-mail: sheila.barrios.esteban@usc.es

Introduction

Protamine (Pr), a small polycationic peptide, is one of the most used cationic polymers to formulate non-viral vectors. Currently, this polymer is gaining importance in gene therapy for the treatment of glioblastoma, the most dangerous brain tumor [1]. Gene therapy has become an interesting therapeutic intervention for brain cancer due to its viable and safe approach compared with the conventional treatment. This therapy also has the capacity to target specific pathways within glioblastoma cells by the introduction of exogenous tumor suppressor sequences that are rendered therapeutically effective by using delivery nanosystems [2]. Protamine nanoparticles (Pr NPs) are an attractive delivery platform due to its safety, non-toxicity, and natural capacity to condense different nucleic acids, such as DNAs, miRNAs, and siRNAs [3]. Based on this information, our research group has been exploring protamine NPs as a gene delivery system using different nucleic cargos for the treatment of glioblastoma.

Materials and Methods

The NPs were formulated by the ionic complexation method combining Pr as cationic polymer and dextran (Dx) as anionic element, using the Pr:Dx ratio 4:1 (*w:w*) (4:1 Pr:Dx NPs). The physicochemical characteristics of this formulation: size, polydispersity index (PDI) and surface charge, were analyzed by Photon Correlation Spectroscopy and Laser Doppler Anemometry. In addition, the morphology was studied by using Transmission Electron Microscopy. The long and short-term stability was examined for one month under storage conditions (4ºC) and for 4h when incubated in cell culture media at 37ºC (pH=7.4), respectively. The association of nucleic acids was studied by agarose gel electrophoresis using an excess of heparin as ionic competitor. Regarding the *in vitro* studies, first, they were optimized in U87MG monolayers and 3D spheroids and then, applied to a panel of primary patient-derived glioblastoma cell lines from both the glioblastoma core and invasive margin (GIN-28, GIN-8 and GCE-28). Cell viability was evaluated by different proliferation and cell death assays such as resazurin, spheroid volume and 7-Aminoactinomycin D membrane permeability. 2D and 3D nanocarrier uptake were examined using 5-TAMRA-labeled NPs by Confocal- and Light Sheet Fluorescence Microscopy. Additionally, we also performed these studies employing NPs loaded with a fluorescently labeled siRNA (Cy5-modified siRNA) in U87MG cells and spheroids. The quantification of the NP-uptake was carried out by conventional Flow Cytometry, and by Imaging Flow Cytometry using a ImageStreamer cytometer. Finally, the transfection efficiency in U87MG cell line was studied using different concentrations of a model plasmid encoding the enhanced Green Fluorescent and Luciferase Proteins (pEGFP-Luc). Quantification was done by flow cytometry and a Luciferase Reporter Gene assay.

Results and Discussion

The formulation consists of a homogeneous population (PDI≤0.2) of spherical NPs composed by protamine, a cationic cell penetrating peptide (CPP) with high campacity to condense the genetic material, and dextran sulfate, which is a natural anionic polysaccharide. The Pr NPs had a diameter below 150 nm (120 ± 7 nm) and a positive surface charge (+34 ± 2 mV). These physicochemical characteristics (Table 1.) allowed this nanosystem to have a high and efficient encapsulation of different nucleic acids (≥90%). In addition, 4:1 Pr:Dx NPs were stable for one month at 4ºC and for 4h in cell culture media at 37ºC.

Table 1. Physicochemical characterization of blank and nucleic acids loaded in 4:1 Pr:Dx NPs. PDI: Polydispersity index, A.E: Association Efficiency.

Sample	Nucleic acids	Size (nm)	PDI	Zeta Potential (mV)	A.E (%)
4:1 Pr:Dx NPs	-	120 ± 7	0.2	+34 ± 2	-
	pDNA	146 ± 1	0.2	+33 ± 5	≥90%
	siRNA	157 ± 16	0.1	+18 ± 4	≥90%
	miRNA	147 ± 23	0.2	+22 ± 3	≥90%

The cell-viability studies showed low toxicity of this nanocarrier in U87MG and patient-derived glioblastoma cells and spheroids in all the assays. Both 2D and 3D uptake confirmed an efficient internalization of these fluorescence-labeled NPs (Figure 1.). Furthermore, the quantification by Flow Cytromety verified that more than 90% of the glioblastoma cells and spheroids were positive for the presente of this nanosystem. Finally, the transfection assay in U87MG cell line showed an efficient capacity of the protamine NPs to transfect glioblastoma cells and spheroids for doses above 1 µg/well.

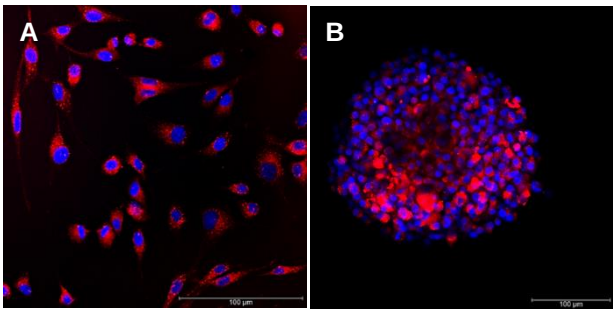

Fig 1. Cellular uptake analyzed by Confocal Laser Sacanning Microscopy in U87MG cells (A) and (B) spheroids after 4h of the removal of 4:1 Pr-TAMRA:Dx NPs. Blue channel: DAPI staining of cell nuclei. Red channel: 5-TAMRA-labeled NPs (7 µg/well, 37ºC).

Conclusions

We have developed a formulation based on protamine NPs with physicochemical properties suitable for the association and protection of different genetic cargos. Their low cellular toxicity, high internalization and their capacity to transfect 2D and 3D glioblastoma models indicated that this formulation could be a promising gene-nanocarrier for glioblastoma treatment.

Acknowledgments

This work was supported by Gobierno de España, Xunta de Galicia (Consellería de Cultura, Educación e Odenación Universitaria (2016-2019, ED431G/05)), European Regional Developtment Fund (ERDF), BritishSpanish Society and (BINV-CS) Bolsas Investigación 2021-Área de ciencias da saúde (Deputación da Coruña).

References

[1] C. Garcia-Mazas, S. Barrios-Esteban, M. Garcia-Fuentes, N. Csaba. Supression of cancer stem cells, *Woodhead Publ Ser Biomater*. 13 (2020) 365-398

[2] W.H. Hsu, P. Sánchez-Gómez, E. Gomez-Ibarlucea, D.P. Ivanov, R. Rahman, A.M. Grabowska, N. Csaba, C. Alexander, M. Garcia-Fuentes. Structure-Optimized Interpolymer Polyphosphazene Complexes for Effective Gene Delivery against Glioblastoma. *Ad. Ther*. 2 (2019) 1-15

[3] S. Reimondez-Troitiño, J.V. González-Aramundiz, J. Ruis-Bañobre, R. López-López, M.J. Alonso, N. Csaba, M. de la Fuente. Versatile protamine nanocapsules to restore miR-145 levels and interfere tumor growth in colorectal cancer cells. *Eur J Pharm Biopharm*. 142 (2019) 449-459.

O1.2: Dexamethasone and melatonin co-loaded PLGA microspheres: potential chronic neuroprotective strategy for glaucoma

M. Brugnera[1;2]*, M. Vicario-de-la-Torre[1;2], V. Andrés-Guerrero[1;2], I. Bravo-Osuna[1;2], I.T. Molina-Martinez[1;2] and R. Herrero-Vanrell[1;2]

[1]*Innovation, Therapy and Pharmaceutical Development in Ophthalmology (InnOftal) Research Group, UCM 920415, Department of Pharmaceutics and Food Technology, Faculty of Pharmacy, Complutense University of Madrid, Plaza Ramón y Cajal s/n, 28040 Madrid, Spain*
[2]*Sanitary Research Institute of the San Carlos Clinical Hospital (IdISSC) San Carlos Clinical Hospital, Calle Profesor Martín Lagos, s/n, 28040 Madrid, Spain*
*e-mail: marcobru@ucm.es

Introduction

Glaucoma is a chronic and multifactorial neuropathy depicted by progressive damage to the optic nerve and death of retinal cells, which lead to irreversible vision loss [1]. Currently, the only evidence-based treatment for this disease addresses reducing intraocular pressure (IOP). However, there are patients with normal values of IOP developing glaucoma. Despite the fact that the pathogenesis of the disease has not been completely established yet, all patients diagnosed with glaucoma are characterized by neurodegeneration [2]. Since retinal cells degeneration is triggered by several molecular pathways, combination therapy could have a potential use as a neuroprotective treatment for glaucoma. Dexamethasone, melatonin and vitamin E, among others, demonstrated achieving encouraging effects to the onset and the progression of this disease [3, 4]. Drug delivery systems, and biodegradable microspheres in particular, can represent the perfect strategies for keeping sustained concentrations of these neuroprotective substances at the retina level for a long time [5]. The purposes of this study were the design of a novel poly (lactic-co-glycolic) acid (PLGA) microspheres formulation (F1) combining the anti-inflammatory drug (dexamethasone) and the antioxidant (melatonin) for intravitreal administration and its *in vitro* characterization. Vitamin E addition to the formulation (F2) was also evaluated.

Materials and Methods

PLGA microspheres (MSs) were manufactured using the oil/water emulsion solvent evaporation technique. Dexamethasone (DX) and melatonin (MEL) were added (2/1:10 w/w). In formulations with Vitamin E addition, a volume of 40 µL was included before the sonication step. Dichloromethane (DCM) and ethanol (EtOH) (25% v/v) were used to dissolve the PLGA and polyvinyl alcohol (PVA) was the surfactant. After 3 hours of maturation, the MSs were separated, selecting one granulometric fraction (38-20 µm) and then lyophilized. In addition, unloaded MSs were elaborated.

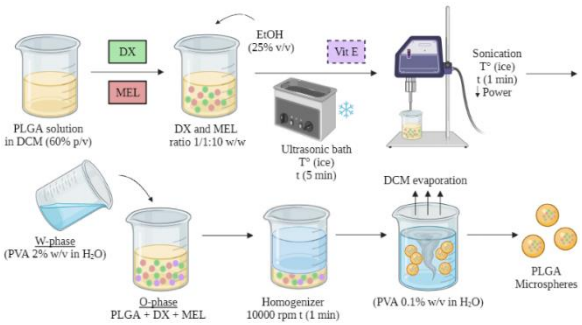

Fig 1. Elaboration of co-loaded PLGA microspheres

Both F1 (DX + MEL) and F2 (DX + MEL + Vitamin E) were evaluated at scanning electron microscopy (SEM) to determine their morphology. Moreover, the two co-loaded formulations were characterized in terms of particle size, encapsulation efficiency and *in vitro* release profile following the procedures described in Figure 2. An HPLC-UV method was previously developed and validated to simultaneously quantify the compounds' content entrapped into the microdevices (encapsulation efficiency assay) and the amounts of each drug co-liberated during the *in vitro* release assay.

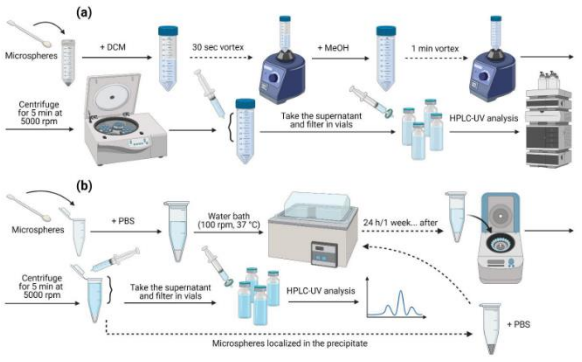

Fig 2. Characterization of DX/MEL co-loaded PLGA microspheres: encapsulation efficiency (a) and *in vitro* release (b) assays

Results and Discussion

F1 showed smooth and spherical shape microspheres, while the presence of pores was visible in F2 surfaces at SEM. This effect is due to the different rate of organic solvent diffusion from the internal to the external phase for the presence of the oily component (Vitamin E). Regarding particle size, both formulations exhibited a unimodal distribution which was included in the 38-20 µm range. DX encapsulation efficiencies were not influenced by the addition of Vitamin E. However, a decrease of the encapsulated MEL was observed for F2 (Table 1).

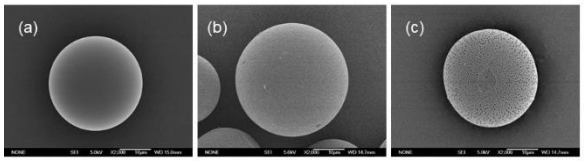

Fig 3. SEM images of unloaded (a), F1 (b) and F2 (c) PLGA-MSs

Table 1. Results of F1 and F2 *in vitro* characterization

PLGA MSs		Particle Size [µm]	Encapsulation Efficiency [µg/mg MSs]	Burst Release [µg/mg MSs]	Release after 90 days [µg/mg MSs]
Unloaded		29.40 ± 5.79	-	-	-
F1	DX	27.70 ± 4.48	89.03 ± 3.31	6.90 ± 0.46	44.36 ± 0.06
	MEL		61.76 ± 3.89	19.20 ± 2.59	43.65 ± 0.10
F2	DX	28.95 ± 3.75	97.51 ± 5.86	11.46 ± 1.70	61.67 ± 0.14
	MEL		46.45 ± 5.72	14.08 ± 0.80	32.00 ± 0.07

Both F1 and F2 released the drugs in a sustained manner after an initial burst (Figure 4). Vitamin E inclusion produced a faster release of DX at 7 days compared to F1. The release of MEL was not modified due to Vitamin E addition. Subsequently, active substances were released in a controlled fashion, being faster for F2 compared to F1. F1 released 0.32 ± 0.02 µg/day DX, while F2 liberated 0.44 ± 0.03 µg/day DX after three months. In the same 90-day interval, F1 released 0.07 ± 0.01 µg/day MEL following the initial 7 days of rapid release, similar to F2 with 0,09 ± 0.02 g/day MEL.

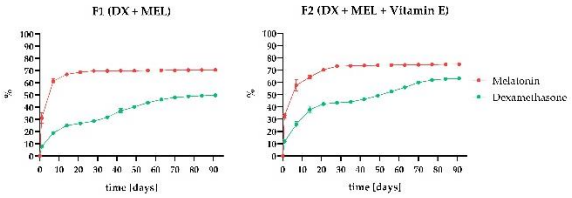

Fig 4. F1 and F2 *in vitro* release profiiles

Conclusions

According to results obtained, combination of DX, MEL and Vitamin E demonstrated being valid as possible long-term therapy due to their three-month *in vitro* co-delivery. Vitamin E presence proved accelerating drugs release from PLGA microspheres. Additional studies will be required for assessing *in vivo* usefulness of the two biodegradable drug delivery devices.

Acknowledgments

This work received funding from the European Union's Horizon 2020 Research and Innovation Programme under the Marie Sklodowska–Curie Actions (grant agreement number 813440; Ocular Research by Integrated Training and Learning (ORBITAL)).

References

[1] C. Guymer, J. Wood, G. Chidlow *et al.* Neuroprotection in glaucoma: recent advances and clinical translation, *Clin. Experiment. Ophthalmol.* 47 (2019) 88-105

[2] J. Tsai, Innovative IOP-Independent Neuroprotection and Neuroregeneration Strategies in the Pipeline for Glaucoma, *J. Ophthalmol.* (2020) 9329310

[3] A. Arranz-Romera, B. Davis, I. Bravo-Osuna *et al.* Simultaneous co-delivery of neuroprotective drugs from multi-loaded PLGA microspheres for the treatment of glaucoma, *J. Control Release* 297 (2019) 26-38

[4] C. García-Caballero, E. Prieto-Calvo, P. Checa-Casalengua *et al.* Six-month delivery of GDNF from PLGA/vitamin E biodegradable microspheres after intravitreal injection in rabbits *Eur. J. Pharm. Sci.* 103 (2017) 19-26

[5] I. Bravo-Osuna, V. Andrés-Guerrero, A. Arranz-Romera *et al.* Microspheres as intraocular therapeutic tools in chronic diseases of the optic nerve and retina, *Adv. Drug Deliv. Rev.* 126 (2018) 127–144

O1.3: Peptide nano-vaccine against SARS-CoV-2 infection

R.C. Acúrcio[1]*, R. Kleiner[2], B. Carreira[1], D. Vaskovich[2], Y. Liubomirski[2], E. Yeini[2], C. Araújo[1], C. Plama[1], A.S. Viana[3], J. Gonçalves[1], R. Satchi-Fainaro[2] and H.F. Florindo[1]

[1] *Research Institute for Medicines (iMed.ULisboa), Faculty of Pharmacy, Universidade de Lisboa, Lisbon, Portugal*
[2] Department of Physiology and Pharmacology, Sackler Faculty of Medicine, Tel Aviv University, Tel Aviv, Israel
[3] Center of Chemistry and Biochemistry, Faculty of Sciences, University of Lisbon, Lisbon, Portugal, Portugal

*e-mail: ritaacurcio@ff.ul.pt

Introducction

To control COVID-19 pandemic, huge efforts of academia, pharma companies, hospitals, and regulatory agencies accelerated the development and approval of safe and effective vaccines within record time. COVID-19 pandemic is still an unmet medical need, as novel variants have emerged in high prevalence regions, reinfecting individuals, and escaping vaccine-elicited immune responses. Studies have also reported that the immunity generated by COVID-19 vaccines approved so far might fade over time.
Nanotechnology-based platforms have shown a paramount role in the development of SARS-CoV-2 vaccines[1]. Here, we present a novel reproducible and safe biodegradable nano-vaccine rationally designed for the co-delivery of SARS-CoV-2 antigens and regulators of immune cell function to generate protective anti-SARS-CoV-2 host responses.

Materials and Methods

SARS-CoV-2 peptides were selected using bioinformatic and epitope mapping tools. Poly(lactic acid) (PLA) and Poly(lactic-co-glycol) (PLGA)-based nanoparticles (NP) incorporating SARS-Cov-2 antigens and immune potentiators were formulated by the double emulsion–solvent evaporation method, following methods already established. Particle size and morphology were determined by dynamic light scattering and Atomic Force Microscopy (AFM), respectively. Animals were immunized two times, 21 days apart with our nanoplatform incorporating the peptides and immune potentiators. Cellular-mediated response was assessed by flow cytometry and ELIspot. ELISA was performed for the detection of peptides or SARS-CoV-2 RBD-specific antibodies (IgM and IgG) in immunized mouse sera.

Results and Discussion

NP presented similar average hydrodynamic diameters, despite the entrapment of large or short peptides, with low polydispersity index. AFM showed spherical particles with a slight roughness surface. NP showed entrapment efficiency (EE) of 70-90%.

A strong cellular-mediated immune response was observed. A balanced T helper (Th) 1 and Th2 cytokine secretion was observed after vaccination, specifically high levels of IFNγ and TNFα (Th1-guided response). Long-lasting high levels of IgM and IgG against SARS-CoV-2 peptides and RBD were observed (Figure 1).

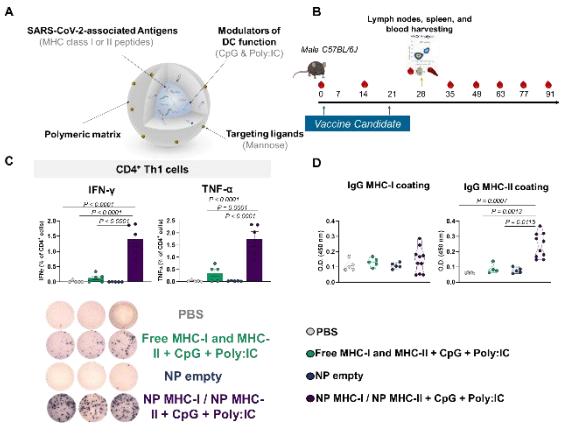

Fig 1. Nano-vaccine elicited a robust T- and B-cell responses.

Conclusions

The developed peptide nano-vaccine elicited robust cellular and humoral responses against SARS-CoV-2.

Acknowledgments

This work was supported by SFRH/BD/131969/2017, UIDB/04138/2020, UIDP/04138/2020 (FCT-MCTES), and LCF/PR/HR19/52160021 (La Caixa Foundation).

References

[1] Florindo, H. F. et al. Immune-mediated approaches against COVID-19. Nature 596, (2021) 630–645.

[2] Conniot, J. et al. Immunization with mannosylated nanovaccines and inhibition of the immune-suppressing microenvironment sensitizes melanoma to immune checkpoint modulators. Nat. Nanotechnol. 14, (2019) 891–901.

O1.4: Smart targeted nanohybrids as dual-approach drug delivery systems against colorectal cancer

J. Gonzalez-Valdivieso[1,2]*, R. Vallejo[2,3], A. Girotti[4], S. Rodriguez-Rojo[3], Mercedes Santos[4] and F.J. Arias[2]

[1]Molecular Imaging Innovations Institute (MI3), Weill Cornell Medicine, 10021 New York, USA
[2]Smart Biodevices for NanoMed Group, University of Valladolid, 47011 Valladolid, Spain
[3]High Pressure Process Group, University of Valladolid, 47011 Valladolid, Spain
[4]BIOFORGE Research Group, University of Valladolid, 47011 Valladolid, Spain
*e-mail: juan.gonzalez.valdivieso@uva.es

Introduction

Poor drug accumulation and adverse side effects are some of the most important problems of current cancer treatments [1]. To overcome this, novel biomaterials constitute a promising approach aiming to develop nanocarriers with improved therapeutic efficacy. Elastin-Like Recombinamers (ELRs) are smart biomaterials for multiple biomedical applications, due to their cell-friendly behavior, thermal sensitivity and lack of immunogenicity [2]. We report herein a novel drug delivery nanosystem comprising the encapsulation of the chemotherapeutic drug Docetaxel (DTX) and recombinant fusion of a small peptide inhibitor of Akt kinase within an ELR scaffold. A DNA aptamer selective for CD44 was chemically conjugated as targeting system against cancer cells.

Materials and Methods

By recombinant DNA technology, the nanohybrids were designed based on an amphiphilic backbone with certain bioactive sequences [3] and DTX was encapsulated by supercritical fluids. Nanohybrids were characterized by DLS, TEM and AFM. The specific inhibition of Akt phosphorylation was determined by western blot analysis, whereas the effectiveness of ELR nanohybrids, internalization pathway and intracellular activation were evaluated *in vitro*. Furthermore, the pharmacokinetic profile and therapeutic accuracy were determined *in vivo* in a colorectal cancer mouse model.

Results and Discussion

The 50 nm nanohybrids selectively affected cell viability and proliferation of colorectal cancer cells compared to endothelial cells, and triggered both apoptosis- and necrosis-mediated cell death. Nanohybrids also remained stable under physiologic conditions, triggered sustained drug release and possessed proper pharmacokinetic profile after systemic intravenous administration. When used in a murine colorectal cancer model, nanohybrids significantly reduced both the number and size of tumor polyps along the colorectal tract. Furthermore, systemic administration induced tissue recovery in terms of morphology of gastrointestinal crypts and tissue architecture.

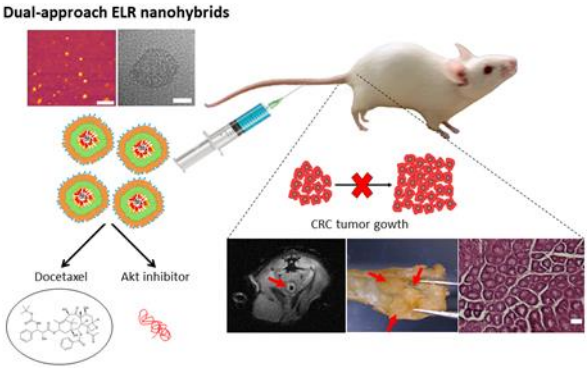

Fig 1. Design, physicochemical characterization and biological validation of dual-approach ELR nanohybrids

Conclusions

Together, these findings indicate that this advanced doubly-loaded nanosystem allows us to achieve successful controlled release of chemotherapeutics in colorectal cancer cells and has a promising potential for cancer treatment.

Acknowledgments

This work was supported by the European Social Fund, the European Regional Development Fund, the MICIUN and the University of Valladolid.

References

[1] J. Shi, P.W. Kantoff, R. Wooster, *et al*. Cancer nanomedicine: progress, challenges and opportunities., *Nat. Rev. Cancer* 17 (2017) 20-37

[2] J.C. Rodriguez-Cabello, F.J. Arias, M.A. Rodrigo, *et al*. Elastin-like polypeptides in drug delivery., *Adv. Drug Deliv. Rev*. 97 (2016) 85-100

[3] J. Gonzalez-Valdivieso, A. Girotti, R. Muñoz, *et al*. Self-assembling ELR-based nanoparticles as smart drug-delivery systems modulating cellular growth via Akt., *Biomacromolecules* 20 (2019) 1996-2007.

Abstracts for Oral Presentation

Session 2: Biomimetic Structures for Diagnosis and Therapy

O2.1: "***Functionalization of a meniscus prosthesis with polymeric coatings for the sustained release of anti-inflammatory drugs***". A. Fernandez Blanco, G. Lou, J. C. Campo, M. J. Alonso, Universidade de Santiago de Compostela. (p.41)

O2.2: "***Exosome-mediated MEK1 silencing is a promising approach against triple negative breast cancer regression***". D. Ferreira, C. Santos-Pereira, M. Costa, J. Afonso, A. Longatto-Filho, F. Baltazar, R. Kalluri, J. Moreira and L.R. Rodrigues, University of Minho. (p.43)

O2.3: "***Etoposide and edelfosine lipid nanomedicines as a synergistic combination therapy for neuroblastoma***". SH. El Moukhtari, G.M. Pelin, M.J. Blanco-Prieto, University of Navarra. (p.45)

O2.4: "***Pollen-based platforms for pulmonary delivery of nanoencapsulated rifabutin***". S. Robla, J.M. Ageitos, R. Ambrus, N. Csaba, Universidade de Santiago de Compostela. (p.47)

O2.1: Functionalization of a meniscus prosthesis with polymeric coatings for the sustained release of anti-inflammatory drugs

A. Fernández-Blanco[1,2,*], G. Lou [1,2], J. Crecente-Campo [1,2] , M.J. Alonso [1,2]

[1]Center for Research in Molecular Medicine and Chronic Diseases (CiMUS), IDIS Research Institute, Universidade de Santiago de Compostela, Santiago de Compostela, Spain

[2]Department of Pharmacology, Pharmacy and Pharmaceutical Technology, School of Pharmacy, Universidade de Santiago de Compostela, Santiago de Compostela, Spain

*e-mail: alfonso.fernandez.blanco@rai.usc.es

Introduction

Knee osteoarthritis (OA) is a joint disease caused by the progressive degeneration of cartilage and bone with a rising prevalence worldwide [1]. One of the causes of this disease is the deterioration of menisci which leads to meniscus removal. The substitution of the damaged meniscus with a non-degradable prosthesis is a recurrent solution for elder patients trying to avoid knee OA [2]. These patients take anti-inflammatory drugs orally to relieve pain for as long as it persists. However, the continued administration of anti-inflammatory drugs can result in off-target side effects, including renal, cardiovascular, and gastrointestinal complications. The intra-articular administration of these drugs is another extended procedure, and a solution for the previously mentioned side effects. Nevertheless, it leads to patient discomfort and discontent [3]. Taking this into account, the local and sustained administration of drugs can enhance the therapeutic effect while limiting side effects and patient uneasiness.

In this work, a functional coating for a meniscus prosthesis, based on biodegradable polymers, was designed to achieve a sustained release of two anti-inflammatory drugs (named as AID1 and AID2) with two different release kinetics that allows the modulation of the inflammatory environment in the joint cavity of the knee (1-4 weeks for AID1 and 3-9 months for AID2). More precisely, the effect of polymer type and molecular weight, and drug loading on the release kinetics were evaluated and optimized during a primary screening, and a functional double-layer polymer/drug prototype was designed afterwards.

Materials and Methods

Two anti-inflammatory drugs (AID1 and AID2), and a wide spectrum of polymers named as polymer A (P_A) characterized by two different monomer1 : monomer2 ratios in P_{A1} and P_{A2}, polymer B (P_B), polymer C (P_C), polymer E (P_E) of low (LMW-P_E) and high molecular weight (HMW-P_E), and polymer D (P_D) were used for the screening of the best combination for the polymer/drug coatings.

Different techniques were used to create these coatings, namely solvent casting to produce single-layer polymer/drug films, and dip-coating for the complete coating of the prosthesis. Drug release studies were performed in sink conditions at 37 °C in PBS containing Tween 80® 1% w/v. The amount of both drugs (AID1 and AID2) released at different time points was quantified by reverse phase ultra-performance liquid chromatography (UPLC). Further characterization of the polymer/drug coatings was carried out using powder X-ray diffraction (XRD), differential scanning calorimetry (DSC), and field-emission scanning electron microscopy (FESEM).

Results and Discussion

A preliminary screening using single-layer polymer/drug films was used to select the most promising polymer or combinations of polymers regarding drug release kinetics. From these studies, polymer P_D was selected for the release of AID1, and P_B and the blend of P_C/P_B for the release of AID2.

Table 1. Summary of the parameters that were taken into account for the drug release studies.

Parameters to be analyzed	
• Polymer type	• Polymer molecular weight
• Polymer concentration	• Polymer1 : Polymer2 ratio
• Drug loading	• Solvent evaporation times
• Polymer film formation techniques	• Dip-coating cycles
• Solvent effect	• Number of polymer/drug layers

Afterwards, the complete coating of the prosthesis with two separated polymer/drug layers was achieved through a two-step dip-coating approach. Considering the results of the initial screenings, the simultaneous release of AID2 from P_C/P_B (first layer) and AID1 from P_D (second layer) was evaluated.

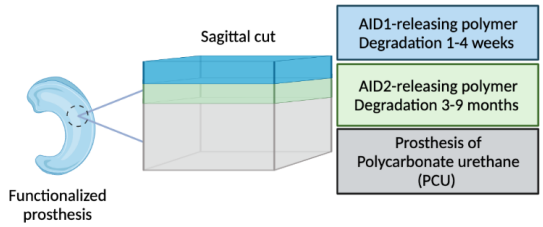

Fig 1. Schematic representation of the functionalized meniscus prosthesis.

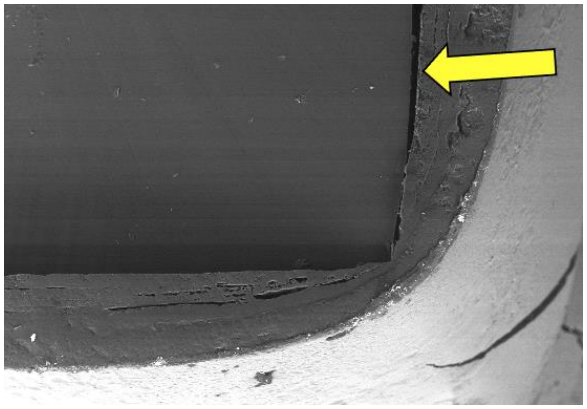

Fig 2. FESEM micrographs of the double-layer polymer/drug system coating the PCU prosthesis. The arrow signals the border of the PCU (towards the left), and the polymer/drug coating (towards the right).

This prototype has shown to fit adequately the desired release profile. The idea of using AID1 was to deal with post-surgical pain whereas the use of AID2 was thought for the control of long-term inflammation and pain relief. In this sense, the double-layer polymer/drug coating was able to keep a controlled release of AID1 from the P_D layer for 2-3 weeks, and a >5 months controlled release of AID2 from P_C/P_B. For this reason, this prototype was further characterized using DSC, FESEM, and XRD techniques.

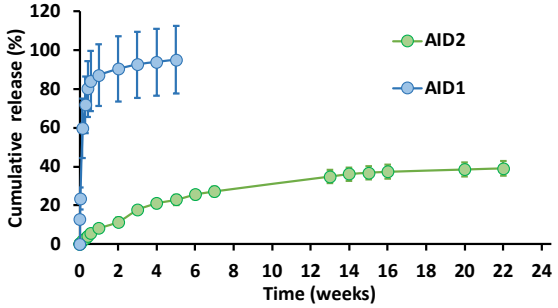

Fig 3. The sequential release of AID1 and AID2 in terms of amount of percentage (%) released from a double-layer polymer/drug coating composed of a first coating of P_C/ P_B with AID2 and the second polymer coating of P_D with AID1. Results are represented as mean ± SD of three polymer/drug coatings.

Conclusions

Using a completely novel double-layer polymer coating for a PCU prosthesis, we obtained a controlled release of both drugs, AID1 and AID2, simultaneously. Then, considering the adjustment of the release of AID1 and AID2 from this prototype to the desired release kinetics, we have decided to select this model for future *in vitro* and *in vivo* investigations.

Acknowledgments

This work was supported by funding from the European Union's Horizon 2020 research and innovation program under grant agreement No 814444 (MEFISTO).

References

[1] D.T. Felson, Epidemiology of hip and knee osteoartrritis, Epidemiol. Rev. 10 (1988) 1–28. https://doi.org/10.1093/oxfordjournals.epirev.a036019.

[2] A. Abbadessa, J. Crecente-Campo, M.J. Alonso, Engineering Anisotropic Meniscus: Zonal Functionality and Spatiotemporal Drug Delivery, Tissue Eng. - Part B Rev. 27 (2021) 133–154. https://doi.org/10.1089/ten.teb.2020.0096.

[3] J.C. Mora, R. Przkora, Y. Cruz-Almeida, Knee osteoarthritis: Pathophysiology and current treatment modalities, J. Pain Res. 11 (2018) 2189–2196. https://doi.org/10.2147/JPR.S154002.

O2.2: Exosome-mediated *MEK1* silencing is a promising approach against triple negative breast cancer regression

D. Ferreira[1]*, C. Santos-Pereira[1;2], M. Costa [3;4], J. Afonso[3;4], A. Longatto-Filho[3;4;5;6], F. Baltazar[3;4], R. Kalluri[7;8;9], J. N. Moreira[10;11] and L. R. Rodrigues[1]

[1]*CEB - Centre of Biological Engineering, University of Minho, Campus de Gualtar, 4710-057 Braga, Portugal*
[2]*Centre of Molecular and Environmental Biology (CBMA), Department of Biology, University of Minho, 4710-057 Braga, Portugal*
[3]*Life and Health Sciences Research Institute (ICVS), University of Minho, Campus of Gualtar, Braga, Portugal*
[4]*ICVS/3B's – PT Government Associate Laboratory, Braga/Guimarães, Portugal*
[5]*Molecular Oncology Research Center, Barretos Cancer Hospital, Barretos, São Paulo, Brazil*
[6]*Laboratory of Medical Investigation (LIM 14), Faculty of Medicine, São Paulo State University, S. Paulo, Brazil*
[7]*Department of Cancer Biology, Metastasis Research Center, University of Texas MD Anderson Cancer Center, Houston, Texas 77005, USA*
[8]*Department of Molecular and Cellular Biology, Baylor College of Medicine, Houston, TX, USA*
[9]*School of Bioengineering, Rice University, Houston, TX, USA.*
[10]*CNC – Center for Neurosciences and Cell Biology, Center for Innovative Biomedicine and Biotechnology (CIBB), University of Coimbra, Faculty of Medicine (Polo 1), Rua Larga, 3004-504 Coimbra, Portugal*
[11]*FFUC – Faculty of Pharmacy, CIBB, University of Coimbra, Pólo das Ciências da Saúde, Azinhaga de Santa Comba, 3000-548 Coimbra, Portugal*

*e-mail: deboraferreira@ceb.uminho.pt

Introduction

Breast cancer is a major public health problem worldwide being the most diagnosed cancer in women [1]. Triple negative breast cancer (TNBC) represents 10-20% of all breast cancers and is characterized by the absence of hormone receptors (progesterone and estrogen) and lack of expression of epidermal growth factor receptor-2. Furthermore, it is also described to have poor prognosis due to its propensity to metastasize to visceral organs early in the clinical course [2–4].
In accordance with the lack of recurrently altered targets at the genomic level, there is a shortage of approved targeted agents for TNBC, remaining cytotoxic chemotherapy the mainstay of treatment. Even though, various distinct molecular signaling pathways have been implicated in TNBC phenotypes. Of these, aberrant activity of the mitogen-activated protein kinase/ extracellular signal-regulated kinase (MAPK/ERK) signaling activity is revealed to be important in the initiation and progression of cancer [5,6]. Therefore, we sought to uncover the potential of MAPK/ERK cascade downregulation in TNBC through the use of an exosome-mediated system loaded with RNA interference (RNAi)-based therapeutics.

Materials and Methods

Exosomes derived from BJ cells were isolated by differential centrifugation and further characterized by nanoparticle tracking analysis, transmission electron microscopy, flow cytometry and western blot. Moreover, *in vitro* uptake experiments and biodistribuition experiments were accomplished to assess performance. These exosomes were further electroporated with MEK1-targeting siRNA (iexo^{MEK1}), being the impact of downregulation in the metastatic phenotype of highly invasive breast cancer cells evaluated by measuring migration, invasion and proliferation. Changes in the regulation of direct and indirect genes were also assessed. Moreover, implantation of TNBC cells treated with iexo^{MEK1} in chicken embryo chorioallantoic membrane (CAM) was also executed.

Results and Discussion

We showed that MEK1-targeting siRNA (siMEK1) led to an efficient downregulation of *MEK1* in different TNBC cell lines, but the effects on the downstream MAPK/ERK cascade are different. Moreover, we also demonstrated that the siMEK1-mediated silencing led to a cell proliferation impairment that can be supported by the induction of apoptosis for all TNBC cell lines under study, including MDA-MB-231, MDA-MB-157 and Hs 578T.
In our study, we also showed a clear decreased ability of all TNBC cells to migrate and invade upon *MEK1* downregulation. Such impairment in migration/invasion was in part explained by the reversion of the epithelial-mesenchymal transition (EMT) phenotype, characterized by the loss of the mesenchymal markers, including vimentin and n-cadherin and by the gain of epithelial markers, namely e-cadherin. Additionally, a clear decrease

of MMP-2 and MMP-9 expression levels was observed for all the cell lines under study.
Furthermore, we confirmed that engineered exosomes loaded with siMEK1 (iexo^{MEK1}) are not altered in their physical properties and overall integrity, being able to induce a powerful downregulation of *MEK1* expression. The *in vivo* experimental data demonstrated that iExo^{MEK1} induces a significant regression of the tumor size in relation to control conditions. Supported by the decrease of the number of recruited blood vessels, a reduction of metastasis and consequent inhibition of the formation of a second tumor was observed for iExo^{MEK1}-treated condition.

Conclusions

In summary, we have here clarified the role of MAPK/ERK suppression using a RNAi-based approach in different TNBC cell lines. Proliferation, migration and invasion impairments explained by the reversion of the EMT phenotype and the MMP-2/MMP-9 downregulation was verified upon *MEK1* downregulation. Additionally, a successful exosome-based platform was generated for the siRNA-targeting *MEK1* loading (iExo^{MEK1}), showing no changes in their physical properties and overall integrity in relation to unmodified exosomes. Ultimately, an *in vivo* tumor regression and angiogenesis decrease were observed after exosome-mediated *MEK1* downregulation, certifying this strategy as a novel promising approach towards TNBC.

Acknowledgments

This work was supported by by the Portuguese Foundation for Science and Technology (FCT) under the scope of the strategic funding of UID/BIO/04469/2020 unit. Débora Ferreira is recipient of a fellowship supported by a doctoral advanced training (call NORTE-69-2015-15) funded by the European Social Fund under the scope of Norte2020 - Programa Operacional Regional do Norte. Débora Ferreira also acknowledges “Liga Portuguesa contra o cancro - Núcleo Regional do Norte (LPCC-NRN) “for her current fellowship.

References

[1] H. Sung, J. Ferlay, R. L. Siegel, M. Laversanne, I. Soerjomataram, A. Jemal, F. Bray, *CA. Cancer J. Clin.* **2021**, *71*, 209.

[2] T. F. S. Mendes, L. D. Kluskens, L. R. Rodrigues, *Adv. Sci.* **2015**, *2*, 1500053.

[3] D. O’Reilly, M. Al Sendi, C. M. Kelly, *World J. Clin. Oncol.* **2021**, *12*, 164.

[4] M. N. Abad, S. Calabuig-Fariñas, M. L. de Mena, M. J. G. S. de Bremond, C. G. González, S. T. Martínez, J. Á. García-García, V. I. González-Cruz, C. C. Herrero, *https://doi.org/10.1177/1758835920986749* **2021**, *13*, DOI 10.1177/1758835920986749.

[5] Braicu, Buse, Busuioc, Drula, Gulei, Raduly, Rusu, Irimie, Atanasov, Slaby, et al., *Cancers (Basel).* **2019**, *11*, 1618.

[6] R. Yaeger, R. B. Corcoran, *Cancer Discov.* **2019**, *9*, 329.

O2.3: Etoposide and edelfosine lipid nanomedicines as a synergistic combination therapy for neuroblastoma

SH El Moukhtari*[1], GM Pelin[3], MJ Blanco-Prieto[1,2]

[1]Department of Pharmaceutical Technology and Chemistry, University of Navarra, 31008 Pamplona, Spain
[2] Instituto de Investigación Sanitaria de Navarra, IdiSNA, 31008 Pamplona, Spain.
[3] Università Degli Studi Di Trieste, 34123, Trieste, italy.
*e-mail: selmoukhtar@alumni.unav.es

Introduction

Neuroblastoma is the most frequent pediatric extracranial solid tumor, and its aggressiveness and heterogeneity are particularly visible for high risk and relapsed patients [1]. Multimodal chemotherapy is often employed to rescue these children but present many limitations such as elevated short- and long-term toxicities [2]. Lipid nanoparticles (LNPs) can solve these quandaries and present the ability to enhance oral bioavailability, among many other applications [3]. LNPs are colloidal nanosystems composed in most cases of biological and biocompatible lipids [4]. These systems can encapsulate a wide variety of chemicals and their composition is usually considered as safe by regulatory agencies. In this study, we encapsulated etoposide (ETP) [5], a conventionally used hydrophobic chemotherapeutic agent and a novel molecule named edelfosine (EDF) that has proven to be effective against other aggressive tumors such as pediatric osteosarcoma [6].

Materials and Methods

Nanoparticles (NP) were formulated by the hot homogenization and ultrasonication method [7] and freeze-dried for preservation. Particle size and homogeneity were measured by dynamic light scattering and nanoparticle tracking analysis while surface charge (ζ potential) was measured by doppler laser velocimetry. Drug content was studied by UPLC-MS/MS for both molecules. NPs' stability and drug release were also evaluated in PBS and simulated gastrointestinal fluids [8]. Finally, cell studies were performed regarding efficacy in 6 neuroblastoma cell lines. Finally, drug combination studies (Chou-Talalay Method [9]) were performed in two neuroblastoma cell lines: SH-SY5Y (MYCN non amplified) and SK-N-BE (2) (MYCN amplified). Combination index (CI) is defined as follows: CI < 1 indicate synergism, CI = 1 indicate additivity, CI > 1 indicate antagonism. Dose reduction index (DRI) was calculated and defined as the measure of the dose fold decrease for each drug when synergistically combined to achieve a given effect, compared with the dose of each drug alone required to engender the same inhibition.

Results and Discussion

ETP and EDF were efficiently loaded into LNPs obtaining a diameter after lyophilization of 170 ± 6.2 nm and 150 ± 17.6 nm for ETP-NP and EDF-NP respectively, presenting homogeneous size distribution *(Table 1)*. Elevated encapsulation efficiency of 81.8% ± 4 for ETP-NP and of 86.9 % ± 12 for EDF-NP was obtained, corresponding to a drug loading value of 13.2 ± 0.7 µg/mg and 35.1 ± 5.1µg/mg respectively. Finally, particles were negatively charged in both cases allowing a stable colloidal suspension, avoiding the coalescence and aggregation of NPs due to the electrostatic repulsion between them.

In vitro stability studies revealed that NPs were stable as particle diameter was maintained in the nanoscale range when added to different simulated fluids (PBS, simulated gastric fluids, and in simulated intestinal fluid in the fasted and fed states). Overall, drug release was sustained for both NPs in PBS. Moreover, although drug release was above 50% for some of the tested formulations in simulated gastrointestinal fluids, it was comparable to what has been observed in the literature so far [3]. We previously demonstrated in other *in vitro* studies that these types of NPs were able to cross the gastrointestinal barrier [10] suggesting that NPs are suitable for *in vivo* studies for *per os* administration.

Cytotoxicity assays revealed that the nanoencapsulation improved or maintained the antiproliferative effect of ETP in all cell lines, whereas for EDF it was maintained in most of them. The overall strong cytotoxicity of the nanosystems against these neuroblastoma cell lines (4/6) showed promising efficacy of the proposed treatments.

However, the nanoencapsulation of EDF restricts its activity in two cell lines that present very similar chromosomal aberrations and are almost morphologically identical [5]. Further studies are needed to elucidate why this lack of efficacy in these particular cell lines.

For combination studies, results indicated a synergistic response when combining LNPs at a ratio (ETP:EDF) of 1:2 for SH-SY5Y cells and 1:1.5 for SK-N-BE (2) cells *(Fig. 1 and 2*). For SH-

SY5Y, a 27.38-fold dose reduction was observed for EDF-NP when combined to ETP-NP. This dose reduction reached almost 50 for SK-N-BE(2). DRI was maintained between 1 and 2 for ETP-NPs in both cell lines, showing slight improvements in dose reduction. Although these results need to be confirmed *in vivo*, this synergism establishes EDF-NP and ETP-NP as a potential novel combination therapy for neuroblastoma treatment.

Table 1. Physicochemical characteristics of the nanomedicines

	Size(nm)	PDI	ζ potential (mV)
ETP-NP	170 ± 6.2	0.26 ± 0.1	21.9 ± 3.4
EDF-NP	150 ± 17	0.23 ± 0.02	-14.7 ± 1.5

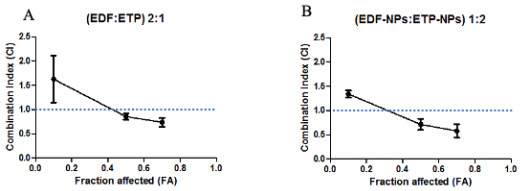

Fig 1. – CI at different cell viability (Fa) values for EDF and ETP, in both free(A) and nanoencapsulated (B) form in SH-SY5Y cells.

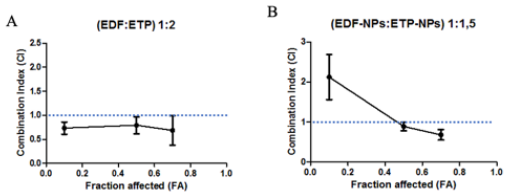

Fig 2 - CI at Fa values for EDF and ETP, in both free (A) and nanoencapsulated (B) form in SK-N-BE(2) cells.

Conclusions

In summary, both NPs were physicochemically adequate and presented strong efficacy in most neuroblastoma cell lines. Moreover, good stability was seen in simulated fluids suggesting their applicability in future *in vivo* studies in an oral treatment setting. Furthermore, the similar synergy observed for LNPs in the tested cell lines highlight a novel therapeutic opportunity for the treatment of neuroblastoma. At present, the pharmacokinetics and biodistribution of these nanoformulations are tested *in vivo* in animal models. In the future, the toxicity and efficacy of the combined nanosystems will be assessed in an animal model of neuroblastoma.

Acknowledgments

This work was supported by NEN Association [Nico contra el cancer infantil 2017 – PVR00157]

References

[1] K.K. Matthay, J.M. Maris, G. Schleiermacher, A. Nakagawara, C.L. Mackall, L. Diller, W.A. Weiss, Neuroblastoma, Nat. Rev. Dis. Prim. 2 (2016) 16078. https://doi.org/10.1038/nrdp.2016.78.

[2] S.E. Lipshultz, T.R. Cochran, V.I. Franco, T.L. Miller, Treatment-related cardiotoxicity in survivors of childhood cancer, Nat. Rev. Clin. Oncol. 10 (2013) 697–710. https://doi.org/10.1038/nrclinonc.2013.195.

[3] S.H. El Moukhtari, C. Rodríguez-Nogales, M.J. Blanco-Prieto, Oral lipid nanomedicines: current status and future perspectives in cancer treatment., Adv. Drug Deliv. Rev. (2021). https://doi.org/10.1016/j.addr.2021.03.004.

[4] B. Lasa-Saracibar, A. Estella-Hermoso de Mendoza, M. Guada, C. Dios-Vieitez, M.J. Blanco-Prieto, Lipid nanoparticles for cancer therapy: state of the art and future prospects, Expert Opin. Drug Deliv. 9 (2012) 1245–1261. https://doi.org/10.1517/17425247.2012.717928.

[5] R. Burgos-Panadero, S.H. El Moukhtari, I. Noguera, C. Rodríguez-Nogales, S. Martín-Vañó, P. Vicente-Munuera, A. Cañete, S. Navarro, M.J. Blanco-Prieto, R. Noguera, Unraveling the extracellular matrix-tumor cell interactions to aid better targeted therapies for neuroblastoma, Int. J. Pharm. 608 (2021) 121058. https://doi.org/https://doi.org/10.1016/j.ijpharm.2021.121058.

[6] Y. González-Fernández, H.K. Brown, A. Patiño-García, D. Heymann, M.J. Blanco-Prieto, Oral administration of edelfosine encapsulated lipid nanoparticles causes regression of lung metastases in pre-clinical models of osteosarcoma, Cancer Lett. (2018). https://doi.org/10.1016/j.canlet.2018.05.030.

[7] A. Estella-Hermoso de Mendoza, M. Rayo, F. Mollinedo, M.J. Blanco-Prieto, Lipid nanoparticles for alkyl lysophospholipid edelfosine encapsulation: Development and in vitro characterization, Eur. J. Pharm. Biopharm. 68 (2008) 207–213. https://doi.org/10.1016/j.ejpb.2007.06.015.

[8] S. Klein, The use of biorelevant dissolution media to forecast the in vivo performance of a drug, AAPS J. 12 (2010) 397–406. https://doi.org/10.1208/s12248-010-9203-3.

[9] T.C. Chou, Drug combination studies and their synergy quantification using the chou-talalay method, Cancer Res. 70 (2010) 440–446. https://doi.org/10.1158/0008-5472.CAN-09-1947.

[10] B. Lasa-Saracíbar, M. Guada, V. Sebastián, M. Blanco-Prieto, In Vitro Intestinal Co-Culture Cell Model to Evaluate Intestinal Absorption of Edelfosine Lipid Nanoparticles, Curr. Top. Med. Chem. 14 (2014) 1124–1132. https://doi.org/10.2174/1568026614660140329225340.

O2.4: Pollen-based platforms for pulmonary delivery of nanoencapsuled rifabutin

S. Robla[1]*, J.M. Ageitos[1], R. Ambrus[2] and N. Csaba[1]

1. *Center for Research in Molecular Medicine and Chronic Diseases (CiMUS) and Department of Pharmacology, Pharmacy and Pharmaceutical Technology, University of Santiago de Compostela, Spain*
2. *Faculty of Pharmacy, Institute of Pharmaceutical Technology and Regulatory Affairs, University of Szeged, Szeged, Hungary.*

*e-mail: sandra.robla.alvarez@usc.es

Introduction

Oral antibiotic therapy has been used for the treatment of respiratory diseases such as tuberculosis, resulting in the emergence of adverse effects and resistance to these therapies. Although the pulmonary route has substantial vascularization and a broad alveolar surface for absorption, lung defense systems and mucociliary clearance pose a challenge to successful pulmonary drug delivery. In order to overcome these barriers, our group has developed pollen-based platforms, taking advantage of their special 3D structure which confers a high resistance and improved bioadhesion to mucosal surfaces for drug delivery.

Materials and Methods

Chamomile (*Matricaria chamomilla*) pollen grains were treated by several methods for the obtention of hollow sporopollenin microcapsules with a nanoporous surface [1], and their *in vitro* distribution profile was evaluated using the Andersen cascade impactor. Blank and rifabutin (RFB)-loaded protamine nanocapsules were prepared following a treatment developed by our group [2] and their physicochemical characterizacion in terms of size, drug association efficiency, stability, as well as their permeability and dissolution in simulated lung media were evaluated. Finally, loading capacity and aerodynamic profile of RFB-loaded protamine NCs in chamomile sporopollenin microcapsules were also studied.

Results and Discussion

Chamomile (size ~20 µm) echinate pollen grains were treated in sequential washing steps with water, acetone, and phosphoric acid for the obtention of hollow sporopollenin microcapsules with a nanoporous surface (Figure 1). This hollow pollen prototype showed a mass aerodynamic diameter (MMAD) of 8 µm and a fine particle fraction (FPF, mass of drug particles <5 µm) of around 30%. They could be efficiently aerosolized and deposited in the lungs, with a high retention in the extra-thoracic as well as in the tracheo-bronchial region compared with untreated pollen.

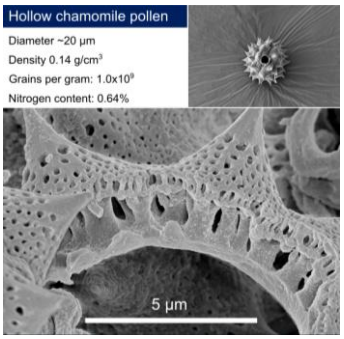

Fig 1. *Matricaria chamomilla* pollen grain (top) and a cross section of its nanoporous surface (below)

Protamine nanocapsules were prepared by solvent displacement technique, and different percentages of rifabutin (1, 2.5 and 5%) were incorporated. Nanocapsules presented a size of around 200 nm and positive charge, with a rifabutin association of 69, 56 and 51%, respectively (Table 1). Nanocapsules presented a spherical shape and they were stable in the freeze-dried form and in suspension under storage after one month. .

Table 1. Size, polydispersity index (PDI), association efficiency (AE) and Drug Loading (DL) of non-loaded and rifabutin (RFB) loaded protamine nanocapsules (prot NCs).

Formulation	Size (nm)	PDI	AE (%)	DL (%)
Blank prot NCs	204 ± 17	<0.1	-	-
1% RFB prot NCs	190 ± 13	<0.1	69 ± 16	0.65%
2.5% RFB prot NCs	199 ± 14	<0.1	56 ± 4	1.39%
5% RFB prot NCs	206 ± 27	<0.1	51 ± 4	2.55%

Diffusion in simulated lung media (Figure 2) of RFB-loaded nanocapsules was slower and more progressive with a linear trend, in a faster way in the case of 1% RFB-loaded nanocapsules. Nanocapsules also showed a linear drug-release pattern with sustained rifabutin release, which was faster in the case of 1% RFB protamine NCs (94% vs 25% for 2.5 and 5% RFB protamine NCs) for the same time frame.

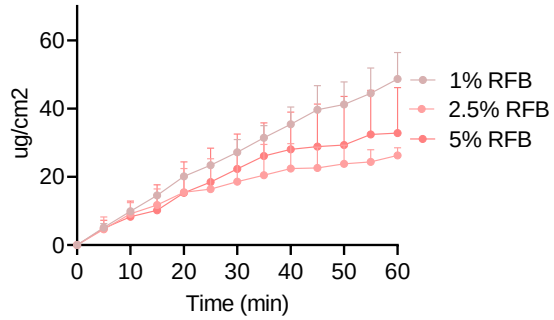

Fig 2. *In vitro* diffusion results of the API (RFB) permeability from the developed 1%, 2.5% and 5% RFB loaded protamine NCs

RFB-loaded protamine nanocapsules were microencapsulated into chamomile hollow sporopollenin platforms (ratio 1:1 w/w) by vacuum. Encapsulation efficiency was of 78%, 61 and 56% for 1, 2.5 and 5% RFB protamine NCs respectively, with a loading capacity of around 50% in all the cases. Aerodynamic distribution showed a MMAD between 10-14 µm and a FPF within 17-24%, being able to reach the respiratory zone, with a main deposition in the extrathoracic region.

Conclusions

Chamomile pollen microcapsules presented a natural microneedle-like design with a reasonable aerodynamic profile for its use in pulmonary drug delivery. Further, the developed protamine nanocapsules revealed considerable entrapment efficiencies of lipophilic rifabutin and satisfactory physical and biological stability.
The developed platform combined the benefits of nanotechnology and the capacity of pollen grains to be anchored to the mucosa for obtaining a multi-step delivery platform. Future studies will be carried out coating pollen grains with excipients in order to improve flow properties.

Acknowledgments

This work was supported by Ministerio de Ciencia e Innovacion RETOS - PID2019-107500RB-I00 and the Erasmus+ program of the European Union.

References

[1] J.M. Ageitos, S. Robla, L. Valverde-Fraga, M. Garcia-Fuentes, N. Csaba, Purification of Hollow Sporopollenin Microcapsules from Sunflower and Chamomile Pollen Grains, Polymers (Basel). 13 (2021) 2094. https://doi.org/10.3390/polym13132094.

[2] L.N. Thwala, A. Beloqui, N.S. Csaba, D. González-Touceda, S. Tovar, C. Dieguez, M.J. Alonso, V. Préat, The interaction of protamine nanocapsules with the intestinal epithelium: A mechanistic approach, J. Control. Release. 243 (2016) 109–120. https://doi.org/10.1016/j.jconrel.2016.10.002.

Abstracts for Oral Presentation

Session 3: Innovative Strategies for Drug Targeting

O3.1: "***Lipid-based non viral gene therapy for Fabry disease:Ex vivo and in vivo evaluation***". J. Rodríguez-Castejón, I. Gómez-Aguado, M. Beraza-Millor, M.A. Solinís, A. del Pozo-Rodríguez and A. Rodríguez-Gascón, University of the Basque Country. (p.51)

O3.2: " ***Treating Neurodegeneration with Synergistic Combinations of Polypeptide-Based Nanoconjugates Targeting Oxidative Stress and Inflammation***". I. Conejos-Sánchez, E. Masiá, M.J. Vicent, Centro de Investigación Príncipe Felipe. (p.53)

O3.3: "***Combining glucose-responsive nanoparticles and iPSCs differentiation: an innovative strategy to treat diabetes***". J.M. Marques, A.M. Carvalho, R. Nunes, J. das Neves, H. Florindo, D. Ferreira, B. Sarmento, University of Porto. (p.55)

O3.4: "***Multifunctional nanoparticles as an anticancer approach for the intracellular delivery of monoclonal antibodies***". A.M. López-Estévez, L. Sanjurjo, J. Pellico, R.T.M. de Rosales, D. Torres, and M.J. Alonso, Universidade de Santiago de Compostela. (p57)

O3.5: "***Non-viral delivery of CRISPR/Cas9 DNA for gene editing via multivalent cationic liposome system***". D.A. Sousa, R. Gaspar, J. O. Ferreira, F.Baltazar, B. Silva 2 and L.R. Rodrigues. University of Minho. (p.59)

O3.1: Lipid-based non-viral gene therapy for Fabry disease: *Ex vivo* and *in vivo* evaluation

J. Rodríguez-Castejón[1;2]*, I. Gómez-Aguado[1;2], M. Beraza-Millor[1;2], M.A. Solinís[1;2], A. del Pozo-Rodríguez[1;2] and A. Rodríguez-Gascón[1;2]

[1]*Pharmacokinetic, Nanotechnology and Gene Therapy Group (PharmaNanoGene), Faculty of Pharmacy, Centro de Investigación Lascaray Ikergunea, University of the Basque Country UPV/EHU, Vitoria-Gasteiz, Spain*
[2]*Bioaraba, Microbiology, Infectious Disease, Antimicrobial Agents, and Gene Therapy, Vitoria-Gasteiz, Spain*

*e-mail: julen.rodriguez@ehu.eus

Introduction

The recent approval of SARS_CoV_2 vaccines has boosted the potential of lipid nanoparticles as nucleic acid vehicles for diseases that lack an effective treatment. Rare monogenic diseases, such as Fabry disease (FD), are a perfect target for gene therapy, where the supplementation of a copy of the defective or missing gene can notably slow down the results of disease progression. In this regard, transduction of hepatocytes for the production of the functional protein is gaining special attention [1]. However, the size of the delivery platform and ligand-functionalization are crutial factors to achive a successful transfection of hepatocytes *in vivo* [2].

In the present work we have developed a solid lipid nanoparticles (SLNs)-based nanovector bearing a pDNA encoding the enzyme α-Galactosidase A (α-Gal A), deficient in FD. We have optimized the size of the nanovector to be around 100 nm, and we have functionalized it with a polysaccharide, galactomannan (GM), to target hepatocytes. In addition, we have evaluated the capacity of the nanovector to increase α-Gal A activity *ex vivo* in primary hepatocytes from Fabry mice, and *in vivo* in a mouse model of FD.

Materials and Methods

SLNs were synthesized with DOTAP, Tween 80 and Precirol® ATO5 by a hot-melt emulsification technique, as previously described [3]. To form the GM nanovector, a pDNA encoding α-Gal A was mixed with protamine, GM and SLNs. The GM nanovector was characterized in terms of size, polydispersity index and zeta potential.

Primary hepatocytes were isolated from 8-week-old Fabry male mice by two-step collagenase perfusion and plated in collagen-coated 6-well culture plates 24 h prior to use. Primary hepatocytes from Fabry mice were treated with the GM nanovector (10 µg of pDNA) and intracellular α-Gal A activity was quantified 72 h post-transfection.

For *in vivo* experiments, the GM nanovector was concentrated to 0.4 µg/µL of pDNA by vacuum centrifugation. Three 8-week-old Fabry male mice were treated with 150 µL of the nanovector (60 µg of pDNA), administered through the lateral tail vein, and were sacrificed 5 days later. Plasma, liver, spleen, heart and kidney were harvested from each mouse to assess α-Gal A activity.

Results and Discussion

The GM nanovector presented suitable characteristics for intravenous administration: hydrodynamic diameter in the nanometre range (103 ± 0.5 nm), cationic zeta potential (+32 ± 1.1 mV) and low polydispersity index (0.1 ± 0.01).

As shown in *Fig 1*, treatment of primary hepatocytes with the GM nanovector resulted in a 1.5-fold increase in intracellular α-Gal A activity with respect to untreated cells.

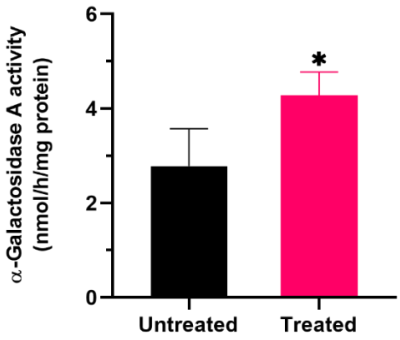

Fig 1. Intracellular α-Galactosidase A activity in primary hepatocytes isolated from Fabry mice 72 h post-transfection with the galactomannan nanovector. Data represent mean ± standard deviation of three biological replicates. * $p < 0.05$ with respect to untreated.

Once we demonstrated the capacity of the GM nanovector to transfect primary hepatocytes, we administered it to Fabry mice by intravenous injection. *Fig 2* features α-Gal A activity in plasma, liver, spleen, heart and kidney of Fabry mice treated with a single dose of the GM nanovector containing 60 µg of pDNA that encodes the enzyme.

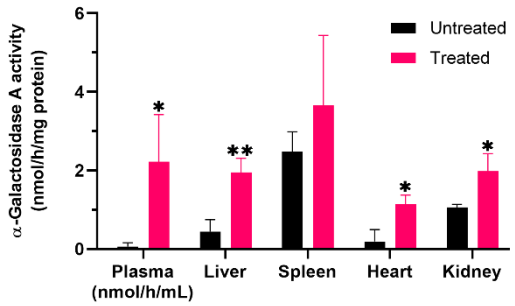

Fig 2. α-Galactosidase A activity in plasma and tissues of Fabry mice 5 days after the administration of the galactomannan nanovector. Data represent mean ± standard deviation of three biological replicates. * $p < 0.05$, ** $p < 0.01$ with respect to untreated.

Five days after the treatment, enzyme activity increased significantly in plasma and all tissues analysed, except in the spleen. It is known that accumulation of nanoparticles in the spleen is size-dependent, with larger nanoparticles accumulating more rapidly; especially nanoparticles greater than 200 nm [4]. Interestingly, the lack of effect in the spleen is most likely due to the reduced size of the GM nanovector (≈ 100 nm) and its capacity to bypass the reticuloendothelial system.

The greatest difference between treated and untreated animals was detected in plasma, where enzyme activity reached levels 35-fold higher than in untreated mice. α-Gal A activity in the liver increased 4-fold compared to untreated mice. The effect in the liver demonstrates the ability of the GM nanovector to access and transfect liver cells, probably related to the particle size smaller than the liver sinusoidal fenestrate (110-140 nm) and the functionalised surface with galactose and mannose groups of the GM that facilitate reaching the hepatocytes [2]. Moreover, enzyme activity significantly increased in heart and kidney of treated mice (6- and 2-fold higher, respectively). These results are of particular relevance as the heart and kidneys are the most affected organs in Fabry patients.

In a previous work [5], we prepared another non-viral vector based on SLNs prepared by a solvent emulsification-evaporation technique, and decorated with dextran (DX) instead of GM. The DX vector was significantly bigger (233 ± 10.5 nm). After the intravenous administration (a single dose of 60 µg of pDNA encoding α-Gal A) to the same animal model of FD, the enzyme activity in the liver did not increase. Therefore, particle size reduction and substitution of DX by GM has a major impact on the transfection of the liver. In fact, the elevation of α-Gal A activity in plasma may reflect hepatocyte transduction and resultant secretion to the bloodstream of the produced enzyme. Importantly, GM nanovector increased enzyme activity in the heart, one of the major target organs in therapies for FD, while DX vector did not. In contrast, unlike the GM nanovector, the DX vector increased enzyme activity significantly in the spleen, most likely due to the size of the vector. The results suggest that the GM nanovector is taken up to a lesser extent by the spleen, avoiding uptake by immune cells that could lead to therapeutic failure.

Conclusions

We have developed a nanosized non-viral vector based on SLNs functionalised with GM to target hepatocytes, although further studies are needed to confirm the type of liver cells transfected. We have shown that formulation-dependent parameters, such as the size of the delivery system and the incorporation of specific ligands, condition the interaction of the vector in the biological milieu and, therefore, its efficacy and safety. These preliminary results point out the importance of performing an *in vivo* optimization of formulation factors in the early steps of the development of non-viral vectors.

Acknowledgments

J. Rodríguez-Castejón thanks the Basque Government (PRE_2020_2_0120) and I. Gómez-Aguado and M. Beraza-Millor thank the University of the Basque Country UPV/EHU (PIF17/067 and PIFG19/36, respectively) for their research grants. This research has been funded by MCIU/AEI/FEDER, UE (RTI2018-098672-B-I00) and by the University of the Basque Country UPV/EHU (GIU20/048).

References

[1] D.P.W. Rastall, A. Amalfitano, Recent advances in gene therapy for lysosomal storage disorders, *Appl. Clin. Genet.* 8 (2015) 157-169

[2] F. Jacobs, S.C. Gordts, I. Muthuramu, *et al*. The liver as a target organ for gene therapy: state of the art, challenges, and future perspectives, *Pharmaceuticals,* 5 (2012) 1372-1392

[3] I. Gómez-Aguado, J. Rodríguez-Castejón, M. Beraza-Millor, *et al*. mRNA-based nanomedicinal products to address corneal inflammation by interleukin-10 supplementation, *Pharmaceutics,* 13 (2021) 1472

[4] N. Hoshyar, S. Gray, H. Han, *et al.* The effect of nanoparticle size on in vivo pharmacokinetics and cellular interaction, *Nanomedicine,* 11 (2016) 673-692

[5] J. Rodríguez-Castejón, A. Alarcia-Lacalle, I. Gómez-Aguado, *et al*. α-Galactosidase A augmentation by non-viral gene therapy: Evaluation in Fabry disease mice, *Pharmaceutics,* 13 (2021) 771

O3.2: Treating Neurodegeneration with Synergistic Combinations of Polypeptide-Based Nanoconjugates Targeting Oxidative Stress and Inflammation

I. Conejos-Sánchez[*,1], E. Masiá[1], and M.J. Vicent*[,1]

[1]*Centro de Investigación Príncipe Felipe, C/ Eduardo Primo Yúfera,3, 46012 Valencia, Spain*
*e-mail: iconejos@cipf.es

Introduction

The lack of effective treatments for neurodegenerative disorders in an aging population combined with growing incidence and increasing societal costs has underscored the need to develop novel therapeutic approaches. An estimated 35% of the disease burden is attributed to brain-related disorders in Europe alone[1].

Alzheimer's Disease (AD) represents one of the most significant global public health challenges; however, the presence of the blood-brain barrier represents a significant obstacle to the delivery of central nervous system-targeted therapeutics[2]. Overall, only 2% of small-molecule drugs and almost 0% of biologic drugs can breach the blood-brain barrier and reach target cell types in the brain[3]. Additionally, the pathology of neurodegenerative diseases such as AD includes alterations in multiple pathways, such as elevated oxidative stress and chronic neuroinflammation. Therefore, combination therapies blocking both these pathways may represent a more efficient treatment strategy.

Due to their intrinsic characteristics, polymer therapeutics and polypeptide-based combination conjugates in particular[4] represent ideal delivery systems for combination-based therapies required to treat AD patients. Preliminary data from our lab demonstrated that the intravenous administration of an Angiopep2-targeted polypeptide-based combination nanoconjugate allowed 1.5% of the given dose to reach the brain. The delivery of a synergistic combination of curcumin and a monoamine oxidase-B inhibitor in this manner improved olfactory memory and spatial learning in models of AD[5] and alcohol-induced neuroinflammation[6]. Biodistribution studies demonstrated the presence of the combination nanoconjugate in blood vessels, where it may act as a drug "depot," and different cell types throughout the brain.

Materials and Methods

Five antioxidant and five anti-inflammatory drugs were screened to identify synergistic combinations in immortalized microglia (BV2) and primary microglia extracted from neonatal P2-P5 mice upon LPS stimulation. Total antioxidant capacity was measured by flow cytometry and DCFH assay. Pro-inflammatory cytokine content was determined by ELISA. Selected drugs were conjugated to poly-L-glutamic acid (PGA)-derivatives of different architecture through bioresponsive linkers. Conjugates were characterized by NMR, CD, and DLS. Cell viability and antioxidant and anti-inflammatory capacities were evaluated in BV2 and mouse primary microglia. Western blotting evaluated a panel of proteins involved in antioxidant and anti-inflammatory responses.

Results and Discussion

After screening in microglia, we identified a synergistic combination of anti-inflammatory and antioxidant drugs. We synthesized a family of single-drug conjugates using pH-responsive linkers. For each approach, we employed differing PGA architectures (linear and star-shaped) and varied drug loadings. After evaluating drug release profiles, we evaluated our nanoconjugate family's anti-inflammation and antioxidant capabilities, which provided evidence for the maintenance of synergism following the creation of polymer-drug conjugates.

Conclusions

We rationally designed a successful combination therapy for AD treatment based on single polymer-drug conjugates targeting oxidative stress and inflammation. We are currently evaluating our combination therapy *in vivo*. We anticipate this our combination-based approach will also be of interest to neurodegenerative diseases other than AD.

Acknowledgments

This work was supported by the Spanish Ministry of Science, Innovation, and Universities (PID2019-108806RB-I00). ICS is funded by AEEC Junior Grant Ref INVES211323CONE. Part of the equipment employed was funded by the Generalitat Valenciana and co-financed with FEDER funds (PO FEDER of Comunitat Valenciana 2014–2020).

References

[1] J. Olesen, *Eur J Neurology*, 10 (5), (2003) 471
[2] B. Obermeier, *Nat med* 19 (12), (2013) 1584
[3] J. Leszek, et al., *CNS Neurol Disord Drug Targets* 2016, 15, 329
[4] T. Melnyk, S. Đorđević, I. Conejos-Sánchez, MJ. Vicent. *Adv Drug Deliv Rev*, 160 (2020) 136–169
[5] A. Duro-Castano et al*, Sci Adv,* 7 (13) (2021)
[6] CM. Cuesta et al, *Nanomedicine*, 34 (2021)

O3.3: Combining glucose-responsive nanoparticles and iPSCs differentiation: an innovative strategy to treat diabetes

Joana Moreira Marques[1;2*], Ana Margarida Carvalho[1], Rute Nunes[1;4], José das Neves[1;4], Helena Florindo[3], Domingos Ferreira[2], Bruno Sarmento[1;4]

[1]*i3S - Instituto de Investigação e Inovação em Saúde, Universidade do Porto, Portugal*
[2]*Faculdade de Farmácia, Universidade do Porto*
[3]*Faculdade de Farmácia, Universidade de Lisboa*
[4]*CESPU – Instituto de Investigação e Formação Avançada em Ciências e Tecnologias da Saúde, Instituto Universitário de Ciências da Saúde*

*e-mail: jcmarques@i3s.up.pt

Introduction

Diabetes mellitus (DM) is one of the biggest health problems nowadays. An estimated 463 million individuals suffer from DM worldwide and this number is expected to rise [1]. Type 1 DM (T1DM) is a chronic auto-immune disease characterized by insulin insufficient secretion due to beta cells destruction [1]. Since T1DM is not preventable and most of the cases are diagnosed after extensive beta cells destruction [2], definitive cure consists in replacing the destroyed pancreas [3]. However, the number of available pancreas or islets is limited, in addition to the need of a lifelong immunosuppressive therapy. In this work, we propose the development of an innovative biomimetic pancreas, comprising beta and alpha cells differentiated from induced pluripotent stem cells (iPSCs) and immobilized in a biofunctional matrix, embedding glucose-responsive nanoparticles (NPs) encapsulating a GLP-1 analogue (*Fig*. 1). The sensitiveness to glucose will be accomplished by the incorporation of the enzyme glucose oxidase (GOx) in the system. In the presence of high levels of glucose, GOx degrades this monoshacaride into gluconic acid, thus decreasing the surrounding pH (-5). Engineered pH-sensitive NPs will respond to the decrease of the environmental pH by releasing their payload.

Materials and Methods

pH-sensitive NPs based on hybrid PLGA/polymethacrylates matrices were produced by a modified solvent emulsification-evaporation method based on the double emulsion technique [4] to encapsulate GLP-1 analogue exenatide or semaglutide. NPs were characterized regarding average size and size distribution by dynamic light scattering, and zeta potential by laser Doppler electrophoresis. Association efficiency (AE) and drug loading (DL) were determined by HPLC. Exenatide and semaglutide *in vitro* release profiles were assessed at different pH (5.0 and 7.4), while secondary structure stability after release was confirmed by circular dichroism. Human WLS-4D1 iPSCs (hiPSCs) were differentiated into beta [5] and pre-alpha cells [6]. The differentiation of hiPSCs was assessed at different stages by flow cytometry through the expression of relevant cell markers. The capacity of differentiated beta cells to secrete insulin was assessed by glucose-stimulated insulin secretion (GSIS) assay [7]. Undifferentiated hiPSCs were immobilized in an alginate hydrogel [8] and cell viablity was evaluated by the resazurin reduction assay [9].

Results and Discussion

Different NPs formulations showed a monodisperse population (PdI <0.170) with an average size ranging from 130 to 155 nm and zeta potential (ZP) around +25-40 mV for higher polymethacrylates ratios, decreasing up to -7 mV for higher PLGA proportions. Two GLP-1 analogues were encapsulated (exenatide and semaglutide) using different DL (between 5% and 15%). For exenatide-loaded NPs, AE values ranged from 34% to 49%, while for semaglutide-loaded NPs, AE ranged from 50% to 65%, depending on PLGA/polymethacrylates ratios. NPs showed a pH-dependent *in vitro* release profile, despite showing a burst release of around 40% at pH 7.4 and 60-70% at pH 5 after five minutes, depending on the peptide. Moreover, both exenatide and semaglutide maintained their secondary structure after 48h of *in vitro* release. hiPSCs were differentiated into insulin-producing cells, however, in the GSIS assay, cells did not show a glucose-responsive behaviour, highlighting the likely need for further improvements regarding beta cells differentiation protocol. Differentiated pre-alpha cells produced both glucagon and insulin, as expected at this stage. The maturation stage will decrease insulin expression, leading to monohormonal, glucagon-producing alpha cells. Undifferentiated iPSCs

remained viable three days after immobilization in alginate, thus supporting the suitability of the protocol developed for cell immobilization.

Conclusions

GLP-1 analog-loaded glucose-responsive NPs were successfully produced. Glucagon- and insulin-producing cells differentiated from hiPSCs were also obtained, even though the last were not responsive to changes in glucose levels. Finally, the protocol developed for iPSCs immobilization in alginate can be easily applied to the immobilization of differentiated cells. Once differentiation protocols are improved, differentiated functional cells can be immobilized in an alginate matrix, thus moving closer to a bioartificial pancreas that could be useful for diabetes therapy.

Ongoing work is focused on the encapsulation of NPs into alginate microparticles and co-encapsulation of this nano-in-micro system with differentiated pancreatic cells in an alginate-based 3D scaffold.

Acknowledgments

The work was funded by the Portuguese Science and Technology Foundation (FCT) (Project PTDC/MED-OUT/30466/2017, POCI-01-0145-FEDER-030466). Joana Marques also acknowledges FCT for financial support through grant PD/BD/145149/2019 (through the PhD Programme in Medicines and Pharmaceutical Innovation, i3DU).

References

[1] International Diabetes Federation, IDF Diabetes Atlas, 9th ed Brussels, Belgium 2019 [https://www.diabetesatlas.org] (last accessed on: May 14th, 2021)

[2] E. Mannucci, M. Monami, I. Dicembrini *et al*. Achieving bA1c targets in clinical trials and in the real world: a systematic review and meta-analysis, *J. Endocrinol. Invest*. 37 (2014) 477-495

[3] S. Pellegrini, E. Cantarelli, V. Sordi *et al.* The state of the art of islet transplantation and cell therapy in type 1 diabetes, *Acta Diabetol*. 53 (2016) 683-691

[4] F. Sousa, A. Cruz, P. Fonte, *et al.* A new paradigm for antiangioenic therapy through controlled release of bevacizumab from PLGA nanoparticles, *Sci. Rep*. 7 (2017) 3736

[5] A. Rezania, J. Bruin, P. Arora, *et al.* Reversal of diabetes wit insulin-producing cells derived in vitro from human pluripotent stem cells, *Nat. Biotechnol*. 32 (2014) 1121-1133

[6] Q.P. Peterson, *et al.* A method for the generation of human stem cell-derived alpha cells. *Nat. Commun.* 11 (2020) 2241-2241

[7] N.J. Hogrebe, *et al*. Generation of insulin-producing pancreatic β cells from multiple human stem cell lines. *Nat. Protoc.* 16 (2021) 4109-4143

[8] L. Ghila, T. A. Legøy, S. Chera. A Method for Encapsulation and Transplantation into Diabetic Mice of Human Induced Pluripotent Stem Cells (hiPSC)-Derived Pancreatic Progenitors, *Methods Mol. Biol.* (2021) 1-23

[9] S.J. Bidarra, C.C. Barrias. 3D Culture of Mesenchymal Stem Cells in Alginate Hydrogels. *Methods Mol. Biol.* 2002 (2019) 165-180

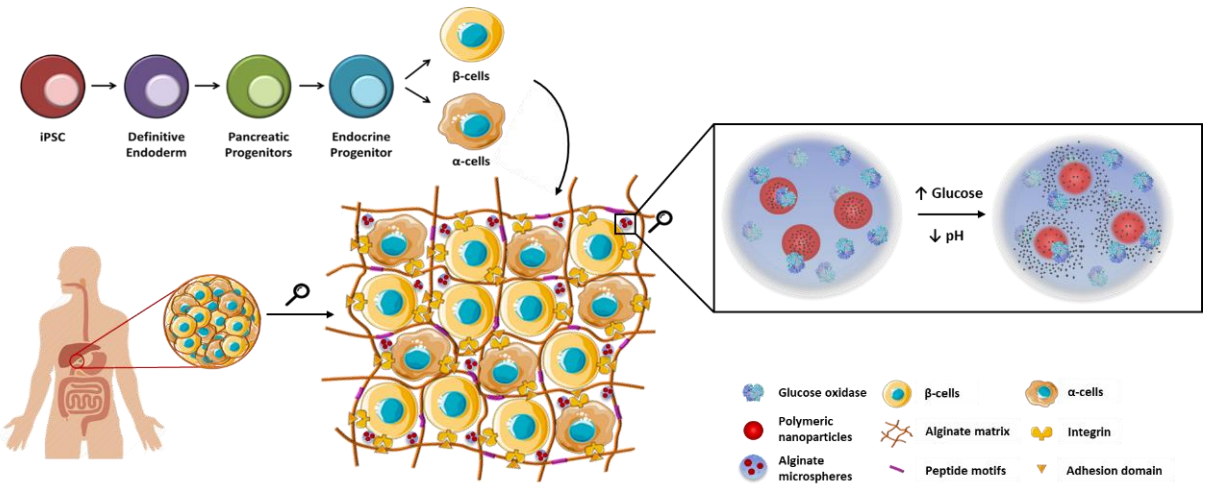

Fig 1. Schematic representation of the overall strategy used in this work.

O3.4: Multifunctional nanoparticles as an anticancer approach for the intracellular delivery of monoclonal antibodies

A.M. López-Estévez[1,2]*, L. Sanjurjo[1], J. Pellico[3], R.T.M. de Rosales[3], D. Torres[2], and M.J. Alonso[1,2]

[1]*Center for Research in Molecular Medicine and Chronic Diseases, IDIS Research Institute, University of Santiago de Compostela, Santiago de Compostela, Spain*
[2]*Department of Pharmacology, Pharmaceutics and Pharmaceutical Technology, School of Pharmacy, University of Santiago de Compostela, Santiago de Compostela 15782, Spain*
[3]*School of Biomedical Engineering & Imaging Sciences, King's College London, St. Thomas' Hospital, London SE1 7EH, UK*

*e-mail: anamarialopez.estevez@usc.es

Introduction

During the last years, cancer research has been focused on the new diagnosis and treatment strategies to reduce cancer mortality. Thus, the necessity to develop cancer therapies with improved specificity and affinity has tipped the balance towars monoclonal antibodies (mAbs). Evidence of this is the number of Abs marketed for the indication of cancer, mainly directed to extracellular membrane-bound receptors and soluble antigens[1]. Despite the remarkable success of mAbs in the clinic, these new treatmens have not overcome their major limitation, their inability to reach intracellular targets. This has become the main constraint to fully exploit their potential due to the intracellular localization of many oncogenes. Therefore, the necessity to reach and interfere with intracellular epitopes[2] while reducing the off-target toxicity and modifying their biodistribution, requires the development of new therapeutic strategies. Thus, nanotechnology offers the opportunity overcome the above limitations through the mAbs association[3].

Therefore, the present work aims to conveniently design hyaluronic acid-based nanoparticles (HA-NPs) containing the model mAb, bevacizumab (BVZ), and the clinically relevant anti-KRAS mAb. Thereafter, NPs were functionalized with the truncated peptide LyP-1 (tLyP-1), which was chosen due to its function as a tumor-penetrating peptide[4]. Cell viability and uptake of NPs studies were performed using different 2D cells lines models. Finally, biodistribution studies were carried out in healthy mice to demonstrate whether the distribution profile of the mAb was modified by the HA-NPs.

Materials and Methods

HA and PEG-lipid were functionalized with the tLyP-1 peptide. The covalent conjugation was confirmed by Proton Nuclear Magnetic Resonance (^{1}H-NMR).

BVZ and anti-KRAS mAbs were loaded to targeted HA-NPs through an assembling technique. Dynamic light scattering (DLS), NPs tracking analysis (NTA), asymmetrical flow field-flow fractionation (AF4), and transmission electron microscopy (TEM) were carried out to a full structural analysis. The colloidal stability was studied at 37ºC in PBS supplemented with 10% of fetal bovine serum (FBS) and in storage conditions at 4ºC. Moreover, freeze-drying studies were performed in the presence of trehalose as cryoprotectant. Furthermore, the association efficiency and release profile of the mAbs were evaluated by an Enzyme-Linked ImmunoSorbent Assay (ELISA).

Cytotoxicity and uptake studies were performed in the murine cell lines CMT167 (lung cancer) and RAW264.7 (macrophages). Cell viability studies were conducted using the Resazurin assay whereas DiD-labeled NPs uptake was evaluated by flow cytometry and confirmed by confocal microscopy. *In vivo* distribution by single-photon emission computed tomography (SPECT) imaging was evaluated in healthy mice after the intravenous administration of radiolabeled BVZ-loaded HA-NPs with ^{89}Zr. As controls, $^{89}ZrCl_4$ and ^{89}Zr-BVZ were used.

Results and Discussion

Herein, HA-tLyP-1 and PEG-lipid-tLyP-1 conjugates were incorporated to BVZ and anti-KRAS-loaded HA-NPs and will be referred to as NP 1 (absence of PEG) and 2 (presence of PEG). Ligand conjugation led to particles with a particle size ranging from 110 to 190nm, PDI<0.3 (DLS, NTA, and AF4 analysis), and negative surface charge. A deeper NPs characterization by TEM indicated a spherical shape. Whereas the colloidal stability studies in relevant biological media led to particles stable up to 8 hours, studies

under storage conditions resulted in stable particles for at least 1 month. Besides, NPs could be freeze-dried and reconstituted preserving their original physicochemical properties. In addition, the capacity of these prototypes to associate both mAbs, led to values from 10 to 80%. As shown in Table 1, significant differences were observed among Abs.

Table 1. Physicochemical characterization of tLyP-1 targeted HA-NPs as a function of the loaded mAb. AE: association efficiency; LC: loading capacity.

tLyP-1 prototype (loaded-mAb)	Particle size (nm) ± SD	AE (%) ± SD	LC (%)
tLyP-1 NP 1 (BVZ)	157 ± 11	38.1 ± 6	15.3
tLyP-1 NP 1 (anti-KRAS)	184 ± 23	11.4 ± 1	6.0
tLyP-1 NP 2 (BVZ)	118 ± 13	80.8 ± 8	32.1
tLyP-1 NP 2 (anti-KRAS)	134 ± 14	27.9 ± 8	11.1

The release pattern at physiological pH indicated that while NP 1 released 100% of the encapsulated BVZ, NP 2 only released 40% after 24 hours of incubation.

As preliminary results, *in vitro* and *in vivo* studies were performed with non-targeted NPs. Viability studies with blank NPs demonstrated a low toxicity profile up to 3 mg/mL. Furthermore, NPs incubation for 4 hours evidenced high uptake in both cell lines. Uptake results were confirmed by confocal microscopy (Figure 1).

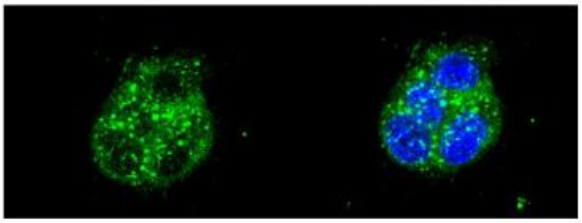

Fig 2. Representative fluorescence confocal microscopy images of the CMT167 uptake of blank NPs 2 after 24 hours of exposure.

The biodistribution profile of the BVZ-loaded NPs 1 was assessed in healthy mice. As expected, while the free antibody remains in blood circulation for long periods (Fig. 2A), in accordance with the half-life of BVZ, prototype 1 is taken up by the mononuclear phagocyte system (Fig. 2B),. These results indicate the capacity of the NPs to modify the distribution profile of the mAb.

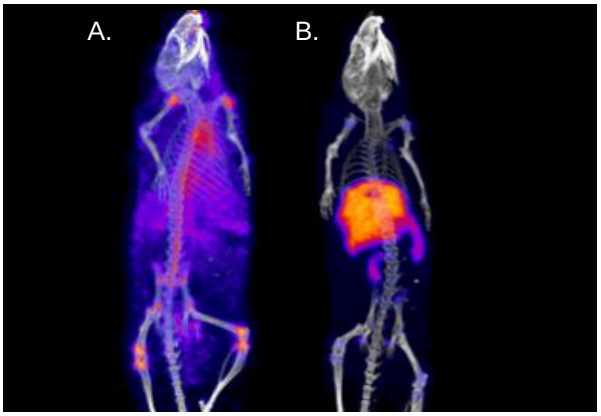

Fig 1. In vivo imaging of ^{89}Zr-labeled BVZ (A.) and ^{89}Zr-labeled NP 1 (B.) intravenously injected in C57BL/6 healthy mice.

Conclusions

tLyP-1 targeted HA-NPs were developed showing an efficient association of BVZ and anti-KRAS mAbs. The required standards in terms of physicochemical properties, stability in relevant biological media and after reconstitution were fulfilled. Overall, *in vitro* and *in vivo* results suggest the suitability of these systems for drugging intracellular targets.

Acknowledgments

This work was supported by the Spanish Ministry of Science, Innovation and Universities - Project Intracel (Ref. SAF2017-86634-R) and the Competitive Reference Groups (Consellería de Educación e Ordenación Universitaria, Xunta de Galicia, Ref: ED431C 2017/09). Ana María López Estévez acknowledges a predoctoral FPU grant from the Spanish Ministry of Science, Innovation and Universities (grant number FPU18/00095).

References

[1] P. Janice M. Reichert, Antibody therapeutics approved or in regulatory review in the EU or US, Antib. Soc. (2020). https://www.antibodysociety.org/resources/ approved-antibodies/ (accessed March 26, 2021).

[2] S. Niamsuphap, C. Fercher, S. Kumble, P. Huda, S.M. Mahler, C.B. Howard, Targeting the undruggable: emerging technologies in antibody delivery against intracellular targets, Expert Opin. Drug Deliv. 17 (2020) 1189–1211.

[3] F. Sousa, P. Castro, P. Fonte, P.J. Kennedy, M.T. Neves-Petersen, B. Sarmento, Nanoparticles for the delivery of therapeutic antibodies: Dogma or promising strategy?, Expert Opin. Drug Deliv. 14 (2017) 1163–1176.

[4] L. Roth, L. Agemy, V.R. Kotamraju, G. Braun, T. Teesalu, K.N. Sugahara, J. Hamzah, E. Ruoslahti, Transtumoral targeting enabled by a novel neuropilin-binding peptide, Oncogene. 31 (2012) 3754–3763.

O3.5: Non-viral delivery of CRISPR/Cas9 DNA for gene editing via multivalent cationic liposome system

D.A. Sousa [1;2*], R. Gaspar [2], C. J. O. Ferreira [2], F. Baltazar [4;5], B. F. B. Silva [2], L. R. Rodrigues [1]

[1]*CEB – Centre of Biological Engineering, University of Minho, Campus de Gualtar, 4710-057 Braga, Portugal*
[2]*INL – International Iberian Nanotechnology Laboratory, Av. Mestre José Veiga, 4715-310 Braga, Portugal*
[3]*CF-UM-UP, Department of Physics, University of Minho, Campus de Gualtar, 4710-057 Braga, Portugal*
[4]*Life and Health Sciences Research Institute (ICVS), School of Medicine, University of Minho, 4710-057 Braga, Portugal*
[5]*PT Government Associate Laboratory, ICVS/3B's—Life and Health Sciences Research Institute/Biomaterials, Biodegradables and Biomimetics, 4710-057 Braga/Guimarães, Portugal*

*e-mail: diana.sousa@ceb.uminho.pt

Introduction

CRISPR/Cas9 gene editing technology has revolutionized medical research by opening new therapeutic possibilities for disease treatment such as cancer, cardiovascular, neuronal and immune disorders [1]. Even with the emergence of this technology, the lack of clinically viable delivery systems continues to hinder CRISPR therapeutic applications. Viral vectors have been sucessfully used for the delivery of CRISPR/Cas9, which whilst efficient, raise safety concerns regarding immunogenicity and insertional mutagenesis [2]. Non-viral vector such as cationic liposomes offer an attractive alternative to viruses given their low immunogenicity, high encapsulation capacity, easy synthesis and functionalization [3]. Their cationic charge mediates strong electrostatic interactions with the negative charges of nucleic acids, leading to the formation of complexes called "lipoplexes". However, cationic lipids efficiency is still not at the level of viruses as delivery vectors. In recent years, multivalent cationic lipids have been proposed as a promising strategy to effectively deliver nucleic acids into target cells [4]. In this work, we explored the potential of multivalent cationic liposomes to deliver plasmid-based CRISPR/Cas9 systems as well as to mediate gene-editing.

Materials and Methods

To study the *in vitro* suitability of multivalent cationic lipid-DNA complexes to deliver CRISPR/Cas9 DNA plasmids, a pentavalent cationic lipid (MVL5) was combined with three different helper lipids: 1,2-dioleoyl-sn-glycero-3-phosphocholine (DOPC), monoleein (GMO) and 1,2-dioleoyl-sn-glycero-3-phosphoethanolamine (DOPE). The lipoplexes were prepared with cationic-to-anionic charge ratios (CR (+/-)) of 3 and 10. To facilitate the detection of transfection in HEK 293T cells by flow cytometry and fluorescence microscopy, a plasmid containing both Cas9/sgRNA and reporter green fluorescence protein (GFP) expression cassettes was used. To evaluate CRISPR-mediated gene editing, a Cas9 expression plasmid containing a sgRNA to target the *GFP* gene was designed, and consequently transfected into HEK 293T cells stably expressing GFP. The depletion of fluorescence signal associated to GFP gene disruption was also assessed by flow cytometry and fluorescence microscopy. The cytotoxicity of MVL5-DNA complexes was assessed using a standard colorimetric cell viability assay.

Results and Discussion

We demonstrated that plasmids encoding Cas9 and sgRNA can be successfully transfected into HEK 293T cells via MVL5-based lipoplexes in a concentration-dependent manner for both CR (+/-). Neverthless, at CR (+/-) 10 lipoplexes showed a superior transfection ability, being comparable to the commonly used commercial transfection reagent Lipofectamine 3000. Regarding gene editing, MVL5-lipoplexes mediated a notable *GFP* gene disruption in HEK 293T-GFP cells, achieving a knockout superior to 50%. However, a non-specific gene knockout was also verified, probably resulting from the considerable cytotoxicity of these formulations. Altogether, these results show that multivalent lipid-based lipoplexes are promising CRISPR/Cas9 plasmid delivery systems, and by further optimization and functionalization could achieve an effective and safe delivery system.

Conclusions

In summary, we have demonstrated the potential of MVL5-based lipoplexes to deliver sgRNA/Cas9 plasmids for gene editing. These formulations exhibited both high transfection efficiency, as well as gene knockout ability, achieving results

comparable to Lipofectamine 3000® commercial reagent. Although MVL5-based formulations also showed considerable cytotoxicy and, probably consequent non-specific gene knockout, their versatility opens significant opportunities for further optimization, either by tuning the cationic-to-anionic CR (+/-) to lower cytotoxicity, or by including additional lipids or surface functionalization, which is important for *in vivo* applications and may constitute an alternative to viral-delivery methods.

Acknowledgments

This work was supported by the Portuguese Foundation for Science and Technology (FCT) under the scope of the strategic funding of UIDB/04469/2020 unit and BioTecNorte operation (NORTE-01-0145-FEDER-000004) funded by the European Regional Development Fund under the scope of Norte2020 - Programa Operacional Regional do Norte and the Project FCOMP-01–0124-FEDER-021053 (PTDC/SAU-BMA/121028/2010). This research was also supported by Microfluidic Layer-by-layer Assembly of Cationic Liposome - Nucleic Acid Nanoparticles for Gene Delivery project (032520) co-funded by FCT and the ERDF through COMPETE2020. Diana A. Sousa (D.A.S) and Celso J.O. Ferreira (C.J.O.F) acknowledge FCT for the grants PD/BD/139083/2018 and SFRH/BD/149199/2019, respectively.

Reference

[1] L. Naldini, *Nature* **2015**, *526*, 351.

[2] Z. Glass, M. Lee, Y. Li, Q. Xu, *Trends Biotechnol.* **2018**, *36*, 173.

[3] A. Akbarzadeh, R. Rezaei-Sadabady, S. Davaran, S. W. Joo, N. Zarghami, Y. Hanifehpour, M. Samiei, M. Kouhi, K. Nejati-Koshki, *Nanoscale Res. Lett.* **2013**, *8*, 102.

[4] N. F. Bouxsein, C. S. McAllister, K. K. Ewert, C. E. Samuel, C. R. Safinya, *Biochemistry* **2007**, *46*, 4785.

Abstracts for Oral Presentation

Session 4: Hydrogels and 3D Models for Drug Delivery Systems

O4.1: "***Biocompatible Injectable Smart Hydrogels-based Depot Systems: A Dual-Anticancer Drug Sustained Release Strategy***". D. Rafael, F. Andrade, M.M. Roca-Melendres, D. Hide, I. Raurell, M. Martell, S. Schwartz, M. Oliva, E. Duran-Lara and I. Abasolo. Vall D'Hebron Institut de Recerca. (p.63)

O4.2: "***Modulating muchoadhesion and mucopenetration in multiresponsive nanogels*** ". M. Calderón, S. Orellano, J. Udabe and A. Sonzogni. University of the Basque Country. (p.65)

O4.3: "***Does it GUT what it takes? A new 3D bioengineered in vitro intestinal model to predict permeability***". M.H. Macedo, A.S. Barros, E. Martinez, C.C. Barrias, B. Sarmento, University of Porto. (p.67)

O4.4: "***Uterine leiomyoma 3D preclinical model for evaluating ganirelix delivery system***". P. García-García, A. Salas, C. Évora, P. Díaz-Rodríguez, T.A. Almeida and A. Delgado, Universidad de La Laguna. (p.69)

O4.5: "***Evaluation of lipid nanosystems for cancer treatment in static and non-static 3D models***". M. Cascallar, A. Martins, M. Ferrero, E. Escorihuela, S. Calabuig-Fariñas, L. Diéguez, E. Jantus-Lewintre, M. de la Fuente. Health Research Institute of Santiago de Compostela (IDIS)/CIBERONC. (p.71)

O4.1: Biocompatible Injectable Smart Hydrogels-based Depot Systems: A Dual-Anticancer Drug Sustained Release Strategy

D. Rafael[1,2]*, F. Andrade[1,3], M.M. Roca-Melendres[1], D. Hide[4,5], I. Raurell[4,5], M. Martell[4,5], S. Schwartz[1], M. Oliva[2,3,6] E. Duran-Lara[7,8], and I. Abasolo[1,2,9]

[1] *Drug Delivery & Targeting, Vall d'Hebron Institut de Recerca (VHIR), Universitat Autònoma de Barcelona (UAB), 08035, Barcelona, Spain.*
[2] *Networking Research Centre for Bioengineering, Biomaterials, and Nanomedicine (CIBER-BBN), Instituto de Salud Carlos III, 28029, Madrid, Spain.*
[3] *Department of Pharmacy and Pharmaceutical Technology and Physicochemistry, Faculty of Pharmacy and Food Sciences, School of Pharmacy, Universitat de Barcelona (UB), 08028, Barcelona, Spain.*
[4] *Liver Unit, Department of Medicine, Hospital Universitari Vall d'Hebron, Vall d'Hebron Institut de Recerca (VHIR), Universitat Autònoma de Barcelona (UAB), 08035, Barcelona, Spain.*
[5] *Centro de Investigación Biomédica en Red de Enfermedades Hepáticas y Digestivas (CIBEREHD), Instituto de Salud Carlos III, 28029, Madrid, Spain.*
[6] *Nanoprobes & Nanoswitches, Institute for Bioengineering of Catalonia (IBEC), 08028 Barcelona, Spain.*
[7] *Bio and NanoMaterials Lab, Drug Delivery and Controlled Release, Universidad de Talca, P.O. Box 747, 1141, Talca, Maule, Chile.*
[8] *Departamento de Microbiología, Facultad de Ciencias de la Salud, Universidad de Talca. P.O. Box 747, 1141, Talca, Maule, Chile.*
[9] *Functional Validation & Preclinical Research (FVPR)/U20 ICTS Nanbiosis, Vall d'Hebron Institut de Recerca (VHIR), Universitat Autònoma de Barcelona (UAB), 08035, Barcelona, Spain.*

*e-mail: diana.fernandes_de_so@vhir.org

Introducction

Cancer is the second leading cause of death worldwide and is still considered an incurable disease, despite the enormous efforts of the scientific community in the last decades [1]. Requirement of high doses of chemotherapy, drug resistance and severe side effects, are major drawbacks regarding cancer therapy [2]. Therefore, new formulations are continuously under research in order to improve drugs therapeutic index. Among a wide range of possibilities, hydrogels (HG) have gained the attention of cancer researchers due to the possibility to create in situ sustained and controlled release drug delivery systems. In particular, the stimuli-responsiveness HG, that are able to change their state from liquid to gel accordingly to external factors such as temperature, pH, light, ionic strength, and magnetic field, have been widely used for drugs and/or genetic material delivery [3].

Materials and Methods

Based in our previous work [4], a novel biodegradable and biocompatible HG formulation consisting in a combination of monomers of NIPAM with monomers of cellulose crosslinked with citric acid and using CAN as initiator/catalysator was optimized for the encapsulation of both hydrophilic (e.g., Doxorrubicin) and hydrophobic (e.g., Niclosamide) drugs. The formulation was extensively characterized through different up-to-date techniques: gelation time, Scanning Electron Microscope (SEM), Fourier-transform infrared spectroscopy (FTIR), Nuclear Magnetic Resonance spectroscopy (1H-NMR)), rheology, and release profile in physiological conditions. Moreover, the biocompatibility in fibroblast cells lines as well as their biological activity in colon (HCT116) and ovarian cancer models (Ovcar-3) were performed. Finally, it was performed an *in vivo* injectability and biocompatibility assay, to evaluate HG behaviour during the injection procedure, its ability to remain *in situ* during several days, and the occurrence of possible adverse effects.

Results and Discussion

The designed formulation present thermo-responsiveness and reversibility (Fig. 1) two of the main important features required for *in situ* injectable HG.

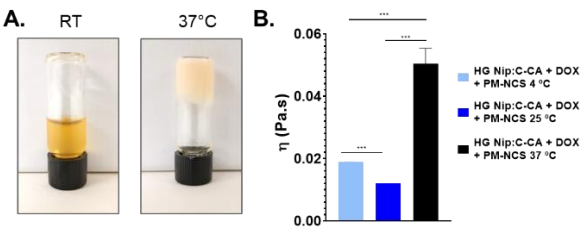

Fig 1. A. Tube inversion test at 25 and 37 ºC. B. Viscosity of formulations at different temperatures. Results are expressed as mean ± SEM, n≥3, ***<0.001.

Moreover, the formulation served for the incorporation of both hydrophobic and hydrophilic anticancer drugs, allowing their sustained slow release over time (Fig. 2). Despite the low percentage release, at 72h, was possible to observe therapeutic efficacy of the formulation in both colorectal and ovarian cancer *in vitro* models (Fig. 3). These results indicate that the formulation could work as a depot system promoting long-term therapeutic efficacy, reducing the number of chemotherapy administrations/cycles required.

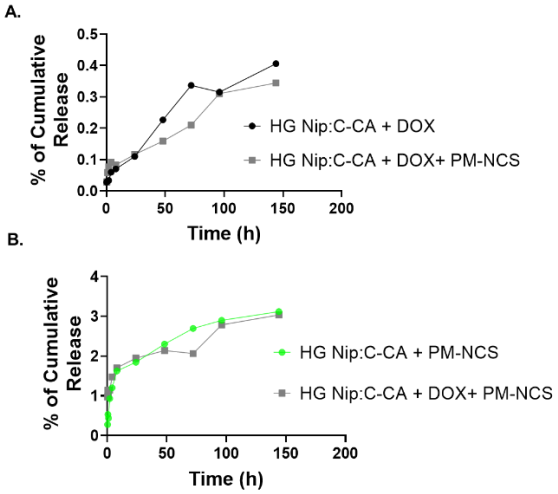

Fig 2. *In vitro* Doxorrubibin (A) and Niclosamide (B) release kinetic profile from prepared formulations. Results are expressed as mean ± SEM, n ≥ 3.

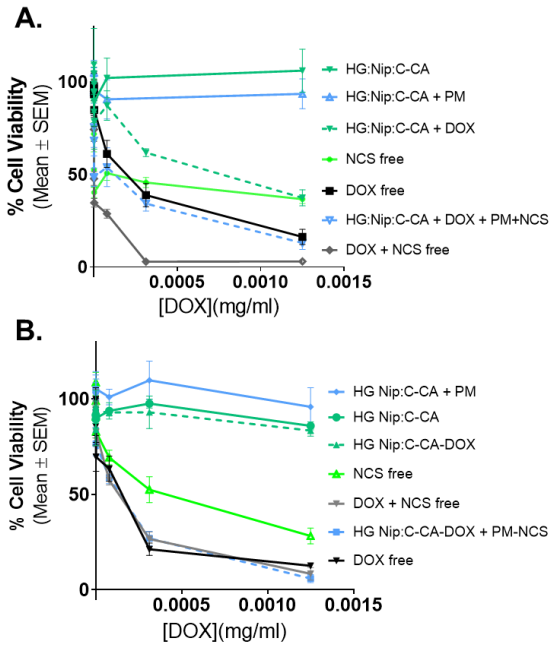

Fig 3. Cell viability curves of HCT116 colorectal (A) and Ovcar-3 ovarian (B) cancer cells exposed to Doxorrubucin and Niclosamide free and released from the formulations over 72h. Results are expressed as mean ± SEM, n ≥ 3.

Moreover, the formulation presented the ideal features in terms of *in vivo* injectability, *in situ* localization, and biocompatibility (Fig. 4).

Conclusions

Taking all the results into consideration, the here presented formulation could work as a platform for the local sustained release of anticancer drugs, bringing a great impact as cancer co-adjuvant therapy or in the case of non-operable tumors.

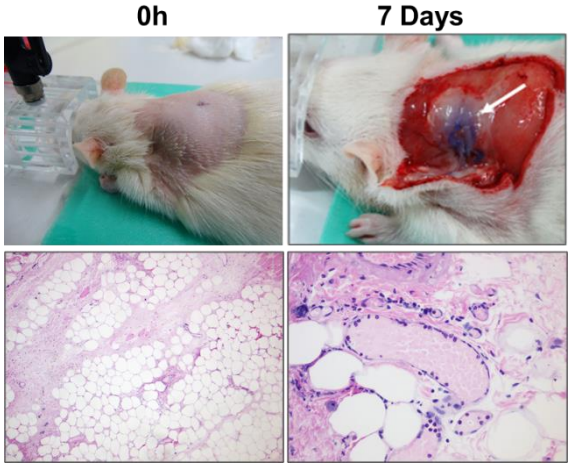

Fig 4. Injectability and *in vivo* biocompatibility (histological analysis) of HG subcutaneousy administered to healthy Wistar rats.

Acknowledgments

This work was supported by the Networking Research Centre on Bioengineering, Biomaterials, and Nanomedicine (CIBER-BBN) which is financed by the Instituto de Salud Carlos III (ISCIII) with assistance from the European Regional Development Fund (ERDF). We also thank the denomination of Consolidated group from Generalitat de Catalunya (2017-SGR-00638). The work was also supported by ANID FONDECYT REGULAR (Chile) through project N◦ 1210476 from Esteban F Durán-Lara.

References

[1] World Health Organization. Cancer. Available from: https://www.who.int/health-topics/cancer

[2] V. Schirrmacher. From chemotherapy to biological therapy: A review of novel concepts to reduce the side effects of systemic cancer treatment., *Int J Oncol.* 54(2) (2019) 407–19

[3] D. Rafael, M.M. Roca-Melendres, F. Andrade, *et al.* Thermo-responsive hydrogels for cancer local therapy: Challenges and state-of-art., *Int J Pharm* 606 (2021) 120954

[4] G. Carreño, A. Pereira, F. Avila-Salas, *et al.* Development of “on-demand” thermo-responsive hydrogels for anti-cancer drugs sustained release: Rational design, in silico prediction and in vitro validation in colon cancer models., *Materials Science & Engineering C* 131 (2021) 112483

O4.1: Modulating mucoadhesion and mucopenetration in multiresponsive nanogels

M. Calderón[1,2]*, S. Orellano[1], J. Udabe[1] and A. Sonzogni[3]

[1]POLYMAT, Applied Chemistry Department, Faculty of Chemistry, University of the Basque Country, UPV/EHU, Paseo Manuel de Lardizabal 3, 20018 Donostia-San Sebastián, Spain.
[2]IKERBASQUE, Basque Foundation for Science, 48009 Bilbao, Spain.
[3]Group of Polymers and Polymerization Reactors, INTEC (Universidad Nacional del Litoral-CONICET), Güemes 3450, Santa Fe 3000, Argentina

*e-mail: marcelo.calderon@polymat.eu

Introducction

Thiol bearing materials recently gained increased interest due to their ability to overcome mucosal clearance and thus to deliver drugs to submucosal layers in sufficient concentrations.[1] To date, mostly free thiol bearing materials have been employed for submucosal delivery of drugs. However, in aqueous environment disulfides and thiols are in a dynamic equilibrium resulting in the occasionally presence of free thiols for disulfide containing materials as well. We thus hypothesize, that disulfide containing materials will perform in a similar manner to thiol bearing particles and are exciting candidates to overcome the mucosal barrier and deliver therapeutic actives to submucosal cells.[2]
The stimuli-responsive nanogel (NG) technology is shaping up as a potential strategy to transport and deliver small molecule drugs as well as therapeutic biomacromolecules.[3] Key features such as nanogel size, polarity/lipophilicity, volume phase transition temperature, surface decoration, targeting ability, etc., have been correlated with the potential of responsive NGs to deliver and release bioactive molecules. In this context, we hereby present the development of redox-sensitive NGs for overcoming restrictive barriers in mucosal drug delivery of therapeutics (Fig. 1). Many NGs have been suggested that exploit biopolymers, such as chitosan, dextran, gelatin or hyaluronic acid to introduce degradability. However, the application of cleavable linker instead of a degradable backbone or biodegradable polymers allows precise control over the mesh sizes, the degradation rate and the size of fragments after degradation. This advantage should enable an accurate tuning of the macroscopic response of the NGs to adapt to the requirements of the specific application.

Materials and Methods

A series of disulfide-bearing crosslinkers suitable for free radical polymerization were employed. Nanogels were prepared by precipitation polymerization with, for instance, N-isopropyl methacrylamide (NIPMAM) as monomer. By varying the crosslinker and monomer feed ratio, the size of the NGs was tuned to values of 40–200 nm. Characterization of the NGs and of their interaction with mucose were performed using dynamic light scattering (DLS), gel permeation chromatography (GPC), ζ-potential, atomic force microscopy (AFM), scanning electron microscopy (SEM), Raman spectroscopy, rheology, and Franz cells. Cytotoxicity and mucopenetration of pristine and protein-loaded nanogels were assayed on Caco2 cells, intestinal mucose, and in human-based models of the bronchial epithelium.

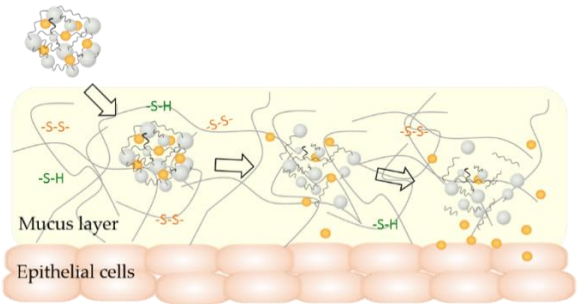

Fig 1. Submucosal delivery of therapeutic actives through interaction of disulfide-containing nanogels

Results and Discussion

A comprehensive screening of monomers and crosslinkers was realized to control the number and location of disulfide linkers within the NGs' structure. The main aim was to assess the degradability of the NGs in reductive conditions and its correlation with their mucoadhesive/mucopenetrating properties.
Systematic analysis of the NG polymerization process revealed the importance of careful polymer choice to form particles with diameters in the 50-200 nm range that yield low polydispersity and intact disulphide-bonds. Aspects related to the crosslinker functionalization, temperature of reaction, monomer/crosslinker ratios, and nature of the monomers showed to play a pivotal role. As

example, utilizing dendritic polyglycerols functionalized with N-methacryloyl N'-propargyoxylcystamine yielded fully degradable NGs (Fig. 2), while using N,N'-bis(acryloyl)cystamine (BAC) as crosslinker, yielded NGs that did not disintegrate into their component parts when incubated in reductive environments.

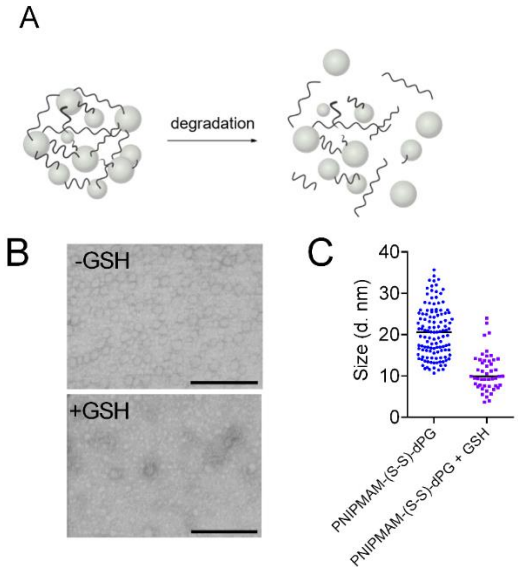

Fig. 2. (A) Glutathione (GSH) induced cleavage of nanogels through reduction of disulfides to thiols. (B) TEM images of PNIPMAM-(S-S)-dPG before and after incubation with 5 ×10^{-3} M GSH for 24 h. Scale bar = 200 nm. (C) Distribution of particle diameter semiquantified using the TEM images.

NG interactions with the mucus and potential mucopenetrating properties were tested with mucin, in gastrointestinal mucus of freshly excised porcine small intestines, and in reconstructed human-based models of bronchial epithelium. Moreover, they are currently being tested in c-elegans regarding their mucoadhesion and in mice, for mucosal vaccinations. The NGs were further loaded with etanercept (ETN) as a model drug for anti-tumour necrosis factor alpha (anti-TNFα) treatment of inflammatory diseases of the GI tract. [4] The penetration of ETN was then demonstrated in three-dimensional human models which emulate characteristics of inflammatory diseases. In all cases, the nature and the amount of disulfide linkages showed to be of great relevance.

Conclusions

The results demonstrated that the incorporation of disulfide bonds provides the NGs not only with degradable points that later enable the cargo release, but also with a programmable capacity for mucoadhesion or mucopenetration. High loading efficiencies and transmembrane transport of highly challenging proteins was demonstrated. Further applications against cystic fibrocys, bovine mastitis and Chagas disease are currently being explored.

Acknowledgments

This work was supported by MINECO (RTI2018-098951-B-I00), CONICET, IKERBASQUE-Basque Foundation for Science, and the Marie-Slodowska-Curie Action under the H2020 framework program, with the project "THERMUCNA" [896775].

References

[1] X. Murgia, B. Loretz, O. Hartwig, M. Hittinger, C.-M. Lehr, Adv. Drug Delivery Rev. 124 (2018), 82-97.

[2] Loryn Theune, doctoral thesis (2019), Freie Universität Berlin, Germany

[3] C. Cuggino, E.R. Osorio Blanco, L.M. Gugliotta, C.I. Alvarez Igarzabal, M. Calderón, Crossing biological barriers with nanogels to improve drug delivery performance, *Journal of Controlled Release* 307 (2019), 221-246.

[4] R. Charbaji, M. Kar, L.E. Theune, J. Bergueiro, A. Eichhorst, F. Stumpff, M. Calderón, S. Hedtrich, Design and testing of efficient mucus-penetrating nanogels – pitfalls of preclinical testing and lessons learned, *Small* 17 (2021), 2007963.

O4.3: Does it GUT what it takes? A new 3D bioengineered *in vitro* intestinal model to predict permeability

M.H. Macedo[1,2,3]*, A.S. Barros[1,2,3], E. Martinez[4,5,6], C.C. Barrias[1,2,3] and B. Sarmento[1,2,7]

[1]*i3S – Instituto de Investigação e inovação em Saúde, Universidade do Porto, Porto, Portugal*
[2]*INEB – Instituto Nacional de Engenharia Biomédica, Universidade do Porto, Porto, Portugal*
[3]*ICBAS – Instituto de Ciências Biomédicas Abel Salazar, Universidade do Porto, Porto, Portugal*
[4]*IBEC - Institute for Bioengineering of Catalonia, Barcelona, Spain*
[5]*CIBER-BBN – Consorcio Centro de Investigación Biomédica en Red de Bioingeniería, Biomateriales y Nanamodicina, Madrid, Spain*
[6]*Electronics and Biomedical Engineering Department, Universitat de Barcelona, Barcelona, Spain*
[7]*CESPU – Instituto de Investigação e Formação Avançada em Ciências e Tecnologias da Saúde, Gandra, Portugal*

*e-mail: macedohelena6@gmail.com

Introduction

The drug development field is constantly requesting tools that can speed up the early pharmacokinetic phases by reducing animal experiments. In oral delivery, understanding the absorption in the small intestine is paramount. *In vitro* models are routinely used but current 2D models are too simplistic, which impacts permeability outcomes [1,2].

Materials and Methods

A new 3D *in vitro* intestinal model was developed, comprising the epithelium, with Caco-2 and HT29-MTX cells resembling the enterocytes and goblet cells, respectively, on top of a 3D layer of collagen with human intestinal fibroblasts (HIF) embedded, mimicking the intestinal lamina propria (3D Co-culture model). An endothelial layer, surrogating the blood capillaries was added to the previous model (3D Complete model) (Figure 1). A 2D Co-culture model (Caco-2 + HT29-MTX) was used as control.
The behavior of the HIF inside the collagen layer was assessed. Models were characterized regarding the expression of intestinal markers and drug transporters. The activity of P-glycoprotein (P-gp) was confirmed with a transport activity with Rhodamine 123 (Rho 123), a substrate of this transporter. Finaly, permeability assays using three model drugs with low, medium and high permeability were performed and values were compared to *in vivo* data from the literature.

Results and Discussion

Fibroblasts embedded in the collagen hydrogel showed increasing metabolic activity along the culture time. Besides, they presented their prototypical elongated shape and secreted fibronectin, remodeling the surrounding matrix (Fig. 2).

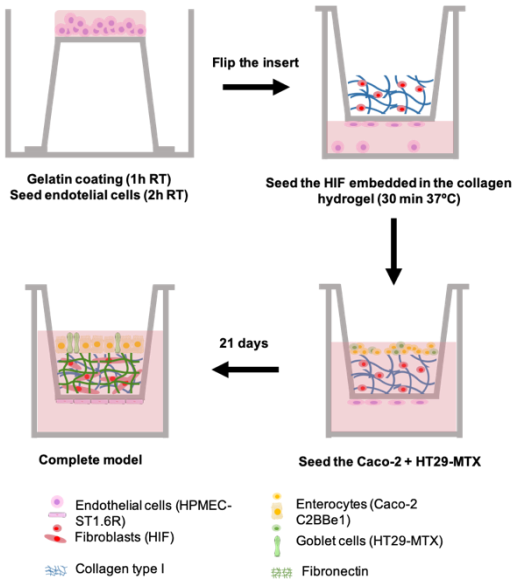

Fig 1. General overview of the procedure to obtain the 3D model

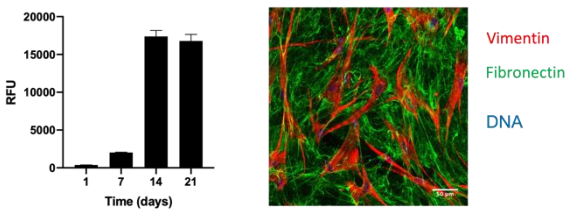

Fig 2. Metabolic activity of HIF along the time in culture and secretion of fibronectin and vimentin after 21 days.

The expression of Sucrase Isomaltase (SI) was lower in the 3D models compared to the 2D. Expression of Intestine Specific Homeobox (ISX) and Villin 1 (Vil1) was similar between models (Fig. 3).

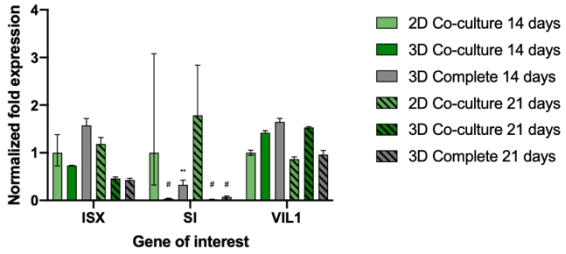

Fig 3. Normalized genetic expression of different intestinal markers in the different models.

The expression of drug transporters was overall more biologically relevant in the 3D models. Specifically, the expression of P-gp and Multidrug Resistence Protein 2 (MRP2), which are normally overexpressed in the 2D models, was decreased in the 3D configurations, which is important since these transporters are responsible for the efflux of innumerous substrates (Fig. 4).

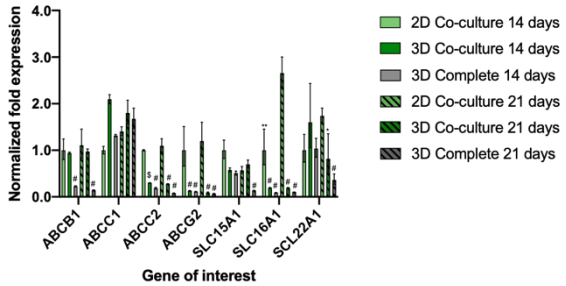

Fig 4. Normalized genetic expression of different intestinal drug transporters in the different models.

A lower activity of P-gp in the 3D models was confirmed with a transport assay with Rho 123 since the compound showed lower permeability and higher efflux in the 2D models (Fig. 5).

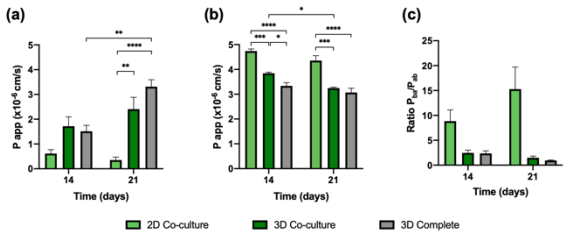

Fig 5. Papp (x10^{-6} cm/s) values of Rho 123 in the models at 14 and 21 days in the (a) apical to basolateral and (b) basolateral to apical directions and (c) ratio of the bidirectional transport.

The 3D Co-culture model was the configuration that presented higher permeability results, being more similar to *in vivo* literature data. The addition of the endothelial layer (3D Complete model) led to a decrease in permeability values. The permeability at different timepoints was different for the 2D and 3D Co-culture models (Fig. 5 and Table 1).

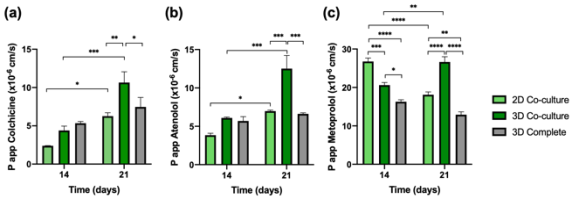

Fig 5. Papp (x10^{-6} cm/s) values of (a) Colchicine, (b) Atenolol and (c) Metoprolol in models at 14 and 21 days

*T*able 1. Literature values of Papp (x10^{-6} cm/s) in the different models and rat small intestine [3].

	P_{app} Rat Small Intestine	P_{app} 2D Co-culture	P_{ap} 3D Co-culture	P_{app} 3D Complete
Colchicine	25	6.3±0.7	10.7±2.4	7.5±2.1
Atenolol	10.7	7.0.±0.2	12.5±3.0	6.6±0.2
Metoprolol	62.4	18.1±1.3	26.6±2.4	12.9±1.3

Conclusions

Two different configurations of a new 3D intestinal model were achieved, and the viability of HIF inside the collagen matrix and secretion of endogenous ECM was confirmed. The 3D models showed a more relevant expression of drug transporters and P-gp activity. This led to better permeability outcomes, specially in the 3D Co-culture model, which presented more similar results to *in vivo* data. It was also possible to conclude that the addition of an endothelial layer led to a decrease in permeability and that permeability results are different at 14 and 21 days, so models should be kept until the last timepoint.

Acknowledgments

This work was supported by FCT – Fundação para a ciência e tecnologia (SFRH/BD/131587/2017).

References

[1] M. H. Macedo, et al., Development of an Improved 3D *in vitro* Intestinal Model to Perform Permeability Studies of Paracellular Compounds. Front. Bioeng, Biotechnol. 8 (2020) 524018

[2] M. H Macedo, et al., Mucus-producing 3D cel culture models. Adv. Drug Deliv. Rev. 178 (2021) 113993

[3] I. Lozoya-Agullo, et al., In Situ Perfusion Model in Rat Colon for Drug Absorption Studies: Comparison with Small Intestine and Caco-2 Cell Model. J. Pharm. Sci. 104 (2015) 3136-3145

O4.4: Uterine leiomyoma 3D preclinical model for evaluating ganirelix delivery system

P. García-García*[1;2], A. Salas[3;4], C. Évora[1;2], P. Díaz-Rodríguez[2;5], T.A. Almeida[3;4] and A. Delgado[1;2].

[1]*Department of Chemical Engineering and Pharmaceutical Technology, Universidad de La Laguna, 38206 La Laguna, Spain*
[2]*Institute of Biomedical Technologies (ITB), Universidad de La Laguna, 38206 La Laguna, Spain*
[3]*Department of Biochemistry, Microbiology, Cell Biology and Genetics, Universidad de La Laguna, 38206 La Laguna, Spain*
[4]*Instituto Universitario de Enfermedades Tropicales y Salud Pública de Canarias, 38206 La Laguna, Spain*
[5]*Department of Pharmacology, Pharmacy and Pharmaceutical Technology, Universidade de Santiago de Compostela, 15782 Santiago de Compostela, España*

*e-mail: pgarciag@ull.edu.es

Introduction

Uterine leiomyomas are the most common benign tumors in women of reproductive age. Given its clear hormonal dependence, the pharmaceutical approach to treat these fibroids has focused mainly on blocking the pituitary-gonadal axis [1,2]. To date, the only treatment approved by the FDA and the EMA consists of gonadotropin-releasing hormone GnRH (GnRHa) analogues that act by inhibiting this axis, leading to numerous adverse effects at the systemic level.

Sustained release systems are characterized by maintaining the delivery of a therapeutic agent, at a previously optimized rate, for prolonged periods. Furthermore, adequately dispersed microparticles within these systems are injectable and, therefore, can be administered locally, thus avoiding unwanted systemic effects. Considering the nature of uterine leiomyomas and that they have GnRH receptors in their cells, the objective of this study was to verify the efficacy of an organotypic culture, previously described [3] as a 3D preclinical model for evaluating a ganirelix (GnRH antagonist) controlled release system to be administered intratumorally to treat leiomyomas.

Materials and Methods

Three female patients aged 41-53 years were enrolled with prior consent in this study. All patients were Caucasian and underwent hysterectomy for menorrhagia without any previous hormonal treatment for at least 3 months. Fresh tissue sectioning was carried out using a vibratome, obtaining slices of 500 µm. Tissue slices were positioned at the air/liquid interface of 0.8 mm thickness alginate scaffold [3].

Ganirelix PLGA microspheres were prepared by double emulsion method (w/o/w). Briefly, 75 µg of ganirelix acetate salt with (GA-M) and without (G-M) 1 mg of ultrapure alginate sodium in 50 µL of water was emulsified with 1.5 ml of a mixture of 250 mg of PLGA 75:25 and 85:15 [80:20] and 0.2 mg of SPAN 60 (HBL=4.7) in methylene chloride solution (DCM) for 1 min. Then, 5 ml of an aqueous solution of 5% poly (vinyl alcohol) (PVA) and NaCl was added and vortexing for 30 s. Afterward suspension was poured in 100 ml of water under magnetic stirring to evaporate the organic solvent for 1.5 h. Microspheres were characterized in terms of size distribution with a Mastersizer 2000 (Malvern Instruments) and the morphology was observed with scanning electron microscopy (SEM). Some microspheres batches were prepared with ^{125}I-Ganirelix as a tracer to determinate the encapsulation efficiency and perform the release assays.

To develop the scaffolds, 2mg of microspheres were dispersed in 100 µl of an aqueous solution of 2% sodium alginate in a cylindrical mold and freeze-dried. Then, alginate was crosslinked with 100 µl of 1% $CaCl_2$ for 3 min and washed two times with sterile MilliQ water and freeze-dried again.

In order to determine the ganirelix effect at tissue level, we were performed a Click-It™ Plus TUNEL assay for in situ apoptosis detection (C10617, Invitrogen) following the manufacturer instruction. Sections were examined under a fluorescence microscope (Leica DM4000B), and images were acquired using a digital camera (Leica DFC300FX). Images obtained from the different fluorescent channels were analyzed using the Image J program, version 1.5a software (NIH). Statistical analysis was carried out with GraphPad Prism v. 8.0 (GraphPad Software).

Results and Discussion

The mean volume diameter of microspheres was 68,9 µm (10%< 25,9 µm, 90% > 131,8 µm), No differences were observed between G-M and GA-M. The encapsulation efficiency was 55 ± 0.76 % and 49.93 ± 5,9% for G-M and GA-M respectively.

According to our starting hypothesis, the alginate binds to proteins by interaction of its negative charge with the positive charge of the ganirelix, it should favor their retention in the system. Contrary to expectations, faster release rate of ganirelix from GA-M than from G-M, was observed (Figure 1). The explanation for this result could be that alginate, which is a very large and water-soluble molecule, diffuses through the matrix, forming pores dragging ganirelix to the aqueous medium.

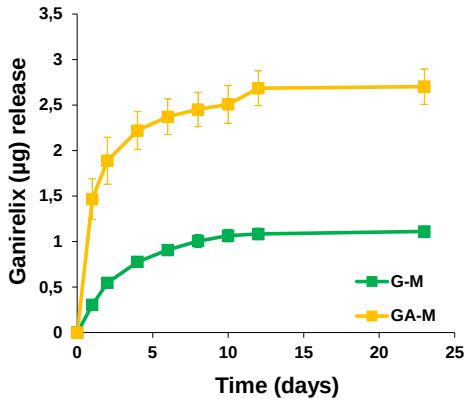

Fig 1. Ganirelix (µg) release from different types of microspheres included in alginate scaffold. Dulbecco's Modified Eagle Medium (DMEM) without supplements was used as release media. The assay was performed at 37ºC and 25 rpm. n=3

Figure 2 shows the results of the TUNEL test for the three fibroids included in the study. A significant increase in the percentage of apoptosis with respect to the control was observed regardless of the composition and the release profile of the microspheres containing ganirelix.

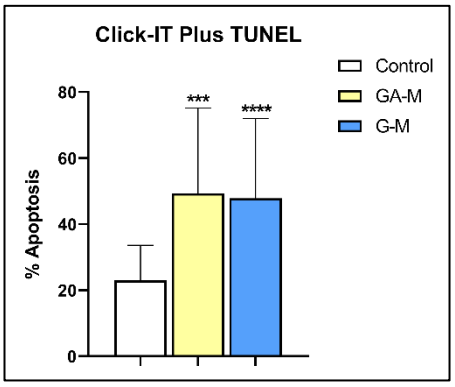

Fig 2. Analysis of immunoreactive cells for the Click-IT TUNEL test expressed as a percentage of apoptosis after six days of drug exposure. Significant increase in apoptosis with both releases compared to the untreated control. *** $p < 0.001$, **** $p < 0.0001$.

Conclusions

The development platform for culture 3D is a good tool to maintain explant cultures and is effective as a preclinical method for evaluating the system developed in this work. Ganirelix microsphere formulation could be useful for treating uterine leiomyomas.

Acknowledgments

This study has been funded by Ministerio de Ciencia, Innovación y Universidades (MICIUN), which is part of the Agencia Estatal de Investigación (AEI), Spain, with joint financing by FEDER funds from the European Union (RTI2018-097324). Patricia García and Ana Salas acknowledges postdoctoral grant "Investigador Posdoctoral Junior, CEI-Canarias" and predoctoral grant "cajasieste" para la formación de doctores" respectively.

References

[1] Bulun, S.E., 2013. Uterine Fibroids. N. Engl. J. Med. 369, 1344–1355.

[2] Islam, M.S., Protic, O., Stortoni, P., Grechi, G., Lamanna, P., Petraglia, F., Castellucci, M.,Ciarmela, P., 2013. Complex networks of multiple factors in the pathogenesis of uterineleiomyoma. Fertil. Steril. 100, 178–193.https://doi.org/10.1016/j.fertnstert.2013.03.007

[3] Salas, A., López, J., Reyes, R., Évora, C., Oca, F.M. De, Báez, D., Delgado, A., Almeida, T.A., 2020. Organotypic culture as a research and preclinical model to study uterine leiomyomas. Sci. Rep. 1–12. https://doi.org/10.1038/s41598-020-62158-w

[4] García-García P., Reyes R., Pérez-Herrero E., Arnau MR., Évora C., Delgado A. 2020. Alginate-hydrogel versus alginate-solid system. Efficacy in bone regeneration in osteoporosis. Mater Sci Eng C Mater Biol Appl. doi: 10.1016/j.msec.2020.111009.

O4.5: Evaluation of lipidic nanosystems for cancer treatment in static and non-static 3D models

M. Cascallar[1,2]*, A. Martins[3], M. Ferrero[2, 4, 5], E. Escorihuela[4, 5], S. Calabuig-Fariñas[2, 4, 5, 6], L. Diéguez[3], E. Jantus-Lewintre[2, 4, 5, 7] and M. de la Fuente[1,2].

[1]*Nano-Oncology and Translational Therapeutics Unit, Health Research Institute of Santiago de Compostela (IDIS), 15706 Santiago de Compostela, Spain.*
[2]*Cancer Network Research (CIBERONC), 28029 Madrid, Spain.*
[3]*Medical Devices Research Group, International Iberian Nanotechnology Laboratory (INL), 4715-330 Braga, Portugal*
[4]*Molecular Oncology Laboratory, Fundación Investigación, Hospital General Universitario de Valencia, 46014 Valencia, Spain*
[5]*Unidad Mixta TRIAL, Centro Investigación Príncipe Felipe—Fundación Investigación, Hospital General Universitario de Valencia, 46014 Valencia, Spain*
[6]*Department of Pathology, Universitat de València, 46010 Valencia, Spain*
[7]*Department of Biotechnology, Universitat Politècnica de València, 46022 Valencia, Spain*

*e-mail: maria.cascallarc@gmail.com

Introduction

Cancer is responsible for millions of deaths each year, and new specific therapies are needed. The development of innovative therapies based on biodegradable and biocompatible nanosystems represents a promising alternative for improving cancer treatment.

A key step to study this type of treatments is the *in vitro* evaluation. The most common experiments are based on 2D cell culture, which provide us information about the efficacy of the treatment. However, 2D assays result in a lack of real tumor representation [1]. Therefore, better models are needed to replicate the tumor structure and its environment. Spheroids allow replicating the 3D appearance of the tumor, and organoids provide with the tumoral extracellular matrix. 3D organ-in-a-chip models are a more advanced and complementary approach that replicates a non-static 3D model, increasing the complexity and allowing a more comprehensive testing of new molecules and drug carriers [2].

In our laboratory, we developed sphingomyelin nanosystems (SNs) for cancer therapy, which are highly versatile allowing the addition of biomolecules and drugs for targeting and treatment of tumor cells. In this work, we aimed to evaluate their efficacy in 2D and 3D cell cultures, as well as, in microfluidic organ-in-a-chip devices.

Materials and Methods

SNs were formulated by the ethanol injection method as previously described [3], [4] and characterized with a ZetaSizer Nano ZS. For carrying out the in vitro assays, SNs were labelled with sphingomyelin-Cy5.

Non-small cell lung cancer cells (NSCLC) (A549 and H1650) were used to perform the 2D and 3D *in vitro* experiments.

Two-channel devices made of PDMS were tailored for this project and used for microfluidic experiments. These chips were composed by one endothelial channel (with HPMEC cells) and one tumor channel (with NSCLC cells).

In all cases, SNs were incubated at different times to evaluate their capacity to be internalized by cells, and to observe their behaviour in different scenes mimicking the tumor.

Results and Discussion

In vitro tests have demonstrated the capacity of SNs to be internalized by the tumor cells. 2D-based models resulted in a high uptake of SNs by the cells. In the same vein, 3D models showed a clear internalization of SNs in all the layers of the structure, giving evidence that SNs are capable to reach the inside of the tumor (*Fig. 1*). This is a very relevant fact considering that the release of the treatment must occur in the whole tumoral tissue to be more effective.

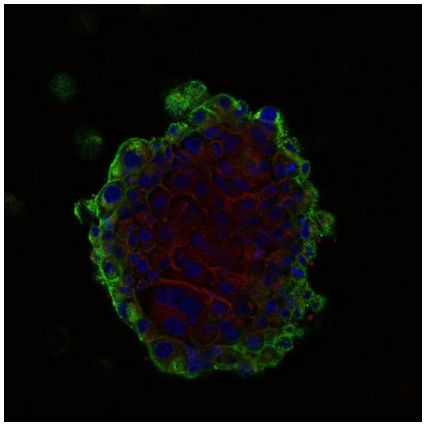

Fig 1. Nanosystems uptake in spheroid.

3D organ-on-a-chip devices achieved a representation of the extravasation process of the nanosystems to the cancer channel, which allows us understanding their capacity to reach the cancer cells and cross the vascular barrier. SNs could overcome the endothelial barrier under a dynamic low and reach cancer cells efficiently.

Conclusions

3D models, static and non-static, are an essential step to evaluate the nanosystems efficacy and their behaviour interacting with the cancer cells in a tumor-like environment. SNs demonstrated to be promising carriers to reach tumor cells, individually, forming spheroids, and under dynamic conditions after having overcome the endothelial layer. Next steps will be the functionalization of the SNs with specific ligands agains cancer, cells, the association of drugs, and screening of the most promising targeted therapies in 3D static and non-static models.

Acknowledgment

This work was supported by the Carlos III Health Institute's METASTARG Project, under the frame of EuroNanoMEd III.

References

1. S. Breslin, L. O'Driscoll, The relevance of using 3D cell cultures, in addition to 2D monolayer cultures, when evaluating breast cancer drug sensitivity and resistance. *Oncotarget*, 7(2016), 45745.
2. I. Van Zundert, B. Fortuni, S. Rocha, From 2D to 3D cancer cell models—the enigmas of drug delivery research. *Nanomaterials*, 1 0(2020), 2236.
3. B. L. Bouzo, M. Calvelo, M. Martín-Pastor, *et al*. In Vitro–In Silico Modeling Approach to Rationally Designed Simple and Versatile Drug Delivery Systems. *The Journal of Physical Chemistry B*, 124 (2020) 5788-5800.
4. S. Díez-Villares, J. Pellico, N. Gómez-Lado, *et al*. (2021). Biodistribution of 68/67Ga-Radiolabeled Sphingolipid Nanoemulsions by PET and SPECT Imaging. *International Journal of Nanomedicine*, 16 (2021), 5923-5935.

Abstracts for Oral Presentation

Session 5: Young Scientist Networking

O5.1: ***"Exploiting the chemotherapeutic and immunomodulatory effect of brain and glioblastoma dual-targeted nanoparticles – a nanomedicine, chemistry and tumor biology therapeutic recipe making use of a novel tumor niche-recapitulating 3D spheroid construct".*** C. Martins, C.M. Barbosa, M. Araújo, S. J. Smith, M. J. Oliveira, D. Lamprou, R. Rahman, J. W. Aylott, B. Sarmento. University of Porto. (p.75)

O5.2: " ***Nanosystems for the development of mRNA vaccines***". M.L. Borrajo, S. Anthiya, G. Lou, and MJ. Alonso. University of Santiago de Compostela. (p.77)

O5.3: "***mRNA Reprograming Matrices for driving chondroblast differentiation in vitro and in vivo***". H. Rilo-Alvarez, A. M. Ledo, M. Lopez-Peña, F. M. Muñoz, A. Vidal, M. Garcia- Fuentes. University of Santiago de Compostela. (p.79)

O5.4: "***Nanoclay-incorporated HA/alginate scaffolds as SDF-1 smart delivery-platforms for bone tissue engineering***". I. Erezuma, I. Lukin, P. García-García, A. Delgado, R. Reyes, C. Evora and G. Orive. University of Basque Country. (p.81)

O5.5: "***Extracellular vesicles from hair follicle and adipose tissue-derived mesenchymal stem cells: Flow cytometry characterization and functional comparison for the treatment of diabetic ulcers***". M K. Las Heras, F. Royo, C. Garcia-Vallicrosa, M. Igartua, E. Santos-Vizcaino, J.M. Falcon-Perez, R Hernandez. University of Basque Country. (p.83)

O5.6: "***Direct powder extrusion 3D printing of polyhydroxybutyrate implants for prolonged drug release***". S. Moroni, M. Tiboni, L. Casettari. University of Urbino. (p.85)

O5.1: Exploiting the chemotherapeutic and immunomodulatory effect of brain and glioblastoma dual-targeted nanoparticles – a nanomedicine, chemistry and tumor biology therapeutic recipe making use of a novel tumor niche-recapitulating 3D spheroid construct

C. Martins[1,2], C.M. Barbosa[1], M. Araújo[1], S. J. Smith[3], M. J. Oliveira[1], D. Lamprou[4], R. Rahman[3], J. W. Aylott[2], B. Sarmento[1]

[1]*Institute for Research and Innovation in Health (i3S), University of Porto, 4200-135 Porto, Portugal*
[2]*School of Pharmacy, University of Nottingham, NG7 2RD Nottingham, UK*
[3]*School of Medicine, University of Nottingham, NG7 2RD Nottingham, UK*
[4]*School of Pharmacy, Queen's University Belfast, BT9 7BL Belfast, UK*

*e-mail: claudia.martins@i3s.up.pt

Introduction

The 5-year survival of glioblastoma (GBM) patients is limited to a dismal 5%, highlighting the need to advance more effective therapies. GBM tissue abnormally overexpresses the L-type amino acid transporter 1 (LAT1), for which L-histidine (His) is an inexpensive and powerful targeting ligand. Thus, we propose the chemical modification of a conventional chemo-immunogenic drug, docetaxel, into a nanomedicine with surface-His (nano-DTX-His) to target GBM tissue via LAT1 adhesive binding and further augment localized cell death. Since nano-DTX-His cannot be used for intravenous therapies due its inability to cross the blood-brain barrier (BBB) *per se*, we further propose its modification with an acid-cleavable Angiopep-2 layer (nano-DTX-His-clv-Angiopep2) to favor endosome-sensitive BBB translocation via binding to the low-density lipoprotein receptor (LDLR). It is of important note that the choice of DTX is based on its IC_{50}, which is around 20.000-times lower in standard U87 GBM cells than the conventional GBM chemotherapeutic, temozolomide [1]. The graphical abstract of this project is presented in Figure 1.

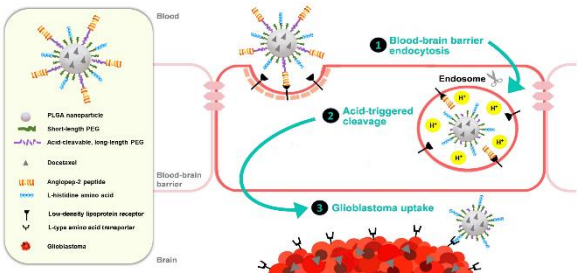

Fig 1. Graphical abstract.

Materials and Methods

Carbodiimide and carbamate hydrolysis were employed to synthesize a poly(lactic-co-glycolic) acid (PLGA) and His-functionalized polyethylene glycol (PEG) conjugate, to serve as the nano-DTX-His matrix. Nano-DTX-His was further manufactured through a scale-up microfluidic technique. To evaluate cell uptake and viability, 2D and 3D models of conventional GBM cell lines (U87, U251, U373) and primary lineages isolated from the GBM invasive margin of human tumors (GIN lineages) were used. To investigate a possible immunogenic cell death, a novel 3D high-throughput model of the GBM microenvironment was developed, including U251 GBM cells, donor-isolated monocytes from hospital buffy coats (differentiated *in situ* into macrophages), and brain primary endothelial cells (scheme of model assembly presented in Figure 2). Finally, nano-DTX-His was modified into nano-DTX-His-clv-Angiopep2 though inclusion of a PLGA-acetal-PEG-Angiopep2 conjugate (Angiopep-2 coupled with a PLGA-acetal-PEG polymer via Thiol-Michael addition) into the final nanomedicine formulation. BBB translocation was preliminarly evaluated in hCMEC/D3 endothelial cell monolayer Transwell® systems.

Results and Discussion

Monodisperse nano-DTX-His was manufactured with c.a. 250 nm and a controlled DTX release over 48 h. The uptake of nano-DTX-His was 3.5-times higher than nano-DTX-ØHis in U87, U251 and U373 GBM cell lines. In GIN lineages, cell uptake was 8-times higher than the controls. 2D studies of cell viability in GIN lineages demonstrated an anti-cancer potential of nano-DTX-His 50% superior compared to the controls, after 4 h flash and 96 h treatments. In a

heterotypic GIN 3D culture, this anti-cancer potential was kept. Moreover, in the 3D high-throughput model of the GBM microenvironment, nano-DTX-His presented 1) a 60% cytotoxicity increase compared to the controls, and 2) the capacity to polarize macrophages into an anti-tumor phenotype. Finally, nano-DTX-His-clv-Angiopep2 presented at least 3-times higher BBB translocation compared to nano-DTX-His and nano-DTX-His-Øclv-Angiopep2 in hCMEC/D3 Transwell® systems.

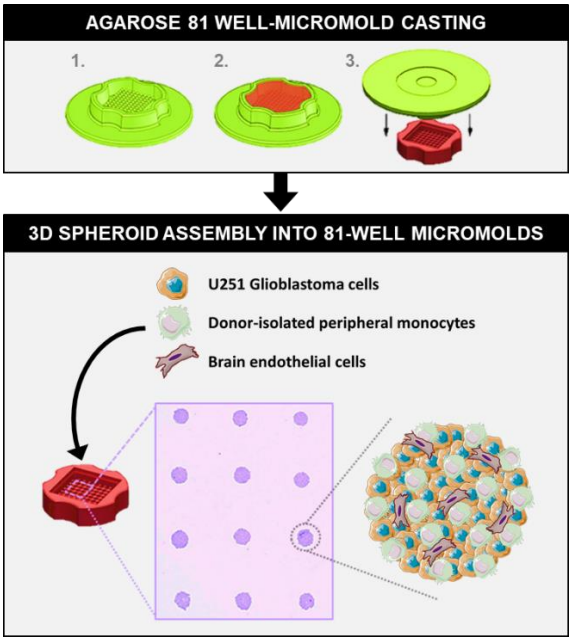

Fig 2. Scheme of assembly of the 3D high-throughput model of the GBM microenvironment, which includes U251 GBM cells, donor-isolated monocytes and brain primary endothelial cells.

Conclusions

Nano-DTX-His demonstrated better properties of cell uptake and cytotoxicity compared to the conventional therapy, in reliable 2D and 3D models of GBM. Moreover, its modification into nano-DTX-His-clv-Angiopep2 allowed the nanomedicine to acquire an ameliorated BBB translocation capacity. Ongoing work focuses on *in vivo* studies.

Acknowledgments

This work was financed by Portuguese funds through FCT - Fundação para a Ciência e a Tecnologia/ Ministério da Ciência, Tecnologia e Ensino Superior in the framework of the project “Institute for Research and Innovation in Health Sciences”, UID/BIM/04293/2019. Cláudia Martins gratefully acknowledges FCT – Fundação para a Ciência e a Tecnologia, Portugal, for financial support (grant SFRH/BD/137946/2018).

References

[1] W. Yang, J. Soares, P. Greninger, *et al*. Genomics of Drug Sensitivity in Cancer (GDSC): a resource for therapeutic biomarker discovery in cancer cells., *J. Nucleic Acids Res.* 41 (2012) D955-D961

O5.2: Nanosystems for the development of mRNA vaccines

Mireya L. Borrajo[1]*, Shubaash Anthiya[1], Gustavo Lou[1], and María José Alonso[1]

[1]*Center for Research in Molecular Medicine and Chronic Diseases, IDIS Research Institute, Department of Pharmacy and Pharmaceutical Technology, School of Pharmacy, Universidade de Santiago de Compostela, 15782, Santiago de Compostela, Spain*

*e-mail: mireya.lopez@rai.usc.es

Introduction

Considering the proven evidence of the effectiveness of mRNA vaccines in the current pandemic situation of COVID-19 disease, the importance of nanotechnology for the delivery of RNA has gained attention [1,2].

Currently, the most efficient nanosystems for the efficient encapsulation, delivery, and endosomal escape of RNA are lipid nanoparticles (LNPs), consisting mainly of lipid, ionizable, and other types of lipidic components [3].

Taking into account all the knowledge generated on the development of LNPs, here we have introduced lipids relevant for RNA transfection onto nanosystems and explored their combination with polymers for the efficient delivery of mRNA, aiming to develop a new generation of mRNA vaccines for the complexation, protection, and transfection of different types of RNA.

Materials and Methods

Nanosystems were prepared by a method designed to improve the control over their physicochemical properties. Size, polydispersity, and surface charge were determined using a Malverns Zeta-Sizer (NanoZS, ZEN 3600, Malverns Instruments). Size distribution and concentration of the nanosystems were performed using Nanoparticle Tracking Analysis (Nanosight NS300, Malverns Instruments), and encapsulation efficiency and final RNA concentration were determined using Quant-iT RiboGreen RNA assay (Invitrogen). Freeze-drying on the nanoformulations was performed using Genesis™ EL (S.P. Industries). *In vitro* studies were performed in HeLa cells, and the potency of transfection of the nanosystems was studied using mRNA encoding Green Fluorescent Protein (mGFP). *In vivo* transfection studies were performed in mice, using mRNA encoding luciferase (mLuc), after intramuscular administration.

Results and Discussion

Two different families of nanosystems were prepared, depending on the presence or absence of polymeric content on their matrix. Pure lipidic nanosystems, of 89 ± 10 nm (PdI = 0.21 ± 0.01) and positive surface charge (49 ± 6 mV); and hybrid nanocarriers (containing a combination of lipids and polymers), of 116 ± 12 nm (PdI = 0.1 ± 0.02), negative surface charge (-24 ± 7 mV) were prepared. Both families of nanosystems presented a high encapsulation efficiency. Freeze-drying process was optimized for hybrid nanosystems, by testing different cryoprotectants and frozen conditions, obtaining similar physicochemical properties after reconstitution of the nanocarriers.

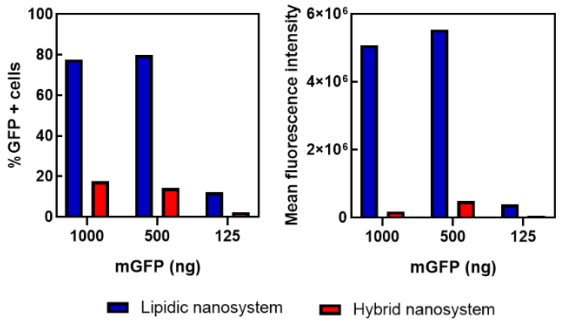

Fig 1. GFP expression in HeLa cells after transfection with lipidic nanosystems (blue) and hybrid nanosystems (red).

In vitro studies showed no cellular toxicity of any of the nanosystems at the concentrations tested. However, in terms of mGFP transfection, lipidic nanosystems reported greater GFP expression than hybrid nanosystems, in terms of percentage of transfected cells and GFP intensity, as depicted in **Fig. 1**.

Subsequent *in vivo* studies, performed after intramuscular administration of the nanocarriers containing mLuc, reported similar transfection efficiency for both kinds of nanostructures (**Fig. 2**).

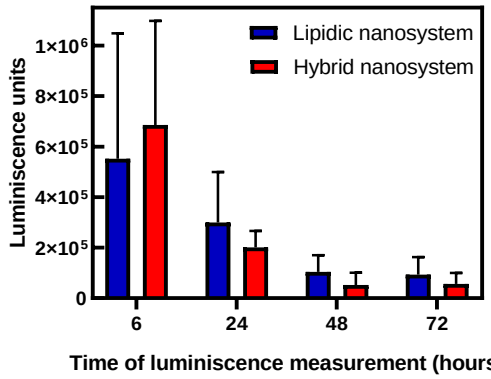

Fig 2. Luciferase expression in the muscle after intramuscular administration of lipidic nanosystems (blue) and hybrid nanosystems (red) (number of mice = 4).

Conclusions

Results showed the promising development of two families of nanocarriers that fulfill the requirements in terms of physicochemical properties to be promising candidates as mRNA transfecting agents, as their transfection efficiency has been proven both *in vitro* and *in vivo*. Lipidic nanosystems seem to perform better in terms of *in vitro* transfection efficiency, as compared to hybrid nanocarriers. However, these data did not correlate with those of the in vivo studies. Therefore, the message of this work is that the value of the in vitro data are not predictive of the in vivo behavior.

Acknowledgments

This work was supported by Insituto de Salud Carlos III project “COVARNA”, under grant agreement COV20-00214, and by the Competitive Reference Groups, Consellería de Educación e Ordenación Universitaria, Xunta de Galicia, Ref: ED431C 2017/09. ML Borrajo acknowledge the finaltial support by the Insituto de Salud Carlos III through the “Contratos i-PFIS: Doctorados ISS-Empresa en Ciencias y Tecnologías de la Salud” grant.

References

[1] N. Chaudhary, D. Weissman, K.A. Whitehead. mRNA vaccines for infectious diseases: principles, delivery and clinical translation. *Nat. Rev. Drug Discov.* 20 (2021) 817-838.

[2] P. Borah, P.K. Deb, N.A. Al-Shar’i, L.A. Dahabiyeh, K.N. Venugopala, V. Singh, P. Shinu, S. Hussain, S. Deka, B. Chandrasekaran, D.M.M. Jaradat. Perspectives on RNA Vaccine Candidates for COVID-19. *Front. Mol. Biosci.*, 8 (2021) 30.

[3] X. Hou, T. Zaks, R. Langer, Y. Dong, Lipid nanoparticles for mRNA delivery, *Nat Rev Mater.* (2021)

O5.3: mRNA Reprogramming Matrices for driving chondroblast differentiation *in vitro* and *in vivo*

H. Rilo-Alvarez[1,*], A. M. Ledo[2], M. Lopez-Peña[3], F. M. Muñoz[3], A. Vidal[4] and M. Garcia-Fuentes[1]

[1]Deparment of Pharmacy, Pharmacology and Pharmaceutical Technology, Center for Research in Molecular Medicine and Chronic Diseases, University of Santiago de Compostela, 15786, Spain.
[2]Respiratory Therapeutic Area, Novartis Institutes for BioMedical Research, Inc. 700 Main Street, Cambridge, MA, 02139, USA
[3]Department Veterinary Clinical Sciences, Faculty of Veterinary, University of Santiago de Compostela, 27002, Lugo, Spain.
[4]Department of Physiology, Center for Research in Molecular Medicine and Chronic Diseases, University of Santiago de Compostela, 15705, Spain.

*e-mail: hector.rilo.alvarez@usc.es

Introducction

The articular cartilage plays a key roll in the proper function of the locomotive system, taking part in the painless movement of joints by covering the bone end in the synovial cavity. Given the high mechanical loads that it supports, articular cartilage is subject to many age-related dysfunctions, chronic diseases as well as traumatic accidents that could lead to its partial destruction. Moreover, articular cartilage lacks the capacity to self-regenerate, originating permanent damages, or scarring tissue in the damaged area [1].

Our purpose is to modulate and enhance the regenerative process by the controlled administration of transcriptions factors (TFs) with a relevant role in the chondrogenic differentiation, like the SOX family [2]. With the aim of regenerate a functional new formed cartilage, the TFs, encoded in mRNA form, were nanocomplexed with a transfection reagent and integrated in fibrin scaffolds that simulate the extracellular environment. These constructs constitute the basic technology of our work, the mRNA Reprogramming Matrices (mRMATRIXs) [3].

Materials and Methods

The therapeutic mRNA used in this work was synthetized by in vitro transcription reactions starting from two different plasmid templates that codify the SOX9 sequence. One of the templates includes a polyT sequence in the final part of the transcript, that generates a poliA stabilizing sequence in the final mRNA molecule, with a specific molecular weight. The other is a standard plasmid lacking the poliT sequence but using a signal sequence for an enzymatic addition of the polyA tail, rendering final sequences of variable molecular weight.

As another potential optimization step of the mRNA, we compared the synthesis of polyA fixed mRNA with and without the addition of chemically modified nucleotides, obtaining, with these inclusion, normal mRNA, or chemically modified mRNA (cmRNA), theorically more stable and less immunogenic.

The integrity, expression potency and ability to triger a differentiation of cartilage of these three types of mRNA were evaluated in adipose tissue-derived mesenchymal stem cells cultures, and later as therapeutic interventions in rabbit knee defects. For these evaluations, mRNA nanocomplexes were administered dispersed in fibrin hydrogels, generated through a reaction between fibrinogen and thombin. Levels of expression of SOX9 and different pro-chondrogenic markers were quantified by qRT-PCR and some characteristic components of the extracellular environment of cartilage, like glycosaminoglycans (GAGs), were evaluated in the new formed tissues.

Results and Discussion

The results of the cell culture studies showed a clear overexpression of chondrogenic markers for mRMATRIXs with all types of active mRNAs, but specially for the systems with cmRNA and the specific polyA molecular weight. The new formed cartilage also showed a higher concentration of GAGs in cultured cartilage when formed from mRMATRIXs activated with cmRNA [Figure 1.].

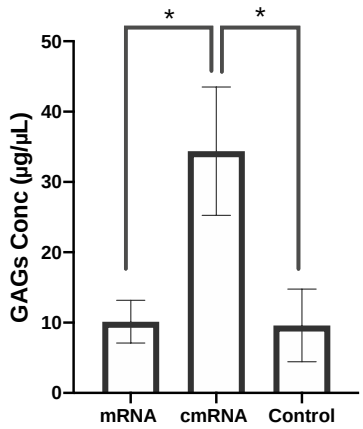

Fig 1. Concentration of GAGs in the new formed cartilage in vitro. P value < 0.05 is expressed as *.

In addition, cmRNA mRMATRIXs in the *in vivo* assays, showed an increased expression of chondrogenic markers compared to the control groups.

Conclusions

Overall, mRMATRIXs activated with nanocomplexes of optimized mRNA therapeutic molecules showed a potent induction of SOX9 and a stable activation of pro-chondrogenic genes *in vitro* and *in vivo*, indicating their great potential for cartilage differentiation.

Acknowledgments

This work was supported by by Ministerio de Economía y Competitividad (MINECO-RETOS, Grant MAT2017-84361-R, Feder Funds), and Xunta de Galicia (Grupos de Referencia Competitiva, Feder Funds). HRA was a recipient of a predoctoral grant from Xunta de Galicia (ED481A-2020/078).

References

[1] Zhao Z., Fan C., Chen F., Sun Y., Xia Y., Ji A., Wang D.-A., Progress in Articular Cartilage Tissue Engineering: A Review on Therapeutic Cells and Macromolecular Scaffolds. *Macromol. Biosci.* 2020, 20.

[2] Rilo-Alvarez H., Ledo A.M., Vidal A. *et al.* Delivery of transcription factors as modulators of cell differentiation. *Drug Deliv. and Transl. Res.* 2021, 11, pp. 426 - 444.

[3] Ledo A.M., Senra A., Rilo-Alvarez H., et al. mRNA-activated matrices encoding transcription factors as primers of cell differentiation in tissue engineering. *Biomaterials*. 2020, 247, 120016.

O5.4: Nanoclay-incorporated HA/alginate scaffolds as SDF-1 smart delivery-platforms for bone tissue engineering

I. Erezuma[1;2]*, I. Lukin[1;2], P. García-García[3], A. Delgado[3], R. Reyes [4], C. Evora[3] and G. Orive[1;2]

[1]NanoBioCel Group, Laboratory of Pharmaceutics, School of Pharmacy, University of the Basque Country (UPV/EHU), Paseo de la Universidad 7, Vitoria-Gasteiz 01006, Spain.
[2]Bioaraba, NanoBioCel Research Group, Vitoria-Gasteiz 01009, Spain.
[3]Department of Chemical Engineering and Pharmaceutical Technology, Universidad de La Laguna, 38200 La Laguna, Spain.
[4]Department of Biochemistry, Microbiology, Cell Biology and Genetics, Universidad de La Laguna, 38200 La Laguna, Spain.

*e-mail: itsasne.erezuma@ehu.eus

Introducction

Bone Tissue Engineering (BTE) is an interdisciplinary field with the formidable aim of restoring or substituting damaged tissues. Current treatments for bone fractures and diseases lack the power to totally repair tissue-involving pathologies. BTE, along with nanotechonology, could provide new tools to overcome the aforementioned obstacles. In this regard, the use of nanoreinforced 3D hydrogels to locally deliver drugs and growth factors is gaining importance [1], considering that nanomaterials have the necessary properties to act as multifunctional smart tools.

Herein, hyaluronic acid and alginate based hidrogels (C2) were created and reinforced with montmorillonate (MMT) nanoclay (M2). The combination of such materials enabled the creation of a bone-mimicking system [2,3]. What is more, these hydrogels may serve as delivery platforms for SDF-1, a potent chemokine that attracts mesenchymal stem cells and promotes bone regeneration. Once its effectiveness in vitro was confirmed, its in vivo efficiency was tested.

Materials and Methods

C2 and M2 hydrogels were prepared using thiol-modified hyaluronic acid, 8-arm PEGacrylate and alginate. In the case of M2, MMT nanoclay was added. A simple mixing technique was applied to form the different hydrogels. For in vitro tests, murine bone marrow-derived mesenchymal stem cells (mMSCs-C57 BL-6J) were added within the scaffolds.

Animal experiments were carried out in conformity with the European Directive (2010/63/UE) on Care and Use of Animals in Experimental Procedures. The animals underwent a surgery and scaffolds were implanted. At 8 weeks postimplantation animals were sacrificed and the defect area was extracted. Histology, histomorphometry and immunohistochemistry studies were performed.

Results and Discussion

C2 and M2 hydrogels were successfully manufactured and tested for bone tissue engineering purposes. First, biocompatibility was examined, since it is a crucial property for scaffolding systems. A Live/Dead assay was performed between days 1 and 14, and both C2 and M2 hydrogels showed good biocompatibility as shown in Figure 1a.

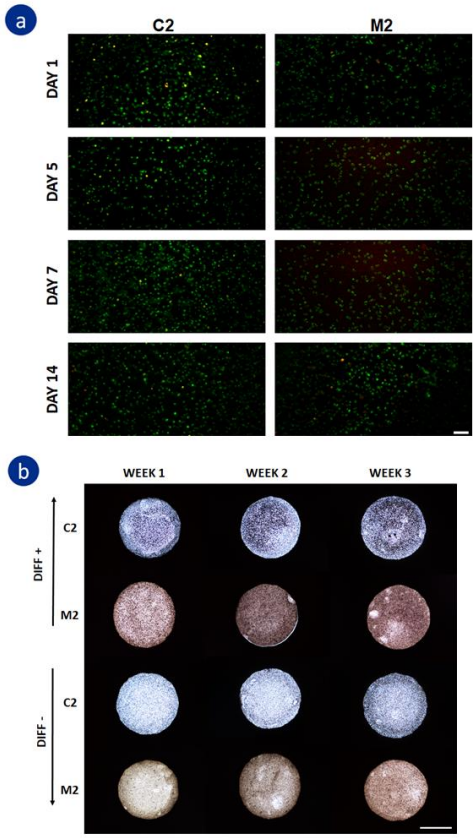

Fig 1. C2/M2 in vitro studies. (a) Live/Dead staining. Scale bar = 100 µm. (b) ALP staining between week 1 and 3. Scale bar = 1 mm.

Afterward, a protein adsorption study was realized as a first attempt to know the retention capacity of designed systems. M2 hydrogels displayed better adsorption ability than C2 ones, 0.241 ± 0.014 and 0.15 ± 0.016 $\mu g_{Protein}/mg_{Hydrgel}$ respectively. This may be due to the electrostetatic interactions generated between the nanomaterial and proteins. Besides, the osteogenic potential was observed in vitro with ALP staining study (Figure 1b). Optical images showed a gradual increase of ALP, which is an early marker of osteogenesis.

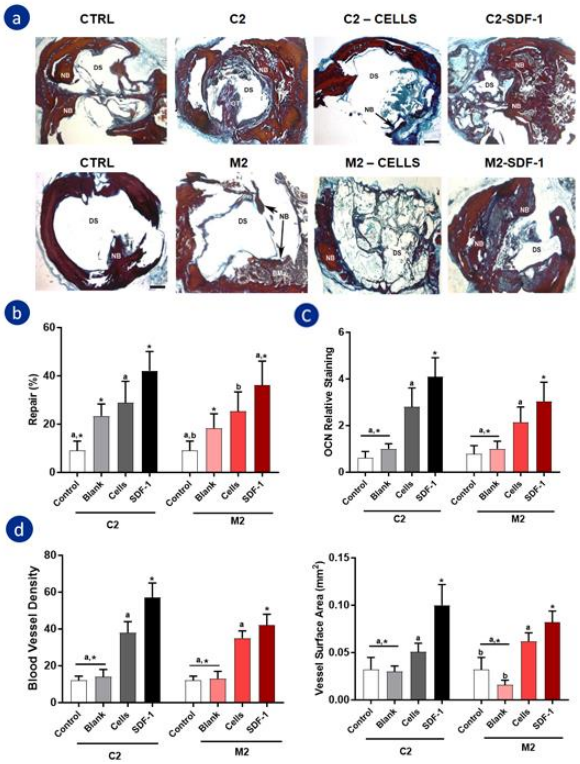

Fig 2. C2/M2 in vivo studies. (a) Representative images with VOF trichrome staining technique, showing the repair response, with both hydrogels. (b) Percentage of bone repair. (c) OCN relative staining in arbitrary units. (d) Blood vessel density and vessel surface area (mm^2) within the ROI. Histograms represent the mean ± SD BMa: Bone marrow, CT: Connective tissue, DS: Defect site, NB: Newly formed bone. Scale bar = 500 µm. *,a,b: p <0.05

Once the potentiality of scaffolds in vitro was confirmed, in vivo tests were performed. Regarding bone repair ability, C2 and M2 blank scaffolds showed greater bone repair compared to control groups after 8 week post-implantation. However, that capacity increased with scaffolds embedded with cells and even more with ones containing SDF-1 (Figure 2a,b). The results of osteocalcin (OCN) expression, marker of late osteogenesis and mineralization, showed a direct correlation with the previous results: higher relative staining was seen in the groups implanted with both hydrogels containing SDF-1 and mMSCs, being higher in the groups treated with SDF-1 (Figure 2c).

Finally, angiogenesis was examined, since it is an essential step for an appropiatte bone regeneration. The analysis of vascularization with anti-CD34 -an endothelial marker-, showed a significant increase of two vascular parameters, blood vessel density and vessel surface area (Figure 2d), in the groups implanted with both hydrogels containing SDF-1 and cells, being superior in the group treated with the chemokine.

Conclusions

HA/alginate scaffolds, fabricated with a simple mixing technique, demonstrated to be biocompatible and bioactive in vitro. Further in vivo studies confirmed their ability to regenerate bone, especially in those carrying SDF-1. Overall, it can be concluded that the developed composites may be useful as delivery-platforms for BTE purposes.

Acknowledgments

This work was supported by the Spanish Ministry of Economy, Industry, and Competitiveness (PID2019-106094RB-I00/AEI/10.13039/501100011033) and technical assistance from the ICTS NANBIOSIS (Drug Formulation Unit, U10) at the University of the Basque Country. We also appreciate the support from the Basque Country Government (Grupos Consolidados, No ref: IT907-16). I. Erezuma and I. Lukin thank to the Basque Government for the PhD grants (PRE_2020_2_0042 and PRE_2020_2_0094, respectively).

References

[1] A.K. Gaharwar, L.M. Cross, *et al.* 2D Nanoclay for Biomedical Applications: Regenerative Medicine, Therapeutic Delivery, and Additive Manufacturing, Adv. Mater. (Weinheim, Ger.). 31 (2019) e1900332.

[2] M. Hasany, A. Thakur, *et al.* Combinatorial Screening of Nanoclay-Reinforced Hydrogels: A Glimpse of the “Holy Grail” in Orthopedic Stem Cell Therapy?, ACS Appl. Mater. Interfaces. 10 (2018) 34924-34941.

[3] I. Erezuma, T. Eufrasio-da-Silva, *et al.* Nanoclay Reinforced Biomaterials for Mending Musculoskeletal Tissue Disorders, Adv. Healthc. Mater. 10 (2021) e2100217.

O5.5: Extracellular vesicles from hair follicle and adipose tissue-derived mesenchymal stem cells: Flow cytometry characterization and functional comparison for the treatment of diabetic ulcers

Kevin Las Heras[1,2], Félix Royo[3,4], Clara Garcia-Vallicrosa[3], Manoli Igartua[1,2,5], Edorta Santos-Vizcaino[1,2,5], Juan M Falcon-Perez[3,4,6] and Rosa Maria Hernandez[1,2,5]*

[1]*NanoBioCel Group, Laboratory of Pharmaceutics, School of Pharmacy (UPV/EHU).*
[2]*Bioaraba, NanoBioCel Research Group, Vitoria-Gasteiz, Spain.*
[3]*Center for Cooperative Research in Biosciences (CIC bioGUNE), Basque Research and Technology Alliance (BRTA), Exosomes Laboratory, 48160 Derio, Spain.*
[4]*Centro de Investigación Biomédica en Red de Enfermedades Hepáticas y Digestivas (CIBERehd), 28029 Madrid, Spain.*
[5]*Biomedical Research Networking Centre in Bioengineering, Biomaterials and Nanomedicine (CIBER-BBN).*
[6]*IKERBASQUE, Basque Foundation for Science, 48013 Bilbao, Spain.*

*e-mail: kevin.lasheras@ehu.eus

Introduction

In the current decade, mesenchymal stromal cells (MSCs) and their extracellular vesicles (MSC-EVs) have proven to elicit different pro-regenerative and immunomodulatory properties that are beneficial for the treatment of chronic wounds [1]. Thanks to the effects of their different mediators, MSC-EVs have demonstrated to play an important role in the proliferation, migration and cell survival of different skin cell populations [2].

Nowadays, one of the most prevalent chronic wounds worldwide are diabetic ulcers. The hyperglycemic status associated with diabetes puts at risk cells survival, causing oxidative stress and delaying the healing of diabetic wounds [3]. Despite adipose tissue derived MSCs (AT-MSCs) have been postulated as the gold standard in regenerative medicine, hair follicle derived MSCs (HF-MSCs) have demonstrated to exert a great potential for chronic wounds healing also *in vivo* [4]. Taken together, we have characterized by flow cytometry the marker expression of MSC-EVs derived from HF-MSCs (HF-EVs) and AT-MSCs (AT-EVs). The presence of different markers could suggests functional properties of EVs useful for the treatment of diabetic ulcers, among other chronic wounds. Finally, we have tested the efficacy of these EVs for the protection of human dermal fibroblasts (HDFs) against cytotoxicity when they are exposed to a hyperglycemic environment.

Materials and Methods

EVs isolation and purification

EVs were isolated and purified from the supernatant of hair follicle MSCs and adipose tissue MSCs. The collected medium was serially centrifuged at 2,000 × g for 10 min at 4ºC to discard cell debris. Then, at 10,000 × g for 30 min

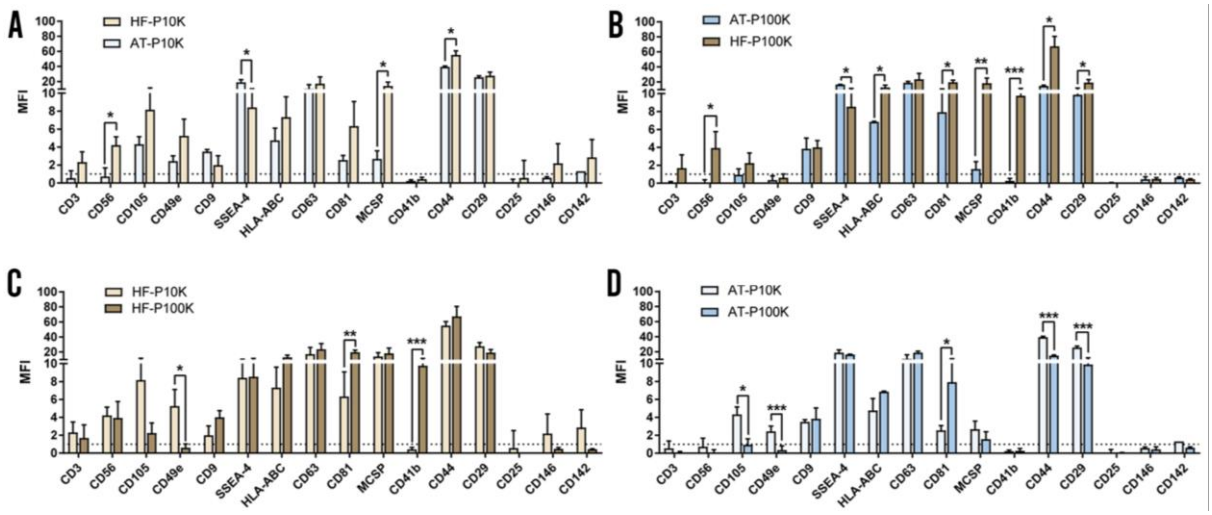

Fig 1. Flow cytometry surface marker analysis. (A) Comparison of EVs surface marker expression between AT-P10K and HF-P10K. (B) AT-P100K and HF-P100K. (C) HF-P10K and HF-P100K. (D) AT-P10K and AT-P100K. * p<0,05 between groups, ** p<0,005 between groups and *** p<0,001 between groups.

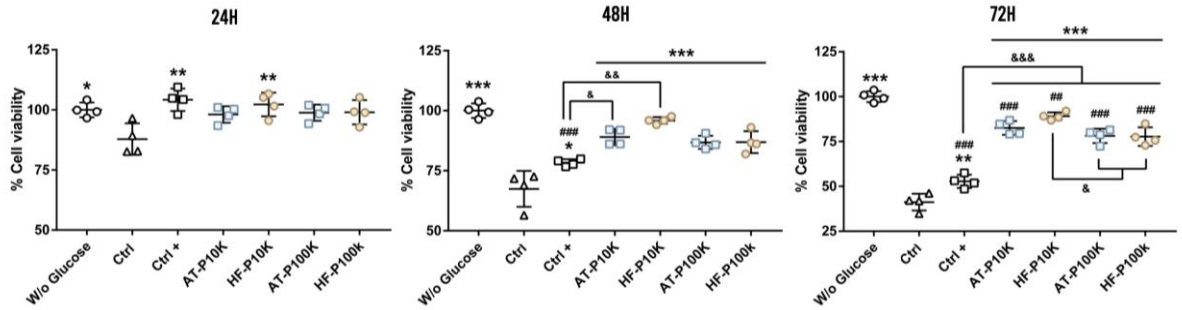

Fig 2. Cell survival under hyperglycemia assay. Percentage of cell viability under hyperglycemia. * p<0,05, ** p<0,005, *** p<0,001 against the control group. ## p<0,005, ### p<0,001 against W/o glucose group. & p<0,05, && p<0,005, &&& p<0,001 between groups.

to obtain medium/large-sized EVs (m-lEVs) — pellet 10K (P10K) — and finally centrifuged at 100,000 × g for 90 min — pellet 100K (P100K) — to obtain small-sized EVs (sEVs).

Bead-based multiplex flow cytometry assay

Samples were processed according to manufacturer's protocol (MACSPlex Exosome Kit, human, Miltenyi Biotec). A dosage of 2 µg of EVs was used for the assay. The flow cytometry analysis was performed using the MACSQuant® Analyzer (Miltenyi Biotec).

Cell survival under hyperglycemia assay

Briefly, HDFs were cultured for 24h. Then, cells were pre-treated with EVs for 6h and exposed to hyperglycemic condition of 150 mM glucose. Cells pre-treated with complete medium were used as positive control. Cells grown without EVs were used as control. The metabolic activity was monitored at 24h, 48h and 72h by CCK8.

Results and Discussion

Marker expression

EVs were evaluated by flow cytometry for the expression of 37 surface protein markers (**Fig. 1**). In addition to the typical MSC-EVs markers — CD9, CD63, CD81, CD105 and SSEA-4 — and HF-MSCs markers — MCSP and CD56 — we observed the expression of several adhesion molecules such as CD29, CD44 and CD49e — principally in P10K EVs —. Another interesting marker slightly found in both P10K EVs — but not in P100K — was CD146. Finally, we only observed CD142 in HF-P10K EVs.

Cell survival under hyperglycemia

As observed in **Fig. 2** we only obtained differences against the control group at 24h in the HF-P10K and positive control groups. However, after 48h and 72h of hyperglycemic exposure, we achieved significant differences in all the EVs treated groups against the control and positive control groups. These results may suggest that MSC-EVs are able to protect HDFs against the hyperglycemic environment of diabetic ulcers. To our knowledge this is the first time that it is described such protective effects of MSC-EVs on HDFs for both pellets and cell types.

Conclusions

In conclusion, in this work, we demonstrated the presence of the classical EV-markers among others involved in biological processes not only in sEVs, but also in m-lEVs for both cell types. Furthermore, our results depicted, for the first time in the literature, that all EVs were able to protect HDFs against a cytotoxic hyperglycemic environment.

Acknowledgments

K. Las Heras thanks the Basque Government for the PhD grant (PRE_2018_1_0412). This project was partially supported by the Basque Government (Consolidated Groups, IT 907-16).

References

[1] J. Cabral, A.E. Ryan, M.D. Griffin, T. Ritter, Extracellular vesicles as modulators of wound healing, Adv. Drug Deliv. Rev. 129 (2018) 394-406.
[2] O.P.B. Wiklander, M.A. Brennan, J. Lotvall, X.O. Breakefield, S. El Andaloussi, Advances in therapeutic applications of extracellular vesicles, Sci. Transl. Med. 11 (2019) 10.1126/scitranslmed.aav8521.
[3] P.A. Shiekh, A. Singh, A. Kumar, Exosome laden oxygen releasing antioxidant and antibacterial cryogel wound dressing OxOBand alleviate diabetic and infectious wound healing, Biomaterials. 249 (2020) 120020.
[4] D. Ma, J.E. Kua, W.K. Lim, S.T. Lee, A.W. Chua. In vitro characterization of human hair follicle dermal sheath mesenchymal stromal cells and their potential in enhancing diabetic wound healing, Cytotherapy. 8 (2015) 1036-51.

O5.6: Direct powder extrusion 3D printing of polyhydroxybutyrate implants for prolonged drug release

Sofia Moroni[1], Mattia Tiboni[2], Luca Casettari[3]

[1]Department Biomolecular Sciences, School of Pharmacy, University of Urbino, 61029, Urbino, Italy
*e-mail: s.moronii@campus.uniurb.it

Introduction

Three-dimensional printing (3DP) is a leading manufacturing technique that has aroused great interest, including in the pharmaceutical field. [1] Among the different 3DP techniques, direct powder extrusion (DPE) is a recent approach that consists of one-step production process, during which the physical blends of the selected materials, are directly processed by a single screw extruder.[2] The continuous evolution of 3D printing required the search for suitable materials, with increasing interest in sustainable and environmentally friendly products, such as biopolymers. Polyhydroxybutyrate (PHB) is biodegradable, biocompatible thermoplastic aliphatic polyester. Owing to the previously mentioned properties it can be employed in drug delivery as alternative biopolymer.[3] The aim of the present work was to explore the innovative technology of direct powder 3d-printing and investigate the potential application of polyhydroxybutyrate to manufacture subcutaneous implants for prolonged drug release.

Materials and Methods

Implants were produced by mixing PHB pellets (the polymer) and paracetamol (the model drug), without the addition of any other solvent, excipient, or plasticizer. Four formulations were manufactured and characterized: i) blank implants, made of pure PHB; ii) PHB + 10% w/w of paracetamol (P); iii) PHB + 20%P and iv) PHB + 30%P. The square shape designs of the implants were developed using CAD software, three sizes of each formulation were produced (side x height: 12x2 mm, 18x2mm, and 24x2 mm). Implants were obtained by directly feding the printing unit with the selected blend, the same printing parameters were followed except for the printing temperature that was set accordingly to the percentage of paracetamol. Printed devices were characterized focusing on the chemical structure, thermal stability, and release profile. Attenuated total reflectance fourier transformed infrared spectroscopy (ATR-FTIR) was performed at 450–4000 cm− 1 with a resolution of 4 cm−1 and a total of 64 scans. For thermal gravimetric analysis (TGA), scans were run from room temperature to 500 ◦C, at a speed rate of 10°C/min under a nitrogen flow rate of 30 mL/min. Finally, the release profile of the formulations was tested using high-performance liquid chromatography (HPLC). The release was performed for 21 days, in phosphate- buffered saline (PBS) pH 7.4, at 37°C.

Results and Discussion

Square shape implants were produced by directly printing the physical mixtures of the selected formulations containing the polymer (PHB) and different percentages of paracetamol (10%, 20% and 30% w/w) (P). One of the main advantages of direct powder extrusion 3DP is that the manifactuing process requires small amount of starting materials, indeed, approximately, 5 mg of each blend were necessary to obtain the desired design (squares of side x height: 12x2 mm, 18x2mm, and 24x2 mm). The printing temperature (170-190°C) was the only parameter that was set according to the formulation, indeed, it showed to be dependent on the amount of loaded paracetamol. This trend has already been observed and can be related to the plasticizing effect of paracetamol on polymers.[4] Printed implants, illustrated in Figure 1, showed good uniformity in dimensions and weight, suggesting that reproducibility was ensured.

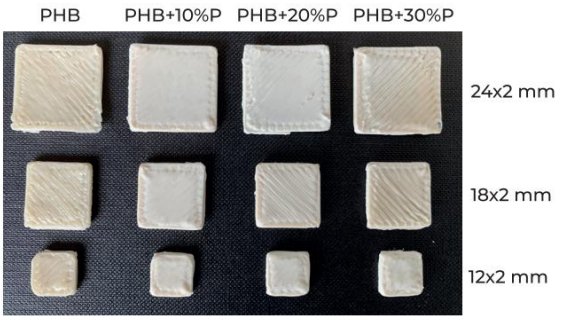

Fig 1. Showing the top view of the printed implants

As the stability of the drug is a fundamental requirment, the thermal behaviour of the printed products was investigated using TGA. Thermograms (data not reported), showed that samples were stable up to at least 200°C,

confirming that no degradation is likely to occur during the printing process.
Moreover, ATR-FTIR was performed to investigate if any interaction arosed between the polymer and the drug. Figure 2 shows the resulting spectra. Indipendently on the formulation, printed implants presented the characteristic peaks of paracetamol (related to the amide group) and PHB (related to the ester group), suggesting that both materials were successfully incorporated in the final products. [5] [6]

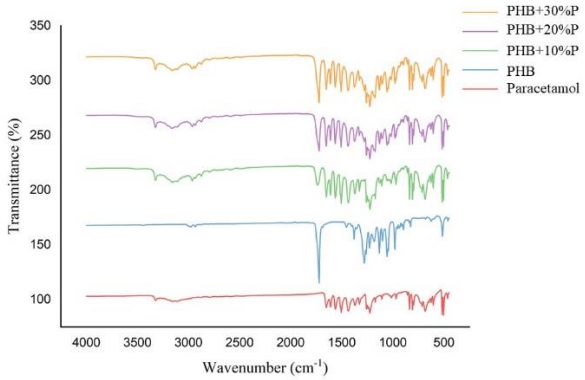

Fig 2. ATR-FTIR spectra of the printed implants and the starting materials

Finally, dissolution tests of the different designs and formulations were evaluated (Figure 3). The release profile of all the formulations demonstrated to be dependent on the dimensions of the devices, and on the amount of paracetamol loaded. Indeed, the formulation PHB+30%P (24x2) ehibited the highest release. Comprehensively, all implants showed a prolonged release of the incorporated drug.

Conclusions

In this work, we demonstrated, for the first time, the potential application of polyhydroxybutyrate and direct powder extrusion 3D-printing technique as tools to manufacture prolonged drug release implants that can be personalized based on patient's needs.

References

[1] Trenfield, S. J., Goyanes, A., Gaisford, S. & Basit, A. W. Editorial: Innovations in 2D and 3D printed pharmaceuticals. International Journal of Pharmaceutics vol. 605 (2021).
[2] Goyanes, A. et al. Direct powder extrusion 3D printing: Fabrication of drug products using a novel single-step process. (2019) doi:10.1016/j.ijpharm.2019.118471.
[3] Giubilini, A., Bondioli, F., Messori, M., Nyström, G. & Siqueira, G. Advantages of Additive Manufacturing for Biomedical Applications of Polyhydroxyalkanoates. (2021).
[4] Macedo, J., Samaro, A., Vanhoorne, V., Vervaet, C. & Pinto, J. F. Processability of poly(vinyl alcohol) Based Filaments With Paracetamol Prepared by Hot-Melt Extrusion for Additive Manufacturing. J. Pharm. Sci. 109, 3636–3644 (2020).
[5] MK, T. Effect of Biofield Treatment on Spectral Properties of Paracetamol and Piroxicam. Chem. Sci. J. 6, (2015).
[6] Ramezani, M., Amoozegar, M. A. & Ventosa, A. Screening and comparative assay of poly-hydroxyalkanoates produced by bacteria isolated from the Gavkhooni Wetland in Iran and evaluation of poly-β-hydroxybutyrate production by halotolerant bacterium Oceanimonas sp. GK1. Ann. Microbiol. 65, 517–526 (2015).

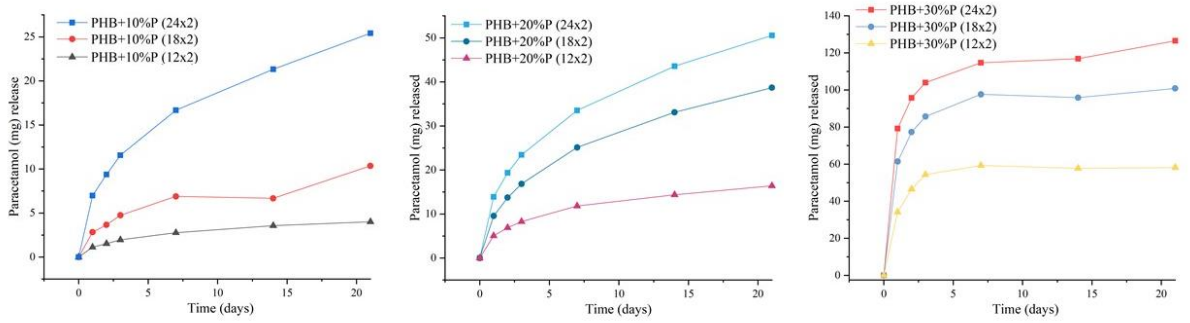

Fig 3. Release studies of A) PHB+10%P B) PHB+20%P C) PHB+30%P

Abstracts for Poster Presentation

Session 1: Technological Tools in Advanced Drug Delivery Systems

P1.1: "*Optimization of PLGA/PEI nanoparticles covered with poly(I:C) for cancer immunotherapy* ". L. Gonzalez-Melero, R.M. Hernandez, E. Santos-Vizcaino, M. Igartua. University of Basque Country. (p.89)

P1.2: "***Amoebicidal Effect of Pitavastatin Nanoparticles in Acanthamoeba castellani Neff*** ". A. Oliva, I. Sifaoui, P. Díaz-Rodríguez, J. Lorenzo, J.E. Piñero. Universidad de La Laguna. (p.91)

P1.3: "***Cell-free synthesis of Ebola virus matrix protein VP40 Virus-like particles***" S. Gutiérrez-Gutiérrez, C. Rivas-Vázquez, A Vidal, M García- Fuentes. Santiago de Compostela. (p.93)

P1.4: "***Chamomilla pollen microcapsules as multistep delivery systems***". J. L. Valverde-Fraga, J. M. Ageitos, S. Robla, N. Csaba. Universidade de Santiago de Compostela. (p.95)

P1.5: "***Gone with the Waste - Quantification of the exact composition of polymeric nanocapsules***" G. Berrecoso, J. Crecente-Campo, M.J. Alonso. Universidade de Santiago de Compostela. (p.97)

P1.6: "***Infliximab microencapsulation by Coaxial Ultrasonic Atomization preserves its biological activity: in vitro evaluation***" I. Lamela-Gómez, J. Blanco-Méndez, F.J. Otero-Espinar, A. Luzardo-Álvarez. Universidade de Santiago de Compostela. (p.99)

P1.7: "***Carvacrol-loaded microcapsules by a coaxial method for varroosis control. Effective parameters on their production***" A. Luzardo-Álvarez, I. Lamela-Gómez, X. Rodríguez-Maciñeiras, E. Fatira, A. Frías-Álvarez, A. Gracia Molina. Universidade de Santiago de Compostela. (p.101)

P1.8: "***Mucoadhesive buccal formulations based on lyophilized liposomes: application to sildenafil citrate***" A. Sánchez Navarro, P. Buján Costas, C. Maderuelo, A. Zarzuelo and M.J de Jesús Valle. Universidad de Salamanca. (p.103)

P1.9: "***Catinonic liposomal formulation for cyclopirox nail administration***" F.J. Otero Espinar, V. De Monte VIdal, V. Díaz Tomé, V. Dominguez Arca, E. Vazquez Lage, M. Casas Parada, G. Prieto Estevez. Universidade de Santiago de Compostela. (p.104)

P1.10: "***Development of a liposomal formulation containing Cyclosporin A for the treatment of dry eye disease***" M.A. González-Cela Casamayor, M.A.

Caballo González, M. Vicario de la Torre, M. Guzmán Navarro, J.M. Benítez del Castillo, E.M. González-Alonso Alegre, A. Rodríguez, B. de las Heras, R. Herrero Vanrell and I.T. Molina Martínez. Complutense University of Madrid. (p.106)

P1.11: "***Budesonide microparticles for ocular administration***" M. Guzmán-Navarro, I. González Criado, J. Rodriguez Villanueva. University of Alcalá. (p.108)

P1.12: "***New treatment for fungal keratitis: A combined eye drops of two antifungals***" V. Díaz-Tomé, X. García-Otero, R. Varela-Fernández, J. Llovo-Taboada, M. González-Barcia, A. Fernández-Ferreiro, F.J. Otero-Espinar. Universidade de Santiago de Compostela. (p.110)

P1.13: "***Bevacizumab-loaded PLGA intravitreal implants prepared by supercritical fluid technology***" C. Bendicho-Lavilla, I. Seoane-Viaño, V. Santos-Rosales, A. Luzardo-Álvarez, C.A. García-Gonzalez, F.J. Otero-Espinar. Universidade de Santiago de Compostela. (p.112)

P1.14: "***Bevacizumab loaded lipidic lyotropic liquid crystals as a promising platform for ocular diseases***" G. Blanco-Fernández, B. Blanco-Fernández, A. Fernández-Ferreiro, F.J. Otero-Espinar. Universidade de Santiago de Compostela. (p.114)

P1.15: "***Development of surface-modified lipid-polymer hybrid nanoparticles: bulk formulation vs microfluidics***" E. Briffault, H. Rouco, P. Diaz-Rodriguez, P. Garcia-Garcia, D. Molina, A. Delgado and C. Evora. Universidad de La Laguna. (p.116)

P1.16: "***Microfluidics for precise tuning of cubosome nanoparticle size***" C.J.O. Ferreira, M. Barros, C. Botelho, M.E.C.D. Real Oliveira, B.F.B. Silva. University of Minho. (p.118)

P1.17: "***Characterization and in vivo evaluation of quercetin-loaded zein nanoparticles***" R. Campión, A.L. Martínez-López, C.J. González-Navarro, E. de Paz-Barragán, C. Matías-Sainz, J.M. Irache. University of Navarra. (p.119)

P1.18: "***A Nanotechnology-based Immunotherapeutic Strategy Against KRAS mutated Colorectal Adenocarcinoma***" F. Andrade, D. Rafael, S. Montero, V.Z. Diaz-Riascos, S. Schwartz, and I. Abasolo. Vall d'Hebron Institut de Recerca. (p.121)

P1.19: "***Self-Illuminating Biocompatible Nanosystems can Induce Apoptosis Via Photodynamic Therapy (PDT)***" M. Abal-Sanisidro, L. Ruiz-Cañas, M.G. Blanco, R. López-López, B. Jr Sainz, M. de la Fuente. Health Research Institute of Santiago de Compostela (IDIS). (p.123)

P1.20: "***Evaluation of Eudragit S100 Nanofibers as pH responsive antimicrobial release system***" L. Miranda-Calderón, C. Yus ,G. Landa, M. Arruebo, G. Mendoza and S. Irusta. Universidad de Zaragoza. (p.125)

P1.21: "***Nucleic acid based medicinal products for Fabry disease: critical formulation factors to ensure effective delivery***" I. Gómez-Aguado, J. Rodríguez-Castejón, M. Beraza-Millor, A. Rodríguez-Gascón, A. del Pozo-Rodríguez and M.A. Solinís. University of Basque Country. (p.127)

P1.22: "***Fluorescence Cross-Correlation Spectroscopy reveals extent of association between liposomes and DNA and the number of DNA molecules per lipid nanoparticle***" R. Gaspar, J.L. Paris, P.A.A. De Beule, B.F.B. Silva. INL - International Iberian Nanotechnology Laboratory. (p.129)

P1.23: "***DOSY as an Alternative Technique to Monitor the Degradation of Polypeptide-Based Drug Delivery Systems***", I. Conejos-Sánchez J.J. Arroyo-Crespo, D. Morelló-Bolumar, S. Stifano, V.J. Nebot and M.J. Vicent. Centro de Investigación Príncipe Felipe. (p.130)

P1.1: Optimization of PLGA/PEI nanoparticles covered with poly(I:C) for cancer immunotherapy

L. Gonzalez-Melero[1,2], R.M. Hernandez[1,2,3], E. Santos-Vizcaino[1,2,3], M. Igartua[1,2,3]*

[1]*NanoBioCel Research Group, Laboratory of Pharmaceutics, School of Pharmacy, University of the Basque Country (UPV/EHU), Vitoria-Gasteiz, Spain.*
[2]*Bioaraba, NanoBioCel Research Group, Vitoria-Gasteiz, Spain.*
[3]*Biomedical Research Networking Centre in Bioengineering, Biomaterials and Nanomedicine (CIBER-BBN). Institute of Health Carlos III, Madrid, Spain.*

*e-mail: manoli.igartua@ehu.eus

Introduction

Polyinosinic:polycytidylic acid (poly(I:C)) is a Toll-like receptor 3 (TLR3) agonist broadly studied for cancer immunotherapy. Poly(I:C) mimics viral double-stranded (ds) RNA, that when activating TLR3 leads to a potent cell-mediated immunity response and secretion of pro-inflammatory cytokines. However, clinical application of poly(I:C) has been limited due to stability and toxicity issues. In this regard, different particulate delivery systems have been developed [1]. Nevertheless, most formulations developed for poly(I:C) delivery are micro sized, and smaller particles have been observed to be taken up by DCs more efficiently [2]. Moreover, surface assembly of poly(I:C), rather than encapsulation, helps in the formulation of the immunostimulant in mild conditions as it avoids the contact with organic solvents [1]. In this study, an easy to prepare formulation of poly (L-lactic-co-glycolic acid) (PLGA) - polyethylenimine (PEI) nanoparticles (NP) covered with poly(I:C) have been developed.

Materials and Methods

NP formulation

PLGA NPs were prepared with the solvent extraction-evaporation of a double emulsion (w/o/w) method, and coated with PEI for a positive charged surface.

The negatively charged poly(I:C) was attached to the surface by interaction with the positive surface of the NPs. Freeze-dryed NPs were incubated with poly(I:C) at 4ºC on a rotating mixer. After 3 hours, NPs were centrifuged. Supernatant was storaged for poly(I:C) indirect measurement, and NPs were resuspended in water for size and Z-potential measurements.

Size and surface charge measurements

The size and size distribution of the NPs were analysed by a dynamic light-scattering technique. The surface charge of the NPs was determined by Z-potential measurements.

Poly(I:C) determination

Poly(I:C) concentrations of the supernatants were measured with a Nanodrop spectophotometer.

Results and Discussion

Poly(I:C) is a negatively charged molecule that is able to bind with the positive charges found on NP surface. A single poly(I:C) molecule can bind more than one NP at the same time, which means that a correct NP:poly(I:C) ratio must be found to avoid NP aggregation and obtain fully covered NPs. For that aim, we first stablished the optimal NP concentration using a fixed concentration of poly(I:C) and increasing concentrations of NPs, and after, we determined the best poly (I:C) concentration using the elected NP concentration with a concentracion range of poly(I:C).

Size analysis was used to determine any aggregation of NP. NPs showed higher aggregation tendency at higher concentrations, with optimal values at 7.5 mg/ml of NP (*Fig 1*).

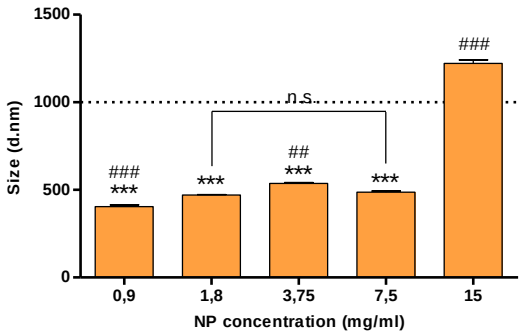

Fig 1. Size of NP at different concentrations, covered with a fixed poly(I:C) concentration (150 µg/ml). ***p<0.001 in regard to 15 mg/ml of NP, and ##p<0.005 and ###p<0.001 in regard to 7,5 mg/ml of NP.

Regarding poly(I:C), low concentration is related to higher aggregation tendency due to its capacity to bind more than one NP. On the contrary, high poly(I:C) concentration allows complete NP covering, less NP interaction, and finally, less aggregation tendency. For nano size, at least 100 µg/ml of poly(I:C) is needed (*Fig 2*).

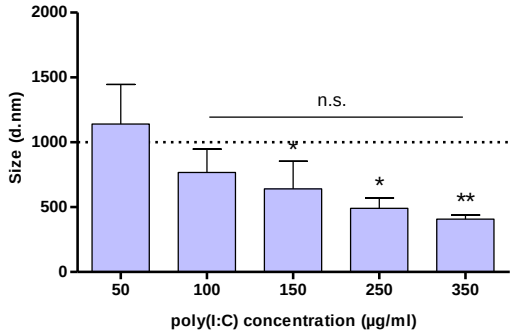

Fig 2. Size of NP covered with increasing poly(I:C) concentrations. *p<0.05 in regard to 50 µg/ml of poly(I:C).

Negatively charged poly(I:C) addition to positively charged NP decreased surface Z-potential. As in size, lower immunostimulant concentrations showed lower NP covering, leading to positive Z-potential values. While increasing poly(I:C) concentration, Z potential decreased until around -20mV values were achieved (*Fig 3*). Results showed good covering efficiency and higher attachment in a dose dependent manner, with no statistical differences from 150 µg/ml on.

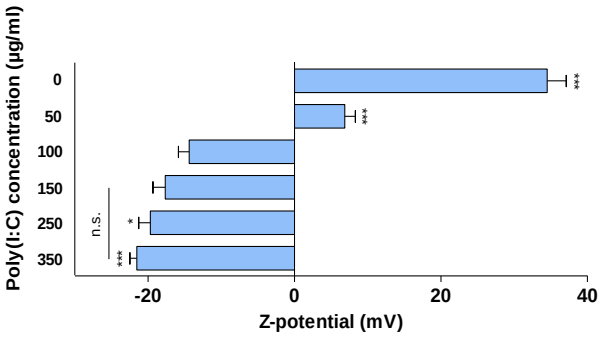

Fig 3. Z-potential of NP covered with different poly(I:C) concentrations. * p<0.05 and ***p<0.001 in regard to 100 µg/ml of poly(I:C).

Concentrations below 50 µg/ml showed complete poly(I:C) attachment, while higher ones leaded to lower covering efficiency (*Fig 4A*). This data indicates that NP surface was completely covered with concentrations above 100 µg/ml of poly(I:C). Moreover, results were in accordance with aggregation and surface potential values (*Fig 2 and 3*). Poly(I:C) loading efficiency describes a logarithmic tendency (y = -38,17ln(x) + 249,6 ; R^2 = 0,9848). In addition, although 100 µg/ml of poly(I:C) showed the minimum concentration needed for NP covering, higher concentrations improved all parameters observed. In that regard, poly(I:C) quantity loaded per mg of NP was determined. *Fig 4B* shows an increased attatchment at higher concentrations, although no statistical differences were observed.

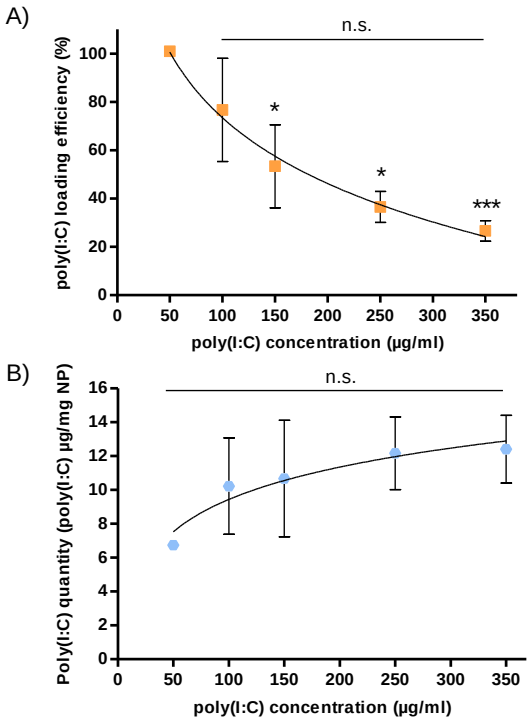

Fig 4. A) Poly(I:C) percentage loaded on the NPs. B) Poly(I:C) quantity loaded per 1 mg of NP.* p<0.05 and ***p<0.001 in regard to 50 µg/ml of poly(I:C).

Taken together, the results showed that complete covering of NP is achieved with 7.5 mg/ml of NPs and with poly(I:C) concentrations at least of 150 µg/ml.

Conclusions

In conclusion, the fact that NPs have been successfully covered with poly(I:C) suggests that the developed NPs could be an interesting system for immune activation. Moreover, w/o/w emulsion allows substances, such as tumor antigens, to be entrapped in the NPs to achieve a complete immune activation to the target of choice.

Acknowledgments

This work was supported by the Basque Government (Grupos Consolidados, IT907-16). Lorena Gonzalez-Melero thanks the University of the Basque Country (UPV/EHU) for the PhD grant.

References

[1] A.M. Hafner, B. Corthésy, H.P. Merkle, Particulate formulations for the delivery of poly(I:C) as vaccine adjuvant, *Adv. Drug Deliv. Rev*. 65 (2013) 1386-1399.

[2] A.L. Silva, R.A. Rosalia, E. Varypataki, S. Sibuea, F. Ossendorp, W. Jiskoot, Poly-(lactic-co-glycolic-acid)-based particulate vaccines: Particle uptake by dendritic cells is a key parameter for immune activation, *Vaccine*. 33 (2015) 847-854.

P1.2: Amoebicidal effect of Pitavastatin Nanoparticles in *Acanthamoeba castellanii* Neff

A. Oliva[1,2,*], I. Sifaoui[1,3], P. Díaz-Rodríguez[4], R. L Rodríguez-Expósito, J. Lorenzo-Morales[1;3,5] and J. E. Piñero[1,3,5]

[1] *Instituto Universitario de Enfermedades Tropicales y Salud Pública de Canarias, Universidad de La Laguna (ULL), Tenerife, 38206, Spain*
[2] *Departamento de Ingeniería Química y Tecnología Farmacéutica, Universidad de La alguna, 38206, Tenerife, Spain*
[3] *Red de Investigación Cooperativa en Enfermedades Tropicales (RICET)*
[4] *Departamento de Farmacología, Farmacia y Tecnología Farmacéutica, Universidad de Santiago de Compostela, 15782, Santiago de Compostela, Spain*
[5] *Departamento de Obstetricia, Ginecología, Pediatría, Medicina Preventiva y Salud Pública, Toxicología, Medicina Legal y Forense y Parasitología, Universidad De La Laguna, La Laguna, 38203, Tenerife, Spain*

*e-mail: Alexis Oliva (amolivar@ull.edu.es)

Introducction

Till present, three generation of statin were developed based on their efficacy to lower the plasma low-density lipoprotein cholesterol (LDL-C) concentration [1]. Recently, several studies have confirmed the antiprotozoal activities of those molecules [2]. Nerveless, the statin remains under-exploited in pharmaceutical industry due to their poorly solubility in aqueous solution. The aim of this study was to develop formulation of PLGA nanoparticles containing Pitavastatin to increase drug's bioavailability in aqueous media suitable for ophthalmic administration.

Materials and Methods

Chemicals

Pitavastatin (calcium salt) was purchased from Cayman chemicals (USA). Poly(lactic-co-glycolic acid Mw 7,000-17,000; PLGA) (50:50) was provided by Evonik, Ltd. (Germany). Pluronic F68 was obtained from Sigma-Aldrich (Germany). Acetonitrile Reag. Ph Eur was provided by Merk (Germany).

Pitavastatin nanoparticles synthesis

Empty and pitavastatin-loaded nanoparticles were obtained by a nanoprecipitation-solvent displacement method. Briefly the required amount of pitavastatin was dissolved in acetonitrile and mixed with a PLGA solution in acetonitrile to get a final PLGA concentration of 5% and a volume of 0.3mL. The mixture was then stirred to get an homogenous solution and, afterwards drop-wise poured on 3 mL of an aqueous solution consisting of 0.3% of Pluronic PF68. The mixture was then kept under continuous stirring for 1 hour to allow the complete removal of the acetonitrile. Nanoparticle suspensions were then sterile-filtered using PES filters of 0.22 µm pore size (Merk Millipore, Irland) and storage at 4 ºC until use.

Nanoparticle characterization

PLGA nanoparticles were characterized in terms of particle size, polydispersity index and surface charge in a Zetasizer nano ZS (Malvern Instruments, UK). To determine nanoparticle size and polydispersity, formulations were placed in polystyrene cuvettes. After that, nanoparticles surface charge was determined as zeta potential (ZP) through particle mobility in an electric field. For this purpose, a potential of ±150 mV was established. All the measurements were conducted in triplicate at 25±1°C.

Biological activity measurement

The trophocidal activity of nanoparticles was done by Almar Blue method against *Acanthamoeba castellanii* Neff.

Results and Discussion

Table 1 shows the physicochemical properties of empty (blank) or pitavastatin-loaded nanoparticles. Both formulations present an average diameter close to 130 nm with a monodisperse size distribution, polidispersity index lower than 0.3. The developed nanoparticles are characterized by a negative surface charge characteristic of PLGA.

Table 1. Physicochemical characterization of blank and Pitavastain-loaded nanoparticles

	Size (nm)	**PdI**	**ZP (mV)**
Blank	125.30 ± 2.00	0.198 ± 0.010	-37.30 ± 0.78
Pitavastatin-loaded	129.83 ± 1.72	0.202 ± 0.010	-19.97 ± 0.70

In the evaluation of the results, it could be observed that the amoebicidal activity was based on a dependent-dose application (Fig 1). Even thought, all the concentration used was able to

inhibit 80% of the present strain. The effect of Pitavastatin on the trohozoite was unsignificant beyond a concentration of 5µM.

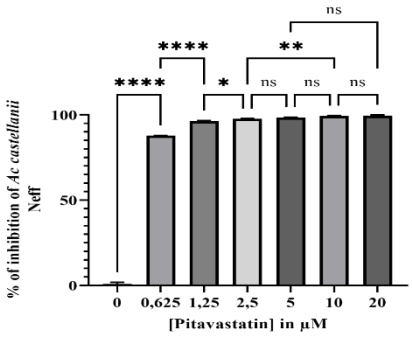

Fig 1. The effect of Pitavastatin Nanoparticles on *A. castellanii* Neff at different dosis. Differences between the values were assessed using one-way analysis of variance (ANOVA).

Conclusions

In summary, nanoparticles loaded with 5µM of Pitavastatin were able to inhibit 90% of the studied parasite; although further evaluation on clinical strains should be processed.

Acknowledgments

This study was supported by PI18/01380 (Fondo Europeo de Desarrollo Regional, FEDER) and RICET (project no. RD16/0027/0001 of the programme of Redes Temáticas de Investigación Cooperativa, FIS RLRE was funded by a grant from Agencia Canaria de Investigación, Innovación y Sociedad de la Información (ACIISI) cofunded by Fondo Social Europeo (FSE) y FEDER, (TESIS2020010117).

References

[1] Maji, D., Shaikh, S., Solanki, D., & Gaurav, K. (2013). Safety of statins. Indian journal of endocrinology and metabolism, 17(4), 636.

[2] Martín-Navarro, C. M., Lorenzo-Morales, J., Machin, R. P., López-Arencibia, A., García-Castellano, J. M., de Fuentes, I., ... & Piñero, J. E. (2013). Inhibition of 3-hydroxy-3-methylglutaryl–coenzyme A reductase and application of statins as a novel effective therapeutic approach against Acanthamoeba infections. Antimicrobial agents and chemotherapy, 57(1), 375-381.

P1.3: Cell-free synthesis of Ebola virus matrix protein VP40 Virus-like particles

S. Gutiérrez-Gutiérrez[1]*, C. Rivas-Vázquez[1,2], A. Vidal[1] and M. García-Fuentes[1,3,4].

[1]*Center for Research in Molecular Medicine and Chronic Diseases, University of Santiago de Compostela, Spain*
[2]*National center of Biotechnology (CNB), CSIC, Madrid, Spain.*
[3]*School of Pharmacy, University of Santiago de Compostela, Spain.*
[4]*Institute of health Research of Santiago (IDIS), Santiago de Compostela, Spain.*

*e-mail: sara.gutierrez.gutierrez@rai.usc.es

Introduction

Peptides and proteins are promising molecules to develop drug delivery system. Their biological kind make them biocompatible, biodegradable, and many present intrinsic molecular recognition patterns [1]. Furthermore, molecular biology and biotechnology tools allow to design sequence-customized proteins resulting in a highly functional active nanoparticle. Unfortunately, there is still a lack of a productive, robust, green, and industry-friendly technology for its obtention.

Herein, we explore cell-free protein synthesis (CFPS) as an alternative method to overcome the limitations of traditional cell-based protein synthesis (CBPS) and applied to develop Virus-like particles (VLPs).
CFPS is an *in vitro* protein synthesis technology based on using the cell machinery strictly needed for protein synthesis. Without cell physiology constraining the reaction conditions, CPFS is an open system focused on protein synthesis from a desired plasmid template and amenable to specific control in any step of the reaction [2].

Materials and Methods

We built VP40 Ebola virus VLPs by expressing a plasmid template in a CFPS system. As a reference, we generated wild VP40 VLPs by cell-transfection in HEK293 and U87 cell lines.
We implemented this technology in the lab through a commercial kit constituted by cell extracts. CFPS reaction conditions, in terms of time and temperature, were optimized for maximum protein expression and proper folding. The resulting VP40 monomer molecular weight was characterized by Western Blot analysis and further VP40 VLPs size were evaluated through Zsizer measurements and their shape by electron microscopy.

Results and Discussion

We produced VP40 VLPs by conventional CBPS, mimicking the natural process of virus replication by traditional cell transfection of an engineered plasmid containing the cDNA sequence of VP40. VP40 VLPs are both released to the supernatant and kept inner the cells. Once we confirmed VP40 was in cell culture medium through Western Blot analysis, VP40 VLPs were purified by a double ultracentrifugation process. The results confirmed the presence of nanoparticles with the shape and size typical for wild-type Ebola virions (Fig. 2A).
Then, we employed the same VP40 plasmid as a template for cell-free protein synthesis system. We confirmed that CFPS was able to produce VP40 monomer through Western Blot analysis. Afterwards, we tested a range of temperatures and reaction times to optimize the yield of this biosynthesis and achieve proper protein folding. We found out that at 27ºC and with 4h of reaction we obtained the nanoparticles most alike those previously produced by CBPS in terms of shape (Fig. 2B). Moreover, size of VP40 VLPs produced by CFPS was ~350 nm of length, close to the ones produced by CBPS, with even, lower polydispersity (Table 1.)

	VP40 VLPs CBPS	**VP40 VLPs CFPS**
size (nm)	369,6 ± 32,34	347,3 ± 70,95
PDI	0,627	0,402

Table 1; Physicochemical characterization of VP40 VLPs produced by CBPS and CFPS (n=3). PDI: polydispersity index.

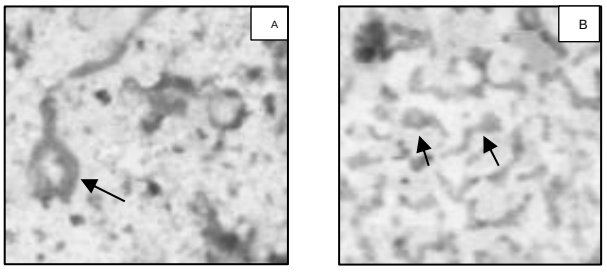

Fig 2AB. STEM images *of VP40 VLPs obtained by CBPS (A) and CFPS (B).*

Among the different synthesis conditions we tested, the higher protein yield obtained was 18,5 μg/μl. For this productivity, we performed the CFPS reaction with 10 μl of cell extract by adding 1μg of VP40 plasmid during 6h at 27ºC. However, at these

conditions VP40 monomers mostly appear aggregated (data not shown). Nevertheless. with just 4h of synthesis at the same temperature the yield was slightly lower 14,45 μg/ μl but resulting VP40 VLPs keep size and shape quite similar to wild virions in a less time-consuming reaction.

Conclusions

Cell-free protein synthesis allows to produce VP40 VLPs like those produce from cell cultures and in pathological cell infections. Moreover, through this technology we can produce VLPs faster and in productive system that allows to control the synthesis conditions.

These studies lay the foundations to produce other functional nanocarriers by this new and robust technology.

Acknowledgments

This work has been founded by Ministerio de Economía, Industria y Competitividad (MINECO-RETOS, Grant MAT2017-84361-R, Feder Founds).

References

[1] Molino NM, Wang SW. Caged protein nanoparticles for drug delivery. Curr Opin Biotechnol 2014 August 01;28:75-82

[2] Gregorio NE, Levine MZ, Oza JP. A User's Guide to Cell-Free Protein Synthesis. Methods Protoc 2019 March 12;2(1):10.3390/mps2010024.

P1.4: Chamomilla pollen microcapsules as multistep delivery systems

L. Valverde-Fraga[1;2]*, J.M. Ageitos[1], S. Robla[1;2], N. Csaba[1;2]

[1]*Department of Pharmacology, Pharmacy and Pharmaceutical Technology, School of Pharmacy, University of Santiago de Compostela, Santiago de Compostela, Spain*
[2]*Center for Research in Molecular Medicine and Chronic Diseases (CiMUS), University of Santiago de Compostela Santiago de Compostela, Spain*

*e-mail: lorena.valverde@rai.usc.es

Introduction

Pollen grains are natural microcapsules with high resistance and improved bioadhesion. In contrast with synthetic microcapsules, pollen grains present a uniform size and a unique tridimensional structure, which makes them interesting candidates for transmucosal drug delivery [1].

Notwithstanding, pollen grains should be purified, in order to eliminate environmental contaminants and possible allergens. The exploration of pollen species with diverse structural characteristics could lead to new application possibilities.

Materials and Methods

A promising candidate for obtaining such microcapsules is *Matricaria chamomilla* grains, in terms of size and structure. In this work we have proposed a protocol to produce stable pollen-based biomimetic microcapsules, as well as a complete characterization of the purification process through different steps by applying microscopy, Fourier transform Infrared Spectroscopy (FTIR), elemental and thermogravimetric analyses.

Finally, as a proof of concept of this potential drug delivery strategy, we have successfully loaded 200 nm nanoparticles with different surface modifications on the hollow pollen surface and inner core.

Nanoparticle association was confirmed using SEM and the association efficiency (AE%) of nanoparticle was estimated by the quantification of the remaining, non-loaded nanoparticles.

For *in vitro* release studies, the pollen grains loaded with fluorescent nanoparticles was incubated in simulated intestinal fluid.

Results and Discussion

At the end of the purification process, we obtained hollow pollen structures with a 3D microneedle-like surface, characterized by a multitude of nanopores, which could be interesting for drug loading and controlled release. The developed purification process was able to eliminate contaminants from the pollen grains and did not compromise its original tridimesional structure and wall morphology [2], while decreasing mass and protein content (Figure 1). Scanning electron microscopy (SEM) and confocal microscopy images showed a surface free of contaminants and the interior was free of celular organelles.

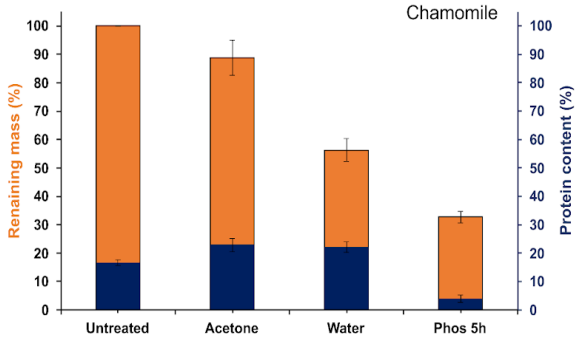

Figure 1: Remaining mass and protein content of pollen samples during purification process. [2]

A complete characterization of the purification process was also performed by microscopy, FTIR (Figure 2), elemental analysis and thermogravimetry [2].

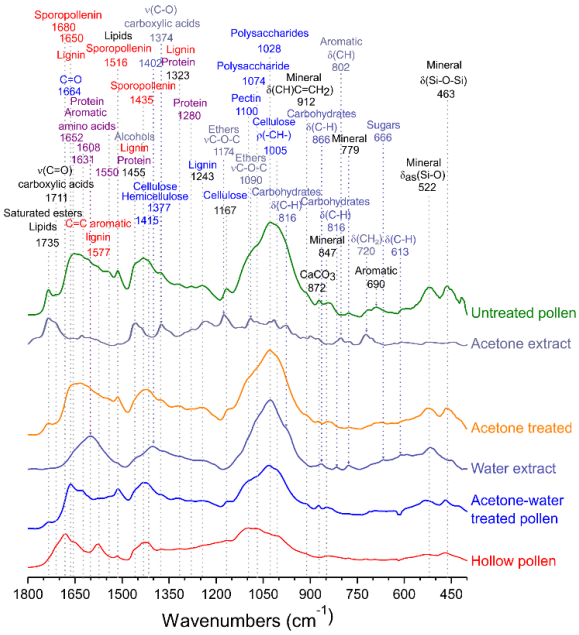

Figure 2: FTIR analysis of pollen samples.

This purification process was tested with chamomile from different origins and it was shown that the results were the same regardless of the origin of the pollen [2].

Finally, polystyrene nanoparticles of different surface modification (carboxylated, aminated and without modification) were loaded in the purified pollen. The SEM images (Figure 3) show that carboxylated nanoparticles were prone to accumulate in the inner part of the pollen, while aminated nanoparticles trended to accumulate in the external and internal surfaces of pollen. Since carboxylated nanoparticles have negative surface charge, internal accumulation can be explained by the different composition of endexine and ectexine, as the latter presents negative groups on its surface. However, it was the nanoparticles without modification that achieved a greater association efficacy (Table 1).

For *in vitro* release studies, the hollow microcapsules loaded with fluorescent nanoparticles was incubated in simulated intestinal fluid.

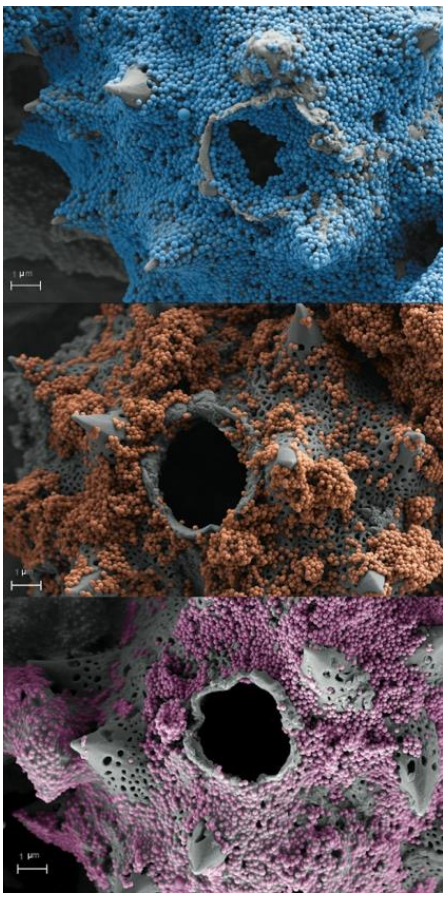

Figure 3: SEM images of pollen grains after association with 200 nm polystyrene nanoparticles (Image was artificially colored in order to increase the contrast). Blue: carboxilated, orange: aminated, pink: without modification)

Table 1: Association efficiency (AE %) of nanoparticles to matricaria pollen grains.

Modification	AE (%)	Burst (%)
Carboxilated	60.19±16.92	1.69±1.50
Aminated	70.54±4.82	1.30±0.25
Without modification	95.33±6.57	0.69±0.37

The nanoparticle release from pollen grains followed an accumulative profile in function of time, with a fast release during the initial 8 h.

In addition, the aminated particles achieved a greater release: 62,38% in 144h as compared with the other tested nanoformulation.

Although the nanoparticles without modification had the greatest association efficiency, they were the ones that presented a lower release profile (9.99% in 144h).

This could be explained taking into account that unmodified nanoparticles presented a higher proportion of aggregation than aminated and carboxylated.

Conclusions

Pollen grains can be treated to eliminate potential allergens from the surface and the inner cavity, without modyfing its original 3D structure and porous wall morphology.

Purified pollen grains could be loaded with different nanoparticles, obtaining a platform that combines the benefits of nanotechnology with the ability of pollen grains to anchor to surfaces, being an interesting candidate for the administration of drugs through the mucosa.

Acknowledgments

This work has received financial support from the Xunta de Galicia (Centro singular de investigación de Galicia accreditation 2019-2022), the European Union (European Regional Development Fund - ERDF), and Ministerio de Ciencia e Innovación, Gobierno de España – FEDER (PID2019-107500RB-I00).

References

[1] Csaba *et al. Purified pollen particles and their use to administrate nanosystems* US20200129575A1

[2] Ageitos JM, Robla S, Valverde-Fraga L, Garcia-Fuentes M, Csaba N. Purification of Hollow Sporopollenin Microcapsules from Sunflower and Chamomile Pollen Grains. Polymers (Basel). 2021 Jun 25;13(13):2094. doi: 10.3390/polym13132094.

P1.5: Gone with the Waste - Quantification of the exact composition of polymeric nanocapsules

G. Berrecoso[1,2,3]*, J. Crecente-Campo[1,2,3], M.J. Alonso[1,2,3]

[1]*Department of Pharmacology, Pharmacy and Pharmaceutical Technology, Univerdade de Santiago de Compostela, 15782 Santiago de Compostela, Spain*
[2]*Centro Singular de Investigación en Medicina Molecular y Enfermedades Crónicas (CiMUS), 15782 Santiago de Compostela, Spain*
[3]*Instituto de Investigación Sanitaria de Santiago de Compostela (IDIS), 15782 Santiago de Compostela, Spain*

*e-mail: german.berrecoso.cuna@usc.es

Introduction

Polymeric nanocapsules (NCs) are versatile nanocarriers that can deliver both hydrophobic and hydrophilic drugs, protecting them from degradation and modulating their biodistribution and clearance. [1]
Characterization of NCs usually simply addresses the actual drug content, named the association efficiency of the loaded drugs. However, since the assembling of the NCs' components is based on physicochemical interactions, the complete incorporation of the rest of components is usually also incomplete.
In this work, we have developed a liquid chromatography (LC) mass spectrometry (MS) methodology for two oils, two polysaccharides, one modified oligopeptide, and seven surfactants that are usual components of NCs. Then, the exact composition of the tested NCs was reported following the developed methodology.

Materials and Methods

NCs of approximately 150 nm were formulated by solvent displacement (SD) [1] or self-emulsification (SE) [2] techniques using several of the following compounds: DL-α-tocopherol (VitE), D-α-tocopherol polyethylene glycol 1000 succinate (TPGS), benzethonium chloride (BZT), Epikuron™ 145V (PC), hexadecyltrimethylammonium bromide (CTAB), 1,2-dioleoyl-3-trimethylammoniumpropane chloride (DOTAP), Miglyol® 812N (TGs), Kolliphor® HS15, Tween® 80 (P80), polysialic acid (PSA), hyaluronic acid (HA), and polyethylene glycol polyglutamic acid (PEG·PGA).
NCs were isolated from the formulation media by ultracentrifugation or tangential flow filtration.
The LC-MS/MS analysis was carried out in a Waters Acquity H-Class UPLC equipped with a C18 or a HILIC column and coupled to a Waters Xevo Triple Quadrupole Detector.

Results and Discussion

The method was validated in terms of specificity, linearity, quantification limits, precision, and accuracy for all the tested molecules.
The association efficiency of the surfactants and polymer resulted to be incomplete and highly formulation-specific.
In general, formulations containing surfactants with polyethylene glycol moieties possessed a higher surfactant association but lower polymer attachment (Table 1).

Table 1. Actual composition of the five tested NCs after isolation. Data is shown as mean ± standard deviation. n=3. MHS15: macrogol 15-hydroxistearate.

Formulation technique	Compound	Concentration ($mg \cdot mL^{-1}$)
SD	VitE	12.99 ± 0.84
	TPGS	3.09 ± 0.32
	HA	0.47 ± 0.08
	BZT	0.26 ± 0.03
SD	TGs	10.55 ± 0.77
	HA	0.47 ± 0.06
	PC	0.42 ± 0.08
	CTAB	0.35 ± 0.08
SD	TGs	13.20 ± 1.60
	PCs	0.46 ± 0.07
	PSA	0.45 ± 0.04
	CTAB	0.31 ± 0.04
SD	VitE	17.07 ± 1.03
	PEG·PGA	0.91 ± 0.25
	DOTAP	0.59 ± 0.02
SE	TGs	55.01 ± 4.22
	P80	13.90 ± 5.26
	MHS15	0.69 ± 0.09
	BZT	0.10 ± 0.02
	HA	0.11 ± 0.01

The highest polymer association was achieved when DL-α-tocopherol, 1,2-dioleoyl-3-trimethylammoniumpropane, and polyethylene glycol polyglutamic acid were used as components, resulting in an attachment of 53 mg of polymer per g of oil.

Conclusions

It is feasible, and highly recommendable, to perform an exact composition characterization of NCs at the laboratory level by LC-MS/MS.
The quantification of all the NCs compounds will facilitate a deeper interpretation of *in vitro* and/or *in vivo* data, e.g. biodistribution profiles, but also facilitate the rational design of new NCs prototypes.

Acknowledgments

This work was supported by the Spanish Ministry of Economy and Industry. Project “Nano-Inmunoterapia: Targeting In-tracelular de Células Tumorales y Tams” 2-INTRATARGET (Ref.: MINECO- PCIN-2017-129/ AEI), under the frame of Eu-roNanoMed III" and by the Competitive Reference Groups, Consellería de Educación e Ordenación Universitaria, Xunta de Galicia, Ref: ED431C 2017/09. G. Berrecoso acknowledges the financial support by the Xunta de Galicia through the “Axudas de apoio á etapa predoutoral 2018” grant, co-funded by the Euro-pean Social Fund “FSE Galicia 2014-2020” (Ref.: ED481A-2018/047).

References

[1] J. Crecente-Campo, M.J. Alonso. Engineering, on-demand manufacturing, and scaling-up of polymeric nanocapsules, *Bioeng Transl Med.* (2018), 38-50.

[2] A. Cadete, A. Olivera, M. Besev, , *et al*. Self-Assembled Hyaluronan Nanocapsules for the Intracellular Delivery of Anticancer Drugs, *Sci Rep*. (2019), 11565.

P1.6: Infliximab microencapsulation by Coaxial Ultrasonic Atomization preserves its biological activity: *in vitro* evaluation

I. Lamela-Gómez[1;2;3]*, J. Blanco-Méndez[1;2;3], F.J. Otero-Espinar[1;3] and A. Luzardo-Álvarez[1;2;3]

[1]*Department of Pharmacology, Pharmacy and Pharmaceutical Technology, Faculty of Sciences, Universidade de Santiago de Compostela, 27002 Lugo (Campus Terra), Spain*
[2]*Department of Pharmacology, Pharmacy and Pharmaceutical Technology, Faculty of Pharmacy, Universidade de Santiago de Compostela, 15705 Santiago de Compostela (Campus Vida), Spain*
[2]*Paraquasil Group, Health Research Institute of Santiago de Compostela (IDIS), Santiago de Compostela, Spain.*

*e-mail: ivan.lamela@usc.es

Introduction

Since the first approval by FDA of the chimeric monoclonal antibody Infliximab (Remicade®) for the treatment of Crohn's Disease (1998) and Rheumatoid Arthritis (1999), anti-TNF-α monoclonal antibodies has become established as a treatment in patients which exhibit a persistent activity of the diseases or an inadequate response to traditional drugs. Concisely, infliximab in single therapy or combination with traditional Disease-Modifying Anti-Inflammatory Drugs (DMARDs) has been demonstrated to exhibit high efficacy in inducing and maintaining pain relief and clinical remission of Rheumatoid Arthritis (RA). Nevertheless, its systemic adverse effects often lead to therapy discontinuation and limit its use as a first-line treatment in RA patients with a non-complicated disease pattern [1].

Local administration of infliximab has been explored as an alternative to achieve a high drug concentration on the site of inflammation and avoid its systemic adverse effects, but its use is limited due to the high clearance rate from the joint [2]. Microencapsulation seems to be an attractive approach to overcome those limitations, allowing us to increase the retention time of the drug into the joint and providing a sustained release profile. Microencapsulating monoclonal antibodies while preserving their stability represents a significant challenge due to their complex secondary and tertiary structure, essential for their biological activity. Coaxial ultrasonic atomization is an innovative approach to obtaining core-shell polymeric microcapsules (MCs) in mind conditions, being a suitable technique for microencapsulation of proteins and labile drugs, as previously reported [3].

This work's main objective is to develop and characterize infliximab-loaded MCs made of Polyactive® 1000PEOT70PBT30 and its polymeric blends with Resomer® RG 502 (PLGA502) and Resomer® RG 503 (PLGA503). Infliximab stability after microencapsulation was also evaluated.

Materials and Methods

Infliximab-loaded microcapsules were fabricated using a coaxial ultrasonic nozzle operated at a fixed frequency (60 kHz) and variable power (Sono-Teck Corp., USA). Three different polymeric compositions were employed to assess their influence on the features of the microparticles (Table 1). Briefly, an infliximab aqueous solution was infused through the inner channel at a constant flow rate of 0.3 ml/min, whereas a 4% (w/w) polymeric dispersion in CH_2Cl_2 was fed through the outer channel (1.5 ml/min). The fine spray generated was collected over a PVA stirring solution, and subsequently, the solvent was removed by rotaevaporation. Finally, microcapsules were washed twice with deionized water, isolated by filtration, and dried under vacuum.

Formulation	Polyactive®	PLGA502	PLGA503
F1	100 %	0 %	0 %
F2	65 %	35 %	0%
F3	65%	0 %	35 %

Table 1. Polymeric composition of the microcapsules

Microparticulate formulations obtained were characterized in terms of process yield, particle size distribution (laser diffraction), ζ potential (Electrophoretic light scattering), surface and inner morphology (SEM), surface hydrophobicity (Rose Bengal adsorption assay) and thermal stability (DSC). Infliximab-polymeric matrix and polymer-polymer physicochemical interactions were studied by FTIR. The structural stability of infliximab released from the microcapsules was analyzed by SDS-PAGE.

Cell compatibility of empty and infliximab-loaded MCs after co-incubation with cells for 24 hours was assessed by XTT cytotoxicity assay in THP-1 cells previously differentiated into macrophages. Moreover, phagocytosis activity of THP-1 derived macrophages in the presence of fluorescent coumarin 6-labelled MCs was investigated.

In vitro neutralization of bioactive TNF-α by free Infliximab and Infliximab-loaded microcapsules was assessed in LPS stimulated THP-1-derived

macrophages. TNF-α activity in the supernatants of THP-1 cells in the absence of treatment and after treatment with free and microencapsulated infliximab was measured by TNF-α bioactivity assay performed in WEHI-13VAR cell line, which exhibits high sensitivity to TNF-α. Cell survival was measured by XTT assay.

Results and Discussion

Spherical microcapsules containing infliximab were successfully prepared by coaxial ultrasonic atomization with high process yield and encapsulation efficiency. All formulations exhibited slightly negative surface charge according to ζ potential results (*Table 2*).

	P.Y (%)	E.E. (%)	ζ Potential (mV)
F1	84.2 ± 2.1	69.7 ± 1.7	-25.3 ± 0.4
F2	94.5 ± 1.9	70.3 ± 1.1	-19.8 ± 0.3
F3	91.3 ± 1.7	80.2 ± 1.4	-20.5 ± 0.4

Table 2. Process yield (PY), Encapsulation Efficiency (EE) and ζ potential of infliximab-loaded MCs

Particle size analysis showed a significant influence of the polymeric composition on particle size distribution. Concisely, F2 exhibited a significantly smaller mean particle size and narrower distribution, probably due to the lower molecular weight of PLGA 502 in comparison to PEOT-PBT and PLGA 503 (*Figure 1*). SEM micrographs showed spherical, smooth surface microcapsules with a core-shell structure.

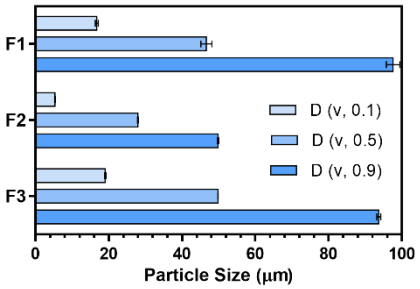

Figure 1. Particle size analysis by laser diffraction

DSC and FTIR analysis confirmed the absence of drug-polymer and polymer-polymer chemical interactions, suggesting that the polymeric blend is a simple mixture of both polymers.

Microcapsule's biocompatibility was assessed in THP-1 macrophages, achieving high viability rates (95-100 %) for all formulations assayed. Further, THP-1-derived macrophages exhibited a high phagocytosis activity after incubation with MCs for 2.5 hours (*Figure 2*).

SDS-PAGE of infliximab p6erformed under reducing and non-reducing conditions showed, respectively, two bands at 25 and 50 KDa and a single band at 150 KDa, confirming the stability of infliximab´s primary structure. TNF-α bioactivity assay showed that the treatment of LPS-

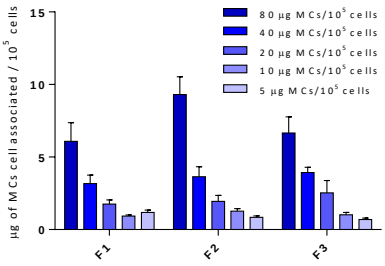

Figure 2. Micrograms of MCs phagocyted by THP-1 macrophages after incubation for 2.5 hours.

stimulated THP-1 macrophages with infliximab-loaded microcapsules leads to the complete neutralization of bioactive TNF-α, confirming that infliximab preserves its biological activity after the microencapsulation process regardless of the polymeric composition *(Figure 3).*

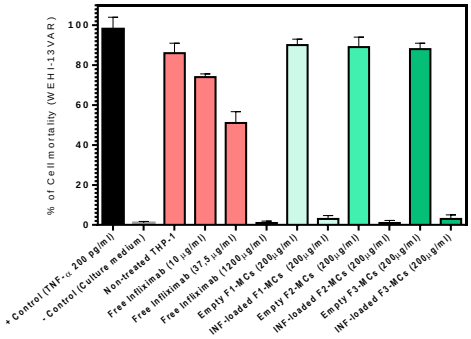

Figure 3. TNF-α biological activity assay results.

Conclusions

Biocompatible Infliximab-loaded microcapsules with satisfactory features for intra-articular administration and macrophage targeting were successfully prepared. Infliximab's biological activity was preserved after microencapsulation as demonstrated by the TNF-α bioactivity assay in WEHI-13VAR cell line. Preliminary results of still unconcluded *In vitro* delivery assays suggested a long-term infliximab delivery profile.

Acknowledgements

ILG acknowledges to "Programa de axudas á etapa predoutoral da Xunta de Galicia".

References

[1] F. Atzeni, L. Gianturco, R. Tallota, V. Varisco, M.C. Ditto, M. Turiel, P. Sarzi-Puttini, Investigating the potential side effects of anti-TNF therapy for rheumatoid arthritis: cause for concern?, *Immunotherapy*. 7 (2010) 353-361.

[2] C.H. Evans, V.B. Kraus and L.A. Setton, Progress in intra-articular therapy, *Nat. Rev. Rheumatol.*10 (2014) 11-22.

[3] S.R. Hwang, D.H. Seo, Y. Byun and J.W. Park, Preparation and in vivo evaluation of an orally available enteric-microencapsulated parathyroid hormone (1-34)-deoxycholic acid nanocomplex, *Int. J. Nanomed.* 11 (2016) 4231-4246.

P1.7: Carvacrol-loaded microcapsules by a coaxial method for varroosis control. Effective parameters on their production.

A. Luzardo-Álvarez[1,2]*, I. Lamela-Gómez[1,2], X. Rodríguez-Maciñeiras[1;2], E. Fatira[3], A. Frías-Álvarez[3,] A. Gracia Molina[3]

[1]*Department of Pharmacology, Pharmacy and Pharmaceutical Technology, University of Santiago de Compostela (Faculty of Sciences-Campus de Lugo), Spain.*
[2] *Paraquasil Group, Health Research Institute of Santiago de Compostela (IDIS), Santiago de Compostela, Spain.*
[3] *University of Las Palmas de Gran Canaria, Spain.*
*e-mail: asteriam.luzardo@usc.es

Introduction

With emerging interest, natural treatments based on Essential Oils extracted from different species of aromatic plants such as *Origanum spp* have evolved as a promising therapeutic tool against the infection of honeybee (*Apis mellifera*) colonies by the ectoparasitic mite *Varroa destructor* [1]. Conventional treatments are based on synthetic acaricides, which have been demonstrated to generate parasite resistance and the accumulation of persistent residues in hive derived products such as honey or wax[2].

In this work, Carvacrol (CRV) represents a potential miticide candidate in honey hives as an alternative to synthetic chemicals. Furthermore, encapsulation technology is explored as an approach to achieve a controlled release of CRV, improve its stability and protect its biological activity under environmental conditions [3]. Concisely, CRV was incorporated in core-shell microcapsules with an oily core surrounded by a hydrogel shell composed of Calcium Alginate and Sodium Carboxymethyl Cellulose (CMC). An experimental design was used to determine the effect of CRV loading and cross-linking agent concentration on the microcapsules' properties in terms of morphology and CRV delivery rate. In order to further investigate the applications of the optimized formulation against varroa mite infestation, *in vivo* assays were performed to test the biological compatibility of the microcapsules in the presence of *Apis mellifera*.

Materials and Methods

Spherical core-shell beads containing CRV were obtained using an Encapsulator B-390 equipped with a coaxial vibration nozzle (Büchi Ibérica S.L.U., Barcelona, Spain) and immediately solidified by ionic gelation technology. To obtain the microcapsules, a mixture of CRV and sunflower Oil (SFO) at different ratios was fed through the inner channel of the coaxial nozzle, whereas a hydrogel containing a 1% of Sodium Alginate and 1% of CMC was infused through the outer channel. The diameter of the nozzle's internal (core) and external (shell) channels were set, respectively, at 900 µm and 450 µm. Operation parameters of Encapsulator B-390 were kept constant and set at an air pressure of 500 mBar, a Frequency of 400 Hz (amplitude 3) and an electrode voltage of 1500 V. In this technique, air pressure promotes the flux of both channels through the nozzle, frequency is a critical parameter to successfully cut the outlet flux into droplets and electrode voltage modulates the repulsion forces between the droplets to avoid its confluence and guarantee its spherical shape. Obtained microcapsules were collected over a $CaCl_2$ stirring solution placed at 24 cm from the nozzle and then incubated for 30 minutes at room temperature to allow the solidification of the beads. Finally, microcapsules were isolated by filtration and stored at 4°C.

Further, a central composite rotatable experimental design was built to assess the influence of the CRV content in the core solution (CRV: SFO mixture; 30.00 - 100.00% w/w) and the concentration of cross-linker agent ($CaCl_2$; 0.97 - 10.03%(w/v)) on the particle size, sphericity, and essential oil delivery profile of the microcapsules. Experimental results were fitted to a regression model, and optimal formulations were selected by surface response methodology

All formulations obtained were characterized in terms of particle size, process yield and carvacrol loading. For particle size analysis, photographs of microparticles were taken against a black background using a high-resolution camera and then were analyzed using the ImageJ software package (National Institutes of Health, USA). A scale was included in all photographs for calibration, and all measurements were performed in triplicate.

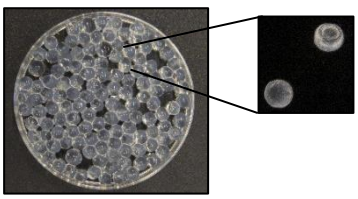

Fig 1. CRV-loaded microcapsules (optimized formulation).

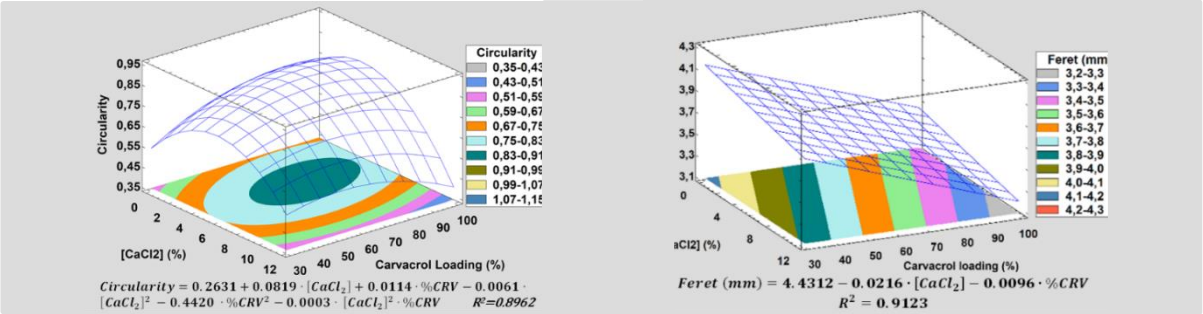

Fig 2. Surface-response graphs for circularity and particle size of CRV-loaded microcapsules.

Bioassays using CRV and CRV-loaded microcapsules in honeybees were performed using microcolonies with 200 adult bees in chambers incubated with water and food at 32°C for 96 hours (n=4).

Results and Discussion

All formulations included in the experimental design were successfully obtained with high loading efficiency and mean sizes between 3.35-4.04 mm, showing a monodisperse distribution. All capsules prepared exhibited spherical shape and high circularity values, ranging between 0.72 and 0.86 (Figure 1). Experimental results of particle size were fitted to a multiple regression linear model, whereas a multiple regression quadratic model describes the influence of the investigated variables on circularity (Figure 2).

The ANOVA analysis showed a statistically significant relationship between both parameters studied and Feret diameter (p-value<5). The linear multiple regression model can explain 91.23% of the variability in particle size. Although both parameters exhibited an inverse proportional relationship with Feret diameter, CRV loading has been demonstrated to have a more significant effect over particle size than [$CaCl_2$]. The influence of the investigated parameters on the circularity of the microcapsules was described by a multiple regression quadratic model, explaining 89.62% of the variability in circularity by changes in CRV loading and cross-linker concentration. As shown in Figure 2, $CaCl_2$ concentration has a greater impact on beads circularity than CRV loading, being the optimal region next to the central point of the experimental design.

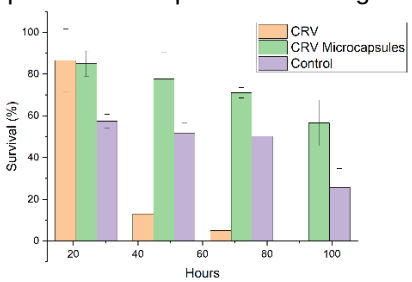

Fig 3. Honeybees' survival in microcolonies (n=4) after exposition to free and microencapsulated CRV. for

At 48h, CRV exhibited mortality of 13,45% of bees compared with non-treated colonies. At 72h, the mortality of CRV was increased to 86.85% due to the high accumulation of volatilized CRV in the chamber. In contrast, the mortality observed with CRV-loaded microcapsules were demonstrated to be significantly lower, showing even higher survival rates compared with control groups (Figure 3).

Conclusions

Microencapsulation of CRV can benefit from biodegradable materials capable of improving its stability and prolonging its release under environmental conditions, increasing its biological activity. Coaxial microencapsulation technology can protect CRV from environmental conditions, stabilizing it in an active core, allowing coating materials to be easily handled for the application. CRV-loaded microcapsules have been shown safe in honeybee microcolonies. Further release studies are going. Also, future long-term studies are needed to confirm these results in colony development and productivity.

Acknowledgements

This work was supported by to "Grupos Operativos Supraautonómicos; Varroaform"; Ministerio de Agricultura, Pesca y Alimentación.

References

[1] Sabahi, Q. et al. Continuous release of oregano oil effectively and safely controls Varroa destructor infestations in honey bee colonies in a northern climate. Exp. App. Acarology. 72: 263-275. 2017.

[2] Higes, M. Assesing the resistance to acaricides in *Varroa destructor* from several spanish locations. Parasitology Res. 119: 3595-3601. 2020.

[3] Bakry A.M. et al. Microencapsulation of oils: a comprehensive review of benefits, techniques and applications. Comprehensive Rev. Food Sci. Food Safety. 15 143-182. 2015.

P1.8: Mucoadhesive buccal formulations based on lyophilized liposomes: application to sildenafil citrate

A. Sánchez Navarro[1,2*], P. Buján Costas[1], C. Maderuelo[1], A. Zarzuelo[1] and M.J de Jesús Valle[1;2]

[1]*Department of Pharmaceutical Sciences, Faculty of Pharmacy, University of Salamanca, 37007, Salamanca, Spain*

[2]Institute of Biomedical Research, University of Salamanca, 37007*, Salamanca, Spain*

*e-mail: asn@usal.es

Introducction

In recent years, buccal formulations have received increasing interest for both systemic and local drug delivery [1]. Fast dissolving tablets and films are useful for patients with swallowing difficulties and mucoadhesive systems have shown excellent results for topical effects. On top of that, drugs that undergo high hepatic extraction or degradation in the gastrointestinal tract may benefit from buccal absorption, via venous drainage to the superior vena cava. The aim of this study was to develop mucoadhesive formulations based on lyophilized liposomes for sustained drug release at the oral cavity. Sildenafil citrate was chosed a prototype drug.

Materials and Methods

Liposomes were prepared by a previous described method based on the mixture of components at 45ºC under ultrasonic agitation, followed by extrusion and pH gradient application for remote drug loading [2].

Next, mannitol (M), lactose (L) sodium alginate (A) and carboxymethylcellulose (C) were assayed as cryo/lyoprotectvive and gelling agents. The following conditions were studied:

- M (2%) + L (2%) + A (1%).
- A (1%) + C (1%)

Samples were lyophilized using a Nuaire Ultralow freezer (-80ºC±3ºC) and a Telstar Cryodos laboratory freeze-dryer. Then compacted using an ecccentric tabletting machine (Bonals BMT) with 11 mm punches.

A swalling assay was performed in an orbital incubator at 36ºC, using artificial salivary fluid. The swallen index (SI) were estimated from initial and final weight of lyophilized tablets (Wi and Wf, respectively), according to the next equation:

$$SI\ (\%) = [(Wf-Wi)/Wi] \times 100$$

In vitro dissolution study was done using USP type II paddle dissolution apparatus, with slow agitation (25 rpm). Each tablet was placed on a small glass piece and submerged into the vessel with Milli-Q water. Samples were withdrawn at regular time intervals for quantification of total and free drug, by a previously described HPLC method [2]. Centrifugation at 4ºC was carried out to separate free drug. For statistical comparison of drug profiles, the similitud factor (*f2*) was estimated.

Results and Discussion

Gelling agents showed crio/lyoprotection ability and protected liposomes from compactation. Figure 1 shows the swelling and and drug release profiles.

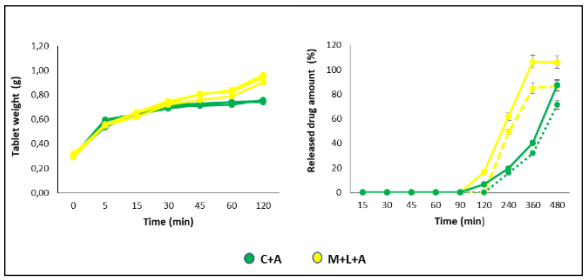

Fig 1. Swelling (left panel) and drug release (right panel) mean profiles.

Differences in sweeling profiles between tablets were not significant, but a significative delay in drug release was observed for tablets with A+C. A lag time (60-90min) was observed, irrespectively of using A or A+C as gelling agent.

Conclusions

1. Gelling agents protected liposomes during lyophilization and cake compactation.
2. A lag time (60-90 min) was observed. The drug release profile was more rapid for tablets with a single gelling agent.
3. Gelling agents in lower % will be assayed to shorten lag time.

Acknowledgments

This work was supported by University of Salamanca.

References

[1] S. Hua. Advances in nanoparticulate drugs delivery approaches for sublingual and buccal administration. *Frontiers in Pharmacology.* 10 (2019) 1-9

[2] M J. de Jesús Valle, et al. Lyoprotective effects of mannitol and lactose compared to sucrose and trehalose. Sildenafil citrate liposomes, as a case study. *Pharmaceutics*. 13 (2021) 1164

P1.9: Catinonic liposomal formulation for cyclopirox nail administration

O. E. Francisco J.[1]*, D M.V. Vinicius[1], D. T. Victoria, A. D. Vicente, V. L. Emilio[1;2], C.P. Matilde[3], P.E. Gerardo[2].

[1]*Pharmacology, Pharmacy, Pharmaceutical Technology Department, Faculty of Phamarcy, University of Santiago de Compostela (USC), Spain.*
[2]*Applied Physical Department, Faculty of Physic, University of Santiago de Compostela (USC), Spain.*
[3]*Physical Chemistry Department, Faculty of Phamarcy, University of Santiago de Compostela (USC), Spain.*
[4]*Clinical Pharmacology. Universital Clinical Hospital Health Research Institute Foundation of Santiago of Compostela, Spain.*

*e-mail: francisco.otero@usc.es

Introducction

Onychomycosis is an infectious disease caused by different species of fungi that affects the nail. The pharmacological management of this disease is complicated due to the poor penetration of drugs administered through the nail plate, which leads the patient to a prolonged topical or oral antifungal therapy. Cyclopirox belongs to the pyridone family and is widely used in the onychomycosis treatment [1].

Liposomes are a vesicular colloidal system formed by phospholipids agregation. Phospholipids can improve permeation into biological matrices and the controlled drug release [2]. Furthermore, the phospholipids are biocompatible, biodegradable and suitable for hydrophobic drugs release.

Materials and Methods

Materials: Gemini tensioactive (GS-12) (USC ReactyCat (GI-1935)), Dypalmitoyl Phosphatidylcholine (DPPC) (Avanti Polar Lipids Inc.), Cyclopirox olamine (Fagron Iberica S. A. U, Spain).

Synthesis of liposomes: The synthesis of liposomes was carried out by lipid film hydration. GS-12, DPPC and CPO were dissolved in chloroform/methanol 5:1. Then, the solution was dried in a rotavapor system (bath temperature 60ºC) until complete dryness. The film obtained was hydrated with MilliQ® water and maintained 20 min in an ultrasonic bath at 60ºC.

DPPC:GS12 ratio was 100:2 (mol:mol). Then, 20, 40, 90, 120 and 150 CPO ratios was added.

Characterization of liposomes: The system characterization was carried out by differential light scattering (DLS), pressure-area isotherm and TEM. The release study was performed by *in vitro* studies in vertical Franz cells using a membrane of 0.22 μm of diameter. Transungeal delivery studies were performed in vertical Franz cells using bovine hoof of equal thickness as biological sustrate.

Drug concentration into the receptor medium (Phosphate saline solution) was determined spectrophotomoetrically

Results and Discussion

Differential light scattering (DLS)

DLS data are shown in table 1. A decrease in particle size was observed until the ratios of DPPC:GS12:CPO approached 100:2:100. The PDI was less than or equal to 0.35 for all mixtures, indicating that the system remains monodisperse. The ζ-potential results showed values above +35mV indicating electrostatic stability. Furthermore, these ζ-potential values enhance the possible bioadhesion of the liposomes to the nail keratin matrix (negative charge).

Table 1. DLS results

Ratio molar DPPC:GS12:CPO	Size radius (nm)	ζ-potencial (mV)	PDI
100:2	56.46	51.2	0.29
100:2:20	40.78	49.1	0.24
100:2:40	38.07	40	0.35
100:2:90	31.1	37.9	0.26
100:2:120	42.54	38.9	0.25
100:2:150	44.7	39	0.32

Pressure-area isotherm

Pressure-area isotherm studies were performed using the Langmuir monolayer technique. Only the drug-free system was used for this study. The incorporation of GS12 in the DPPC monolayer in the proportion used in liposomes increases the maximum pressure at which the DPPC monolayer can be compressed, as can be seen in *Figure 1*. This indicates an increase in the stability of the monolayer, and can be extrapolated to the liposomal system, understanding that GS12 provides stability to the colloidal system.

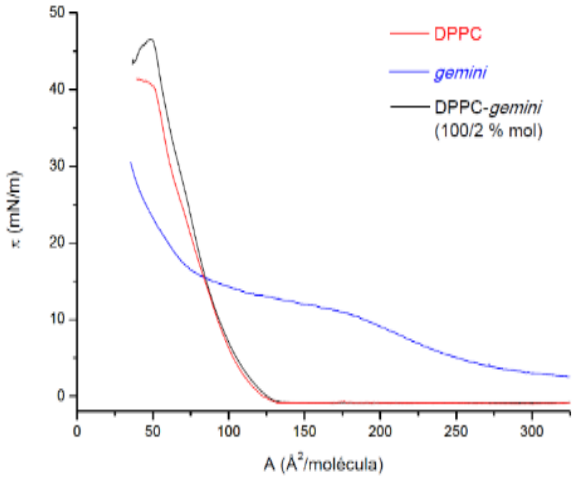

Fig 1. Pressure-area isotherms

TEM

The results of the electron microscopy study show *in Figure 2* a unilamellar structure consisting of an aqueous compartment and a lipid bilayer. The observed sizes agree with those obtained by DLS.

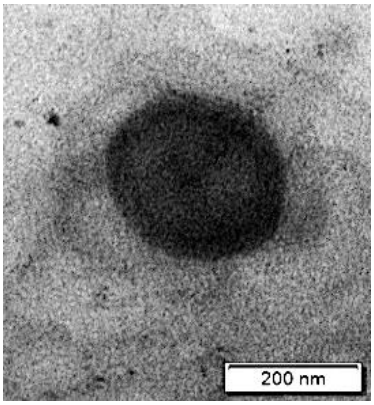

Fig 2. Structure of liposomes by TEM

In vitro release studies

Release studies were performed in comparison with a commercial formulation of ciclopirox, Onytec®. The release profiles observable in *Figure 3* were fitted to order one kinetics, where the R^2 of the liposomal formulation and Onytec® are 0.97 and 0.99 respectively. The liposomes show a less intense and less erratic release compared to Onytec®.

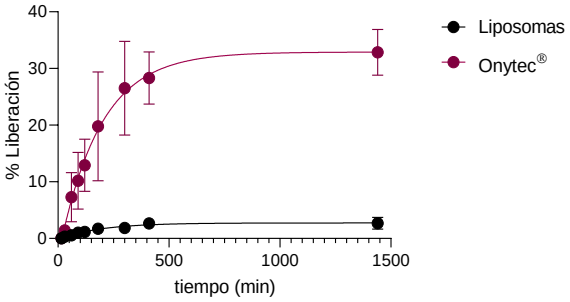

Fig 3. Percentage of drug release

Transungeal delivery

The transungual penetration profiles are shown in Figure 4. They have been adjusted to the steady state release where the flow rate is kept constant. In this trial another formulation Ciclochem® was incorporated into the study. In the case of liposomes, a latency period of 9 days is observed. The Onytec® achieves a similar flux to that of the liposomes with the difference that it does not have a latency time.

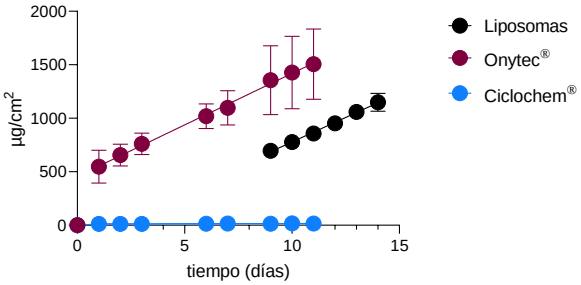

Fig 4. Drug flow adjustments in the various formulations.

Conclusions

Based on the studies, it has been possible to obtain SVU-type liposomes observable in TEM. The designed system is abled to encapsulate the CPO, improving its retention in the nail. The same physicochemical properties of the liposomes make them candidates for nail administration.

References

[1] Westerberg DP, Voyack MJ. Onychomycosis: Current Trends in Diagnosis and Treatment. 2013;88(11):12.

[2] Singh N, Kushwaha P, Ahmad U, Abdullah M. Proliposomas: Una aproximación para el desarrollo de liposoma estables. Ars Pharm. 5 de agosto de 2019;60(4):231-40.

P1.10: Development of a liposomal formulation containing Cyclosporin A for the treatment of dry eye disease

M.A. González-Cela Casamayor [1;2]*, M.A. Caballo González[1;2], M. Vicario de la Torre[1;2;3], M. Guzmán Navarro[4], J.M. Benítez del Castillo[1;3;5], E.M. González-Alonso Alegre[1,6], A. Rodríguez[1,6], B. de las Heras[1], R. Herrero Vanrell[1;2;3] and IT. Molina Martínez[1;2;3]

[1]Innovation, Therapy and Pharmaceutical Development in Ophthalmology (InnOftal) Research Group, UCM 920415, Faculty of Pharmacy, Complutense University of Madrid, 28040 Madrid, Spain
[2]Pharmaceutics and Food Technology Department, School of Pharmacy, Complutense University of Madrid (UCM), IdISSC, 28040 Madrid, Spain
[3]Thematic Research Network in Ophthalmology (Oftared) Carlos III National Institute of Health, 28040 Madrid, Spain
[4]Biomedical Sciences Department, Pharmacy and Pharmaceutical Technology Unit, Faculty of Pharmacy, University of Alcalá, Ctra. de Madrid-Barcelona (Autovía A2), 28805 Alcalá de Henares, Madrid, Spain.
[5]Ocular Surface and Inflammation Unit, San Carlos Clinical Hospital, C/Profesor Martín Lagos, s/n, 28040 Madrid, Spain
[6]Complutense Veterinarian Clinical Hospital, Medicine and Animal Surgery Department, School of Veterinary, Complutense University of Madrid, 28040 Madrid, Spain
*e-mail: mirigo04@ucm.es

Introduction

Dry eye disease (DED) is a pathology caused by a deficit in tear production or an increase in tear evaporation, leading to inflammatory processes that causes severe discomfort. Most patients regularly use over-the-counter eyedrops (artificial tears). Artificial tears are continuously evolving so that include novel technological tools such as the use of liposomes, pharmaceutic nanosystems that help restore the natural tear film. Liposome´s structure, constituted by an external lipid bilayer and an inner aqueous core, might help to restore the homeostasis of the tear film. Also, if the liposomes are dispersed in an aqueous solution of a bioadhesive polymer such as the case of hyaluronic acid, the artificial tear resembles the preocular tear film.

When the symptoms of DED are more serious and persistent, other therapeutic options are used highlighting the ophthalmic anti-inflammatory agent, Cyclosporine A (CyA). CyA has shown clinical benefits in improving signs and symptoms from chronical inflammation. However, it has such a low hydrosolubility that requires the inclusion of hydrophobic vehicles for its formulation that can cause discomfort and low tolerance after instillation.

The aim of this work was to develop and characterize a liposomal formulation able to simulate the natural tear film encapsulating CyA to improve signs and symptoms of DED. The clinical efficacy of this tear substitute based on CyA-loaded liposomes was tested in dogs suffering of DED.

Materials and Methods

Liposomes were prepared using the lipid film hydration method previously described [1]. The lipid phase was composed of phosphatidylcholine, cholesterol and vitamin E in a ratio of 8:1:0.02. The formulation developed was composed by 20 mg/mL phosphatidylcholine and 0.1% CyA. Drug-loaded liposomes were dispersed in a 0.4% sodium hyaluronate solution (CyA-L-HaNa). The *in vitro* characterization includes physico-chemical studies (particle size, pH, osmolarity, surface tension and viscosity). *In vitro* tolerance of the formulations was determined using human conjunctival (IOBA-NHC) and corneal (HCLE) cell lines by the MTT technique (exposures of 15 min, 1 and 4 hours).

CyA content (assay) was determined by HPLC with a modified analytical procedure [2] that was validated in our laboratory.

A short-term stability study was performed under two storage conditions, room temperature (RT) and at 2-8ºC, at different times after CyA-L-HaNa preparation. Physico-chemical properties were evaluated at 0, 1 and 6 months, while CyA content and *in vitro* tolerance were quantified at 0, 1, 3 and 6 months after elaboration and stored at RT and 2-8ºC.

The efficacy of the liposomal formulation CyA-L-NaHa was studied in 20 client-owned dogs with DED immune-mediated or associated to endocrine disorders that also had Schrimer test <15 mm/min in both eyes. Dogs were divided into two groups: group I (n=10), dogs showed a Schirmer test between 10-15 mm/min (mild dry eye disease) and group II (n=10), dogs with Schirmer test <10 mm/min (moderate to severe dry eye disease).

A drop of the tear substitute CyA-L-HaNa was topically applied on both eyes every 8-h daily for 60 days by owners in the home setting. A complete ophthalmic examination was performed

prior to treatment and 60 days after starting the treatment (0 and 60 days) in dogs by veterinarians. This examination included Schirmer test (STT), fluorescein corneal staining, evaluation of the ocular discharge, corneal thickness measured by ultrasound pachymetry (SP100 Tomey, Nürnberg, Germany) and corneal sensitivity using a esthesiometer Cochet-Bonet (Luneau Ophtalmologie, Paris, France).

Results and Discussion

The hypotonic CyA-L-HaNa formulation had a particle size around 200 nm and a neutral pH. The surface tension was around 30 mN/m and the viscosity close to 6 mPas. Moreover, the formulation showed high stability as the physico-cemical parameters remained unchanged during 6 months when the formulation was stored at RT and 2-8ºC (Table 1).

Table 1. Physiochemical parameters of the liposomal formulation developed (CyA-L-HaNa) at RT and under refrigeration (2-8ºC).

Condition	Room Temperature (RT)		2-8ºC	
	1 month	6 months	1 month	6 months
Mean particle size	204.7 ±8.3	199.9 ±1.6	200.7 ±1.2	198.7 ±9.6
pH	7.33 ±0.04	7.40 ±0.02	7.37 ±0.03	7.41 ±0.01
Osmolarity (mOs/L)	204.6 ±4.9	200.4 ±6.4	202.6 ±2.1	197.2 ±2.1
Surface tension (mN/m)	29.2 ±0.4	30.2 ±0.8	28.8 ±0.9	29.6 ±0.7
Viscosity (mPa.s)	6.26 ±0.19	6.32 ±0.08	6.25 ±0.12	6.27 ±0.25

The content of CyA was analyzed for a 6-month storage period at RT and 2-8ºC by HPLC in a liposomal formulation without polymer. After 6 months of storage at 2-8ºC, drug entrapped in the liposomes was 97.3% ± 2.7, while the CyA content decreased to 90.3% ± 2.0 in the formulation stored at RT.

After the incubation times tested (15 minutes, 1 and 4 hours), no cell death was detected for any storage condition in both cell lines.

Owners reported an improvement in their dog's eye health treated with CyA-L-HaNa. After treatment for 60 days with CyA-L-HaNa formulation, a significant improvement ($p<0.001$) was observed in tear production (STT) for both groups. The average tear production increase was 40% in mild cases and 192% in moderate to severe cases (Fig 1). In general terms, dog's ocular surface improved after treatment with the test formulation. Group I showed no positive fluorescein corneal staining after therapy, though significant differences were not found in the groups at the end of the treatment. Ocular discharge decreased in both animal groups, and there was a significant decrease ($p=0.021$) in moderate to severe group. Corneal thickness and sensitivity decreased at the end of the study in both groups, although the high dispersion among the animals did not allow us to find significant differences.

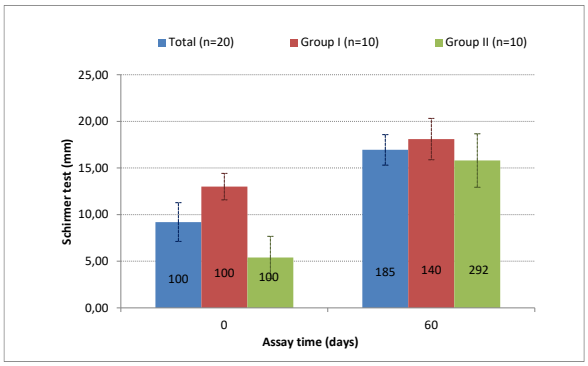

Figure 1: Tear production (STT) in dogs suffering dry eye disease.

Conclusions

Treatment with the liposomal formulation of Cyclosporine A and sodium hyaluronate was safe and effective at improving clinical signs of dry eye disease in dogs and can be considered as a potential treatment for DED.

Acknowledgments

This work was supported by the Research Group UCM 920415, Innovation, Therapy and Pharmaceutical Development in Ophthalmology (InnOftal) and the ISCII-FEDER RETICS (OFTARED) (RD16/0008). FEDER-CICYT FIS-PI17/00079 and PI17/00466. M.G.C. thanks for a PhD fellowship from the Spanish MECD (FPU18/03445).

References

[1] M. Vicario de la Torre, JM. Benítez-del-Castillo, *et al*. Design and characterization of an ocular topical liposomal preparation to replenish the lipids of the tear film. Investig. Ophthalmol. Vis. Sci. 55 (2014) 7839-7847.

[2] G.C. Kahn, L.M. Shaw, M.D. Kane MD. Routine monitoring of cyclosporine in whole blood and kidney tissue using high performance liquid chromatography. J Anal Toxicol. 10.1 (1986) 28-34.

P1.18: Budesonide microspheres for ocular administration

M. Guzmán-Navarro[1,2,3]*, I. González Criado[1], J. Rodriguez Villanueva[2]

[1]*Department of Biomedical Sciences. Lab Pharmaceutical Technology, Univerdad de Alcalá, 28801 Alcalá de Henares, Spain*
[2]Research Group Bioanalytical, Metabolomic and Pharmaceutical Techniques (TECBIOMETFAR) *UAH*
[3]Research Group Innovation, Therapy and Pharmaceutical Development in Ophthalmology (INNOFTAL) *UCM*

*e-mail: manuel.guzman@uah.es

Introduction

Corticosteroids are one of the drugs used for the treatment of inflammatory eye diseases. Several drug delivery systems (DDS) have been developed to be administered by topical (surface diseases) or by different routes to the posterior ocular segment [1].
Biodegradable and nonbiodegradable intravitreal implants used today contain dexamethasone, brimonidine, fluocinolone or ganciclovir [2]. They can release these drugs for extended periods of time, but its administration and the withdrawal of those nonbiodegradable, needs a minor surgical intervention, causing some injuries such as retinal detachment, cataracts... etc.
Budesonide (BDS) is a synthetic corticosteroid that has high glucocorticoid and feeble mineralocorticoid effects. In comparison to cortisone [3], budesonide topical effect is approximately 100 times more potent, while that of dexamethasone is only 20-30 times greater.
The aim of this work has been the development and optimization of biodegradable microspheres (MSs) made with lactic-glycolic copolymer acids (PLGA) and loaded with the glucocorticoid budesonide (BDS), as an alternative to implants for the treatment of neurodegenerative pathologies to the posterior segment of the eye. MSs can be administered with small gauge needles and allow to achieve sustained drug levels in the vitreous humor.

Materials and Methods

Poly (D,L lactic-*co*-glycolic acid) 50:50 (PLGA) copolymer Mw 35,000 g/mol was supplied by Boehringer Ingelheim, Polyvinyl alcohol (PVA) 72,000 g/mol by Merck; Budesonide (BDS) by Sigma-Aldrich, PEG 6 isostearate by Gattefossé, human serum albumin (FITC-has) fluorescein isothiocyanate by Tebu-bio and the solvents (ethyl acetate, acetone) by Scharlab.
MSs were prepared by a solvent extraction-evaporation technique [4] (S/O/W) at 10,000 rpm for 15 min, followed by magnetic stirring for 24h. Several formulations were made with a constant BDS:PLGA ratio (1:10) with or without PEG 6 isostearate and FITC-HSA. Ethyl acetate and acetone mixtures were used as organic phase and aqueous PVA solutions as dispersing phase. Subsequently, MSs of the appropriate size can be selected by filtration through sieves or nylon cloth. MSs particle size and its Z potential was obtained by using a Malvern apparatus (Mastersizer 3000 Hydro EV and a Zetasizer Pro) and its morphology by SEM (Zeis DSM 950).
BDS encapsulation efficiency (EE) was calculated after drug extraction from MSs with 70:30 acetonitrile: water and quantification at 226 nm by spectrophotometry (UV/Vis LAMBDA 325 Perkin Elmer).
Calorimetric studies were performed on a DSC3 Mettler Toledo at 1ºC/5min from 10ºC to 300 ºC.
To estimate FITC-HAS incorporation into the MSs, Confocal microscopy (Leica TCS-SP5) and Flow cytometry were used (MACSQuant 10, Miltenyi Biotecwere).
HeLa cell MTT assays were performed in sterile plates and wells (Cultex SLU), in DMEM culture medium supplemented with 10% fetal bovine serum, 2% penicillin-streptomycin and 2% amphotericin B (Difco and Sigma-Aldrich).

Results and Discussion

The average *particle size* of BDS-loaded PLGA MSs with PEG-6 isostearate and FITC-HSA was 18,04± 10,78 µm and its zeta potential -15 mV. Their 50th and 80th percentiles turned out to be less than 2.5 µm and 20 µm.

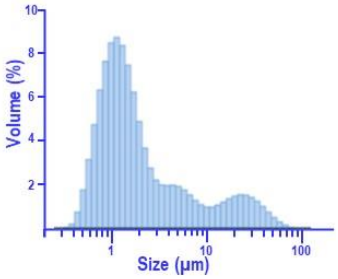

Fig 1. Size distribution of BDS-loaded PLGA MSs by Dynamic Light Scattering (DLS)

MSs observed by *scanning electron microscopy* (SEM) show spherical particles with a smooth surface that corroborates the results obtained by DLS analysis (Fig 2).

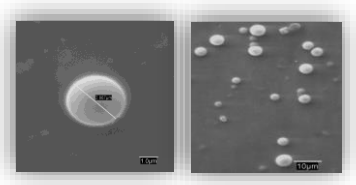

Fig 2. SEM microphotographs of BDS-loaded MSs

BDS encapsulation efficiency (EE) in MSs is greatly influenced by PEG-6 isostearate. MSs without it encapsulate 97,83±1,29% of BDS, but it is reduced to 53,74±0,67% when PEG-6 isostearate is included.

Figure 3 shows the *DSC thermograms* of: raw materials ingredients (BDS, PLGA and PVA) and MSs with PEG-6 stearate and FITC-HAS unloaded and loaded-BDS. It can be seen that the peak corresponding to the glass transition temperature (Tg) of the raw material polymer, (54ºC) is reduce and becomes wider in both BDS-loaded and unloaded MSs formulations. This fact may be due to the oily excipient (PEG-6 stearate) present in both MSs. On the other hand, the BDS melting peak (259ºC) disappears in loaded MSs, suggesting that drug could be probably dispersed as an amorphous state in the MSs matrix to which the PEG-6 isostearate could also collaborates. Although not very significant, it is also observed that some traces of PVA remain in the MSs.

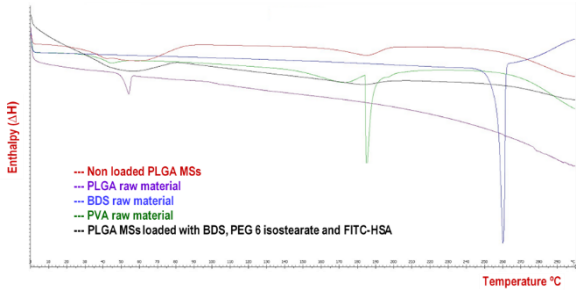

Fig 3. Differential Scanning Calorimetry of raw materials and PLGA MSs (loaded-BDS and unloaded).

Fluorescein-labeled human serum albumin has been included in the MSs formulation with three objectives: as a protein model, to be able to observe its incorporation into MSs and its possible internalization inside cells.

To evaluate *MSs cell viability* an in vitro assay has been performed with HeLa cells (figure 4).

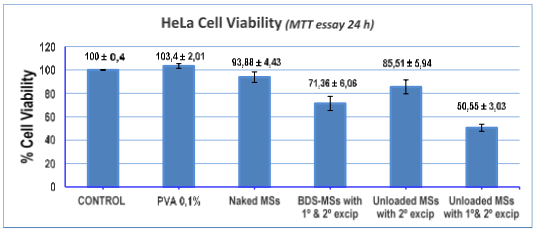

Fig 4. HeLa cell viability of MSs tested by MTT essay.

HeLa cells viability is not affected by naked MSs (without BDS, nor excipients (1) PEG-6 isostearate, nor (2) FITC-HSA), nor by the PVA aqueous dispersion. PEG-6 isostearate was included in the MSs formulation to modulate the release kinetics of BDS. However, it significantly reduces cell viability up to 50%.

After HeLa cells incubation with the BDS-loaded MSs, cultures were observed with the *confocal microscope* (argon lamp 458 nm). Images (fig. 5) show that the most intense staining belongs to the MSs but also a weaker staining appears in cells.

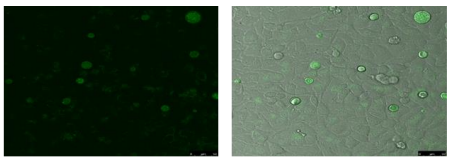

Fig 5. Confocal laser microphotographs of PLGA MSs, loaded with BDS and FITC-HAS.

Flow cytometry studies (fig. 6) confirm that FITC-HSA is incorporated into PLGA MSs, as was observed by confocal microscopy. The mean fluorescence intensity of MSs without FITC-HSA (a) is 1.44 units, while those containing stained albumin (b) is approximately 10 times higher.

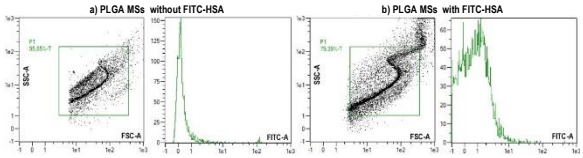

Fig 6. Flow cytometry of unloaded and BDS-loaded MSs

Conclusions

- A BDS DDS has been developed for intravitreal administration with small-gauge needle that could avoid some inconveniences associated to implants.
- The ability of this technique to encapsulate compounds of peptide nature has confirmed.
- PEG-6 stearate causes cytotoxicity in HeLa cells, so it is not an adequate excipient for MSs.

Acknowledgments

This work has been supported by funds of UAH and TECBIOMETFAR and INNOFTAL groups.

References

[1] S.A. Gaballa et al. Corticosteroids in ophthalmology: drug delivery innovations, pharmacology, clinical applications, and future perspectives *Drug Deliv. and Transl. Res*. 11 (2021) 866–893.

[2] D.G. Waller, A.P. Samson ed Corticosteroids (glucocorticoids and mineralocorticoids) in Medical Pharmacology and Therapeutics (2014): 503-511

[3] P. García-Estrada et al. Polymeric Implants for the Treatment of Intraocular Eye Diseases: Trends in Biodegradable and Non-Biodegradable Materials *Pharmaceutics* 13(5) (2021) 701.

[4] J. Rodriguez-Villanueva et al. Optimising the controlled release of dexamethasone from a new generation. *Eur.J.Pharm.Sci. 92 (2016) 287–297.*

P1.12: New treatment for fungal keratitis: A combined eye drops of two antifungals

D. T. Victoria[1,2], G. O. Xurxo[1], V. F. Rubén[1], LL. T. José[4], G. B. Miguel[3], F.F. Anxo[2,3] and O. E. Francisco J[1].

[1]Pharmacology, Pharmacy and Pharmaceutical Technology. University of Santiago de Compostela (USC). Santiago de Compostela. Spain.
[2]Clinical Pharmacology Group. Health Research Institute Foundation of Santiago de Compostela (IDIS). Santiago de Compostela. Spain
[3]Pharmacy Department, University Clinical Hospital Santiago de Compostela (SERGAS). Santiago de Compostela, Spain.
[4]Microbiology Department, University Clinical Hospital Santiago de Compostela (SERGAS). Santiago de Compostela, Spain.

*e-mail: victoriadiaztome@gmail.com

Introducction

Fungal keratitis (FK) is a severe disease of difficult treatment that can produce vision loss. FK can be caused by filamentous fungi such as Fusarium and Aspergillus spp or yeast such as Candida albicans. The ophthalmic FK treatment requires the use of topical ophthalmic antifungal drugs for a prolonged time and frequent instillations. Nowadays, topical voriconazole and natamycin are used like first-line therapies. Some *in vitro* studies have demonstrated more antifungal activity when the voriconazole and Natamycin are combinated [1].

In the present study, the development of a new eye drops that combines voriconazole and natamycin is presented.

Materials and Methods

Natamycin was purchased from LabNetwork®; Voriconazole was procured by Normon®; hyaluronic acid (HA) was obtained from Acofarma®; 2-hydroxypropyl-β-cyclodextrin (HPβCD) from Roquette®; 2-hydroxypropyl-γ-cyclodextrin (HPγCD) was purchased from Sigma Aldrich®; Liquifilm® was obtained from Allergan® Pharmaceuticals.

Preparations of formulations

The HPβCD concentration was stablish by phase solubility diagrams. The inclusion complex obtained between Natamycin/HPβCD was studied by NRM studies. The solubility diagrams and NMR studies of Voriconazole were studied in previous work [2]. 40% HPβCD (p/v) was dissolved in MilliQ® (SNV) water or Liquifilm® (LNV) eye drops. Them, 1% voriconazole (p/v) and 0.7% Natamicyn (p/v) were added and shaked until complete solubilization. 0.4% HA (p/v) was added to the water solution (AHNV).

Ex vivo corneal Permeability studies

Entire and epithelium-free corneas were used for the test. Bovine corneas were isolated and 0mounted on Franz diffusion cells. The cornea was placed on the receptor chamber, and the donor chamber was attached and filled it with 500µl of each formulation. The voriconazole and Natamycin determination was performed in a UHPLC system.

Ocular irritation test

BCOP trial was performed with fresh bovine corneas. Corneal transparency and fluorescein permeability were measured before of contact with the cyclodextrin solutions. HET-CAM assay was performed to quantify the irritation potential.

Disk diffusion method for the antifungal susceptibility study.

Mueller-Hinton agar plate were inoculated with *Candida albicans* ATCC 90231 (1), *Candida albicans* ATCC 90028 (3), *Aspergillus fumigatus* (2), *Paelomyces lilacinus* (4) and *Fusarium solani* (5). Disk were impregnated with 20 µL of formulation: Natamycin/HPβCD, Voriconazole/HPβCD, Natamycin/Voriconazole/HPβCD and Natacyn. The plates were incubated for 48 hours. Afterwards, the diameter of the inhibition zones was measured and compared.

Results and Discussion

Ex vivo corneal Permeability studies

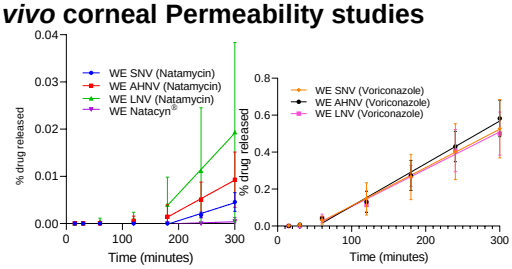

Fig 1. Corneal permeability profile of Natamycin/Voriconazole/HPβCD and Natacyn in corneas with epitelium

The apparent permeability (Ppa) of Natamycin through corneas with epithelium was observed from the formulations developed (Ppa $1.8 \cdot 10^{-10}$, $3.11 \cdot 10^{-10}$ and $6.09 \cdot 10^{-10}$ cm^2/s SNV,AHNV and LNV, respectly) in contrast to the commercial formulation Natacyn® ($2.56 \cdot 10^{-12}$ cm^2/s).

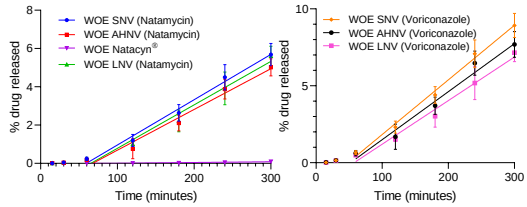

Fig 2. Corneal permeability profile of Natamycin/Voriconazole/HPβCD and Natacyn in corneas without epitelium

The apparent permeability of natamycin through de-epithelialized corneas from the formulations developed (Ppa $1.126 \cdot 10^{-7}$, $1.01 \cdot 10^{-7}$ and $1.08 \cdot 10^{-7}$ cm^2/s SNV,AHNV and LNV, respectly) was higher than the permeability of the commercial formulation Natacyn® ($2.54 \cdot 10^{-10}$ cm^2/s).

Ocular irritation test

BCOP

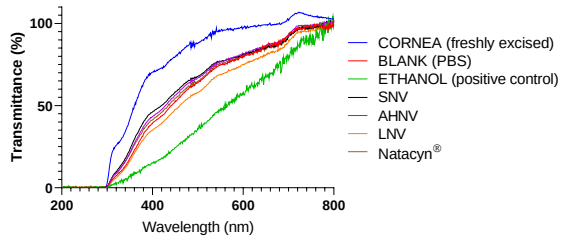

Fig 3. Transmittance representation obtained after the instillation of formulations after 10 min drug treatment and 120 min PBS treatment.100% corresponds to the total light transmitted through bovine corneas incubated in PBS.

Natamycin/Voriconazole/HPβCD formulations did not modificate corneal transparency.

The fluorescein corneal permeability has not been affected for any formulation.

HET-CAM

None of the formulations produced damage to the blood vessels of the CAM after 5 min of contact, all of which can be classified as non-irritating.

Disk diffusion method for the antifungal susceptibility study.

Specie / Form.	*1*	*2*	*3*	*4*	*5*
1	*68-70*	*31*	*64-66*	*65-68*	*11*
2	*60*	*30*	*58*	*60*	*-*
3	*68-70*	*30*	*68-70*	*60*	*11-12*
4	*100*	*-*	*100*	*100*	*-*
5	*80*	*55*	*80*	*90*	*30*

Table 1. Inhibition zones (mm) of antifungal formulations

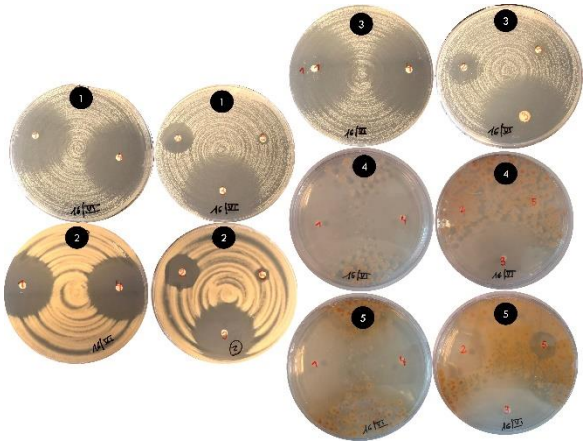

*Fig 3. Inhibition zones of five studied fungal species:1. Candida albicans ATCC 90231, 3. Candida albicans ATCC 90028, 2. Aspergillus fumigatus, 4. Paelomyces lilacinus and 5. Fusarium solani. Formulations: 1. Voriconazole/HP*βCD, 2. Natamycin/HPβCD, 3. Natamycin/Voriconazole/HPβCD, 4. VFEND® (Voriconazole/SBECD), 5. Natacyn®.

The inhibition of fungal growth by Voriconazole was the same for all species tested and showed superior efficacy for *Paelomyces lilacinus.*

Natamycin/HPβCD show a greater inhibition than Natacyn, due to its better diffusion through the disk.

The Natamycin/Voriconazole/HPβCD combination formulation shows no differences with the Vori / HPβCD o Vfend® formulation.

Conclusions

The natamycin and voriconazole corneal permeability was improved in the ephitelium presence or abscense. The antifungal susceptibility by diffusion disks of natamycin/HPβCD was better than commercial Natacyn® due to the improvement in the diffusion through the disk. No synergism was observed between natamycin and voriconazole. The developed formulations have not shown irritation signs. The results obtained shown the interest on these formulation for the treatment of fungal keratitis.

References

[1] Sradhanjali S, Yein B, Sharma S, Das S. In vitro synergy of natamycin and voriconazole against clinical isolates of Fusarium, Candida, Aspergillus and Curvularia spp. Br J Ophthalmol. 2018;102(1):142–5.

[2] Díaz-Tomé V, García-Otero X, Varela-Fernández R, Martín-Pastor M, Conde-Penedo A, Aguiar P, et al. In situ forming and mucoadhesive ophthalmic voriconazole/HPβCD hydrogels for the treatment of fungal keratitis. Int J Pharm. 2021 Mar 15;597:120318

P1.13: Bevacizumab-loaded PLGA intravitreal implants prepared by supercritical fluid technology

C. Bendicho-Lavilla[1]*, I. Seoane-Viaño[1,2], V. Santos-Rosales[3], A. Luzardo-Álvarez[1], C.A. García-Gonzalez[3] and F.J. Otero-Espinar[1]

[1]*Department of Pharmacology, Pharmacy and Pharmaceutical Technology. Paraquasil Group. Faculty of Pharmacy. University of Santiago de Compostela (USC), 15782, Spain*

[2]*Department of Pharmaceutics, UCL School of Pharmacy, University College London, 29-39 Brunswick Square, London WC1N 1AX, UK*

[3]*Department of Pharmacology, Pharmacy and Pharmaceutical Technolog., I+D Farma Group (GI-1645), Faculty of Pharmacy. University of Santiago de Compostela (USC), 15782, Spain*

*e-mail: carlos.bendicho@gmail.com

Introducction

Bevacizumab (BVZ) (Avastin®) is a monoclonal antibody that inhibits vascular endothelial growth factor (VEGF). It is currently used off-label as a therapy for eye diseases such as age-related macular degeneration and diabetic retinopathy [1]. It is administered once a month by intravitreal injection [1].

The main complications are associated with frequent intravitreal injections, which also cause patient discomfort as it is an invasive method [2]. Therefore, a controlled and prolonged release system of BVZ is needed to increase the time between injections [3].

This work proposes the design and preparation of biodegradable intravitreal implants of poly(lactic-co-glycolic acid) (PLGA) loaded with BVZ using supercritical CO_2 foaming technology [3], which has the advantage of manufacturing implants in the absence of organic solvents, with high loadings and at low temperatures.

Materials and Methods

Design and formulation of the implant

Powdered mixtures of PLGA of different molecular weights (50:50 lactic/glycolic, 16-38 kDa) were prepared in a 1:1 ratio. To the polymeric mixture, 50 µL of a commercial BVZ solution (Avastin®) was added and placed in the oven for 30 minutes at 35 ºC for solvent evaporation. The mixture was homogenised and inserted into a plastic probe of dimensions close to those of the desired implant. The material was then subjected to processing with supercritical CO2.

Manufacture of implants using supercritical CO2

The manufacture of the implants was carried out using a high-pressure autoclave (Thar Process, PA, USA); agitation (700 rpm); 100 bar; 60 minutes.

The influence of the processing temperature (35-40 ºC) and the depressurisation speed (0.9-7.2 g/min) of the system on the final morphology and the yield profiles of the implants obtained was evaluated.

Physical appearance and size of the implants

Macroscopic analysis was carried out by observing the external structure of the intravitreal implants through a magnifying glass with an electronic camera (Olympus® SZ-CTV/Olympus® SC100).

In vitro release

The release of the intravitreal implants was performed using Franz cells (5.5 mL) with artificial vitreous humour in the donor chamber and PBS pH 7.4 in the receptor chamber at 37 ºC and 100 rpm agitation. At each preset time, 0.5 mL was removed from the recipient and replaced with fresh PBS. Samples were analysed by ultra high-performance liquid chromatograph (UPLC, Waters) at a wavelength of 280 nm.

Results and Discussion

Morphological evaluation

The intravitreal implants were cylindrical in shape with uniform surface and colour (Figure 1).

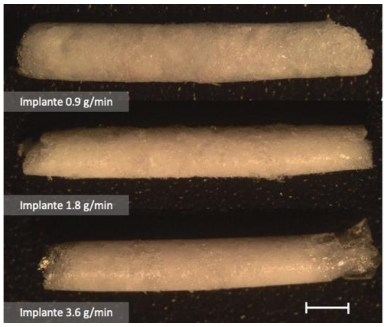

Fig. 1. Macroscopic appearance of the intravitreal implants. Scale bar 2.5 mm.

In vitro release

As can be seen in Figure 2, PLGA implants result in a significantly higher level of diffused BVZ than free BVZ. The release profile of the implants varies with the rate of depressurisation of the supercritical CO_2 system. This is due to the modification in the number and size of pores produced in the implant during the foaming process.

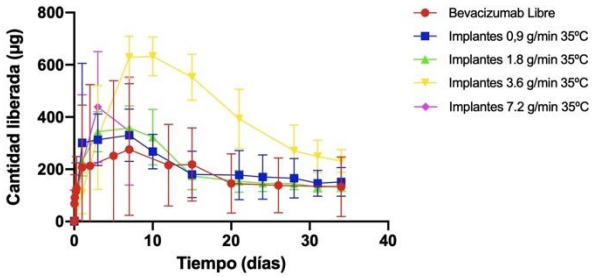

Fig 2. In vitro release of free BVZ and BVZ from intravitreal implants processed with different depressurisation conditions.

In all formulations a decrease in the amount of BVZ is observed after 8-10 days. This is probably due to an aggregation process of the BVZ molecules in the release medium. Incorporation into the implant seems to improve the stability of the antibody, obtaining higher quantities and for longer periods of time, although there is a significant decrease in the concentration of the antibody.

The percentage of antibody diffusing to the recipient is low: 25% in Avastin® or 50% in the 3.6 g/min implant. This low diffusion can be attributed to the presence of negatively charged hyaluronic acid which may interact electrostatically with the positive charges of the antibody, preventing its diffusion towards the receptor.

Future work will study whether the incorporation of stabilisers could prevent the formation of aggregates. Avastin® includes surfactants and other stabilisers in its composition to prevent aggregation of the antibody.

Also, improvements in the implant manufacturing process and modifications in the polymer blending will be evaluated. Antibody stability studies after processing will be made.

Conclusions

In the proposed work, biodegradable BVZ-loaded PLGA intravitreal implants were designed and manufactured using the supercritical CO_2 foaming technique. This method avoids the use of organic solvents, has high loading yields and has the ability to easily modify drug release from the implants.

Acknowledgments

This work was supported by Ministry of Science and Innovation (RTI2018-099597-B-100)

References

[1] The Royal College of Opthalmologists. New NICE Age Related Macular Degeneration guidance supports potential cost savings for the NHS [Internet]. The Royal College of Ophthalmologists. 2018 [cited 2021 Sep 30]. Available from: https://www.rcophth.ac.uk/2018/01/new-nice-age-related-macular-degeneration-guidance-supports-potential-cost-savings-for-the-nhs/

[2] Yorston D. Anti-VEGF drugs in the prevention of blindness. Community Eye Health. 2014;27(87):44–6.

[3] Santos-Rosales V, Magariños B, Starbird R, Suárez-González J, Fariña JB, Alvarez-Lorenzo C, et al. Supercritical CO2 technology for one-pot foaming and sterilization of polymeric scaffolds for bone regeneration. Int J Pharm. 2021 Aug 10;605:120801.

P1.14: Bevacizumab loaded lipidic lyotropic liquid crystals as a promising platform for ocular diseases

G. Blanco-Fernández [1]*, B. Blanco-Fernández[;3], A. Fernández-Ferreiro [4;5] and F.J. Otero-Espinar [1;6]

[1]*Department of Pharmacy, Pharmacology and Pharmaceutical Technology, School of Pharmacy, Univerdad de Santiago de Compostela, 15782*
Santiago de Compostela, Spain
[2]CIBER in Bioengineering, Biomaterials and Nanomedicine, CIBER-BBN, 28029,
Madrid, Spain
[3]Institute for Bioengineering of Catalonia (IBEC), The Barcelona Institute of Science and Technology,
Baldiri Reixac 10-12, 08028
Barcelona, Spain
[4]Grupo de Farmacología, Fundación Instituto de Investigación de Santiago de Compostela (FIDIS), 15706,
Santiago de Compostela, Spain
[5]Department of Pharmacy, Hospital Clínico Universitario de Santiago de Compostela (SERGAS), 15706,
Santiago de Compostela, Spain
[6]Grupo Paraquasil, Fundación Instituto de Investigación de Santiago de Compostela (FIDIS), 15706,
Santiago de Compostela, España

*e-mail: guillermo.blanco.fernandez@rai.usc.es

Introducction

Diabetic retinopathy (DR) and age-related macular degeneration (AMD) are prevalent diseases in the society that can cause blindness in long-term. Proliferative DR and neovascular AMD, are provoked by the neovascularisation of the ocular blood vessels due to an stimulation provided by vascular endothelial growth factor (VEGF) [1]. Their treatment is based on the intravitreal injection of an anti-VEGF antibody, as this This treatment is administered bimonthly, with the consequent risk and associated discomfort for the patient.

Lipidic lyotropic liquid crystals (LLCs) are platforms formed by concentration changes of some lipids, at a range of temperatures, when they are in a solvent such as water. The advantage of these systems is their structural variety and the possibility of transition from one structure to another, their thermodynamic stability, their biocompatibility and their viscosity, which gives them excellent properties for controlled drug release [2].

The aim of this work we will develop and characterize lipidic LLCs for the controlled release of bevacizumab, as a potential treatment for proliferative DR and neovascular AMD.

Materials and Methods

Materials: Capmul GMO-50 (Abitec Corporation). Pluronic F127 (Sigma), Tween 80 (Acofarma). Mili-Q water. Avastin 25mg/mL was donated by Complejo Hospitalario Universitario de Santiago de Compostela (Spain).

Methods:

-Preparation of the implants. For F1, Pluronic F127 was added to the avastin solution in an ice bath. Then, GMO and ths antibody solution were heated at 45 ºC, and then mixed. For F2, Tween 80 was also incorporated.

-Syringability. Formulations were drawn into 5 mL syringes with 18 G needles. The plunger was displaced 20 mm to determine the maximum force required to extrude the formulations through the needle, which was measured with a Shimadzu AGS-X universal materials machine with its 1 kN load cell.

-Implants characterization. Implants structure was evaluated by polarized microscopy and by scanning electron microscopy (Zeiss Evo LS 15). The antibody release was conducted in artificial vitreous humour (5 mL,100 rpm, 37 ºC). The antibody released was determined by UPLC (waters), with the Bioresolve column, at 280nm.

Results and Discussion

Both F1 and F2 showed good extrusion capabilities through the syringe. Implants made by extruding the formulation through a microneedle showed good homogeneity when viewed with SEM. These implants had birefringence when viewed with a petrographic microscope. Finally, formulations showed a controlled release over time (Figure 1).

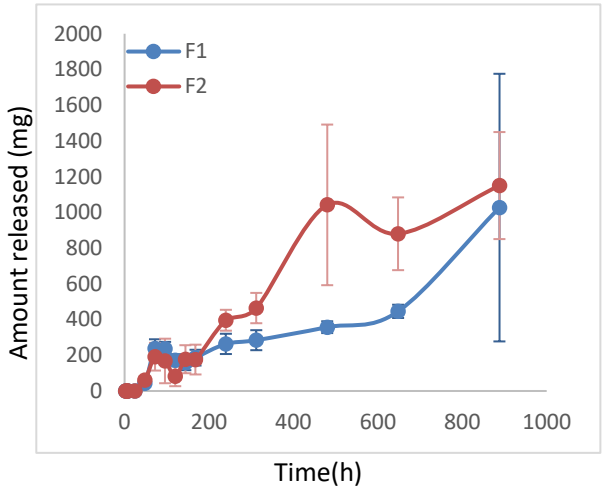

Fig 1. Bevacizumab release from the implants

Conclusions

The birefringence confirmed the formation of LLCs, their were homogeneous and showed a long-term bevazizumab release. These findings suggest that these two formulations could be promising platforms for the treatment of DR and AMD. Further studies to determine the antibody integrity the formulation properties and in vitro experiments to determine their efficacy will

Acknowledgments

GBF is grateful to the department of soil and agricultural chemistry for allowing the use of their petrographic miscroscope.

References

[1] R. Angermann, T. Rauchegger, Y. Nowosielski, M. Casazza, A. Bilgeri, H. Ulmer, C. Zehetner, Treatment compliance and adherence among patients with diabetic retinopathy and age-related macular degeneration treated by anti-vascular endothelial growth factor under universal health coverage, Graefe's Arch. Clin. Exp. Ophthalmol. 257 (2019) 2119–2125. https://doi.org/10.1007/s00417-019-04414-y.

[2] A. Yaghmur, M. Rappolt, A.L.U. Jonassen, M. Schmitt, S.W. Larsen, In situ monitoring of the formation of lipidic non-lamellar liquid crystalline depot formulations in synovial fluid, J. Colloid Interface Sci. 582 (2021) 773–781. https://doi.org/10.1016/j.jcis.2020.08.084.

P1.15: Development of surface-modified lipid-polymer hybrid nanoparticles: bulk formulation vs microfluidics

E. Briffault[1*#], H. Rouco[1#], P. Diaz-Rodriguez[2], P. Garcia-Garcia[1], D. Molina[1], A. Delgado[1] and C. Evora[1]

[1]*Department of Chemical Engineering and Pharmaceutical Technology, Universidad de La Laguna, 38206 La Laguna, Spain*
[2]*Department of Pharmacology, Pharmacy and Pharmaceutical Technology, Universidad de Santiago de Compostela, 15782 Santiago de Compostela, Spain*
[#]The authors contributed equally to the work
*e-mail: alu0100945362@ull.edu.es

Introduction

Lipid-polymer hybrid nanoparticles (LPNPs) have been attracted increasing attention during the last years in the nanotechnology field due to their ability to combine the positive features of both lipid and polymeric nanocarriers, such as good stability, integrity, and easy surface-functionalization [1]. This last feature is of great interest in the controlled drug delivery field, as the introduction of compounds such as drugs or antibodies at the surface of the nanocarriers, could increase their drug loading capacity or target them to specific sites. However, despite these promising features, it should be considered that hybrid nanoparticle preparation by bulk formulation methods hinders their large-scale manufacturing [2]. Microfluidic techniques constitute an interesting alternative, as they enable the rapid and uniform mixing of small volumes of inmiscible liquids in micro channels, allowing a better control over the final product [2]. Therefore, this work is focused on analysing the effect of lipid-polymer hybrid nanoparticles characteristics obtained by microfluidic devices (M) or bulk single-step nanoprecipitation (SSN) over nanocarriers surface functionalization with two different compounds, a drug, and an antibody.

Materials and Methods

Nanoparticle formulation: SSN technique consisted in adding an organic phase composed by a cationic lipid and a polymer onto an aqueous phase containing a phospholipid and a phospholipid-polymer conjugate. The mixtures were then kept under constant stirring until complete evaporation of the organic solvent. In the case of the M-based approach, the above-mentioned organic and aqueous phases were injected into a micromixer chip (Dolomite microfluidics, UK) at a flow rate of 0.6 and 1.5 ml/min, respectively. In order to obtain drug or antibody surface-modified nanoparticles, the phospholipid-polymer conjugate was partially replaced by a similar one containing a terminal NHS group. The nanocarriers were then concentrated by ultrafiltration using 15 ml 100 kDa Amicon® filters, and finally allowed to interact for 1 hour at RT with a solution of the drug or the fluorescently-labelled antibody.

Nanoparticle characterization: both naked and surface-modified nanocarriers were characterized in terms of particle size, polydispersity index (PdI) and zeta potential (ZP) in a Zetasizer Nano ZS. All the measurements were performed in triplicate at 25±1ºC. In the case of the surface-modified nanocarriers, the characterization was performed before and after the incubation step with the drug or the antibody, and results are expressed as the increase in size (Δ size), PdI (Δ PdI) and ZP (Δ ZP) of the functionalized nanocarriers regarding the initial ones.

Association efficiency assessment: With the aim of evaluating the antibody associated to the nanoparticle shell, the functionalized nanocarriers were centrifuged using 300 kDa ultrafilters. After that, the fluorescence of the subnatant was measured at 590/20-645/40 nm, and the association efficiency percentage (AE%) was calculated according to the following equation 1.

$$AE\ (\%) = \frac{Fl\ Total\ ab - Fl\ ab}{Fl\ Total\ ab} \times 100 \qquad \text{(eq. 1)}$$

Where *Fl Total ab* is the fluorescence of a solution containing an equivalent antibody concentration to that used in the formulations, and *Fl ab* is the fluorescence of the subnatant. Similarly, in order to determine the association efficiency of the drug to the nanoparticles, the functionalized formulations were centrifuged using 10 kDa Amicon® ultrafilters. Then, the absorbance of the subnatant was determined at 334 nm, and the (AE%) was finally determined using the following equation 2.

$$AE\ (\%) = \frac{Abs\ Total\ drug - Fl\ drug}{Abs\ Total\ drug} \times 100 \qquad \text{(eq. 2)}$$

Results and Discussion

The physicochemical characterization of the formulations obtained through SSN and M-based techniques revealed the existance of several differences between them. In this way, M-based nanoparticles exhibited a small particle size of just 129±1 nm, while the size increase notably in the case of the nanocarriers prepared through SSN, reaching almost 200 nm. This particle size reduction might be due to the the reduction on the mixing time of both aqueous and organic phases enabled by the use of a micromixer chip, as suggested in previous works [3]. Furthermore, zeta potential seemed to be highly positive in the case of M-based formulations (51±1 mV), while neutral values were obtained for those obtained by SSN (-3±2 mV). This phenomenon could be associated with the high flow rate used in the M-based formulation process, which triggers an increase in the surface charge of the nanoparticles [4]. On the other hand, the formulation procedure employed seemed to have a negligible impact over the polydispersity of the nanocarriers. In this way, PdI values of 0.27±0.05 and 0.26±0.00, were obtained for SSN- and M-based hybrid nanoparticles, respectively.
Concerning surface-modified nanoparticles, it is interesting to note that the formulations obtained through both procedures were succesfully functionalized with the two compounds under evaluation, as can be gathered from Table 1.

Table 1. Association efficiency of the different surface-modified nanoparticles.

Procedure	Functionalization	AE%
SSN	Antibody	96±5
M	Antibody	87±5
SSN	Drug	66±3
M	Drug	45±4

Furthermore, as can be derived from Table 2, the physicochemical characterization of the functionalized nanocarriers with both the drug and the antibody revealed an increase in particle size (Δ size) regarding the original formulations. In addition, a reduction in the zeta potential (negative Δ ZP) of the functionalized nanoparticles displaying the highest AE% values was observed. Interestingly, these modifications in the nanocarriers physicochemical properties might support the high functionalization percentages obtained. In this way, the Δ Size observed might be related with the generation of an antibody or drug monolayer at the nanoparticle-solvent interface. Whereas the negative Δ ZP of the functionalized nanocarriers might be associated with the negative charge displayed by both the drug and the antibody. Conversely, the PdI of the surface-modified nanoparticles seemed to remain almost unaltered.

Table 2. Physicochemical characterization of the surface-modified nanoparticles.

Formulation	Δ Size (nm)	Δ PdI	Δ ZP (mV)
Ab-NPs (SSN)	2±16	0.04±0.03	-13±5
Ab-NPs (M)	36±18	0.08±0.02	-18±4
Drug-NPs (SSN)	65±8	0.05±0.06	-12±2
Drug-NPs (M)	1±6	-0.17±0.3	10±7

Conclusions

This study demonstrated that lipid-polymer hybrid nanoparticles were successfully prepared by both SSN, and M. The obtained nanocarriers were also efficiently functionalized with a drug and an antibody. Furthermore, it was found that the M-based approach enabled a more precise control over critical parameters, such as particle size, making it an interesting substitute of traditional formulation procedures.

Acknowledgments

This study has been funded by Ministerio de Ciencia, Innovación y Universidades (MICIUN), which is part of the Agencia Estatal de Investigación (AEI), Spain, with joint financing by FEDER funds from the European Union (RTI2018-097324). Patricia García acknowledges postdoctoral grant “Investigador Posdoctoral Junior, CEI-Canarias

References

[1] P. Garcia-Garcia, E. Briffault, M. Landin *et al*, Tailor-made oligonucleotide-loaded lipid-polymer nanosystems designed for bone gene therapy, *Drug Deliv Transl Res.* 11 (2021) 598-607.

[2] N. Tahir, A. Madni, W. Li, *et al*. Microfluidic fabrication and characterization of Sorafenib-loaded lipid-polymer hybrid nanoparticles for controlled drug delivery, *Int J. Pharm.* 581 (2020) 119275.

[3] J.X. Wang, Q.X. Zhang, Y. Zhou, *et al*. Microfluidic synthesis of amorphous cefuroxime axetil nanoparticles with size-dependent and enhanced dissolution rate, Chemical Engineering Journal. 162 (2010) 844-51.

[4] M.M. Hasani-Sadrabadi, S.P. Hajrezaei, S.H. Emami *et al*. Enhanced osteogenic differentiation of stem cells via microfluidics synthesized nanoparticles, *Nanomedicine.* 11 (2015) 1809-19.

P1.16: Microfluidics for precise tuning of cubosome nanoparticle size

C.J.O. Ferreira[1;2;3]*, M. Barros[1;2], C. Botelho[3], M.E.C.D. Real Oliveira[2], B.F.B. Silva[1]
[1]*INL-International Iberian Nanotechnology Laboratory, 4715-330 Braga, Portugal;*
[2]*CF-UM-UP Physics Centre, Minho University, 4710-057 Braga, Portugal;*
[3]*CEB-Centre of Biological Engineering, Minho University, 4710-057 Braga, Portugal*
*e-mail: celso.ferreira@inl.int

Introduction

Cubosomes are nano-sized dispersions of bicontinuous cubic phases in water, ideal to deliver bioactive molecules in therapeutic applications [1]. Typically they are prepared either by fragmenting the cubic phase in excess water using high energy input, or using solvent-shifting approaches [2]. In both cases, poor experimental control at the micron-scale (e.g. poor control on concentration gradients), limits the fine tuning of the particle properties and results in cubosomes with broad size distributions.

Microfluidics enables the control and manipulation of fluids at the micron-scale. Its micron-sized channels lead to laminar flow regimes and enhanced experimental control. In this regime, hydrodynamic focusing can be used to decrease the mixing time between different components by decreasing the distances that molecules must travel for total mixing.

In this work, in order to achieve rapid and controlled mixing at the micron-scale, we employ the solvent-shifting method in a microfluidic device [3]. The ultimate goal is to obtain cubosomes of tunable narrow size distributions.

Materials and Methods

Using a COC microfluidic device composed by a cross-junction where 3 inlets and one outlet meet, an ethanol-lipid solution is flowed in the central inlet, which is squeezed by two side streams of water with stabilizer (F127). As the lipid-ethanol solution narrows, ethanol and water are mixed in a controlled way by diffusion, leading to the formation of cubosomes.
The obtained cubosomes were compared with the ones obtained following a solvent-shifting approach using a bulk methodology. To do so, the concentration of all components was adjusted to the same as in the microfluidic methodology.
Particles size was determined by Dynamic Light Scattering, and the structure by Small Angle X-ray Scattering.

Results and Discussion

The flow rate ratio (Q_R) is defined by the ratio between the centre inlet to the side inlets. By manipulating the Q_R between the lipid solution to the stabilizer solution, we manipulate the width in which the hydrodynamic focusing occurs, influencing the assembly time in a homogeneous way. As a result, an increase in Q_R results in a decrease of the particle size. This is contrast with particles assembled with the bulk methodology, where the size is kept constant, except for higher dilution ratios where it increases. This reinforces that by manipulating the flow conditions (especially Q_R), we can tune the cubosome size.
SAXS measurements show that the particles obtained using this microfluidic methodology have a Pn3m crystallographic spacegroup, as expected for this concentration and temperature range [4].

Conclusions

We showed that by the use of microfluidics, the sizes of cubosomes can be manipulated in the 130-210 nm range. Since nanoparticle size is a key parameter in drug delivery, this constitutes a relevant step towards the design of new and more efficient formulations.

Acknowledgments

This work was supported by the Microfluidic Layer-by-Layer Assembly of Cationic Liposome – Nucleic Acid Nanoparticles for Gene Delivery project (032520) co-funded by FCT and the ERDF through COMPETE2020. CJOF is supported by the FCT fellowship SFRH/BD/149199/2019.

References

[1] A. Zabara, R. Mezzenga, Controlling molecular transport and sustained drug release in lipid-based liquid crystalline mesophase, *J. Control. Rel.* 188 (2014) 31-43

[2] P.T. Spicer, K.L. Hayden, *et al*. Novel process for producing cubic liquid crystalline nanoparticles (cubosomes), *Langmuir.* 17 (2001) 5748-5756

[3] A. Jahn, S.M. Stavis, *et al*. Microfluidic mixing and the formation of nanoscale lipid vesicles, ACS Nano. 4(2010) 2077-2087

[4] J. Barauskas, T. Landh, Phase Behavior of the Phytantriol/Water System, Langmuir, 19 (2003) 9562-9565

P1.17: Characterization and *in vivo* evaluation of quercetin-loaded zein nanoparticles

R. Campión[1]*, A.L. Martínez-López[1], C.J. González-Navarro[2], E. de Paz-Barragán[3], C. Matías-Sainz[3] and J.M. Irache[1]

[1]*Department of Chemistry and Pharmaceutical Technology, University of Navarra, Pamplona, Spain*
[2]*Center for Nutrition Research, University of Navarra, Pamplona, Spain*
[3]*CNTA, National Centre for Food Technology and Safety, San Adrián, Spain*

*e-mail: rcampion@alumni.unav.es

Introduction

The flavonoid quercetin is present in most fruits and vegetables, such as onion, cranberry, or broccoli, and it can produce a wide range of pharmacological effects, as anti-inflammatory, antidiabetic, or cardioprotective ones [1]. However, the use of quercetin is limited due to its poor oral bioavailability, which is given by a poor aqueous solubility and its instability in physiological media. These drawbacks can be solved by encapsulating the flavonoid in drug delivery systems [2].

Zein is the major storage protein of maize, GRAS (Generally Recognized as Safe) considered by the FDA, with some advantages like its biodegradability, its prize, or the origin in renewable sources [3]. In this work, we aim to encapsulate quercetin in zein nanoparticles, with the objective of protecting the flavonoid and increasing its bioavailability.

For that purpose, two kinds of nanoparticles as oral carriers for quercetin were developed and compared (nanospheres and nanocapsules). Moreover, two *in vivo* experiments were carried out: the effect of these formulations on the fat content in *Caenorhabditis elegans*, and a pharmacokinetic study in Wistar rats.

Materials and Methods

Nanospheres and nanocapsules were formed by a desolvation method and dried by Spray Drying [4]. The size, polydispersity index and zeta potential were determined. The quercetin loading in the nanoparticles was also quantified by HPLC.

An *in vivo* evaluation assay was performed in *C. elegans* (N2 strain), in which the effect of free and encapsulated quercetin was evaluated in the fat accumulation of L4 larval stage synchronized worms.

A pharmacokinetic study was also performed (protocol number 056-19, Ethical Committee Experimentation of the University of Navarra), in which free and encapsulated quercetin was administered (15 mg/kg) to Wistar rats, and plasma quercetin concentration was analyzed at different time points by LC-MS Orbitrap.

Results and Discussion

The size of the nanoparticles was in the range between 225 and 255 nm, with a polydispersity index lower than 0.15, and a negative zeta potential (Table 1).

Table 1. Characterization of zein nanospheres (NP) and nanocapsules (NP-O). NP-Q: quercetin-loaded nanospheres; NP-O-Q: quercetin-loaded nanocapsules. n = 3.

	Size (nm)	Zeta potential (mV)	Loading (μg/mg NP)
NP	228 ± 6	-40.6 ± 1.6	-
NP-O	247 ± 5	-42.1 ± 0.9	-
NP-Q	226 ± 2	-41.8 ± 4.0	74.8 ± 0.8
NP-O-Q	254 ± 5	-44.5 ± 2.1	74.1 ± 7.8

In *C.elegans* (Figure 1), quercetin decreased the accumulation of fat in a 6% with respect to control, while quercetin-loaded nanospheres decreased this value to 12%. Nevertheless, quercetin-loaded nanocapsules had no difference with the control.

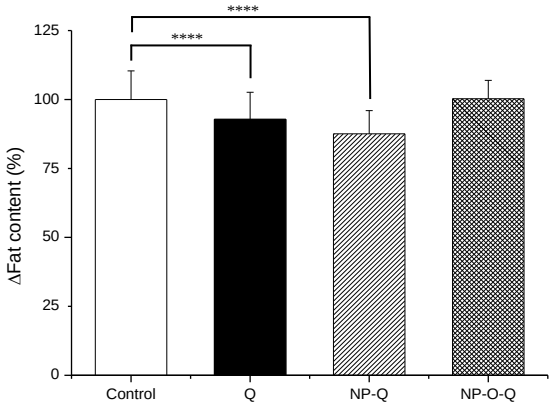

Fig 1. Fat accumulation in *C. elegans* (n ≥ 90). Q: quercetin; NP-Q: quercetin-loaded nanospheres; NP-O-Q: quercetin-loaded nanocapsules. p < 0.0001.

In the pharmacokinetic study in Wistar rats (Figure 2), different pharmacokinetic parameters were calculated, being the relative oral bioavailability of quercetin 9% for quercetin suspension, 37% for quercetin-loaded nanospheres and 25% for quercetin-loaded nanocapsules.

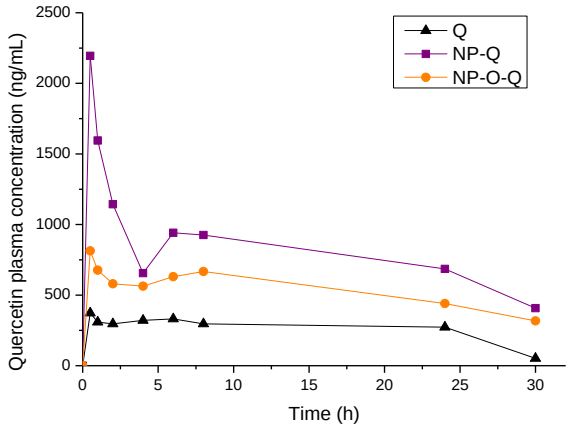

Fig 2. Plasma levels of quercetin in rats after a single dose (n ≥ 5). Q: quercetin; NP-Q: quercetin-loaded nanospheres; NP-O-Q: quercetin-loaded nanocapsules.

The inclusion of an oil in nanoparticles may be useful for the encapsulation of lipophilic compounds because it could increase the payload, modulate its release in order to obtain more sustained profiles, and increase its oral bioavailability by increasing the lymphatic absorption. . However, in this particular case, the formulation of quercetin in nanocapsules did not offer any of these advantages when compared with the conventional nanospheres.

Conclusions

Quercetin was successfully encapsulated in zein nanospheres and nanocapsules. It was demonstrated that quercetin decreases fat accumulation in *C. elegans*, and this effect is increased when the flavonoid is encapsulated in zein nanospheres. In rats, the encapsulation of quercetin in zein nanoparticles increased the absorption of the flavonoid after a single dose. The inclusion of an oil in the nanoparticles did not improve the physicochemical properties, the efficacy or the pharmacokinetic profile compared to nanospheres.

References

[1] M. Bule, A. Abdurahman, S. Nikfar, M. Abdollahi, M. Amini, Antidiabetic effect of quercetin: A systematic review and meta-analysis of animal studies, *Food Chem Toxicol*. 125 (2019) 494-502

[2] X. Cai, Z. Fang, J. Dou, A. Yu, G. Zhai, Bioavailability of Quercetin: Problems and Promises, *Curr Med Chem*. 20 (2013) 2572-82

[3] J.M. Irache, C.J. González-Navarro, Zein nanoparticles as vehicles for oral delivery purposes, *Nanomedicine*, 12 (2017) 1209-11

[4] R. Penalva, C.J. González-Navarro, C. Gamazo, I. Esparza, J.M. Irache, Zein nanoparticles for oral delivery of quercetin: Pharmacokinetic studies and preventive anti-inflammatory effects in a mouse model of endotoxemia, *Nanomedicine Nanotechnology, Biol Med*. 13 (2017) 103-10

P1.18: A Nanotechnology-based Immunotherapeutic Strategy Against KRAS Mutated Colorectal Adenocarcinoma

F. Andrade[1,2]*, D. Rafael[1,3]*, S. Montero[1,2], V.Z. Diaz-Riascos[1,4], S. Schwartz[1], and I. Abasolo[1,2,4]

[1] *Drug Delivery & Targeting, Vall d'Hebron Institut de Recerca (VHIR), Universitat Autònoma de Barcelona (UAB), 08035, Barcelona, Spain.*
[2] *Department of Pharmacy and Pharmaceutical Technology and Physicochemistry, Faculty of Pharmacy and Food Sciences, School of Pharmacy, Universitat de Barcelona (UB), 08028, Barcelona, Spain*
[3] *Networking Research Centre for Bioengineering, Biomaterials, and Nanomedicine (CIBER-BBN), Instituto de Salud Carlos III, 28029 Madrid, Spain.*
[4] *Functional Validation & Preclinical Research (FVPR)/U20 ICTS Nanbiosis, Vall d'Hebron Institut de Recerca (VHIR), Universitat Autònoma de Barcelona (UAB), 08035, Barcelona, Spain.*

*e-mail: diana.fernandes_de_so@vhir.org and fernanda.silva@vhir.org
(These authors contributed equally to the work)

Introducction

Colorectal adenocarcinoma (CRC) has a high prevalence worldwide [1]. A high percentage of the CRC patients present a mutation in a well-known gene called Kirsten rat sarcoma viral oncogene homolog (KRAS). When this mutation is present, there is an aberrant activation of the KRAS protein that will activate molecular cascades responsible for cell malignancy and tumor development [2]. Also, the presence of this mutation could be associated with poor prognosis, low survival rate and drug resistance. Unfortunately, until now any study as succeed to develop effective therapies specifically against the KRAS mutated cancers [3]. We believe that the most efficient and specific way to achieve this objective is to deliver a specific antibody against the KRAS isoform present in each tumor to the interior of the tumor cells. The antibodies by itself do not have the capacity to internalize into the cells and required the help of carriers with a nanometric size [4].

Materials and Methods

Based in our previous works [5], Pluronic® F127-based polymeric micelles (PM) was used for the intracellular delivery of the KRAS antibodies. PM were fully characterized in terms of their mean diamenter, polydispersity index and zeta potential. Moreover, were assessed their internalization and biological efficiacy in different KRAS-mutated and non-mutated celllines, using flow cytometry and cytotoxicity assays, respectively. The affectation of the KRAS-medidated biological cascade after the treatment with the PM encapsulating the anti-KRAS antibody (PM-KRAS) was assessed by RT-qPCR and Western Blot techniques. Finally, the effect of the proposed formulation was validated *in vivo* in a colon cancer model. For this propose, female athimic mice with 6-7 weeks (Hsd:Athymic Nude-Fox) will subcutaneously injected with HCT116 parental colon cancer cells for tumor formation. Posteriorly, the animals were treated 3X a week during 3 weeks with the formulaion and the tumor growth was evaluated in comparison with the control group (animals treated only with the PM vehicle). *In vivo* studies were performed by the ICTS "NANBIOSIS", at CIBER-BBN's in vivo Experimental Platform for Functional Validation & Preclinical Research (FVPR).

Results and Discussion

The Pluronic® F127 micelles previously optimized by the group for the encapsulation of other drugs and biomolecules [5-7], were now used for the intracellular delivery of antibodies. As expected, the formulation presented all the ideal features for intravenous administration, i.e., mean diameter, polydispersity, morphology, and safety.
In terms of *in vitro* efficacy, it was possible to observe a strong inhibition of cell proliferation for the HCT116 colon cancer cells (G13D KRAS mutation) treated with the PM-KRAS formulation. On the contrary, no effect in terms of cell proliferation reduction was observed in the non-mutated cell line HCT8 (Fig. 1). In both cell lines any cytotoxic effect was detected in cells treated with the free KRAS antibody.
A similar profile was also observed in pancreatic cancer cell lines with and without KRAS mutation.

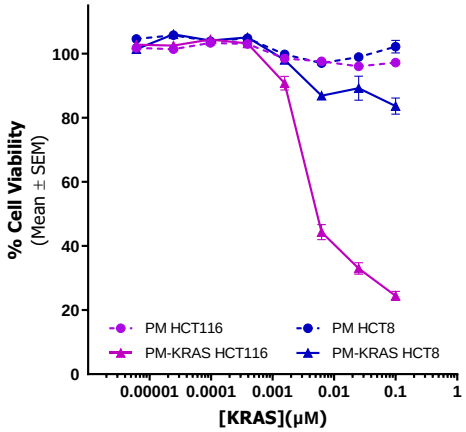

Fig 1. In vitro citotixicity assay in HCT116 and HCT8 colon cancer cll lines treated with PM-KRAS and PM. Results are expressed as mean ± SEM, n≥3

Due to the *in vitro* promising results, the formulation was tested *in vivo* in a subcutaneos colon cancer tumor bearing mice model. After 3 weeks of treatement with the PM-KRAS injected 3 times a week it was possible to observe a clear decrease in the tumor volume, when comparing with the mice treated with the empty micelles (Fig. 2). Importantly, any adverse effects were registered during the time of the treatment.

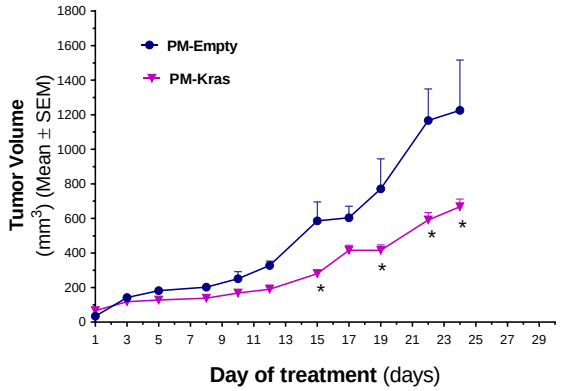

Fig 2. *In vivo efficacy assay. Tumor volume over the time*. Results are expressed as mean ± SEM, n ≥ 3.

Conclusions

Taking all the results into consideration, the here presented formulation demonstrated to be able for to deliver antibodies intracellularly in its active form. Consequently, it was possible to effectivley block the KRAS pathway in colon cancer KRAS mutated cells, promoting the inhibition of cell proliferation *in vitro*. More importantly, the treatment with PM-KRAS significanctly impaired the tumor growth in an *in vivo* colon cancer model.

Acknowledgments

This work was supported by the Networking Research Centre on Bioengineering, Biomaterials, and Nanomedicine (CIBER-BBN) which is financed by the Instituto de Salud Carlos III (ISCIII) with assistance from the European Regional Development Fund (ERDF). We also thank the denomination of Consolidated group from Generalitat de Catalunya (2017-SGR-00638).

References

[1] World Health Organization. Cancer. Available from: https://www.who.int/health-topics/cancer

[2] M. Meng, K. Zhong, T. Jiang, *et al*. The current understanding on the impact of KRAS on colorectal cancer. Biomed Pharmacother.140 (2021) 111717

[3] M. Cefalì, S. Epistolio, M.C. Palmarocchi, *et al.* Research progress on KRAS mutations in colorectal cancer. J Cancer Metastasis Treat 7 (2021) 26

[4] T.A. Slastnikova, A.V. Ulasov, A.A. Rosenkranz, *et al*. Targeted Intracellular Delivery of Antibodies: The State of the Art. Front Pharmacol. 9 (2018) 1208

[5] S. Montero, J. Seras-Franzoso, F. Andrade, *et al.* Intracellular Delivery of Anti-SMC2 Antibodies against Cancer Stem Cells. Pharmaceutics 12(2) (2020) 185

[6] F. Andrade, D. Rafael, M. Vilar-Hernández, et al. Polymeric micelles targeted against CD44v6 receptor increase niclosamide efficacy against colorectal cancer stem cells and reduce circulating tumor cells in vivo. J Control Release 331 (2021) 198-212

[7] P. Gener, S. Montero, H. Xandri-Monje, et al. Zileuton™ loaded in polymer micelles effectively reduce breast cancer circulating tumor cells and intratumoral cancer stem cells. Nanomedicine 24 (2020) 102106

P1.19: Self-Illuminating Biocompatible Nanosystems can Induce Apoptosis Via Photodynamic Therapy (PDT)

Abal-Sanisidro M[1]*, Ruiz-Cañas L[5], Blanco MG[3], López-López R[2,4], Sainz B Jr[5,6], de la Fuente M[1,4]*

[1]*Nano-Oncology and Translational Therapeutics Unit, Health Research Institute of Santiago de Compostela (IDIS), 15706 Santiago de Compostela, Spain.*
[2]*Translational Medical Oncology Group (ONCOMET), Health Research Institute of Santiago de Compostela (IDIS), 15706 Santiago de Compostela, Spain.*
[3]*Center for Research in Molecular Medicine and Chronic Diseases (CiMUS), Santiago de Compostela, Spain.*
[4]*Cancer Network Research (CIBERONC), 28029 Madrid, Spain.*
[5] *Department of Cancer Biology, Instituto de Investigaciones Biomédicas "Alberto Sols" (IIBM), CSIC-UAM, 28029 Madrid, Spain; jclopez@iib.uam.es (J.C.L.-G.); lmartin@iib.uam.es (L.M.-H.).*
[6]*Chronic Diseases and Cancer, Area 3-Instituto Ramon y Cajal de Investigación Sanitaria (IRYCIS), 28029 Madrid, Spain*

*e-mail: marce.abal.san@gmail.com

Introduction

Pancreatic cancer is one of the most difficult cancers to treat due to its pathological features, presenting a death rate of around 80% [1]. Therefore, the development of new strategies to address this tumor are essential. Photodynamic Therapy (PDT) has proven to be efficient for treating external lesions such as melanoma. Besides, this therapy provides a new approach to its treatment and has some proven advantages compared to chemotherapy, radiotherapy and immunotherapy. Nevertheless, due to the poor penetration of light, conventional PDT is not adequate for treating internal organs [2]. In this study, we aim to determine the potential of self-illuminating Sphingomyelin Nanosystems (SI-SNs), to mediate a localized and controlled antitumoral response in pancreatic cancer using Rose Bengal (RB) as a photosensitizer [3]. For that, we propose to decorate biocompatible SNs [4] with the bioluminescent protein RLuc8 and to load them with the photosensitizer Rose Bengal (RB). The aim of this study was to fully characterize the developed SI-SNs and to obtain the first proof-of-concept of the potential of this new nanosystem to mediate PDT in pancreatic cancer, as well as to explore the potential *in vivo* application by determining the ability of the nanosystems to self-illuminate *in vivo*.

Materials and Methods

Sphingomyelin Nanosystems (SNs) were prepared by ethanol injection and characterized in terms of their hydrodynamic diameter, polydispersity index (PDI) and zeta potential (ZP) using a Nanosizer 2000® (Malvern Instruments). SNs were loaded with the photosensitizer Rose Bengal. Then, SNs were decorated covalently with RLuc8, a bioluminescent protein, which is a *Renilla reniformis* luciferase mutant, in order to obtain SI-SNs. This RLuc8 enzyme is activated with an appropriate substrate (Coelenterazine, CTZ) to produce the PDT process within the whole nanosystem. *In vitro* studies have been carried out in pancreas to liver metastatic cancer cells L3.6pl. MTT assay has been performed with the nanosystem components separately and forming the complete SI-SNs. Reactive Oxygen Species (ROS) evaluation by fluorescence method was also tested to confirm apoptosis induction after PDT treatment. Biodistribution of SI-SNs was assessed in healthy mice up to 24h as a first hint that SI-SNs was able to emit light inside healthy living being.

Results and Discussion

After the protein's association was carried out SI-SNs was characterized by different methodologies such as HPLC-MS, MALDI-TOF, Transmission Electron Microscopy (TEM) and Nanoparticle Tracking Analysis (NTA) showing homogenous morphology and efficacious protein incorporation onto SNs. The physicochemical properties of SI-SNs were determined by DLS and LDA. Stability was assessed by monitoring the mean nanoparticles size upon storage and after incubation with biorelevant media. SI-SNs were efficiently internalized into pancreatic cancerous cells, cytotoxicity assays were also performed indicating low SI-SNs toxicity at concentrations as high as 10 mg/mL and PDT treatment was successfully evaluated *in vitro* after performing ROS assays (fig. 1). As a first proof of concept *in vivo*, SI-SNs biodistribution was followed up in IVIS after its activation in healthy

mice.

Table 1. Physicochemical Characterization Measured by DLS and LDA (Results are Expressed as Mean ± Standard Deviation, n = 3).

Formulation	Size (nm)	PdI	ZP (mV)
SNs	57 ± 3	<0.2	- 37 ± 2
SI-SNS	165 ± 4	<0.1	- 34 ± 1
SI-RB-SNs	200 ± 2	<0.2	- 40 ± 2

SNs – Sphingomyelin Nanosystems
SI-SNs – Self-illuminating Sphingomyelin Nanosystems
SI-RB-SNs - Self-illuminating Rose Bengal Sphingomyelin Nanosystems.

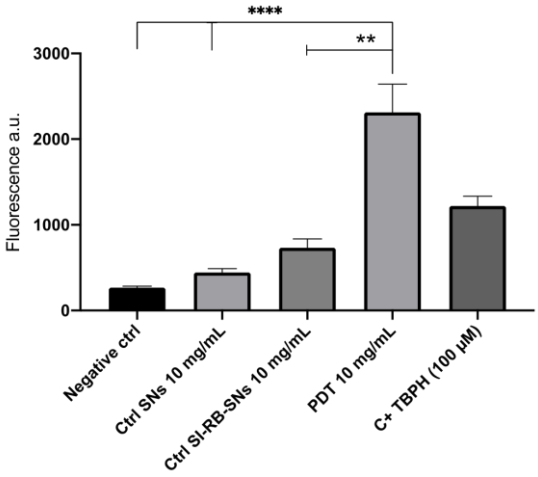

Fig 1. ROS evaluation *in vitro* of SI-RB-SNs confirming the successfully PDT process and the apoptosis induction within pancreatic tumoral cells.

Conclusions

We have stablished the proof of concept of the potential of a versatile and biodegradable nanoplatform, SNs, to have an application in PDT, based in the activation of an encapsulated photosensitive drug by a bioluminescent protein attached onto the SNs surface. SI-SNs have demonstrated an optimal colloidal stability through time and in biorelevant media, while they emit light up to 6 months, confirming the bioluminescent functionality. SI-SNs show a good cell uptake and low toxicity at high concentrations. More importantly, SI-SNs can promote ROS generation within cancer cells to induce apoptosis and therefore have the potential to deliver a PDT process into the very deep pancreatic cancer cells without irradiation of an external laser. Preliminary *in vivo* studies, confirm their ability to emit light after retroorbital injection. Next experiments will be aimed to translate this work to pancreatic *in vivo* models.

Acknowledgments

This work was supported by ISCIII/FEDER funds (AC18/00107), ERA-NET Euronanomed III PANIPAC project.

References

1. https://www.cancer.gov/research/progress/annual-report-nation. NCI. (2021)
2. Yang Y, Hou W, Liu S, Sun K, Li M, Wu C, Biodegradable Polymer Nanoparticles for Photodynamic Therapy by Bioluminescence Resonance Energy Transfer, *Biomacromolecules*, 19(1), 201-208 (2018).
3. Kim S, Jo HC, Jeon M, Choi MG, Hahn SK, Yun SH, Luciferase–Rose Bengal conjugates for singlet oxygen generation by bioluminescence resonance energy transfer, *Chem.Commun*.,53,4569-4572 (2017).
4. Bouzo, B. L., Calvelo, M., Martín-Pastor, M., García-Fandiño, R., & de la Fuente, M. (2020). In Vitro–In Silico Modeling Approach to Rationally Designed Simple and Versatile Drug Delivery Systems. The Journal of Physical Chemistry B, 124(28), 5788-5800.

P1.20: Evaluation of Eudragit S100 nanofibers as pH responsive antimicrobial reease system

L.G. Miranda-Calderon[1,2*], C. Yus[1,2],G. Landa[1,2],M. Arruebo[1,2,3,4], G. Mendoza[3,4] and S. Irusta[1,2,3,4] .

1. Instituto de Nanociencia y Materiales de Aragón, CSIC-Universidad de Zaragoza, España.
2. Department of Chemical Engineering, University of Zaragoza, 50018 Zaragoza, España.
3. Aragon Health Research Institute, 50009 Zaragoza, España.
4. Networking Research Center on Bioengineering, Biomaterials and Nanomedicine, CIBER-BBN, 28029 Madrid, España.
*e-mail: laumiranda270@gmail.com

Introduction

Drug administration using controlled release polymeric systems offers a wide range of benefits including higher effectiveness, lower toxicity and improved patient compliance compared to the administration of the corresponding free drug. Dosage forms based on electrospun polymeric nanofibers have been used as controlled drug release systems in advanced wound dressings to promote a fast wound healing [1]. Among these materials, intelligent polymers are widely studied due to their ability to respond to endogenous or exogenous stimuli including differences in pH, ionic strength, reductive character or under the presence of specific triggering biomolecules [2]. Particularly, the pH-sensitive copolymer Eudragit® S100 (ES100) possesses pH-dependent solubility that has been widely exploited as enteric drug coatings [3].

In this work, polymeric dressings based on ES100 and loaded with different pharmaceutical agents: antibiotics and natural and synthetic antiseptics are assembled by electrospinning. The fabricated dressings were physico-chemically characterized and their pH-responsiveness evaluated at the specific pH values identified during wound healing.

Materials and Methods

ES100 solution (30% w/v) was prepared in a DMF:EtOH (4:1) mixture that was stirred overnight at RT. For Rifampicin (RIFA), Chlorhexidine (CHXD) and Thymol (THY)-loaded dressings, the adequate amount of the therapeutic agent (2.5%, 5% and 20% w/w, respectively, referred to the polymer) was added to the solution and then stirred. A 10 mL syringe was filled with the resulting solution and fed to a Yflow 2.2 D500 electrospinner (Electrospinning Machines/R&D Microencapsulation, Spain) equipped with a flat plate collector. The flow rate was set at 1.0 mL/h, the distance between the tip of the needle and the collector was fixed at 15 cm with a voltage of 15-18kV.

The characterization of the drug-eluting dressings was carried out using different techniques: scanning electron microscopy (SEM) to determine the morphology and the average diameter of the nanofibers, drug release was carried out in three buffers of varied pH (i.e., pH 5.5, 7.4, 8.2) corresponding to healthy, lacerated, and wounded-infected skin, respectively. Monitoring the absorption of the drugs released from the dressings through UV-Vis spectroscopy, we demonstrated a pH-dependent drug release. The minimum inhibitory concentration and maximum bactericidal concentration for RIFA and THY were determined by using the standard microbial test of decimal plate dilutions against Gram-positive (*S. aureus*) and Gram-negative (*E. coli*) bacteria. For the evaluation of the antimicrobial action of CHXD a Kirby-Bauer disk diffusion test was carried out against the same bacteria.

Results and Discussion

Morphological characterization reveals well-defined fibers having nanometric diameters as can be observed in the SEM images (Fig 1 a-d). Fiber size histograms show homogeneous and narrow diameter distributions 1160 ± 245 nm for ES100 30% (w/w), 536.66 ± 82 nm for ES100 30% RIFA 2.5%, 854.45 ± 111 nm for ES100 30% CHXD 5%, and 655.90 ± 93 nm for ES100 30% THY 20% (Fig 1 e-h, respectively). The decrease in the voltage needed to produce homogeneous RIF loaded ES100 fibers would be the reason for the lower diameter in this case. The effect of applied voltage can also be noticed in CHXD and THY ES100 loaded fibers.

The drug loading and encapsulation efficiency of each dressing are described in Table 1 along with the yield of every synthesis, showing that RIFA and THY loaded in ES100 show higher therapeutic loading ability than CHXD. The different EE for the three drugs could be related to their different physical properties. Furthermore, the release of each drug after 24h is shown (Table 1) according to the pH of the release media: 100% of loaded RIFA was released at pH above 7, when the fibers started to be affected, while in an acid buffer only 25% of loaded RIF was released. There is the expected CHXD release increase when the pH changes from 5.5 to 7.4, but further

increase to 8.2 lead to a decrease in the amount of released drug.

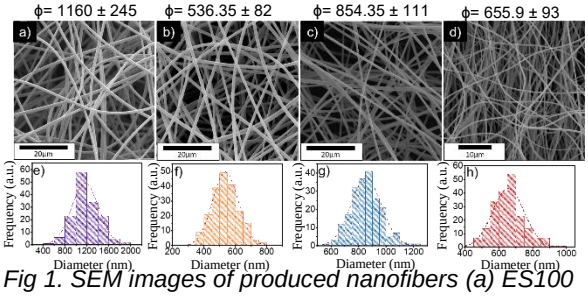

Fig 1. SEM images of produced nanofibers (a) ES100 30% (b) ES100 w/RIFA 2.5%, (c) ES100 w/CHXD 5%, (d) ES100 w/THY 20% and diameter distribution histograms (e-h) n=200.

This effect could be related to an ionization of the released CHXD at the pH of the dissolution medium, higher than the CHXD pKa, that causes its re-adsorption on the fibers surface. THY release was negligible and independent of the buffer pH, probably due to polymer-drug interactions according to FTIR results (not shown) and to the high hydrophobicity of THY that would hinder its release at any pH in aquous medium.

Table 1. Nanofiber yield of Eudragit ES100, DL (w/w %) and EE (%) and release profiles at different pH of each fiber with pharmaceutical agent. Mean ±SD (N = 6)

Loaded Drug	Yield (%)	D.L. (%)	E.E. (%)	D.R. pH 5.5 24h (%)	D.R. pH 7.4 24h (%)	D.R. pH 8.2 24h (%)
2.5% Rifampicin	79	2.33	94 ± 5	25.1 ± 5	100 ± 2	100 ± 5
5% CHXD	93	1.56	32 ± 2	23.4 ± 2	72 ± 7	34 ± 9
20% Thymol	61	11	64 ± 3	N/A	N/A	N/A

Antibacterial tests for ES100 RIFA and THY were carried out being the RIF minimum bactericidal concentration (MBC) for *S. aureus* 0.1 mg/ml and 1.5 mg/ml for THY while for *E. coli* 2 mg/ml and 1 mg/ml were the MBC doses, respectively. Furthermore, minimum inhibitory concentration (MIC) was very low for ES100 RIFA in *S. aureus* assays (0.0125 mg/ml) and also in this range for *E. coli* (0.25 mg/ml) pointing to its higher efficiency compared to THY loaded fibers due to the antibiotic character of RIFA vs the antiseptic characteristics of THY.

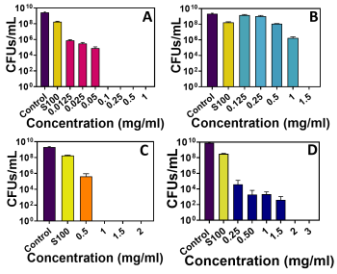

Fig 2. Minimum Inhibitory Concentration (MIC) and Minimum Bactericidal Concentration (MBC) for (A) ES100 w/Rifa (B) ES100 w/Thy vs S. aureus and (C) ES100 w/Rifa, (D) ES100 w/Thy vs E. coli.

In the case of ES100 w/CHXD, a Kirby-Bauer test was performed to measure the zone of inhibition using electrospun dressings having 12 (1.5 ± 0.3 mg), 16 (2 ± 0.5 mg) and 20 mm (2.7 ± 0.2 mg) in diameter showing an increase in the zone of inhibition after 24h of contact, which is indicative of their large antibacterial activity.

Specifically, ES100 CHXD displayed an increase in the inhibition halo diameter of 2-3 mm in the case of *E. coli* while for *S. aureus* samples the increase was lower (< 2 mm), pointing to a slightly higher efficiency of the fabricated dressings against Gram negative bacteria.

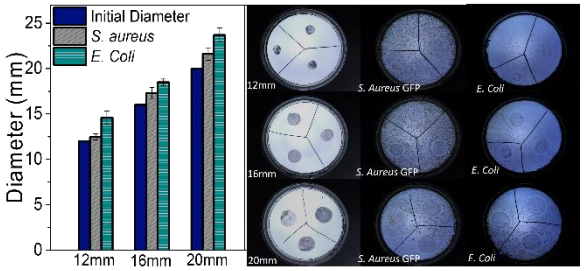

Fig 3. Inhibition halo form by ES100 w/CHXD against S. aureus and E. coli.

Conclusions

Polymeric wound dressings based on ES100 loaded with different pharmaceutical agents were fabricated by electrospinning, maintaining the chemical and morphological stability of the loaded therapeutic molecule and showing pH-responsiveness. Additionally, this drug-eluting system can be used as advanced wound dressings, thanks to their high drug loading ability and their demonstrated antibacterial activity against Gram-positive and Gram-negative bacteria.

Acknowledgments

This work was supported by the Ministry of Economy and Competitiveness of Spain (grant number CTQ2017-84473-R). CIBER-BBN is an initiative financed by the VI National R+D+i Plan 2008-2011, Iniciativa Ingenio 2010, CIBER actions are financed by the Carlos III Health Institute (Spain) with the help of the European Regional Development Fund. L.G. is also grateful for the support of CONACYT, grant CVU710618 (Mexico). G.M. gratefully acknowledges the support from the Miguel Servet Program (MS19/00092; Instituto de Salud Carlos III).

References

[1] Chunder A, *et. al.* Fabrication of Ultrathin Polyelectrolyte Fibers and Their Controlled Release Properties. *Colloids Surf.* , B (2007); 58:172.

[2] Joshi M. Role of eudragit in targeted drug delivery. *Int J Curr Pharm Res* (2013); 5:58-62.

[3] Ding Y, *et. al.* Core-Shell Eudragit S100 Nanofibers Prepared via Triaxial Electrospinning to Provide a Colon-Targeted Extended Drug Release. *Polymers* (2020); 12:E2034.

P1.21: Nucleic acid based medicinal products for Fabry disease: critical formulation factors to ensure effective delivery

I. Gómez-Aguado[1,2]*, J. Rodríguez-Castejón[1,2], M. Beraza-Millor[1,2], A. Rodríguez-Gascón[1,2], A. del Pozo-Rodríguez[1,2] and M.A. Solinís[1,2]

[1] *Pharmacokinetic, Nanotechnology and Gene Therapy Group (PharmaNanoGene), Faculty of Pharmacy, Centro de Investigación Lascaray Ikergunea, University of the Basque Country UPV/EHU, Vitoria-Gasteiz, Spain*

[2] *Bioaraba, Microbiology, Infectious Disease, Antimicrobial Agents, and Gene Therapy, Vitoria-Gasteiz, Spain*

*e-mail: itziar.gomez@ehu.eus

Introduction

Fabry Disease (FD) is a metabolic disorder caused by mutations in *GLA* gene, resulting in a defficiency of α-galactosidase A (α-Gal A) enzyme activity. Therefore, a progressive deposition of glycosphingolipids occurs, mainly within the lysosomes of vascular endothelial and smooth muscle cells [1].

The liver is a specialised organ in protein synthesis, and it could be an opportunity to treat FD by transfecting hepatocytes with nucleic acids that encode α-Gal A. In this way, the lliver could act as a protein factory to later release it and restore the enzyme deficiency in the affected organs. However, the design of suitable non-viral delivery systems targeting hepatocytes still remains a challenge [2].

Solid Lipid Nanoparticles (SLNs) are regarded as one of the most promising non-viral gene delivery systems, due to their wide versatility and efficacy of transfection. In fact, SLNs are such as moldeable tool that they can deliver any type of genetic material [3].

The aim of this work was the design of mRNA-and pDNA-medicinal products based on SLNs and the evaluation of their capacity to transfect a liver-derived cell line (Hep G2).

Materials and Methods

Four different SLNs were formulated to prepare the delivery systems. SLNs were synthesized with Tween 80 and Precirol® ATO5 and a combination of cationic and ionizable lipids. Two of them were prepared with DOTAP as cationic lipid, and two different techniques: solvent evaporation/emulsification (SLN_{EE}) and hot-melt emulsification (SLN_{HM}) [4]. The other two were formulated with a mix of DOTAP and the ionizable lipid DODAP (DOTAP/DODAP), and they were prepared by the same two methods. In order to obtain the final vectors, mRNA or pDNA encoding green fluorescent protein (GFP) was complexed with protamine (P), a polysaccharide (dextran (DX) or galactomannan (GM)) and SLNs.

SLNs and vectors were characterized in terms of size and zeta potential. Thereafter, transfection efficacy, intensity of fluorescence, indicative of the amount of protein produced by transfected cells, and cell viability were evaluated in Hep G2 cells by flow cytometry.

Results and Discussion

The preparation method influenced the physicochemical features of the SLNs and vectors, in terms of particle size and surface charge. SLNs with the same composition but prepared by different methods, varied in particle size. It ranged from 93.3 nm in the case of SLN_{HM} to 198.7 nm in the case SLN_{EE}. The size of vectors (Table 1) containing SLN_{EE} ranged from 156.9 nm to 246.6 nm, whereas the size of vectors bearing SLN_{HM} ranged from 91.8 nm to 201.1 nm. All formulations showed a PDI lower than 0.4 and a positive charge, between + 29.7 mV to +45.9 mV.

Table 1. Size of SLN_{EE}- and SLN_{HM} based vectors.

			mRNA	pDNA
DOTAP	**SLN_{EE}**	**DX**	246.8 ± 1.3	176.4 ± 0.4
		GM	198.1 ± 0.6	156.9 ± 2.4
	SLN_{HM}	**DX**	132.3 ± 1.9	91.8 ± 1.0
		GM	136.5 ± 0.7	98.3 ± 0.9
DOTAP/ DODAP	**SLN_{EE}**	**DX**	210.1 ± 0.8	165.8 ± 1.7
		GM	209.6 ± 2.4	158.8 ± 2.5
	SLN_{HM}	**DX**	203.4 ± 1.1	117.5 ± 1.1
		GM	201.1 ± 3.6	119.1 ± 1.2

All formulations were able to transfect Hep G2 cells (Figure 1), although differences in transfection capacity were observed depending on the preparation method, the composition of SLNs and the type of nucleic acid.

The highest percentages of transfected cells were achieved with pDNA formulated with SLN_{EE} composed by DOTAP/DODAP mixture.

The influence of the type of cationic lipid included in the SLNs was different depending on the type of nucleic acid carried. mRNA transfection was more effective with DOTAP-SLNs in terms of both percentage of transfected cells and protein production. Nevertheless, pDNA formulated in DX-SLN$_{EE}$, DX-SLN$_{HM}$ and GM-SLN$_{EE}$ composed by DOTAP/DODAP transfected a higher number of Hep G2 cells, although with a similar production of GFP per cell, than those composed by DOTAP.

Cell viability was higher than 85%, although formulations prepared with DOTAP/DODAP presented the highest values.

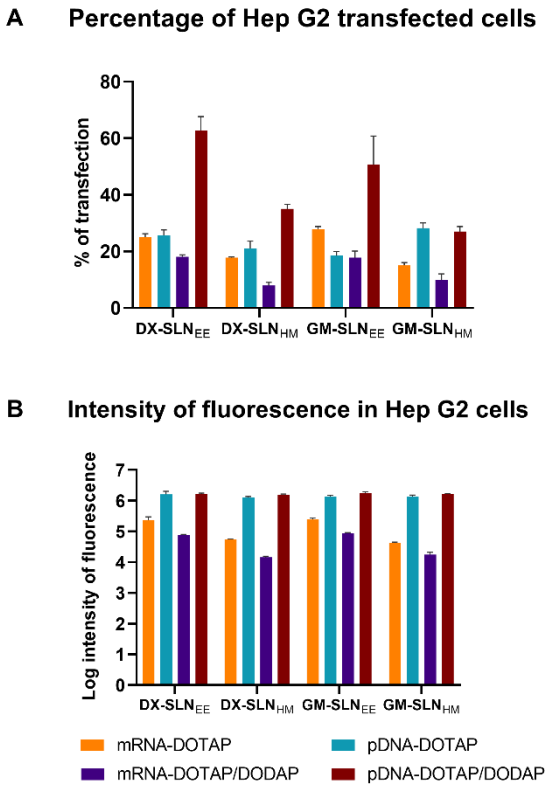

Fig 1. Transfection efficacy in Hep G2 cells after the addition of SLN$_{EE}$ and SLN$_{HM}$ vectors. A: Percentage of transfected cells. B: Log of intensity of fluorescence.

The transfection process is influenced by different factors which are formulation- and cell-dependent, such as the entry mechanism. The main mechanism used by SLNs to enter inside the cells is endocytosis, which is associated with intracellular endosomal/lysosomal pathways. Indeed, endosomal escape plays an important role in the release of the nucleic acid into the cytoplasm, and consequently, in the transfection efficacy. The ability of the ionizable lipid DODAP to become protonated in the acidic environment destabilizes the endosomal membrane and facilitates the release of the nucleic acid [5].

In the case of pDNA vectors the presence of DODAP in the formulations increased transfection efficacy in Hep G2; the endosomal escape seems to be an important limitation for DNA nanomedicines targeted to hepatocytes. The nuclear entry, one of the main drawbacks for DNA transfection, seems not to be a limiting step in this case, which may be due to the presence of protamine, rich in nuclear localization signals.

The bottleneck for an mRNA successful therapy in hepatocytes seems to be its instability in the cytoplasm. The design of specific delivery systems adapted to the nucleic acid features are necessary to protect the genetic material allowing a suitable intracellular disposition to favour the transduction process.

Conclusions

The formuation of SLNs-based vectors with the ionizable lipid DODAP, designed to improve the endosomal escape, is appropriate for pDNA therapies targeted to hepatocytes, since it increases their transfection efficiency. Conversely, increasing mRNA protection without compromising release into the cytoplasm are the critical points to be considered for proper nanosystem design.

Acknowledgments

I. Gómez-Aguado and M. Beraza-Millor thank the University of the Basque Country UPV/EHU (PIF17/067 and PIFG19/36, respectively) and J. Rodríguez-Castejón thanks the Basque Government (PRE_2020_2_0120) for their research grants. This work was supported by MCIU/AEI/FEDER, UE (RTI2018-098672-B-I00) and by the University of the Basque Country UPV/EHU (GIU20/048).

References

[1] J. Rodríguez-Castejón, A. Alarcia-Lacalle, I. Gómez-Aguado, *et al*. α-Galactosidase A augmentation by non-viral gene therapy: evaluation in fabry disease mice. *Pharmaceutics.* 13(6) (2021) 771.

[2] R.N. Aravalli, J.D. Belcher, C.J. Steer. Liver-targeted gene therapy: approaches and challenges. *Liver Transpl*. 21(6) (2015) 718-737.

[3] A. del Pozo-Rodríguez, M. A. Solinís and A. Rodríguez-Gascón. Eur J Pharm Biopharm. 109 (2016) 184–193.

[4] I. Gómez-Aguado, J. Rodríguez-Castejón, M. Beraza-Millor, *et al.* mRNA-based nanomedicinal products to address corneal inflammation by interleukin-10 supplementation. *Pharmaceutics*. 13(9) (2021) 1472.

[5] P.R. Cullis and M.J. Hope. Lipid Nanoparticle Systems for Enabling Gene Therapies. *Mol Ther*. 25 (2017) 1467-1475.

P1.22: Fluorescence Cross-Correlation Spectroscopy reveals extent of association between liposomes and DNA and the number of DNA molecules per lipid nanoparticle

R. Gaspar, J.L. Paris, P.A.A. De Beule[1], B.F.B. Silva[1]*

[1]*INL – International Iberian Nanotechnology Laboratory, Av. Mestre José Veiga, 4715-310 Braga, Portugal*

*e-mail: bruno.silva@inl.int

Introducction

The formation of lipid-nucleic acid nanoparticles (LNPs) is driven by electrostatic interactions between cationic lipids and nucleic acids. While high-resolution methods such as cryo-TEM and SAXS exist to determine the LNPs' structure, quantifying the association between lipids and DNA/mRNA is more cumbersome. In this regard, Fluorescence Cross-Correlation Spectroscopy (FCCS) can provide further insights into the association behavior and be a valuable tool in formulation development. By labeling lipids and DNA with two spectrally-resolved fluorescent dyes, FCCS can follow the correlations between the motions of lipids and DNA as they diffuse in-and-out of a confocal volume. Hence the cases where lipids and DNA move together in the same particles can be distinguished from those where they move independently [1-3].

Materials and Methods

Liposomes were constituted by cationic DOTAP and neutral DOPC lipids at different compositions, and mixed with DNA at various charge ratios (ρ_{chg}). DNA was fluorescently labelled with YOYO-1 (green) and liposomes with Texas-Red. FCCS measurements were performed on a Zeiss LSM 780-NLO microscope.

Results and Discussion

The co-localization between DNA and liposomes can be accessed through the relative amplitudes of the cross-correlation and auto-correlation functions of the labelled species (Fig. 1). This allows following the incorporation of DNA into LNPs as a function of ρ_{chg}, providing a fast estimate of the lipid composition needed to fully encapsulate DNA [4]. Full incorporation of DNA is achieved at ρ_{chg}~2. Further analysis provides the average number of DNA plasmids incorporated per LNP [3-4], which is a quantity difficult to access with other techniques. Importantly, at ρ_{chg}<1 liposomes with less cationic lipid are able to incorporate more DNA than liposomes with more cationic content, but at ρ_{chg} >1 the opposite happens [4]. This is of relevance for LNP design.

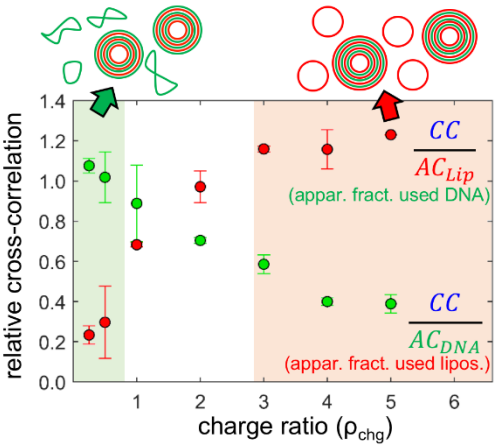

Fig 1. Relative cross correlation functions vs. ρ_{chg}. For ρ_{chg} <1 there is excess DNA in solution and practically all liposomes are co-localized with DNA (CC/AC_{DNA} ~1). For ρ_{chg}>2 there is excess of liposomes in solution and practically all DNA is co-localized with liposomes (CC/AC_{Lip} ~1).

Conclusions

The results show that FCCS is a powerful method, directly probing LNP formation and extent of lipid-DNA association, hence providing new insights that are difficult to achieve with traditional methods.

Acknowledgments

This research is supported by Microfluidic Layer-by-layer Assembly of Cationic Liposome - Nucleic Acid Nanoparticles for Gene Delivery project (032520) co-funded by FCT and the ERDF through COMPETE2020. JLP is supported by a postdoctoral fellowship from the Ramón Areces Foundation.

References

[1] K. Bacia, P. Schwille, *Nat. Protoc.* 2 (2007) 2842
[2] D. Merkle, S.P. Lees-Miller, D.T. Cramb, *Biochemistry* 43 (2004) 7263
[3] A.I. Gómez-Varela, R. Gaspar, A. Miranda, J.L. Assis, R.R.H.F. Valverde, M. Einicker-Lamas, B.F.B. Silva, P.A.A. De Beule, *J. Biophotonics* 14 (2021) e202000200
[4] R. Gaspar, J.L. Paris, P.A.A. De Beule, B.F.B. Silva, MS in preparation

P1.23: DOSY as an Alternative Technique to Monitor the Degradation of Polypeptide-Based Drug Delivery Systems

J.J. Arroyo-Crespo[#,1], I. Conejos-Sánchez[#,2], D. Morelló-Bolumar[#,1], S. Stifano[1], V.J. Nebot[1] and M.J. Vicent[*,2]

[1]*Polypeptide Therapeutic Solutions, S.L. (PTS), Av. Benjamin Franklin 19 46980 Paterna, Valencia, Spain*
[2]*Polymer Therapeutics Lab. Prince Felipe Research Center. Av. Eduardo Primo Yúfera,3, 46012 Valencia, Spain*

e-mail: iconejos@cipf.es # Authors with Equal Contribution

Introduction

Safety concerns regarding non-biodegradable polymer-based drug delivery systems have fostered an interest in polypeptides as functional biodegradable carriers[1]. Polypeptides can overcome specific challenges in drug delivery, and advances in controlled polymerization techniques, material bioresponsiveness, analytical methods, and scale-up-manufacture processes have supported their development.
Polypeptides undergo natural degradation within the body thanks to enzymatic activity and/or the presence of acidic/oxidative stress. Polypeptide degradation improves drug availability and cellular uptake while ensuring metabolic clearance and reducing accumulation-related side effects. A deeper understanding of degradation may contribute to the optimal control of industrial polypeptide production in terms of reproducibility and quality; however, extensive studies of polypeptide biodegradability under various microenvironments and complex biological matrices represents an analytical challenge. While size exclusion chromatography (SEC) represents the most common technique to monitor polypeptide degradation, the increasing number/diversity of molecular species in solution during polypeptide degradation hampers the application of this tool.
For this reason, we have evaluated the use of diffusion-ordered NMR spectroscopy (DOSY)[2] as an alternative technique to complement/replace SEC as a means to monitor polymer degradation. Herein, we present a comprehensive comparison of these quantitative analytical approaches to assess polymer biodegradation rates.

Materials and Methods

Poly-L-ornithine (PLO), poly-L-glutamic acid (PGA), polysarcosine (PSar), hyaluronic acid (HA), and poly(ethylene glycol) (PEG) were subjected to degradation under optimized enzymatic or hydrolytic/oxidative conditions. NMR experiments were acquired at 27 °C (300K) on a Bruker Avance III 300 MHz Bruker spectrometer equipped with a 5 mm TBI broadband probe. Data were processed with Mestrenova software (Bruker GmbH). SEC analysis employed an AF2000 system (Postnova Analytics, Landsberg, Germany) configured to work in GPC mode.

Results and Discussion

We selected two enzymatically degradable polypeptides: **PGA**, which we cleaved using the cysteine protease cathepsin B (overexpressed in certain cancers and other pathological conditions), and **PLO**, which we cleaved with a protease cocktail including endo-, amino-, and carboxy-peptidases. We also selected the proteolytically-resistant **PSar**, which we subjected to oxidative degradation (a condition linked to multiple pathologies including inflammation, chronic diseases, and cancer). To evaluate the utility of DOSY beyond polypeptides, we also included **HA**, which we cleaved with hyaluronidase, and non-biodegradable **PEG**, which we subjected to harsh acidic hydrolysis.
We monitored the successful degradation of all polymers by SEC and DOSY. Importantly, SEC profiles supported myriad interpretations and unclear conclusions; however, DOSY allowed us to consistently track loss in molecular weight over time.

Conclusion

We provide evidence for DOSY as a highly utile technique that can help to monitor/describe polypeptide degradation under in vivo-like biological scenarios.

Acknowledgments

This work was supported by the "la Caixa" Foundation under the framework of the Healthcare Research call 2019 (LCF/PR/HR19/52160021; NanoPanther) and the Spanish Ministry of Science, Innovation, and Universities (RTC-2017-6600-1, PID2019-108806RB-I00). ICS is funded by AEEC Junior Grant Ref INVES211323CONE. Part of the equipment employed was funded by the Generalitat Valenciana and co-financed with

FEDER funds (PO FEDER of Comunitat Valenciana 2014–2020).

References

[1] T. Melnyk, S. Đorđević, I. Conejos-Sánchez, MJ. Vicent, Therapeutic potential of polypeptide-based conjugates: Rational design and analytical tools that can boost clinical translation. *Adv Drug Deliv Rev*, 160 (2020) 136–169

[2] P. Groves, Diffusion ordered spectroscopy (DOSY) as applied to polymers, *Polym. Chem*.,8 (2017) 6700-6708

Abstracts for Poster Presentation

Session 2: Biomimetic Structures for Diagnosis and Therapy

P2.1: "*In vitro production, isolation and characterization of Ebola virus-like particles* ". R. Mellid-Carballal, C. Rivas, M. Garcia-Fuentes. Universidade de Santiago de Compostela. (p.135)

P2.2: "***Self-assembling dendrimer for the delivery of antisense NAMs into bacteria*** ". M. Gomes, I. Resende, S. Pereira, L. Peng, R. S. Santos, N. F. Azevedo. University of Porto. (p.137)

P2.3: "***Transtympanic delivery of the pneumoccal endolysin MSlys via PEGylated liposomes***" M. D. Silva, K. Ray, F. M. Gama, A. K. Remenschneider, and S. Sillankorva. University of Minho. (p.139)

P2.1: In vitro production, isolation and characterization of Ebola virus-like particles

R. Mellid-Carballal[1]*, C. Rivas[1,2], and M. Garcia-Fuentes[1,2,3,4]

[1]*Center for Research in Molecular Medicine and Chronic Diseases, Univerdade de Santiago de Compostela, 15782*
A Coruña, Spain
[2]*National Centre for Biotechnlogy (CNB), CSIC, 28049 Madrid, Spain*
[3]*Department of Pharmacology, Pharmacy and Pharmaceutical Technology, University of Santiago de Compostela, Spain*
[4]*IDIS Research Institute, Santiago de Compostela, Spain*

*e-mail: rocio.mellid.carballal@usc,es

Introduction

VP40 matrix protein of Ebola virus is known to be responsible of virus assembly and release. In fact, it has been shown that the expression of VP40 matrix protein in cells is sufficient to induce the formation of particles similar to those of the Ebola virion [1].

Considering the technological advantages that virus-like particles (VLPs) can offer in the field of drug and vaccine delivery [2,3], we are studying several methods for the isolation of Ebola VLPs from cell culture supernatant. Besides, we are using different methods to precisely characterize these particles and for identifying the release of other byproducts such as VP40 containing extracellular vesicles.

Materials and Methods

To produce Ebola virus-like nanoparticles, HEK293T cells were transfected with a plasmid encoding VP40 matrix protein and cell culture supernatant was collected 48 hours after transfection.

For the isolation of VLPs from the cell culture supernatant, different ultracentrifugation protocols were studied.

Finally, different techniques were used to characterize the isolated products, including Western blot analysis, Dynamic Light Scattering (DLS), Asymmetric Flow Field Flow Fractionation (AF4) and Transmission Electron Microscopy (TEM).

Results and Discussion

Firstly, we have checked the presence of VP40 matrix protein both in cells and in cell culture media 48 hours after transfection. A band for VP40 was clearly observed both for transfected cells and for the correspondent cell culture supernatant (Fig. 1)

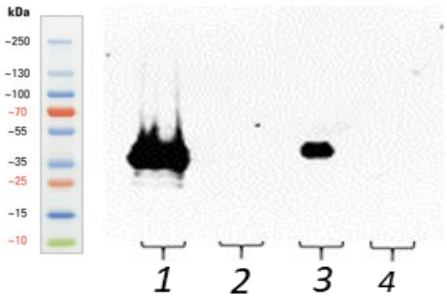

Figure 1. Evaluation of VP40 expression by Western blot.1: transfected cells; 2: control cells; 3: supernatant from transfected cells; 4: control supernatant.

After isolation from cell culture supernatant by ultracentrifugation, we observed the presence of particles with similar size and shape to the Ebola virion by TEM (Fig. 2).

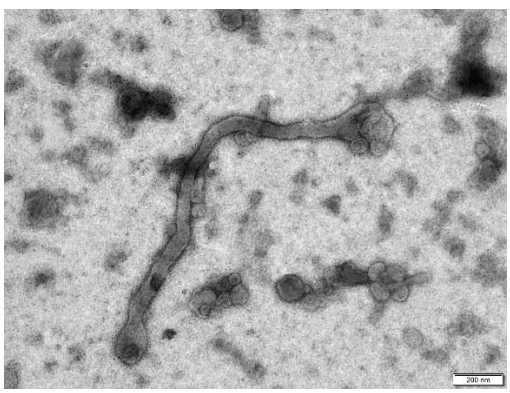

Figure 2. TEM image of VLPs obtained from oligomerization of VP40 matrix protein.

Finally, we have characterized the VLPs in terms of physicochemical properties using DLS and AF4 techniques.

DLS analysis showed particle sizes in the nanometric range with a relatively high polidispersity, logical for biosynthesized particles. Regarding their surface charge, it was negative in any of the solvents used as external phase (Table 1).

	Size (nm)	PDI	ZP (mV)
VLPs (H_2O)	464,8 ± 273,6	0,5	-12,5 ± 5,5
VLPs (PBS)	505,4 ± 127,3	0,5	-10,2 ± 4,7
VLPs (STE)	357,9 ± 82,9	0,3	-22,6 ± 2,8

Table 1. Physicochemical characterization of VLPs in different suspension buffers (n>3). PDI: polydispersity index. ZP: zeta potential.

AF4 analysis further supported our previous results. Our VLPs showed an average radius of 133 nm and a polydisperse population, as we can deduce from the width of the peak.

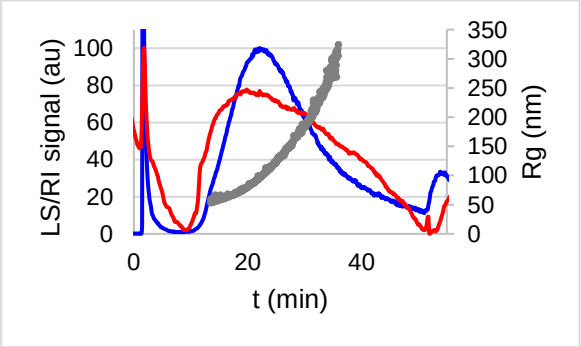

Figure 3. Fractograms of a sample of VLPs (blue: Light Scattering signal; red: Refraction Index signal) and particle size (grey dots: radius of gyration). Results obtained by Asymmetric Flow Field Flow Fractionation.

Conclusions

The unique expression of VP40 matrix protein in HEK293T cells leads to the formation and release of virus-like particles, which can be isolated from the cell culture supernatant making use of ultracentrifugation methods. These particles showed similar characteristics to the Ebola virion, regarding both size and shape.

Due to their biological origin and their intrinsic ability for nucleic acid delivery, they are promising platforms for the transport of therapeutic cargo into cells.

Acknowledgments

This work was supported by Ministerio de Economía, Industria y Competitividad (MINECO-RETOS, Grant MAT2017-84361-R, Feder Funds).

References

[1] L.D. Jasenosky, G. Neumann, I. Lukashevich, Y. Kawaoka, Ebola Virus VP40-Induced Particle Formation and Association with the Lipid Bilayer, J. Virol. 75 (2001) 5205–5214. https://doi.org/10.1128/jvi.75.11.5205-5214.2001.

[2] M.J. Rohovie, M. Nagasawa, J.R. Swartz, Virus-like particles: Next-generation nanoparticles for targeted therapeutic delivery, Bioeng. Transl. Med. 2 (2017) 43–57. https://doi.org/10.1002/btm2.10049.

[3] A.M. Wen, N.F. Steinmetz, Design of virus-based nanomaterials for medicine, biotechnology, and energy, Chem. Soc. Rev. 45 (2016) 4074–4126. https://doi.org/10.1039/c5cs00287g.

P2.2: Self-assembling dendrimer for the delivery of antisense NAMs into bacteria

M. Gomes[1], I. Resende[1], S. Pereira[1], L. Peng[2,3], R. S. Santos[1], N. F. Azevedo[1]

[1] *LEPABE - Laboratory for Process Engineering, Environment, Biotechnology and Energy, Faculty of Engineering, University of Porto, Rua Dr. Roberto Frias, 4200-465 Porto, Portugal*
[2] *CINaM - Centre Interdisciplinaire de Nanoscience de Marseille, Paris, France*
[3] *CNRS - Centre National de la Recherche Scientifique, Paris, France*

*e-mail: mggomes@fe.up.pt

Introduction

Antimicrobial resistance is an escalating public health issue, with estimates indicating it will cause around 10 million annual deaths by 2050 [1]. Nucleic acid mimics (NAMs) can become an alternative to traditional antibiotics, providing specific antibacterial therapy while protecting the beneficial microbiome. NAM sequences can be designed to target genes essential for the survival of specific bacteria and, when in the cytosol, they can, through hybridization, inhibit the expression of the target mRNA, leading to bacterial death. However, the bacterial envelope is not permeable to nucleic acids [2]. While the potential of dendrimers for intracellular delivery of nucleic acids has been extensively reported, these studies have been essentially limited to mammalian cells [3].

Materials and Methods

Herein, we assess the potential of a self-assembling dendrimer [3] as a delivery system of NAMs into bacteria via turbidity reduction assay (TRA). For this study, all NAMs were designed to target the essential *acpP* gene in *Escherichia coli* (*E. coli*).

Initially, NAMs composed of locked nucleic acid (LNA)/2'OMe RNA were complexed with the dendrimer, at different N/P ratios, to form dendriplexes and tested against *E. coli* ATCC 25922.

Afterwards, a 2-step therapy strategy was considered, isolating the effect of the dendrimer and the antisense NAMs. *E. coli* was first treated with the dendrimer (4 h incubation), followed by dendrimer removal and *E. coli* incubation with NAMs (up to 20 h). As NAMs, the previously used LNA/2'OMe sequence was tested, as well as an equivalent sequence composed of peptide nucleic acid (PNA). As a positive control, the conjugate of this PNA with the cell-penetrating peptide $(KKF)_3K$ was used, as it is already proven to permeate and inhibit *E. coli* growth [4].

Results and Discussion

For the dendriplexes: although a considerable growth inhibitory effect was obtained, this was mainly an effect of the dendrimers and not the NAMs, as the dendrimers by themselves often presented a higher effect than the resulting dendriplexes.

Regarding 2-step therapy, this approach relies on the dendrimer to permeabilize the bacterial envelope and benefits from the specificity provided by NAMs. This strategy showed a substantial inhibitory effect for the treatments including a PNA-based NAM.

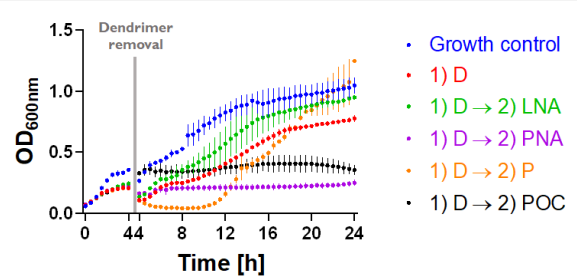

Fig 1. Evaluation of the inhibitory effect of 2 step-therapy with dendrimer (D) for the first 4 h, followed by the LNA-based NAM (LNA), the PNA-based NAM (PNA), the cell penetrating peptide (P) or the peptide-oligonucleotide conjugate (POC) (all at 60 µM), for the following 20 h.

Conclusions

A promising combination (dendrimer followed by PNA-based NAM) was identified, which highlights the dendrimer's permeabilization potential.

Future studies will focus on validating these results via time-kill assays, as well as re-evaluating the dendriplex strategy, considering the association with the PNA-based NAM.

Acknowledgments

This work was financially supported by:

(i) Base Funding - UIDB/00511/2020 of the Laboratory for Process Engineering, Environment, Biotechnology and Energy –

LEPABE - funded by national funds through the FCT/MCTES (PIDDAC);

(ii) Project “LEPABE-2-ECO-INNOVATION” – NORTE-01-0145-FEDER-000005, funded by Norte Portugal Regional Operational Programme (NORTE 2020), under PORTUGAL 2020 Partnership Agreement, through the European Regional Development Fund (ERDF);

(iii) PhD grant No SFRH/BD/118018/2016 funded by Fundação para a Ciência e a Tecnologia (FCT);

(iv) European Union’s Horizon 2020 research and innovation programme under grant agreement No 810685.

References

[1] O’Neil J. Tackling drug-resistant infections globally: Final report and recommendations. *Review on Antimicrobial Resistance*. 2016; 4-15.

[2] Santos RS, Figueiredo C, Azevedo NF, Braeckmans K, De Smedt SC. Nanomaterials and molecular transporters to overcome the bacterial envelope barrier: Towards advanced delivery of antibiotics. *Advanced Drug Delivery Reviews*. 2018; 136–137:28–48.

[3] Dhumal D, Lan W, Ding L, Jiang Y, Lyu Z, Laurini E, et al. An ionizable supramolecular dendrimer nanosystem for effective siRNA delivery with a favorable safety profile. *Nano Research*. 2021;12(1).

[4] Pereira S, Yao R, Gomes M, Jørgensen PT, Wengel J, Azevedo NF, *et al*. Can Vitamin B12 Assist the Internalization of Antisense LNA Oligonucleotides into Bacteria? *Antibiotics*. 2021;10(379).

P2.3: Transtympanic delivery of the pneumococcal endolysin MSlys via PEGylated liposomes

M. D. Silva[1,2,3,4]*, K. Ray[3,4], F.M. Gama[1], A. K. Remenschneider[3] and S. Sillankorva[2]

[1]*CEB−Centre of Biological Engineering, University of Minho, 4710-057 Braga, Portugal;*
[2]*INL−International Iberian Nanotechnology Laboratory, 4715-330 Braga, Portugal;*
[3]*Department of Otolaryngology, Massachusetts Eye and Ear, 02114 Boston, Massachusetts, United States*;
[4]*Wyss Institute for Biologically Inspired Engineering, 02115 Boston, Massachusetts, United States*
*e-mail: mdanielasilva@ceb.uminho.pt;

Introduction

Streptococcus pneumoniae is the most common pathogen that causes acute otitis media [1]. For decades, systemic antibiotic therapy has been the gold standard treatment for these infections. However, the increasing antibiotic resistance has prompted research for novel topical antibiotic alternatives. Endolysins, peptidoglycan hydrolases encoded by bacteriophages, have attracted a lot of attention, even for controlling *S. pneumoniae* [2]. Nevertheless, the efficacy of topically applied endolysins is impaired by the trilaminar tympanic membrane (TM), that acts as protective barrier preventing the permeation of compounds from the ear canal into the middle ear. Liposomal formulations, including PEG-decorated liposomes, have been shown to improve drug permeation through the TM. We have previously characterized a novel pneumococcal endolysin (MSlys) [2] and its encapsulation in liposomes, which were physicochemically characterized and assessed with regards to the *in vitro* release, cytotoxicity and antipneumococcal activity [4]. However, little remains known about its permeation ability and subsequent activity through an intact TM. In this study, we evaluated the permeation ability of MSlys-loaded PEGylated liposomes across different *ex vivo* models and compared it to the permeation of the free MSlys.

Materials and Methods

Liposomes composed of L-α-lecithin and PEG2000 PE loaded with the MSlys endolysin were prepared by thin film hydration technique. The *ex vivo* permeation of free MSlys and of MSlys-loaded liposomes through porcine skin, as well as sheep and human TMs, was evaluated using Franz diffusion cells incubated at 37 ˚C. The antimicrobial efficacy of samples collected from the receptor chamber after permeation across the human TMs was tested against a clinical *S. pneumoniae* otitis media isolate. Moreover, samples were analyzed by SDS-PAGE to confirm the presence of the endolysin.

Results and Discussion

The encapsulation of MSlys in the PEGylated liposomes improved its transdermal and transtympanic permeation, which efficacy was related with the thickness of the tissue (higher for TMs than for the skin). Furthermore, following 2 h of MSlys-loaded liposomes permeation through human TM, the samples collected significantly reduced *S. pneumoniae* cells as compared to free endolysin samples. However, antipneumococcal activity was not observed after 4 h of permeation. SDS-PAGE analysis confirmed increased levels of MSlys permeated through the human TM using liposomes. Prolonged incubation periods (≥ 48 h) demonstrated protein degradation in the permeated samples.

Conclusions

Endolysin-loaded liposomes show promising results for transtympanic treatment of pneumococcal otitis media during a short period of time. Repeat dosing of endolysin-loaded liposomes or use of endolysins with improved stability and efficacy would be beneficial.

Acknowledgments

This study was supported by the Portuguese Foundation for Science and Technology (FCT) under the scope of the strategic funding of UIDB/04469/2020 unit. MDS is supported by FCT fellowship SFRH/BD/128825/2017 and SS by the individual scientific employment program contract 2020.03171.CEECIND.

References

[1] M.D. Silva, S. Sillankorva, Otitis media pathogens – A life entrapped in biofilm communities, Crit. Rev. Microbiol. (2019) 1–18.
[2] M.D. Silva, H. Oliveira, A. Faustino, S. Sillankorva, Characterization of MSlys, the endolysin of *Streptococcus pneumoniae* phage MS1, Biotechnol. Reports. e00547 (2020).
[3] M.D. Silva, J.L. Paris, F.M. Gama, *et al.*, Sustained release of a *Streptococcus pneumoniae* endolysin from liposomes for potential otitis media treatment, ACS Infect. Dis. 7 (2021) 2127–2137.

Abstracts for Poster Presentation

Session 3: Innovative Strategies for Drug Targeting

P3.1: "*Ultraflexible lipid vesicles allow in vitro skin permeability of Cyanocobalamin: a potential treatment for Vitamin B12 deficiency* ". A.J. Guillot, P. Merino, T.M. Garrigues, A. Melero. University of Valencia. (p.143)

P3.2: " ***Targeted cathelicidin nanomedicines as novel glucoregulator for diabetes therapy*** ". C. Cristelo, F. M. Gama, B. Sarmento. University of Porto. (p.145)

P3.3: "***Preclinical basis of nanostructured lipid carriers (NLC) loaded with aflibercept: design, development and characterization***" X. García-Otero, V.F. R. Varela-Fernández, J. Blanco-Méndez, M. González-Barcia, P. Aguiar, A. Fernández-Ferreiro and F. J. Otero-Espinar. Universidade de Santiago de Compostela. (p.146)

P3.4: "***Infliximab-loaded PLGA nanoparticles: design, development, and physicochemical characterization***" R. Varela-Fernández, X. García-Otero, M.I. Lema-Gesto, M. González-Barcia, and F.J. Otero-Espinar. Universidade de Santiago de Compostela. (p.148)

P3.5: "***Inulin-PCL nanoparticles as an adjuvant delivery system for highly purified recombinant antigens***" S. Jesus, J. Panão Costa, H. Duarte, M. Colaço, O. Borges. University of Coimbra. (p.150)

P3.6: "***Novel polypeptide-based conjugates for mitochondrial targeting***" C. Pegoraro, I. Conejos-Sánchez, M.J. Vicent. Centro de Investigación Príncipe Felipe. (p.152)

P3.7: "***Receptor-targeted nanocarriers modulate cannabinoid anticancer activity through delayed cell internalization***" M. Durán-Lobato, J. Álvarez-Fuentes, M. Fernández-Arévalo, L. Martín-Banderas. Universidad de Sevilla. (p.153)

P3.8: "***3D printed tacrolimus suppositories for the treatment of ulcerative colitis***" I. Seoane-Viaño, J.J. Ong, A. Luzardo-Álvarez, M. González-Barcia, A. Basit, F.J. Otero-Espinar, A. Goyanes. Universidade de Santiago de Compostela. (p.155)

P3.9: "***Development of shear-responsive microaggregates based on PLGA nanoparticles for targeted delivery***" M.M. El-Hammadi; R. Otero-Candelera; L. Martín-Navarro; J. Álvarez-Fuentes; L. Martin Banderas. Universidad de Sevilla. (p.157)

P3.1: Ultraflexible lipid vesicles allow in vitro skin permeability of Cyanocobalamin: a potential treatment for Vitamin B12 deficiency.

A.J. Guillot[1]*, P. Merino[1], T.M. Garrigues[1] and A. Melero[1]

[1]*Department of Pharmacy and Pharmaceutical Technology and Parasitology, Faculty of Pharmacy, University of Valencia. Avda Vicent Andrés Estellés s/n, Burjassot (46100), Valencia, Spain.*

*e-mail: antonio.guillot@uv.es

Introducction

Vitamin B12 deficiency is the most common cause of certain hematologic pathologies, neuropsychiatric symptoms, and other issues [1]. Its prevalence in developed areas, such as North America and Europe, varies from 2.9-25.7% depending on cut-off serum levels values (<148 y <256 pmol/L respectively) [2]. Also, it has been administered topically successfully for the treatment of skin illnesses, such as atopic dermatitis and psoriasis [3]. Despite of this positive outcomes, cyanocobalamin permeability through the skin is a challenge because of its high molecular size (1355 Da), unable to overcome the skin barrier fuction exerted by the *stratum corneum*. Research in the pharmaceutical technology field has allowed the development of resources and systems for enhancing transdermal drug diffusion [4]. Different research groups have previously developed Vitamin B12 liposomes, transferosomes and ethosomes with the aim to improve vitamin photostability and achieve a better local and systemic action after a topic and oral administration, respectively [5]. The main goal of this research was to evaluate the cyanocobalamin *in vitro* permeability form lipid vesicles through full thickness procine skin.

Materials and Methods

Lipid vesicles preparation

Liposomes (L), transferosomes (T) and ethosomes (E) were prepared by the thin-film hydration method, based in our previous work (Table 1) [6]. Once MLV were obtained, their size was reduced by sonication and membrane extrusion. After size reduction liposomes were purified by centrifugation and dyalisis methods to remove any rest of free drug.

Entrapment efficiency

Entrapment efficiency (EE) was determined directly by calculating the amount of B12 encapsulated in lipid vesicle dispersions after vesicle disruption using the following equation:

$$EE\ (\%) = (Qe/Qt) \cdot 100$$

Table 1. Composition of the different cyanocobalamin lipid vesicles and purification methods used. C: centrifugation; D: dyalisis.

Components (% w/v)	L1	L2	T1	T2	E
Phospohipon 90G®	4.5	4.5	4.5	4.5	3
Cholesterol	0.135	0.135	-	-	-
Tween 80	-	-	0.675	0.675	-
B_{12}	1 [1]	0.2 [2]	1 [1]	0.2 [2]	0.2 [1]
Reconstitution solvent (mL)	10 PBS	10 PBS	10 PBS	10 PBS	10 H_2O
Purification method [3]	C+D	C+D	D	D	-

Vesicle size, PDI and Z-potential

Particle size (average diameter) and polydispersity index (PDI) were measured by means of a Malvern nanozetasizer (Malvern, UK). Dynamic light scattering (DLS) mode was used to measure the vesicular size and PDI and laser doppler electrophoresis (LDE) was used to determine zeta-potential. The temperature was set at 25 ºC in all cases. Each sample (n = 3) was analysed in triplicate.

Vesicle visualization

Transmission Electronic Microscopy (TEM) was used to visualize the lipid vesicles. A drop of the vesicle dispersion was diluted (1:1000) and poured into a coper grid and dried for 4 min. Excess of the dispersion was removed and a drop of phosphotungstic acid solution (2%) was applied and dried for 1 min.

In vitro permeability through porcine skin

The cyanocobalamin skin permeability of the four formulations was evaluated using a static Franz diffusion cell setup (12 mL PBS as receptor solution; 1.76 cm^2 of diffusional area). The skin permeability of the liposomal formulations was compared with the skin permeability of a cyanocobalamin solution 0.5% (w/v). The *in in vitro* experiments were carried full thickness porcine skin. The studies where skin used were approved by the Ethical Committee of the University of Valencia, under the protocol number H1540295606992.

Results and Discussion

Vesicle characterization

In general, characterization results do not differ statistically from previously reported ones (Table 2). As expected, zeta-potential values were negative for all formulations. Size and PDI measurements obtained from all vesicles were optimal for transdermal delivery purposes, since they were below 300 nm and 0.3, respectively.

Table 2. Characterization of the cyanocobalamin-lipid vesicles in terms of size, PDI, zeta-potential and entrapment efficiency (EE).

	L1	L2	T1	T2	E
Size (nm)	283 ±6.02	284 ±11.9	177 ±3.51	171 ±3.01	145 ±15.04
PDI	0.226 ±0.01	0.205 ±0.02	0.223 ±0.01	0.244 ±0.03	0.201 ±0.03
Zeta-potential (mV)	-9.7 ±0.3	-10.3 ±0.2	-6.2 ±0.2	-5.7 ±0.5	-5.3 ±0.4
Entrapment efficiency (%)	19.96 ±1.95	36.52 ±2.62	21.80 ±0.93	30.59 ±2.73	-

Vesicle visualization

Multilamellar vesicles were observed (Figure 1), since it has been reported that the thin-film method uses to produce heterogeneous vesicles in relation to lamellae number. They present spherical-like shape, although certain irregularity and ovoid-like shapes can be denoted, due to the necessary drying sample process of this technique.

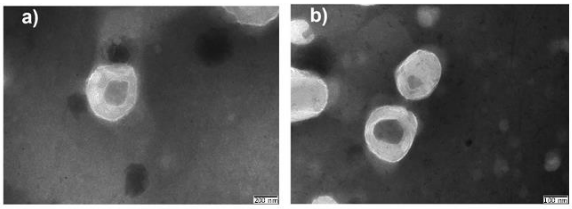

Figure 1. Representative TEM images of cyanocobalamin lipid vesciles.

In vitro permeability through porcine skin

The permeability parameters calculated for each formulation and condition are presented in Table 3. The cyanocobalamin diffusion for 32 h was almost neglectable when it was administered in aqueous solution (S). The developed lipid-vesicle formulations facilitated notably the vitamin B12 permeability through the skin, as Figure 8 reflects. The calculated fluxes from all formulations tested were as follows: T1 ≥ E ≥ L1 > T2 ≥ L2 > S, being 0 for the solution without carriers, as expected. Among the formulations containing a similar drug amount, transferosomes and ethosomes showed higher fluxes compared to liposomes, what can be explained because of their flexibility and the presence of chemical permeability enhancers included into their bilayer.

Table 3. In vitro permeability parameters of cyanocobalamin delivered from the different lipid vesicle formulations through intact porcine skin

	Maximal flux (μg/cm^2/h)	Kp ·10^{-7} (cm/s)	Lag time (h)	Dose (mg/mL)
S	-	-	-	50
L1	1.00 ±0.56	1.26 ±0.7	23.8 ±0.39	2
L2	0.44 ±0.19	1.61 ±0.68	22.9 ±1.11	0.67
T1	1.73 ±0.77	2.40 ±1.07	14.5 ±1.63	2
T2	0.50 ±0.10	2.23 ±0.45	17.6 ±1.55	0,61
E	1.51 ±0.35	2.08 ±0.48	17.5 ±2.14	1.3

Conclusions

Topical delivery of cyanocobalamin is possible using ultraflexible lipid vesicles (transferosomes and ethosomes). Therefore, the possibility of treating the Vitamin B12 deficiency topically, avoiding oral and parenteral routes disadvantages, is now open using these nanocarriers. According with the data presented in this work, T1 transferosome formulation presents the highest transdermal flux through the skin, and can therefore further studied as an alternative for the treatment of this vitamin deficiency.

Acknowledgments

This work is part of the grant PID2020-114530GA-100 funded by MCIN/AEI/10.13039/501100011033 and by "ERDF A way of making Europe".

References

[1] Green, R. Vitamin B12 Deficiency from the Perspective of a Practicing Hematologist. *Blood. 129* (2017) 2603-2611

[2] Allen, L. H. How Common Is Vitamin B-12 Deficiency? *Am J Clin Nutr. 89* (2009) 693S-6S.

[3] Januchowski, R. Evaluation of Topical Vitamin B (12) for the Treatment of Childhood Eczema. *J Altern Complement Med*. *15* (2009) 387–389.

[4] Paudel, K. S.; Milewski, M.; Swadley, C. L.; Brogden, N. K.; Ghosh, P.; Stinchcomb, A. L. Challenges and Opportunities in Dermal/Transdermal Delivery. *Ther Deliv*. *1* (2010) 109–131.

[5] Guillot, A. J.; Jornet-Mollá, E.; Landsberg, N.; Milián-Guimerá, C.; Montesinos, M. C.; Garrigues, T. M.; Melero, A. Cyanocobalamin Ultraflexible Lipid Vesicles: Characterization and In Vitro Evaluation of Drug-Skin Depth Profiles. *Pharmaceutics*. *13* (2021),418

P3.2: Targeted cathelicidin nanomedicines as novel glucoregulator for diabetes therapy

C. Cristelo[1;2]*, F. M. Gama[2], B. Sarmento[1]

[1] *i3S - Instituto de Investigação e Inovação em Saúde, Universidade do Porto, Portugal;*
[2] Centro de Engenharia Biológica, Universidade do Minho, Braga, Portugal
*e-mail: cecilia.cristelo@i3s.up.pt

Introduction

Type 1 diabetes (T1D) is an autoimmune condition resulting in the destruction of the insulin-producing β cells. With no cure available for this disease, patients depend on insulin administration to control glycaemia. The recovery of β cells by promoting its replication, neogenesis or by reprogramming of other pancreatic cells, offers a promising strategy to revert T1D. Cathelicidin is an antimicrobial peptide that has been shown to improve β cell function and neogenesis. This work aims to develop a delivery system for a cathelicidin-derived peptide specifically to β cells, aiming at promoting their function and increase cellular mass. To achieve the specific delivery to β cells, the peptide was loaded on PLGA nanoparticles (NPs). The NPs were surface-decorated with exenatide, an agonist of the GLP-1 receptor, expressed by β cells.

Materials and Methods

NPs were produced by double emulsion solvent evaporation and characterized using dynamic light scattering (DLS), nanoparticle tracking analysis (NTA) and transmission electron microscopy (TEM). The association efficiency and drug loading of the cathelicidin-derived peptide (LLKKK18) were determined using fluorescamine assay. The effects of the nanoformulation on glucose-stimulated insulin secretion (GSIS) by INS-1E cells were evaluated by ELISA, and on cell viability using MTT. The biological interaction was studied using flow cytometry and fluorescence microscopy.

Results and Discussion

NPs loaded with the cathelicidin-derived peptide LLKKK18 and surface-functionalized with exenatide presented a mean size around 100 nm, a narrow size distribution (PdI of 0.14 ± 0.02), zeta potential of -9.6 ± 0.7mV and stability up to 20 days at 4ºC in PBS. The association efficiency and LLKKK18 loading were 85% and 4%, respectively. LLKKK18 was released very slowly from PLGA NPs in PBS. In the first 24h around 20% LLKKK18 was released, and it nearly stabilized in the first 5 days, after which it started to slowly increase.

Soluble LLKKK18 improved GSIS; however, when loaded in NPs it had no significant effect on insulin release. NP functionalization with exenatide showed a slight increase of insulin release compared to non-funcionalized NPs under high glucose concentration. Soluble LLKKK18 significantly increased the cellular viability after 96h of incubation with INS-1E cells; the study of the effect from LLKKK18 NPs on cell viability is ongoing.

Different strategies have been undertaken to improve β cell targeting. NPs were functionalized with exenatide with or without a PEG spacer before C-terminal cysteine, for site-specific conjugation to maleimide. Functionalization was performed either post NP production or using a previously functionalized polymer. In all strategies, NP interaction with INS-1E cells was minor and functionalization did not favour interaction. The expression of GLP-1R by INS-1E cells was slightly greater than the negative control (L929 cells), but still underexpressed. Ongoing studies are being carried out using a GLP-1R transfected cell line.

Conclusions

We successfully obtained cathelicidin-loaded, and exenatide-functionalized NPs with a monodisperse distribution and a slow release. The functionalization of NPs was not efficient in promoting the interaction with β cells possibly related with the low expression of the GLP-1R by INS-1E cells. The ability of the nanoformulation to to improve GSIS and replication is still to be clarified.

Acknowledgments

This work was supported by Fundação para a Ciência e a Tecnologia/Ministério da Ciência, Tecnologia e Ensino Superior (POCI-01-0145-FEDER-007274). Cecília Cristelo gratefully acknowledges FCT for financial support (fellowship SFRH/BD/139402/2018).

P3.3: Preclinical basis of nanostructured lipid carriers (NLC) loaded with aflibercept: design, development and characterization

X. García-Otero[1;2]*, V.F. R. Varela-Fernández[1], J. Blanco-Méndez[1;2], M. González-Barcia[3], P. Aguiar[2], A. Fernández-Ferreiro[3] and F. J. Otero-Espinar[1]

[1]*Department of Pharmacy, Pharmacology and Pharmaceutical Technology, Universidad de Santiago de Compostela (USC), 15782 Santiago de Compostela, Spain*
[2]*Molecular Imaging Group, Health Research Institute of Santiago de Compostela (IDIS), 15706 Santiago de Compostela, Spain*
[3]*Clinical Pharmacology Group, Health Research Institute of Santiago de Compostela (IDIS), 15706 Santiago de Compostela, Spain*

*e-mail: xurxo.garcia.otero@gmail.com

Introduction

Aflibercept is a recombinant fusion protein consisting of portions from the extracellular domains of the human VEGF receptors 1 and 2 fused with the Fc (fragment crystallizable) portion of the human IgG1. US Food and Drug Administration agency (FDA) and the European Medicines Agency (EMA) had approved aflibercept for the treatment of exudative age-related macular degeneration (AMD), choroidal neovascularization (CNV), diabetic macular oedema (DME) and macular oedema secondary to central and branch retinal vein occlusion (RVO) [1]. Its mechanism of action is based on binding to vascular endothelial growth factor (VEGF), thus inhibiting its binding to its receptors Flt 1 (VEGFR 1) and KDR (VEGFR 2), located on the surface of endothelial cells, causing a reduction in angiogenesis, the main pathophysiological mechanism involved in these diseases.
Resistance mechanisms have been identified, including altered antigen expression or binding, impaired complement-mediated cytotoxicity (CMC) or antibody-dependent cellular cytotoxicity (ADCC). Following this, encapsulation of this antibody in nanometer-sized lipid systems is proposed in order to increase its stability, confer protection and vectorize the antibody to the desired site [2].

Materials and Methods

The preparation of aflibercept-loaded NLCs was carried out using a modified double emulsion/evaporation technique. Two types of NLC were prepared, one with an aqueous core and the other with a gelled core. A previous factorial study was carried out in order to assess the optimal composition of the NLCs, as well as the conditions of the preparation process.
Physicochemical characterization in terms of size, size distribution and surface charge of aflibercept-loaded NLCs was carried out using a dynamic light scattering (DLS) technique. The study of the morphology of NLCs was performed by transmission electron microscopy (TEM), after staining with phosphotungstic acid, placement on copper plates and subsequent drying.

The determination of the production yield was carried out by a direct method, based on the ratio between the amount of final and initial product. In turn, the evaluation of the production efficiency and loading capacity of the NLCs was carried out by a high-performance liquid ultracromatography (UPLC) technique through a gradient diffusion method designed for the detection of aflibercept.
The effect of the amount of aflibercept on the physicochemical characteristics of NLCs has been evaluated in terms of size, size distribution and surface charge and subsequently correlated with the values of encapsulation efficiency and loading capacity.

Results and Discussion

The preparation procedure of NLCs loaded with aflibercept has been adequate, allowing the encapsulation and stabilization of this antibody in nanometer-sized systems.
NLCs loaded with aflibercept presented as a very uniform and homogeneous population, without aggregation or precipitation. In addition, they showed adequate surface charge values derived from the intrinsic charge of the lipids, an aspect that guarantees their stability over time.

Both types of NLC had an aqueous core, are round, uniform and with a smooth surface. Therefore, it would be a repertoire-type lipid system, useful for controlled release processes of aflibercept.
High values were obtained for production yield, encapsulation efficiency and loading capacity, ensuring that the preparation method is suitable for aflibercept encapsulation.

Conclusions

A nanostructured lipid system is proposed, for the first time, for the encapsulation of aflibercept as a way to increase its stability, reduce the possible effects associated with its administration and improve its bioavailability. Its design and development were reinforced by a consistent basis of *in vitro* characterization. Furthermore, this NLC system showed suitable physicochemical characteristics for aflibercept delivery.

Acknowledgments

This work was supported by Ministerio de Ciencia, Innovación y Universidades (RTI2018-099597-B-100). XGO and RVF are grateful to IDIS (Health Research Institute of Santiago de Compostela) for financing his predoctoral research fellowship.

References

[1] Drug Approval Package: Eylea (Aflibercept) [Internet] [cited 2021 Oct 29]. Available from:https://www.accessdata.fda.gov/drugsatfda_docs/nda/2011/125387s0000TOC.cfm

[2] Luan J, Zhang D, Hao L, Li C, Qi L, Guo H, Liu X, Zhang Q. Design and characterization of Amoitone B-loaded nanostructured lipid carriers for controlled drug release. Drug Deliv. 2013 Nov;20(8):324-30. doi: 10.3109/10717544.2013.835007. Epub 2013 Sep 13. PMID: 24032657.

P3.4: Infliximab-loaded PLGA nanoparticles: design, development, and physicochemical characterization

R. Varela-Fernández[1;2;3*], X. García-Otero[1,4], M.I. Lema-Gesto[3], M. González-Barcia[4], and F.J. Otero-Espinar[1,5]

[1]*Department of Pharmacology, Pharmacy and Pharmaceutical Technology. University of Santiago de Compostela (USC). Campus vida. Santiago de Compostela. Zip Code: 15782. Spain. francisco.otero@usc.es.*
[2]Pharmacy Service of the Complejo Asistencial Universitario de León (CAULE). León. Zip Code: 24071. Spain. rvarelaf@saludcastillayleon.es
[3]Clinical Neurosciences Group. University Clinical Hospital, Health Research Institute of Santiago de Compostela (IDIS). Travesía da Choupana s/n Santiago de Compostela. Zip Code: 15706. Spain. mariaisabel.lema@usc.es.
[4]Clinical Pharmacology Group. University Clinical Hospital, Health Research Institute of Santiago de Compostela (IDIS). Travesía da Choupana s/n Santiago de Compostela. Zip Code: 15706. Spain. miguel.gonzalez.barcia@sergas.es.
[5]Paraquasil Group, Health Research Institute of Santiago de Compostela (IDIS). Travesía da Choupana s/n Santiago de Compostela. Zip Code: 15706. Spain.

*e-mail: ruben.varela.fernandez@rai.usc.es

Introducction

Infliximab is a chimeric monoclonal antibody against tumour necrosis factor (TNF)-alpha that has shown efficacy in several diseases, including Crohn's disease and rheumatoid arthritis, among others, with a disease-modifying activity and rapid onset of action [1].

Several resistance mechanisms were identified, including altered antigen expression or binding, impaired complement-mediated cytotoxicity (CMC) or antibody-dependent cellular cytotoxicity (ADCC) [2]. For this reason, infliximab encapsulation in nano-sized polymeric systems is proposed in order to increase its stability, confer protection, and vectorize the antibody to the desired site [3].

Materials and Methods

Infliximab (Inflectra®) was provided by the Hospital Pharmacy Service of the University Clinical Hospital of Santiago de Compostela. Resomer RG Resomer 503 H (PLGA) were supplied by Evonik® (Germany). Polyvinil alcohol (PVA) was bought from Sigma Aldrich (Germany) The rest of reagents were of analytical grade and all solvents complied with the limits established by the USP XXII and the European Pharmacopoeia.

Infliximab-loaded PLGA nanoparticles were prepared by a modified double emulsion/solvent evaporation method. Different compositions were tested in order to select the formulation with better characteristics. Evaluation and characterization were carried out in terms of size, particle size distribution, morphology, production yield (PY), encapsulation efficacy (EE) and loading capacity (LC).

Particle size and size distribution were measured by a light scatering technique, while morphology was evaluated by transmission electron microscopy (TEM). Production yield (PY), encapsulation efficacy (EE) and loading capacity (LC) were obtained by experimental procedures. Additional assays may be included in order to support previous assays.

Results and Discussion

The preparation procedure of the infliximab-loaded PLGA NPs has proven to be appropriate for the encapsulation and stabilization of the antibody into nano-sized systems. The infliximab-loaded PLGA NPs appeared as a very uniform and homogeneous population, with an aqueous core, round and smooth. High values were obtained for production yield, encapsulation efficiency and loading capacity, ensuring that the preparation method is suitable for infliximab encapsulation.

Conclusions

A nanostructured polymeric system for the encapsulation of infliximab was proposed for the first time, as a way to increase its stability, reduce the possible side effects, and improve its bioavailability. Its design and development were reinforced by an *in vitro* consistent characterization basis. Furthermore, this PLGA NPs system showed physicochemical characteristics suitable for infliximab delivery.

Acknowledgments

This work was supported by by the Ministry of Science, Innovation and Universities (RTI2018-099597-B-100). RVF and XGO acknowledge IDIS (Health Research Institute of Santiago de Compostela) for their predoctoral contract grant funding.

References

[1] Siddiqui MA, Scott LJ. Infliximab: a review of its use in Crohn's disease and rheumatoid arthritis. Drugs. 2005;65(15):2179-208. doi: 10.2165/00003495-200565150-00014. Erratum in: Drugs. 2006;66(10):1359. PMID: 16225377.

[2] Strand V, Balsa A, Al-Saleh J, Barile-Fabris L, Horiuchi T, Takeuchi T, Lula S, Hawes C, Kola B, Marshall L. Immunogenicity of Biologics in Chronic Inflammatory Diseases: A Systematic Review. BioDrugs. 2017 Aug;31(4):299-316. doi: 10.1007/s40259-017-0231-8. PMID: 28612180; PMCID: PMC5548814.

[3] Varela-Fernández R, García-Otero X, Díaz-Tomé V, Regueiro U, López-López M, González-Barcia M, Lema MI, Otero-Espinar FJ. Design, Optimization, and Characterization of Lactoferrin-Loaded Chitosan/TPP and Chitosan/Sulfobutylether-β-cyclodextrin Nanoparticles as a Pharmacological Alternative for Keratoconus Treatment. ACS Appl Mater Interfaces. 2021 Jan 27;13(3):3559-3575. doi: 10.1021/acsami.0c18926. Epub 2021 Jan 11. PMID: 33428398.

P3.5: Inulin-PCL nanoparticles as an adjuvant delivery system for highly purified recombinant antigens

S. Jesus[1]*, H. Duarte[1;2], J. Panão Costa[1;2], M. Colaço[1;2] and O. Borges[1;2]

[1]Center for Neuroscience and Cell Biology, University of Coimbra, Coimbra, Portugal
[2] Department of Pharmaceutical Technology, Faculty of Pharmacy, University of Coimbra, Coimbra, Portugal

*e-mail: scjesus@cnc.uc.pt

Introduction

Inulin is a natural polysaccharide, that belongs to the fructans class. It has fructose monomers linked by β (2→1) glycosidic bonds that make inulin resistant to hydrolysis in human gastrointestinal tract and is only digested by bacteria in the colon [1]. Inulin is non-toxic and safe for humans and it was given FDA GRAS recognition (Generally Recognised As Safe) in 2002 [1]. Inulin, unlike other polysaccharides, can generate crystalline forms or as it is described and known in literature, isoforms. Seven isoforms were identified so far, with Gamma-Inulin (GI) and Delta-Inulin (DI) being widely reported in the literature for its immunological effects [2].
Polycaprolactone (PCL) NPs have been previously explored as an adjuvant/vaccine delivery system by our group with sucess [3]. Additionaly, this hydrophobic polymer has a great ability to blend with other polymers. Consequently, the work herein presented aims to develop Inulin/PCL nanoparticles, characterize them and assess their immunotoxicity. These outputs will constitute the first steps towards the development of a new vaccine adjuvant.

Materials and Methods

Inulin particles (INP) were produced by nanoprecipitation, when 1 mL of Inulin (5 mg/mL) was added dropwise to 2 mL of acetone with 1 % of Pluronic®. Then, acetone was evaporated and the final suspension was centrifuged and the pellet ressuspended in 1 mL of MilliQ water or pyrogen-free water (*in vitro* studies). Formulations PCL-inulin NPs (PINP) and PCL NPs (PNPs) were produced by the same technique, using 0.125 % PCL dissolved in the organic phase.

The formulations were characterized regarding its size and zeta potential using Dynamic Light Scattering and Electrophoretic Light Scattering, respectively. Protein loading capacity studies were developed with bovine serum albumin (BSA), mioglobin (MYO) and lysozime (LYS) and using DC™ protein assays. The effects of the particles on RAW 264.7 cells were tested using MTT assay. Their immunomodulatory effects were assessed through nitric oxide (NO) production assay in RAW 264.7 cells and cytokine production in monocyte-derived dendritic cells (Mo-DCs).

Results and Discussion

Inulin and PCL based particles were successfully obtained with a nanoprecipitation technique followed by the evaporation of the organic solvent over 48 h at 27ºC. Three different formulations were developed - Inulin particles (INP), PCL-Inulin particles (PINP) and PCL particles (PNP) - whose phisicochemical characterization is summarized in table 1.

Table 1. Physicochemical characterization of Inulin and PCL based particles after centrifugation: size distribution and zeta potential (ZP) measured in water. Data are presented as mean ± SEM, n = 19 (each in triplicate).

	Size ± SD (nm)	Zeta potential ± SD (mV)
INP	1320.86 ± 564.01	-3.76 ± 2.58
PINP	301.26 ± 64.25	-16.06 ± 4.53
PNP	275.32 ± 77.92	-20.86 ± 3.64

Importantly, when these particles were freeze dried, resuspension in water resulted in PINP and PNP formulations with a slightly larger particle size: 394.57 nm and 347.73 nm, respectively. INP on its turn, had a size of 1050 nm after resuspension, which is smaller than initially assessed, and possibly indicates that some agglomerates were dissociated.

The ability of these particles to encapsulate/entrap an antigen was assessed by testing three different model proteins: BSA, MYO and LYS. Proteins at 1.25 mg/mL, 2.5 mg/mL and 5 mg/mL were mixed with the aqueous solution prior to the nanoprecipitation. At the end of the production and 48 h incubation, particles were centrifuged and supernatants evaluated for the amount of free protein. For the ratio 1:1 NP:protein, all three formulations presented

similar results, achieving almost 50 % loading capacity for MYO and around 20 % for LYS.

In vitro cell viability experiments were performed in RAW 264.7 cells with a range of concentrations varying from 1.22 µg/mL to 2500 µg/mL of each formulation (Fig.1).

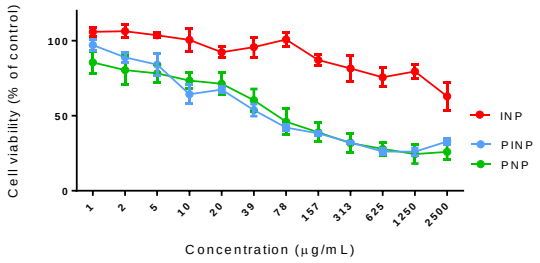

Figure 1. *Cell viability assay (MTT) on RAW 264.7 cells. Serial dilutions of INP, PINP and PNP were incubated with the cells for 24 h. Results are expressed as mean ± SEM, n ≥ 3.*

The results showed that INP are extremelly cytocompatible, as only the higher concentration (2500 µg/mL) had a significant effect of cell viability (< 70 %). On its turn, PINP and PNP induced similar results on cells, with a significant decrease in cell viability starting around 10 µg/mL. A reason for this higher toxicity, is likely to be related with the composition and with the size of the particles. Both PINP and PNP have a core of PCL, a hydrophobic polymer. Several studies have reported similar effects on cell viability for PCL nanoparticles [4]. Also, smaller particles are linked to more cellular damages, due to their higher ability to enter the cell [5].

At last, to unravel some immunomodulation effects, different assays were performed, such as the analysis of the NO production by RAW 264.7 cells and the analysis of cytokines production on Mo-DCs (TNF-α, IL-6, IL-10, and IL-12). None of the formulations have induced NO production at the tested concentrations (1.25 µg/mL, 2.5 µg/mL, 20 µg/mL and 40 µg/mL). As for the production of cytokines by DCs, upon stimulation with PINP particles at 2 µg/mL have shown no significant induction of cytokines, since all cytokine concentrations were similar to the negative control. However, at 4 µg/mL, PINP were found to induce a small concentration of IL-12 and IL-10 in one donor. This result *per si* has no significance, and such variability between donors must be attenuated by performing further assays.

Conclusions

The developed work enabled us to obtain a reproducible production method for the preparation of PCL-Inulin particles by a nanoprecipitation method. These particles are cytocompatible in a considerable range of concentrations and are not expected to induce pro-inflammatory effects, as demonstrated by the lack of cytokine induction on Mo-DCs. Consequently, they constitute a promising candidate to be further studied as a vaccine adjuvant, for instance for the hepatitis B antigen.

Acknowledgments

This work was supported by the European Regional Development Fund (ERDF), through the Centro 2020 Regional Operational Programme, under project CENTRO-01-0145-FEDER-000008:BrainHealth 2020, and through the COMPETE 2020—Operational Programme for Competitiveness and Internationalisation and Portuguese national funds via FCT – Fundação para a Ciência e a Tecnologia, under projects PROSAFE/0001/2016, POCI-01-0145-FEDER-030331, UIDB/04539/2020, UIDP/04539/2020 and grants 2020.10043.BD and SFRH/BD/139142/2018.

References

1. Afinjuomo, F., et al., *Inulin and Its Application in Drug Delivery.* Pharmaceuticals, 2021. **14**(9): p. 855.
2. Petrovsky, N. and P.D. Cooper, *Advax™, a novel microcrystalline polysaccharide particle engineered from delta inulin, provides robust adjuvant potency together with tolerability and safety.* Vaccine, 2015. **33**(44): p. 5920-5926.
3. Jesus, S., et al., *Poly-ε-caprolactone/chitosan nanoparticles provide strong adjuvant effect for hepatitis B antigen.* Nanomedicine, 2017. **12**(19): p. 2335-2348.
4. Jesus, S., et al., *Unravelling the Immunotoxicity of Polycaprolactone Nanoparticles—Effects of Polymer Molecular Weight, Hydrolysis, and Blends.* Chemical Research in Toxicology, 2020. **33**(11): p. 2819-2833.
5. Sukhanova, A., et al., *Dependence of Nanoparticle Toxicity on Their Physical and Chemical Properties.* Nanoscale Research Letters, 2018. **13**(1).

P3.6: Novel polypeptide-based conjugates for mitochondrial targeting

C. Pegoraro, I. Conejos-Sánchez*, M.J. Vicent*
Polymer Therapeutics Lab. Prince Felipe Research Center, Valencia, Spain
E-mail: cpegoraro@cipf.es

Introduction

Mitochondrial dysfunction contributes to conditions ranging from neurodegeneration and ischemia-reperfusion injury to obesity, diabetes, and cancer[1]. Mitochondrially-targeted drug delivery platforms have gained attention as possible therapeutic approaches to disease treatment. Polypeptide-based drug delivery platforms offer several advantages, including tightly controlled synthesis, easy scale-up, tunable conformation design, biodegradability, structural versatility, and multivalency[2]. Furthermore, the characteristics of polycationic polypeptides such as polyornithines (PLOs)[3], which include cell penetration and efficient cellular uptake, lend themselves well to mitochondrially-targeted drug delivery platforms.
In our present study, we functionalized PLO with well-described mitochondria targeting moieties. We focused on TPP[4], a delocalized lipophilic cation targeting the mitochondria negative membrane potential, and SS31[5], a Szeto-Shiller peptide with a high affinity for cardiolipin.

Materials and Methods

We synthesized and characterized two platforms with a theoretical endocytic pathway: PLO(PEG)-SSlink-TPP-Lys-Cy5 (trivalent compound) and PLO-PEG-TPP/SS31-Cy5 (with different loading percentages of TPP and SS31). We labelled our platforms with a near-infrared dye (Cy5) for later cellular uptake studies in the triple negative breast cancer MDA-MB 231 cell line.

Results and Discussion

Our preliminary results have provided evidence of mitochondrial colocalization for the trivalent compound (Fig 1).

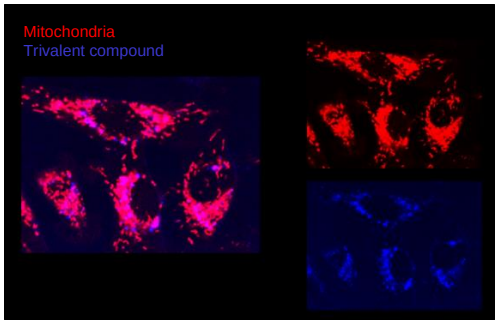

Fig 1. Cellular internalization studies in MDA-MB 231 by confocal fluorescence microscopy

This suggests that TPP targeting provides better targetability for PLO than SS31. TPP-targeted carrier also presented a bigger size and a spherical shell conformation in comparison with the other candidates.

Conclusions

In conclusion our preliminary results have provided evidence of mitochondrial colocalization for the trivalent compound, proposing this carrier as the basis for drug conjugation to create an efficient mitochondrially-targeted drug delivery platform.

Acknowledgments

This work was supported by the EU Horizon2020 Funded ITN BIOMOLMACS: Molecular Machines Functioning in Cells (H2020-MSCA-ITN-2019. Proposal n. 850418). Fondo Europeo de Desarrollo Regional (FEDER) included in the Operative Program FEDER of the Valencian Community 2014–2020. ICS is funded by AEEC Junior Grant Ref INVES211323CONE. Parent PLO was kindly provided by PTS SL (Valencia, Spain).

References

[1] N. Badrinath, S.Y. Yoo, Mitochondria in cancer: In the aspects of tumorigenesis and targeted therapy, Carcinogenesis. 39 (2018) 1419–1430.
[2] T. Melnyk, S. Đorđević, I. Conejos-Sánchez, M.J. Vicent, Therapeutic potential of polypeptide-based conjugates: Rational design & analytical tools that boost clinical translation, Adv. Drug Deliv. Rev. 160 (2020) 136–169.
[3] I. Conejos-Sanchez, E. Gallon, A. Niño-Pariente, J. Smith, A. Fuente, L. Di Canio, S. Pluchino, R. Franklin, MJ. Vicent, Polyornithine-based polyplexes to boost effective gene silencing in CNS disorders, Nanoscale. 12 (2020), 6285-6299.
[4] J. Zielonka, J. Joseph, A. Sikora, M. Hardy, O. Ouari, J. Vasquez-Vivar, G. Cheng, M. Lopez, B. Kalyanaraman, Mitochondria-Targeted TPP Compounds Syntheses, Mechanisms of Action, Therapeutic & Diagnostics, Chem. Rev. 117 (2017) 10043–10120.
[5] A. V Birk, S. Liu, Y. Soong, W. Mills, P. Singh, J.D. Warren, S. V Seshan, J.D. Pardee, H.H. Szeto, The mitochondrial-targeted compound SS-31 re-energizes ischemic mitochondria by interacting with cardiolipin, J. Am. Soc. Nephrol. 24 (2013) 1250–1261.

P3.7: Receptor-targeted nanocarriers modulate cannabinoid anticancer activity through delayed cell internalization

M. Durán-Lobato*[1], J. Álvarez-Fuentes[1], M. Fernández-Arévalo[1], L. Martín-Banderas[1]

[1]*Department of Pharmacy and Pharmaceutical Technology, Facultad de Farmacia, Universidad de Sevilla, c/Prof. García González nº2 41012, Sevilla, Spain*

*e-mail: mduran@us.es

Introducction

Δ9-tetrahydrocannabinol (THC) is known for its antitumor activity and palliative effects. However, its unfavorable physicochemical and biopharmaceutical properties, including low bioavailability, psychotropic side effects and resistance mechanisms associated to dosing make mandatory the development of successful drug delivery systems. In this work, previously developed THC-loaded poly(lactic-co-glycolic acid) nanoparticles (PLGA NPs) were optimized by introducing a targeting ligand and a multifunctional fluorescent labelling. Transferrin (Tf), a targeting moiety for cancer cells based on a higher expression of the Tf receptor in tumor cells [1-4], was coupled to the nanoparticles to modulate their interaction with the target cells. In addition, a double fluorescent labeling of the formulations, both through chemical linkage to the polymer and through dye encapsulation, was performed in order to selectively track the internalization pathway and intracellular fate of both the carrier and the cargo. The resulting formulations were evaluated in order to correlate the modulation of their anticancer effect with their cell internalization mechanics.

Materials and Methods

Δ9-THC was provided by THC Pharma GmbH, (Frankfurt/Main, Germany). Poly(DL-lactide-co-glycolide) Resomer®RG 502H was obtained from Evonik-. Poly(vinyl alchohol) (87 – 90% hydrolyzed, Mw: 30,000 – 70,000) PVA, Nile Red, Rhodamine B, human transferrin (Tf), N-(3-Dimethylaminopropyl)-N′-ethylcarbodiimide hydrochloride (EDC·HCl), N-Hydroxysuccinimide (NHS), fluorescein isothiocyanate isomer I (FITC), sucrose and genistein were purchased from Sigma-Aldrich (St Louis, MO; USA). All solvents employed were of HPLC or analytical grade. Deionized and filtered water was used in all the experiments (Milli-Q Academic, Millipore, Molsheim, France).

The RP-HPLC analysis was carried out with a Hitachi LaChrom® (D-7000) Series HPLC (Waters column 3 µm, 4.6x100 mm, at 25.0 ± 0.1ºC)

For cell line experiments, human colon adenocarcinoma cells (Caco-2) cells were obtained from the European Collection of Cell Cultures (ECACC); number 86010202 (Salisbury, UK).

PLGA NPs were produced by a modified emulsion solvent evaporation method (SEV) and Tf was conjugated on the surface of PLGA NPs and THC-PLGA NPs by the carbodiimide method described elsewhere. In the case of fluorescently labeled formulations, FITC was covalently coupled to PLGA also by the carbodiimide method, prior to particle production. Double-labeled fluorescent PLGA NPs were obtained by encapsulating either Nile Red or Rhodamine B into FITC-PLGA NPs.

Results and Discussion

Monodispersed populations of spherical nanostructures able to provide a sustained release of THC were obtained, in agreement our previous works on THC-PLGA NPs. No statistically significant difference was induced by the Tf coupling procedure or the presence of this moiety on the nanoparticle surface.

Caco-2 culture, a cancer cell model bearing both cannabinoid and Tf receptors, were employed to analyze the performance of the formulations. Upon incubation with the cells, both plain THC-PLGA NPs and Tf-modified THC-PLGA NPs avoided moderate cell viability increases exerted by free THC at short incubation times, which have been associated in the literature to drug resistance mechanisms. Furthermore, Tf-THC PLGA NPs exerted a cell viability decrease down to 17% vs. 88% of plain nanoparticles, however their internalization was significantly slower than plain nanoparticles. Uptake studies in the presence of inhibitors indicated that the nanoparticles were internalized through cholesterol-associated and clathrin-mediated mechanisms. Overall, the observations suggested that the improved THC antitumor effect was potentially due to increasing the presence of the nanocarriers, and hence

maximizing the amount of drug locally released, at the surface of cells bearing cannabinoid receptors, instead of improving internalization.

Conclusions

The results obtained highlight the promising potential of THC-loaded nanocarriers and their modulated interaction at the cell surface for the development of optimized antitumor therapies.

Acknowledgments

M. D-L is especially grateful to the V Plan Propio de Investigación of the Vicerrectorado de Investigación from the University of Seville for the postdoctoral fellowship Contrato Puente Posdoctoral. L.M.-B. is especially grateful for the financial support from Junta de Andalucía. Authors are also grateful to Dr. Modesto Carballo for the technical assistance with Flow Cytometry analysis and the Biology and Microscopy Services of CITIUS for their technical assistance. The authors specially acknowledge Junta de Andalucía, Spain (Project Nr. P09- CTS5029) for the financial support.

References

[1] Yoshikawa, T. & Pardridge, W. M. Biotin delivery to brain with a covalent conjugate of avidin and a monoclonal antibody to the transferrin receptor. J. *Pharmacol. Exp. Ther.* 263 (1992) 897–903

[2] Yan, F., Wang, Y., He, S., Ku, S., Gu, W., & Ye, L. Transferrin-conjugated, fluorescein-loaded magnetic nanoparticles for targeted delivery across the blood-brain barrier. *J. Mater. Sci. Mater. Med.* 24 (2013) 2371–2379

[3] Ulbrich, K., Hekmatara, T., Herbert, E. & Kreuter, J. Transferrin- and transferrin-receptor-antibody-modified nanoparticles enable drug delivery across the blood-brain barrier (BBB). *Eur. J. Pharm. Biopharm.* 71 (2009) 251–256

[4] Sahoo, S. K. S. K., Ma, W. & Labhasetwar, V. Efficacy of transferrin-conjugated paclitaxel-loaded nanoparticles in a murine model of prostate cancer. *Int. J. Cancer* 112 (2004) 335–340

P3.8: 3D printed tacrolimus suppositories for the treatment of ulcerative colitis

I. Seoane-Viaño[1,2]; J.J. Ong[2]; A. Luzardo-Álvarez[1]; M. González-Barcia[3]; Abdul Basit[2,4]; F.J. Otero-Espinar[1]; Álvaro Goyanes[2,4,5]

[1]*Department of Pharmacology, Pharmacy and Pharmaceutical Technology. Paraquasil Group. Faculty of Pharmacy. University of Santiago de Compostela (USC), 15782, Spain.*
[2]*Department of Pharmaceutics, UCL School of Pharmacy, University College London, 29-39 Brunswick Square, London WC1N 1AX, UK.*
[3]*Pharmacy Department, University Clinical Hospital Santiago de Compostela (SERGAS) (CHUS), 15706, Spain.*
[4]*Departamento de Farmacología, Farmacia y Tecnología Farmacéutica, I+D Farma Group (GI-1645), University of Santiago de Compostela, 15782, Spain.*
[5]*FabRx Ltd., 7B North Lane, Canterbury CT2 7EB, UK*

*e-mail: i.seoane.viano@usc.es

INTRODUCTION

Three-dimensional printing (3DP) is an additive manufacturing technology that enables the production of bespoke objects in a layer-by-layer manner. This technology offers unique benefits for the manufacturing of pharmaceutical products such as the development of patient-tailored medicines, with complex geometries, loaded with multiple APIs and with customised drug release kinetics [1]. In particular, semi-solid extrusion (SSE) is based on the deposition of semisolids (gel or pastes) in sequential layers through a syringe-based tool-head nozzle to create the 3D object, and it is highly relevant to print objects using soft materials, such as lipid-based excipients [2]. Self-emulsifying drug delivery systems (SEDDS) are lipid-based isotropic mixtures of oils, surfactants and co-surfactants that form kinetically stable oil-in-water (O/W) emulsions under mild agitation. This approach is especially useful for enhancing drug solubility of poorly water-soluble drugs, which are solubilized in the small drops of oil. Tacrolimus is a macrolide antibiotic with potent immunosuppressive properties commonly used in the management of medication-resistant Crohn´s disease (CD) and ulcerative colitis (UC), the two main disease categories of Inflammatory Bowel Disease (IBD), which is an inflammatory condition that affects the digestive system. The low oral bioavailability and low water solubility of tacrolimus makes it a suitable candidate for inclusion in a lipid-based rectal dosage form.

The aim of this study is to develop self-emulsifying suppositories (SES) loaded with the immunosuppressant drug tacrolimus for the treatment of IDB using a pharmaceutical SSE 3D printer to produce patient-tailored suppositories.

MATERIALS AND METHODS

3D design

The software 123D Design (Autodesk Inc., USA) was used to design the templates of the suppositories with three different sizes. The smallest size was 8 mm diameter x 24.77 mm height, the medium size was 9 mm x 27.87 mm and the biggest size was 12 mm x 36 mm (Figure 1).

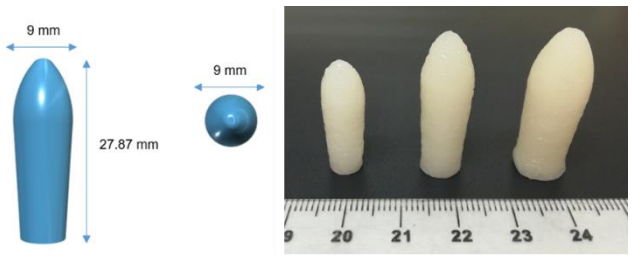

Fig 1. 3D model of the medium size suppository (left) and final 3D printed suppositories in three different sizes (right).

Semi-solid extrusion 3D printing

Pre-selected ratios of lipid excipients and drug (Table 1) were mixed in a glass beaker. The mixtures were heated up to the melting point of each mixture (42 ºC for Gel 44 and 48 ºC for Gel 48) under magnetic stirring until the complete solubilization of the drug in the lipid excipients. The mass was immediately transferred to a 5 mL extrusion syringe with a tapered extrusion tip (0.58 mm orifice) and allowed to solidify at room temperature. Then, the syringe was placed into the pharmaceutical 3D printer with the semisolid extrusion tool (FabRx Ltd, UK).

Formulation	Gelucire 44/14 (% w/w)	Gelucire 48/16 (% w/w)	Coconut oil (% w/w)	Tacrolimus (%w/w)
Gel 44	79.94	0	19.94	0.12
Gel 48	0	79.94	19.94	0.12

Table 1. Formulation composition.

Characterization of the 3D printed suppositories

3D printed suppositories were characterization by Transmission electron microscopy (TEM), Scanning electron (SEM) and Fourier transform-infrared spectroscopy (FT-IR). Moreover, the syringe extrusion force required for printing the melted mixtures, the in vitro drug release profiles, drug content and disintegration time of the final suppositories were evaluated. Furthermore, to characterize the formed emulsion, the self-emulsification time, particle size and ζ potential were also determined.

RESULTS AND DISCUSION

Previous works have demonstrated the potential of 3DP to tailor oral medicines to individual patients, and the feasibility of this technology to prepare tailored medicines in hospital settings [1]. This study we have proved that it was feasible to prepare drug-loaded suppositories without a mould or other physical support using 3DP technology. The printed suppositories were well-defined and with an acceptable consistency for normal handling. Two different compositions of printing material were tested. During the printing process, the syringe temperature was set at 42 ºC for Gel 44 formulation and to 48 ºC for Gel 48. The suppositories were printed in two positions, horizontally and vertically (Figure 2) and in three different sizes (Figure 1). The printing time for the suppositories printed vertically was 4 min 30 s and 2 min 16 s for those printed horizontally.

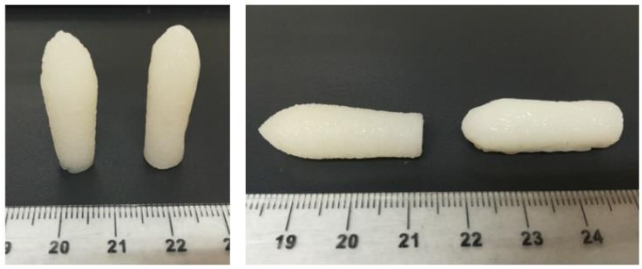

Fig 2. In each picture, Gel 44 SES printed in horizontal position (right) or vertical position (left).

SEM images showed the deposition of individual layers connected to each other forming a solid low porosity object (Figure 3).

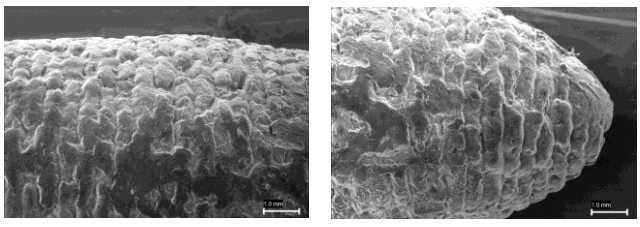

Fig 3. SEM images of different sections of Gel 44 SES printed in vertical position.

Extrusion force studies showed that the extrusion force required for Gel 48 extrusion was higher, even at higher temperatures, than that required for Gel 44 extrusion.

The disintegration time of Gel 44 SES was close to the 30 min limit recommended by the European Pharmacopeia, whereas Gel 48 SES demonstrated a higher disintegration time which could be ascribed to the higher melting points of the material. In the same way, in vitro drug release profiles showed that Gel 44 SES released drug at a faster rate than Gel 48.

Gel 44 SES showed faster microemulsification time than Gel 48 SMES, which also justifies its shorter disintegration time. Moreover, mean size of lipid droplets of both formulations was between 1-1.5 µm, and the stability of the emulsion was given by ζ potential of emulsion droplets, which was – 14 mV for Gel 44 and – 20 mV for Gel 48, which means that Gel 48 emulsion was more stable. TEM microphotographs were obtained to directly visualize the lipid droplets, showing globules with spherical shapes and sizes consistent with the dynamic light scattering (DLS) measurements.

FT-IR spectra showed that the major infrared peaks of the actives did not change within the formulations as compared to control spectra of tacrolimus alone, which means there were no detectable interactions between the drug and the lipid excipients. **CONCLUSIONS**

In the present study, we have successfully prepared for the first time customised lipid-based suppositories with different sizes and containing a specific dose of the drug, which can be tailored to the dose requirements of each patient reducing the risk of adverse effects.

REFERENCES

[1] A. Goyanes, CM. Madla, A. Umerji, et al. Automated therapy preparation of isoleucine formulations using 3D printing for the treatment of MSUD: first single-centre, prospective, crossover study in patients. Int. J. Pharm. 2019:118497.

[2] I. Seoane-Viaño, N. Gómez-Lado, H. Lázare-Iglesias, et al. 3D printed tacrolimus rectal formulations ameliorate colitis in an experimental animal model of inflammatory bowel disease. Biomedicines, 8 (12) (2020), p. 563

P3.9: Development of shear-responsive microaggregates based on PLGA nanoparticles for targeted delivery

Mazen M. El-Hammadi[1], Remedios Otero-Candelera[2,3,4], Lucía Martín-Navarro[1], Josefa Álvarez-fuentes[1], Lucía Martin Banderas[1,2*]

[1]*Department of Pharmacy and Pharmaceutical Technology, Facultad de Farmacia, Universidad de Sevilla, Sevilla, Spain.*
[2]*Instituto de Biomedicina de Sevilla (IBIS)-Campus Hospital Universitario Virgen del Rocío, Sevilla, Spain.*
[3]*Hospital Universitario Virgen del Rocío, Sevilla, Spain.*
[4]*CIBERES, Instituto de Salud Carlos III, Madrid, Spain.*

*e-mail: luciamartin@us.es

Introduction

Obstruction of critical blood vessels as in thrombosis and aterosclerosis is a leading cause of death and long-term adult disability worldwide. Effective treatment requires quick and invasive interventions through the systematic infusion of thrombolytic agents or the placement of a catheter in the affected vessel. Moreover, non-selective distribution of the thrombolytic drug increases bleeding risk. Blood vessels with luminal stenosis (narrowing) show a significant increase in fluid shear stress (>1000 dyne/cm2) compared to normal vessels (~70 dyne/cm2), a fact that can be exploited for targeting delivery to obstructed vessels.

The objective of present work is to prepare microscale aggregates of PLGA NPs with the ability to breakup under high shear stress into their forming NPs, which in turn adhere more effectively to the vessel surface compared with larger aggregates.

Materials and methods

Negatively and positively charged NPs were prepared based on poly(ethylene glycol) (PLGA) using an emulsion-solvent evaporation method. Nanoparticles surface charge was modulated by using carboxylic or amine species. Next, the microaggregates were prepared by mixing the negatively and positively charged NPs using a high-speed homogenizer. Optimized aggregates were achieved by controlling different parameters as: (i) composition of NPs; (ii) NPs ratio; or (iii) homogenization conditions (speed, duration). The produced NPs and aggregates were extensively characterized. To test the ability of the microaggregates to collapse under high shear stress, they were injected through a microfluidic device specially designed to mimics different vascular grading stenosis (low, medium, high) (see Fig. 1).

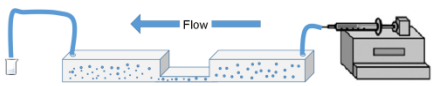

Figure 1. Set-up for shear-induced dissociation of aggregates assay

Furthermore, HUVEC cells were cultivated in the microfluidic system and labelled aggregates (Nile red-negative NPs and (FITC-positive NPs) were injected into the microchannel and observed under fluorescence microscope.

Results and Discussion

Particle size and zeta potential were 268.5 nm, -20.1mV and 179.2 nm, +20.9 mV for negative and positive NPs, respectively. The microaggregates had a globular shape and an average diameter of 6 µm (Figue 2).

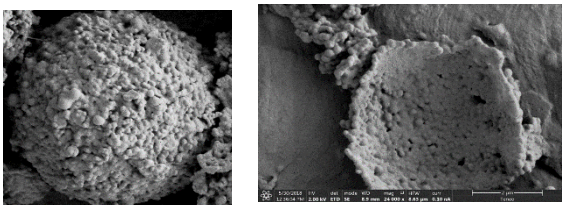

Figure 2. SEM images of a micro-aggregate and a cross-section of an aggregate of microparticles showing its interior and where the individual nanoparticles can be differentiated

Aggregates passed through the microchannel contained ~30% of NPs as a result of aggregates collapse under the elevated shear. In addition, examination under fluorescence microscope provided another evidence for aggregates breakup.

Conclusions

The PLGA-based microaggregates show promise for targeted treatment of thrombosis, arteriosclerosis and thrombosis-associated disorders such as COVID 19 infection.

Acknowledgments

We specially thank funding from Junta de Andalucía (Consejería de Economía, Conocimiento, Empresas y Universidad) Project. Medicamentos innovadores basados en nanomedicina (AT17_5548_USE)

Authors also thank Biology and Microscopy Services from Centro de Investigación, Tecnología e Innovación (CITIUS, Universidad de Sevilla) for technical assistance.

References

[1] Korin N, et al. Science, 337(2012) 738-42.

[2] Berrocoso Domínguez E, et al. Nanomedicine, 13 (2017):2623-2632.

P3.10: Lipid-polymeric hybrid nanoparticles funcionalized with a specific aptamer: cellular uptake and citotocicity

P. Díaz-Rodríguez[1,2*], P García-García[2,3], C. Évora[2,3] and A. Delgado[2,3]

[1] *Department of Pharmacology, Pharmacy and Pharmaceutical Technology, Universidade de Santiago de Compostela, 15782 Santiago de Compostela, España*
[2]*Department of Chemical Engineering and Pharmaceutical Technology, Univerdad de La Laguna, 38206 La Laguna, Spain*
[2]Institute of Biomedical Technologies (ITB), Universidad de La Laguna, 38206 La Laguna, Spain

*e-mail: patricia.diaz.rodriguez@usc.edu.es

Introducction

Nanoparticles (NPs) present a great potential as drug delivery systems to treatment different diseases [1]. However, the development of effective pharmaceutical formulations able to target specific tissues/cells remains a challenge. Specifically for NPs, to ensure their therapeutical activity, they must be elaborated in such a way they are able to overcome a series of biological barriers that limit their ability to release their content in the target cells. Furthermore, some therapeutic agents must follow a specific intracellular pathway to escape the endosomal-lysosomal pathway and exert their effect on an intracellular target. Nucleic acid aptamers are a kind of short RNA or single-stranded DNA oligonucleotides. Aptamers can target widely varying molecules and even whole cells or viruses [2]. Due to their high specificity, binding affinity, and low nanomolar dissociation constants to their targets, aptamers are very attractive as targeting ligands to be combined with NPs to develop targeted drug delivery systems.

The aim of this work is to test the celular uptake and explore the intracelular trafficking of lipid-polymer nanoparticles functionalized with an aptamer. The toxicity of the nanoparticles in the target cells, mouse Mesenchymal Stem Cells (mMSC), will also be tested.

Materials and Methods

Lipid-polymer hybrid nanoparticles (LPNPs) were developed by a single-step nanoprecipitation method similarly to already published [3]. Additionally, the aptamer was linked using a click chemistry approach. No further details of the formulation procedure can be provided as the procedure is under the process of intellectual property protection.

In vitro assays were carried out with naked and aptamer-NPs using primary mMSC isolated from FVB mice as previously described [3]. *Cytotoxicity assays:* cell monolayers were incubated for 24 hours with naked or aptamer-NPs suspensions in DMEM at variable concentrations (0.1 µg/ml-1.41 mg/ml) and cell viability was measured by an XTT assay (Roche).

NPs cell uptake: coumarin-6 labelled LPNPs were used to test NPs uptake. Cells were incubated with the NPs' suspensions for 2 hours. Then, the cells were washed with DPBS, tripsinized and after centrifugation analyzed with the Tali® Image-Based Cytometer (Thermofisher). The percentage of cell uptake was calculated by counting the fluorescent cells, stained with coumarin-6, and total cells. Alternatively, NPs uptake was visualized by confocal microscopy and transmission electron microscopy (TEM). For the confocal microscopy cells were seeded in a culture slide (Falcon®, CultureSlides) and treated with the NPs suspensions for 2 hours, washed and fixed with paraformaldehyde 4%. Afterwards, cells were permeabilized and incubated with 50 µg /ml rhodamine phalloidin (Thermo Fisher Scientific, USA) for 40 minutes. Then, wells were washed and incubated with DAPI for 5 minutes. Finally, cells were visualized using a confocal microscope. The internalization pathway followed by the NPs was evaluated by transmission electron microscopy. Cells were treated for 1, 2 and 24 hours with the NPs suspensions. Then, fixed with 2% glutaraldehyde in 0.1 M sodium cacodylate buffer (SC buffer) for at least 1h at 4°C. After fixation, all procedures were carried out on ice. Fixed cells were washed and stained with 1% OsO4 in 0.1M SC buffer for 45 min. Coverslips were placed in 2% uranyl acetate buffer for 45 min and samples were dehydrated. Then, samples were incubated with Ducurpan:Acetone 50/50 for 1 hour, and two times more in fresh Durcupan. Coverslips embedded in Durcupan resin were cuted into 60-nm ultrathin sections and mounted on 300 mesh grids. Samples were then visualized on a transmision electron microscope.

Results and Discussion

The treatment of mMSC with the different nanoparticles' concentrations did not show any

toxicity. Only a slight decrease in cell viability was observed at the highest concentration (1.41 mg/mL) but even in this case, cell viability remained higher than 70%. If we estimate the concentration of NPs in the bloodstream of a human being after administration of a 500 mg dose, the expected concentration of NPs in the blood would be approximately 0.1 mg / mL at the time of injection and it will decrease as a consequence of the distribution. Therefore, taking into account the wide range of NPs concentrations used to carry out this study, our results indicate that both, nacked NPs and the aptamer functionalized one are safe as no signs of cytotoxicity were detected.

Together with cytocompatibility, cell uptake can be desired when NPs are designed for intracellular delivery of therapeutic agents. The number of cells positive for coumarin-6 (encapsulated in NPs) was assessed using an image-based cytometer. The images showed that both types of particles were highly internalized by cells. Despite not observing differences in the number of positive cells for both types of NPs, the labeling intensity was higher for the aptamer-LPNPs which could indicate a higher number of internalized NPs per cell. This could be caused by a different route of internalization between the two types of NPs.

The intracellular localization of NPs was studied both by fluorescence microscopy and transmission electron microscopy. The images obtained by both methods indicate the LPNPs, independtly of the incorporation of aptamer, are located in the cytoplasm of the cells.

Conclusions

The developed LPNPs with or without aptamer did not produce any cell toxicity in a wide range of concentrations. Moreover, the cellular uptake process seems to be favored in the aptamer functionalized nanoparticles. Both confocal microscopy and TEM results show the designed LPNPs reach the cell cytoplasm.

Acknowledgments

This study has been funded by Ministerio de Ciencia, Innovación y Universidades (MICIUN), which is part of the Agencia Estatal de Investigación (AEI), Spain, with joint financing by FEDER funds from the European Union (RTI2018-097324). Patricia Garcia-Garcia acknowledges the postdoctoral grant “Investigador Posdoctoral Junior, CEI-Canarias”.

References

[1] Yetisgin AA., Cetinal S., Zuvin M., Kosar A., Kutlu O. Therapeutic Nanoparticles and Their Targeted Delivery Applications. Molecules (2020). 25: 2139.

[2] F. Ding, Y. Gao, X. He Recent progresses in biomedical applications of aptamer-functionalized systems. Bioorganic & Medicinal Chemistry Letters (2017) 27: 4256–4269

[3] García-García P., Briffault E, Landin M, Evora C, Diaz-Rodriguez P, Delgado A. Tailor-made oligonucleotide-loaded lipid-polymer nanosystems designed for bone gene therapy. Drug Deliv Transl Res (2021). 11: 598-607.

P3.11: Organs toxicity of oligonucleotide aptamer-lipid-polymer nanoparticles for osteoporosis

R. Reyes[1,2]*, P. García-García[2,3], P. Díaz-Rodríguez[4], M.R. Arnau[2], C. Évora[2,3] and A. Delgado [2,3]

[1] *Department of Biochemistry, Microbiology, Cell Biology and Genetics, Universidad de La Laguna, 38206 La Laguna, Spain*
[2]Institute of Biomedical Technologies (ITB), Universidad de La Laguna, 38206 La Laguna, Spain
[3]*Department of Chemical Engineering and Pharmaceutical Technology, Univerdad de La Laguna, 38206 La Laguna, Spain*
[4]*Department of Farmacoloxía, Farmacia e Tecnoloxía Farmacéutica, Univerdade de Santiago de Compostela. Spain*

*e-mail: rreyesro@ull.edu.es

Introducction

Oligonucleotide delivery systems have emerged to improve the clinical application of this type of therapeutic agents to treat some diseases. Osteoporosis is a progressive bone disease characterized by loss of bone mass and alterations in its structure that affect the microarchitecture of the bone increasing the fracture risk. The osteoporosis could be a good candidate to be treated with ASO-aptamer- lipid-polymer-nanoparticles (A-A-LPNPs) to stimulate the canonical Wnt-beta catenin pathway and promote bone formation. For this, it is necessary to take into account, among others, an important issue concerning ASOs drug, the specific delivery of oligonucleotide to target tissue, which will affect both the efficacy and the toxicity of the treatment [1]. Although few studies focus on the detection of NPs toxicity, some signs of toxicity have been reported in animals treated with silica NPs and solid lipid NPs [2,3]. For this reason, this study aims to evaluate the in vivo biocompatibility/ toxicity profile of the A-A-LPNPs previously developed in our laboratory. Toxicity was analyzed in vital organs after intravenous administration of nanoparticles

Materials and Methods

LPNPs for ASO encapsulation were prepared following a single-step nanoprecipitation method and functionalized with the aptamer by maleimin reaction to obtain the A-A-LPNPs.

18 osteoporotic mice were divided in 3 groups of 6 mice each and 50 µl of saline solution (SS), or of A-A-LPNPs control and A-A-LPNPS suspensions, were injected respectively via vein tail per month. After 3 months animals were anesthetized and fixed by intracardiac perfusion with 10% formalin buffered, the organs (spleen, liver, lung, kidney, heart, brain and bone) were extracted and prepared for histological analysis as previously described [4]. Briefly, the organs were post fixed by immersion for 24 hours in the same fixative, and embedded in Paraplast®. Sections of 5 µm thick were obtained with a microtome (Shandon Finesse 325). The sections were stained with hematoxylin-erythrosine (H-Er) for topographical study. Sections were analyzed by light microscopy (LEICA DM 4000B) and the images were captured with a digital camera (Leica DFC300FX).

Results and Discussion

Lipid NPs and polymeric NPs are usually considered safe drug delivery systems. The LPNPs were prepared with biocompatible and GRAS excipients. All the organs analyzed showed a normal macroscopic appearance of the three experimental groups (SS, A-A-LPNPs control and A-A-LPNPs). Neither the microscopic analysis showed differences in in the organs of animals treated with A-A-LPNPs with respect to the organs of the control group. No significant change was observed in the organs, neither in tissue architecture nor alterations in cell structure with respect to the SS group. The liver showed a normal structure with hepatocytes arranged in cords around the sinusoid capillaries, and normal size and morphology (Fig. 1). The vascular spaces of portal and hepatic systems present normal size and morphology as well as the bile ducts (Fig. 1). The kidney shows a normal tissue structure both, in cortex and medulla, observing renal corpuscles of normal size and morphology in which the simple flat epithelium of Bowmann's capsule is observed (Fig 1). The proximal convoluted tubules dominate the parenchyma of renal cortex, showing the characteristic simple cubic epithelium of intense eosinophilic stain and the brush border in the apical domain of epithelial cell (Fig. 1). The distal tubules, of simple cuboidal

epithelium, are observed in fewer number showing a wider lumen (Fig. 1).
In addition, the rest of the organs analyzed, spleen, lung, heart and brain, showed, a normal histological structure, without changes or significant alterations with respect to SS group.

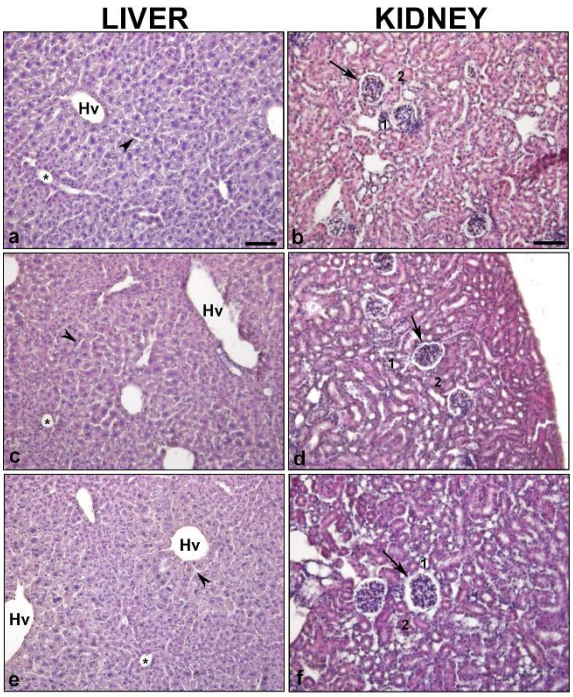

Fig 1. **Histological evaluation**. Semi-panoramic images showing the liver and kidney in the three experimental groups (SS: a-b, A-A-LPNPs control: c-d and A-A-LPNPs: e-f). A normal tissue structure is observed without changes at the cellular level. Liver: HV. Hepatic vein, Asterisks: Portal vein, arrowheads: sinusoid capillaries. Kidney: 1: Distal convoluted tubule, 2: Proximal convoluted tubule, Arrows: Renal corpuscles. (H-Er). Scale bars: 80 µm.

No study on the toxicity of LPNPs was found in the consulted literature. That is why we have focused this work on the search for signs of toxicity in the organs where these NPs accumulate. The LPNPs were designed with an aptamer to target osteoporotic bone, the results will be published soon but are currently subject to patent secrecy. We can anticipate that the results are hopeful and that no toxicity has been detected in the skeleton of the mice injected with the indicated regimen. Likewise, the spleen, liver or lung, which are the organs in which NPs are usually distributed according to their size, presented normal tissue structure. Also, the kidney, the organ of excretion of these NPs, does not present any histological damage. Finally, although these LPNPs are not expected to cross the BBB, the analysis of brain tissue is normal. Future studies with different dosage guidelines will be necessary to confirm the safety of these NPs.

Conclusions

The administered nanoparticles do not cause significant histological alterations in tissue structure nor changes at cellular level in the analyzed organs.

Acknowledgments

This work was supported by the EDER/Ministerio de Ciencia e Innovación—Agencia Estatal de Investigación RTI2018-097324-B-I00 and by the Spanish Ministry of Science, Innovation and Universities (MICINN), State Research Agency (AEI) and the European Regional Development Funds (ERDF) (PGC2018-094503-B-C21).

References

[1] X. Chi, P. Gatti and T. Papoian Safety of antisense oligonucleotide and siRNA-based therapeutics. *Drug Discovery Today* 22 (2017) 823-833

[2] R. Mohammadpour, M. Yazdimamaghania, D. L. Cheneya *et al.* Subchronic toxicity of silica nanoparticles as a function of size and porosity. *J. Control Rel.* 304 (2019) 216–232

[3] M. Padilha Mendonça, A. Radaic, F. Garcia-Fossa *et al.* The in vivo toxicological profile of cationic solid lipid nanoparticles. Drug Delivery and Translational Research 10 (2020) 34–42

[4] A. Hernández, E. Sanchéz, I. Soriano *et al*. Material-related effects of BMP-2 delivery systems on bone regeneration. Acta Biomater 8(2) (2012) 781-91.

P3.12: Immunotoxicological properties of yeast-derived glucan particles

J. Panão Costa[1;2]*, M. Colaço[1;2], S. Jesus[1] and O. Borges[1;2]

[1]Center for Neurosciences and Cell Biology Coimbra, Portugal
[2]Faculty of Pharmacy, University of Coimbra, Portugal

*e-mail: jpanao94@gmail.com

Introduction

The excitement around particulate systems has risen in recent times, particularly in the field of drug delivery and vaccinology. Despite the growing number of studies on particulate-based systems, their adverse effects on the organism are not often accounted for [1]. Given the unique properties of particulate systems, it is critical to perform a detailed risk assessment during pre-clinical development, to determine their unexpected toxicity profile and to prevent any harmful reaction on humans or the environment [2]. Thus, *in vitro* assays are essential to identify valuable candidates and to anticipate any toxicological problems, expediting their potential translation into the clinic [1, 2].

β-glucans are natural polysaccharides found in many organisms such as fungi, bacteria, and some algae. They can be divided in soluble glucans and insoluble glucan particles (GPs). GPs are porous and hollow cell wall microspheres, and they are generally purified from the yeast *Saccharomyces cerevisiae*, being mainly composed of β-1,3-D-glucan, and trace amounts of mannoproteins and chitin [3].

Due to their β-glucan content and other pathogen-mimicking characteristics, GPs are targeted to phagocytic cells, like DCs and macrophages, making them interesting candidates to use in immunotherapies or as a vaccine platform [4]. Besides their use as a payload delivery system, these yeast-derived β-glucan particles were already studied for their potential adjuvant and immunostimulant effects [5].

GPs are promising particulate delivery systems with immunological adjuvant properties, yet their toxicological profile is not fully documented. Thus, the purpose of this study was to assess the immunotoxicity and biocompatibility of GPs *in vitro*.

Materials and Methods

GPs were purified from *Saccharomyces cerevisiae*, through successive alkaline, acidic, and organic extractions at high temperatures [3]. Three types of GPs were tested, varying the extent of alkaline extractions. GPs obtained through protocol with just two alkaline extractions were called GPs A. To produce GPs B and GPs C, four and six 1 h washes in NaOH 1 M were performed, respectively. GPs were characterized regarding their size, zeta potential (ZP) and protein loading capability. Their morphology was visualized by transmission electron microscopy. Several immunotoxicity studies were completed in RAW 264.7 macrophage cell line, namely cytotoxicity assay (MTT), reactive oxygen species (ROS) and nitric oxide (NO) production and inhibition of NO production. Hemolysis assay was evaluated on whole blood and human peripheral blood mononuclear cells (PBMCs) were used to assess GPs' cytotoxicity and ability to induce IL-6 and TNF-α production. GP internalization by human monocytes was visualized by confocal microscopy.

Results and Discussion

In terms of size and size distribution, the three types of GPs did not show meaningful differences amongst them, presenting sizes around 5 µm. Regarding particles' surface charge, GPs exhibited a slightly negative charge when suspended in water.

Table 1. GPs' physicochemical properties. Mean particle size (µm), and zeta potential (mV) value of empty GPs measured in water; GPs A – n = 4; GPs B – n = 4; GPs C – n = 1

	Size (µm) ± SEM	ZP (mV) ± SEM
GPs A	4.50 ± 1.16	-6.94 ± 0.81
GPs B	5.62 ± 2.78	-4.93 ± 1.37
GPs C	6.24 ± 1.54	-7.70 ± 0.04

GPs were able to internalize all the protein added irrespective of the GP production protocol. Through TEM, no significant differences were observed between GPs A and GPs B, however GPs C were difficult to focus, possibly due to the harsher purification protocol that may have partially destroyed the integrity of the outer shell.

Studies assessing the impact on cell viability (RAW 264.7) and hemocompatibility upon

stimulation with the particles show that GPs C have a cytotoxic effect on RAW 264.7 and are slightly hemolytic, unlike GPs A and GPs B.

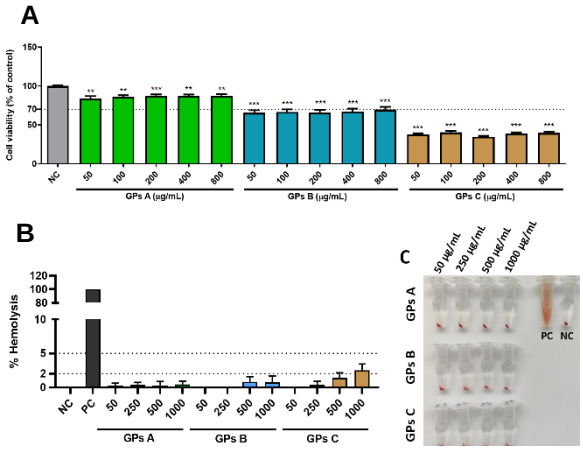

Fig 1. Cytotoxic effect of GPs. (A) Cytotoxicity assay (MTT), performed in RAW 264.7 cells after 24 h. Data presented as mean ± SEM, n = 4; GPs A – n = 3; GPs B – n = 3; GPs C – n = 1. (B) Hemolytic effect of different concentrations of GPs in human whole blood (mean ± SEM, n = 3, three independent experiments, each condition in triplicate). Results are expressed in comparison with cells treated with Triton X-100 (positive control (PC), 100% hemolysis) and with cells treated only with PBS (negative control (NC), 0% hemolysis). (C) Visual evidence of the tubes containing diluted total blood after being incubated with the controls.

Concerning the particles' effect on oxidative stress, only higher concentrations of GPs C were able to increase ROS production on RAW 264.7 cell line. Studies assessing NO production in the same cell line revealed that all kinds of GPs were unable to enhance NO production. On the other hand, almost all GPs' concentrations inhibited, to some extent, NO production in LPS-stimulated macrophages.

Furthermore, GPs A and GPs B showed no cytotoxity on PBMCs, on all concentrations tested. IL-6 and TNF-α production on PBMCs was stimulated by all concentrations of GPS B, while only higher concentrations of GPs A were able to induce the same effect. Regarding PBMCs uptake, GPs A were successfully internalized by human monocytes, as expected since particulate β-glucans bind to the dectin-1 receptor on the surface of these cells.

Conclusions

Despite all three types of GPs showed similar physicochemical properties and demonstrated no significant effect on the oxidative stress in the RAW 264.7 cell line, GPs C appeared to be more cytotoxic and hemolytic. Additionally, all tested GPs seem to have immunomodulatory activity on human immune cells, specifically regarding pro-inflamatory cytokine induction.

To conclude, GPs are a promising particulate delivery systems or adjuvant, given their biocompatibility and immunomodulatory activity.

Acknowledgments

This work was supported by the European Regional Development Fund (ERDF), through the Centro 2020 Regional Operational Programme, under project CENTRO-01-0145-FEDER-000008:BrainHealth 2020, and through the COMPETE 2020—Operational Programme for Competitiveness and Internationalisation and Portuguese national funds via FCT – Fundação para a Ciência e a Tecnologia, under projects PROSAFE/0001/2016, POCI-01-0145-FEDER-030331, UIDB/04539/2020, UIDP/04539/2020 and grants 2020.10043.BD and SFRH/BD/139142/2018. The authors thank Dr. Luísa Cortes and Dr. Mónica Zuzarte for their expertise and assistance in confocal microscopy and transmission electron microscopy, respectively.

References

[1] S. Jesus, A.P. Marques, A. Duarte, E. Soares, J. Panão Costa, M. Colaço et al., Chitosan Nanoparticles: Shedding Light on Immunotoxicity and Hemocompatibility. Front Bioeng Biotechnol. 2020;8(February).

[2] A.B. Engin, A.W. Hayes. The impact of immunotoxicity in evaluation of the nanomaterial's safety. Toxicol Res Appl. 2018; 2:1–9.

[3] E.R. Soto, G.R. Ostroff. Characterization of multilayered nanoparticles encapsulated in yeast cell wall particles for DNA. Bioconjug Chem. 2008;19(4):840–8.

[4] E. Soto, G. Ostroff. Glucan particles as carriers of nanoparticles for macrophage-targeted delivery. ACS Symp Ser. 2012;1119:57–79.

[5] V. Vetvicka, L. Vannucci,P. Sima. B-Glucan As a New Tool in Vaccine Development. Scand J Immunol. 2019;91(2):0–2.

P3.13: The influence of curcumin-encapsulated glucan nanoparticles on oxidative stress in liver cells

M.Colaço[1;2]*, O. Borges[1;2], T. Roquito[1;2], J. Panão Costa[1;2] and S. Jesus[1]

[1]Center for Neuroscience and Cell Biology, University of Coimbra, Coimbra, Portugal
[2] Department of Pharmaceutical Technology, Faculty of Pharmacy, University of Coimbra, Coimbra, Portugal

*e-mail: olga@ci.uc.pt

Introduction

Liver cancer, despite recent technological and scientific advancements, is still a problematic disease that requires more research on prevention and treatment. It is estimated to be the 4th major cause of cancer death worldwide (8.2 %), and the 6th most commonly diagnosed cancer (4.7 %), being more prevalent in males, in Asian countries and in countries with lower human development index. Hepatocellular carcinoma (HCC) is the most common form of liver cancer, comprising 75 % to 85 % of all cases [1]. Many researchers have been studying the role of the oxidation/reduction balance in the liver to look for options to treat HCC. It is accepted by the scientific community that higher levels of reactive oxygen species (ROS) can contribute to cancer cell death, in part due to the fact that cancer cells have an increased metabolism and therefore a higher rate of ROS production, which makes these cells more susceptible to increases in oxidative stress [2]. Curcumin is a relatively simple polyphenol that has been associated with anticarcinogenic and prooxidant properties, mostly depending on its concentration and on the present chemical environment [3]. However, the curcumin molecule possesses very poor pharmacokinetics, which limits its practical applications. The encapsulation of curcumin in nanoparticles is one of the possible solutions to solve this problem. Therefore, this work investigates the encapsulation of curcumin in glucan NPs and its effect on oxidative stress in liver cancer cells.

Materials and Methods

Curcumin-encapsulated glucan nanoparticles (NPs) with 100 nm (GluCur 100 NPs) and with 380 nm (Glu 380 NPs) were produced based on a method previously published by our group with minor modifications to encapsulate the drug [4]. The particles were characterized regarding its oxidative stress potential in liver cancer cells. Cell viability studies, ROS production, nitric oxide induction and intracellular reduced glutathione (GSH) levels were investigated in HepG2 cells previously incubated with GluCur 100 NPs, GluCur 380 NPs, free drug as well as its corresponding blank NPs, Glu 130 and Glu 355 NPs.

Results and Discussion

Curcumin-encapsulated and blank glucan NPs of different sizes (Glu 130, GluCur 100, Glu 355 and GluCur 380 NPs) were successfully produced and once more characterized regarding its size and zeta potential, which was slightly negative, when suspended in water. Studies assessing the impact on cell viability (splenocytes and HepG2 cells) upon stimulation with the particles and the free drug showed that the smaller NPs consistently caused a higher percentage of cell death, as well as the curcumin-encapsulated NPs comparatively to their bare counterparts. Concerning the particles' effect on oxidative stress in HepG2 cells, GluCur 380 NPs displayed an increased induction of ROS, in viable cellular concentrations, that seems the result of an additive effect between curcumin and the curdlan delivery system (Glu 355 NPs). It was also observed that both curcumin-encapsulated glucan NPs induce NO production in liver cancer cells, although the concentration required to observe such effect is completely different. The free drug was also capable to induce NO on its own, but only on concentrations higher than 32 µM, which is far from the quantity of curcumin that was encapsulated in the particles. Finally, regarding the evaluation of the intracellular GSH levels, HepG2 cells stimulated for 1 h with the particles revealed that smaller curcumin-encapsulated particles were able to significantly reduce the levels of intracellular GSH, in a similar extent to the positive control, diethyl maleate. However, subsequent cell viability assays showed that at those particles' concentrations tested, a reduced cell viability was observed. With this data, further GSH quantification assays were performed with lower concentrations of NPs, but this time it was not noticed any effect in GSH concentration.

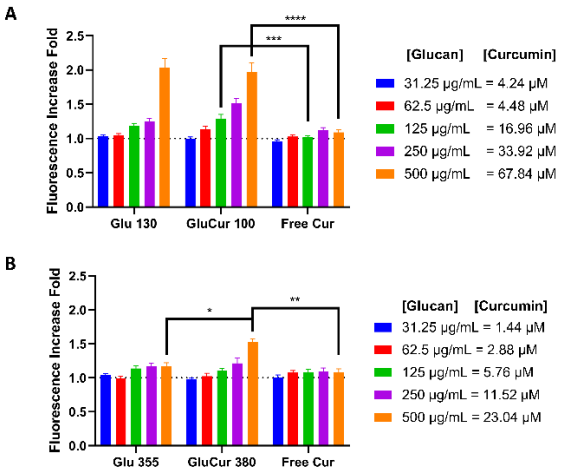

Fig 1. Induction of ROS production by HepG2 cells after 1 h of incubation with nanoparticles and curcumin. (A) Representation of statistically significant differences between Glu 130 NPs, GluCur 100 NPs and its corresponding free curcumin. (B) Representation of statistically significant differences between Glu 355 NPs, GluCur 380 NPs and its corresponding free curcumin. Data are presented as mean ± SEM, n = 5.

Conclusions

GluCur 100 NPs showed a greater ability to induce oxidative stress, demonstrated by ROS production and NO induction in HepG2 cells. Therefore, we theorize that smaller curcumin-encapsulated glucan NPs present a considerable ability to be used as part of an immunotherapy, specifically for treatment of hepatocellular carcinoma.

Acknowledgments

This work was supported by the European Regional Development Fund (ERDF), through the Centro 2020 Regional Operational Programme, under project CENTRO-01-0145-FEDER-000008:BrainHealth 2020, and through the COMPETE 2020—Operational Programme for Competitiveness and Internationalisation and Portuguese national funds via FCT – Fundação para a Ciência e a Tecnologia, under projects PROSAFE/0001/2016, POCI-01-0145-FEDER-030331, UIDB/04539/2020, UIDP/04539/2020 and grants 2020.10043.BD and SFRH/BD/139142/2018.

References

[1] Bray, F., J. Ferlay, I. Soerjomataram, R.L. Siegel, L.A. Torre, and A. Jemal, *Global cancer statistics 2018: GLOBOCAN estimates of incidence and mortality worldwide for 36 cancers in 185 countries.* CA: A Cancer Journal for Clinicians, 68 (2018) 394-424

[2] Gorrini, C., I.S. Harris, and T.W. Mak, *Modulation of oxidative stress as an anticancer strategy.* Nature Reviews Drug Discovery, 12 (2013) 931-947

[3] Kobayashi, H., M. Murata, S. Kawanishi, and S. Oikawa, *Polyphenols with Anti-Amyloid β Aggregation Show Potential Risk of Toxicity Via Pro-Oxidant Properties.* International Journal of Molecular Sciences, 21 (2020) 3561

[4] Colaço, M., A.P. Marques, S. Jesus, A. Duarte, and O. Borges, *Safe-by-Design of Glucan Nanoparticles: Size Matters When Assessing the Immunotoxicity.* Chemical Research in Toxicology, 33 (2020) 915-932

P3.14: Preparation, characterization and efficacy of polylactide glycolide-chitosan nanoparticles loaded with Curcuma

J. Molpeceres*, C. Tizón, G. Yagüe and M.R. Aberturas

[1]*Department of Biomedical Sciences, Faculty of Pharmacy, Univerdad de Alcalá, 28871 Alcalá de Henares, Spain*

*e-mail: jesus.molpeceres@uah.es

Introducction

CCM (curcumin) is a lipophilic polyphenol obtained from the root of turmeric, which has been, traditionally used in medicine due to its antioxidant, anti-inflammatory and antibiotic properties (1). Therefore, CCM is deemed as a potential antitumoral and CNS drug. However, its poor aqueous solubility and permeability (BCS class IV) results in low bioavailability limiting CCM´s therapeutic efficacy. Nanotechnology has been evaluated for the development of novel non-toxic and efficient CCM formulations in order to overcome the mentioned issues (2). Polylactide-glycolide (PLGA) copolymers are EMA and FDA approved biodegradable materials in nanoparticle (NP) preparation. However, the negatively charged surface of PLGA NP prevents an efficient interaction with the cell's membrane (3). One of the most widely used biodegradable, biocompatible and non-toxic natural polymers to obtain NP is chitosan (CS). Due to the primary amino groups in its structure CS is positively charged at physiological pH granting NP mucoadhesion and internalization across negatively charged cell membranes (4,5). Nevertheless, its molecular weight and degree of deacetylation may imply differences in the physicochemical properties of the NP obtained (6). Thus, the objective of this piece of research was to prepare and characterize hybrid cationic NP made from PLGA and 20, 30, 50 and 600 (H) KDa CS (NPH-CS) containing CCM and to evaluate their therapeutic efficacy *in vitro* using different cell lines.

Materials and Methods

NP were obtained by the solvent evaporation method. An organic phase containing PLGA and CCM was emulsified with a 1% PVA aqueous phase by using an ultrasonic tip for 5 minutes at 280 mW. After the removal of the organic solvent under vacuum, excess PVA was removed by centrifugation at 12,000xg for 15 min and the NPHC pellet was re-suspended in ultrapure water. NPHC-CS were obtained following the same steps but re-suspending the pellet in a 0,1% CS solution/0,5% acetic acid followed by an incubation period of 15 min at 37ºC. Afterwards, excess CS was removed by centrifugation at 20,000xg for 15 min, and the NPHC-CS pellet was finally re-suspended in ultrapure water. These procedures were also reproduced in the absence of CCM to obtain placebo NP (NPHB or NPHB-CS) that were used as a control. CCM aqueous dispersions were also prepared by the same method in the absence of CS. Particle size and ζ-potential analysis, yield, drug encapsulation rate and dissolution studies were conducted to characterize the NP. Also, their efficacy were evaluated in PANC-1 and BxPC3 pancreatic cancer cell lines (10000 cells/well).

Results and Discussion

As shown in table 1, CCM was efficiently entrapped in NPH with no influence of the CS coating or mw. However, slightly higher NPH sizes were obtained in NPHC formulations (table 2). When CS was present the surface charge was positive and slightly higher values were obtained for increasing mw. All formulations responded to unimodal size distributions.

Table 1. Entrapment efficiency (EE), recovery and yield of NP (s.d.).

Id	EE (%)	Rec (%)	Yield (%)
NPHC-CS20	73.80 (5.6)	103.64 (5.4)	74.85 (14.4)
NPHC-CS30	73.94 (5.7)	113.34 (5.8)	84.92 (7.2)
NPHC-CS50	73.64 5.8	109.55 7.4	77.73 8.6
NPHC-CSHMW	73.56 5.7	101.88 12.9	69.09 8.6
NPHC	74.48 5.9	90.88 1.5	76.29 13.0

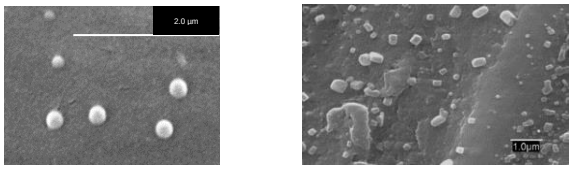

Fig 1. SEM micrograph of NPH and CCM (right).

Figure 1 shows smooth and spherical NP with no drug crystals.

Table 2. Particle size, PDI and ζ-potential of NP.

Id	Size (nm)	PDI	ζ-pot mV
NPHC-CS20	234 5,2	0,14 0,1	7,3 0,3
NPHC-CS30	233 0,9	0,13 0,1	11,8 5,1
NPHC-CS50	238 0,3	0,14 0,1	11,6 0,5
NPHC-CSH	241 2,6	0,17 0,1	12,4 2,4
NPHC	231 2,3	0,05 0,0	-12,8 2,2
NPHB-CS20	212 7,5	0,08 0,0	5,7 5,8
NPHB-CS30	208,8 4,8	0,07 0,0	9,4 2,4
NPHB-CS50	210,9 3,8	0,07 0,0	10,1 0,4
NPHB-CSH	214,6 1,7	0,088 0,0	13,0 4,6
NPHB	210 1,1	0,062 0,0	-15,9 4,7

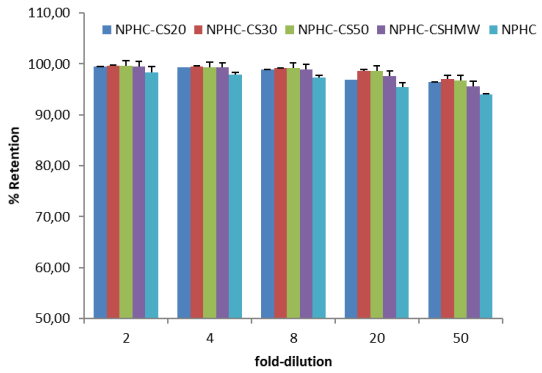

Fig 2. CCM retention by NPHC upon dilution

CCM was retained inside NPH even upon high dilution at RT (fig. 2). However, at 37ºC and under sink conditions in PBS about 80% of CCM was quickly released from NPH and the rest (20%) more slowly. These values changed to 50-60% and 30%, respectively in the presence of the CS coating regardless of the polymer mw (fig. 3). The activity of CCM on PANC-1 and BxPC3 cells was very different. As shown in figure 4, empty NPH has no effect but the effects of encapsulated CCM on BxPC3 cells was comparable to the one obtained with 5 or 50 µg/ml free drug even at low concentration (20µl NP equivalent to 28 µg/ml CCM) and regardless of the CS coating. However, it was not very significant on PANC-1 (results not shown).

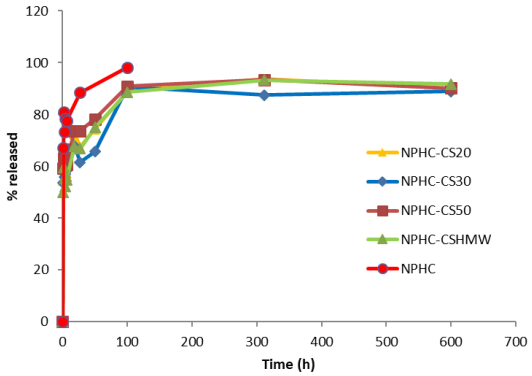

Fig 3. Drug release from NPH

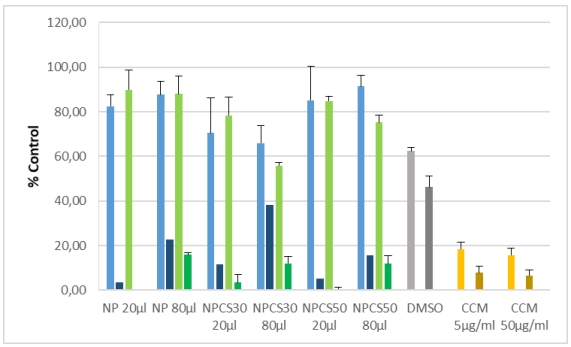

Fig 4. Cytotoxicity of NP and CCM on BxPC3 cells. (n>4) (empty NP: light coloured; CCM loaded NP: dark coloured; blue: 24h, green: 48h)

Conclusions

CCM loaded hybrid PLGA-CS NP show promising for the treatment of some pancreatic cancer.

Acknowledgments

The authors are grateful to Isabel Trabado for technical help regarding the cell culture experiments.

References

[1] S. A Noureddin, R. M.El-Shishtawy, K. O. Al-Footy, *Eur. J. of Med. Chem.* 182 (2019) 111631. doi:10.1016/j.ejmech.2019.111631

[2] P. Anand, P., A.B. Kunnumakkara, R. A. Newman, B.B. Aggarwal, *Mol. Pharm.* 4(6), (2007) 807-818. doi:10.1021/mp700113r

[3] T. Dou, J. Wang, C. Han, X. Shao, J. Zhang,W. Lu, *Int. J. Biol. Macromol.* 138, (2019) 791-799. doi:10.1016/j.ijbiomac.2019.07.168

[4] T. A. Ahmed, B.M. Aljaeid, *Drug Des. Dev. Ther.* 10, (2016) 483-507. doi:10.2147/DDDT.S99651

[5] A. Bernkop-Schnürch, A., S. Dünnhaupt, *Eur. J. Pharm. Biopharm.* 81(3), (2012) 463-469. doi:10.1016/j.ejpb.2012.04.007

[6] S. Sabnis, L.H. Block, L. H. *Int. J. Biol. Macromol.* 27(3), (2000) 181-186. doi:10.1016/S0141-8130(00)00118-5

P3.15: Polymeric nanoparticles loaded anti-viral peptide efficiently inhibits SARS-CoV-2

A. Mali[1;3]*, C. Zannella[1], S. Anthiya[3], M. Galdiero[1], G. Franci[2], M.J. Alonso[3,4]

[1]*Department of Experimental Medicine, section Virology and Microbiology, University of Campania "Luigi Vanvitelli", Naples 80138, Italy*
[2]Department of Medicine, Surgery and Dentistry "Scuola Medica Salernitana", University of Salerno, Salerno, Italy
[3]Center for Research in Molecular Medicine and Chronic Diseases (CiMUS), University of Santiago de Compostela, 15782 Santiago de Compostela, Spain
[4]Department of Pharmacy and Pharmaceutical Technology, University of Santiago de Compostela, 15782 Santiago de Compostela, Spain

*e-mail: avinashkrishna.mali@unicampania.it

Introduction

The coronavirus disease 2019 (COVID-19) is a severe pneumonia-like disease that has evolved into a pandemic due to its highly contagious and virulence nature of novel severe acute respiratory syndrome coronavirus 2 (SARS-CoV-2). During the past two-decade, animal coronaviruses (beta-CoVs) with the ability to jump species barriers have caused two deadly human outbreaks and this spillover ability makes it a candidate for future pandemics. The fundamental limitation of the current intramuscular vaccination approach using nanoparticles loaded mRNA, DNA viral vectors, or subunit protein is that they are not primarily designed to elicit mucosal immunity [1]. As the virus mainly enters and spreads through the nasal passage, developing an antiviral strategy that could effectively inhibit viral replication in the nasal cavity could be used as a tool not only to reduce the viral infection (prophylaxis) but also reduce transmission [2]. Developing intranasal antiviral formulations could help in reducing human-to-human transmission, thereby bringing the pandemic under control.

Our group has previously shown effective intranasal peptide and protein delivery using polymeric nanoparticle [3,4]. This nanoparticle can be easily produced under mild conditions with tunable size, surface charge, and *in vitro* release properties which facilitate the adsorption and encapsulation of therapeutic protein, peptides, and antigens [3,4]. Importantly, some biopolymers such as chitosan can enhance the nasal adsorption/absorption of peptide drugs improving the resident time and it is critical for our current application to reduce the frequency of infection and to neutralize the virus. In this study, we have rationally developed promising polymer conjugates and polymeric nanoparticle that show effective *in-vitro* inhibition of SARS-Cov-2.

Materials and Methods

Preparation of polymer- anti viral peptide conjugates: Chemical conjugation strategy was developed using the maleimide-thiol conjugation chemistry. Initially, maleimide conjugation to polymer-A was performed with N-hydroxy succinimide (NHS) and 1-(3-Dimethylaminopropyl)-3-ethyl carbodiimide (EDC). Reaction conditions were optimized to get the required degree of substitution. The reaction mixtures were dialyzed with a membrane (MWCO-7500Da) to remove impurities and lyophilize them for further use. The maleimide modification of polymer-A and subsequent peptide conjugation (either with peptide-X or peptide-Y) was confirmed by proton NMR**.**

Nanoparticles preparation and characterization: The nanoparticle was prepared by ionic interaction between the polymer A-peptide conjugate and a counter-polymer (polymer-B) in a mild aqueous condition. The resulting nanoparticle were fully characterized by dynamic light scattering (Zetasizer Nano-ZS®, Malvern Instruments, UK) and Nanoparticle tracking analysis (Nano Sight NS300, Malvern Instruments, UK).

***In-vitro* SARS-CoV-2 Neutralization Assay:** The free anti-viral peptides (X, Y), polymer-peptide conjugates (A-X, A-Y), and the nanoparticle (A-X/B or A-Y/B) were incubated with SARS-CoV-2 virions for 2

hours, then the mixture was added on Vero-76 cells and incubated for 1 hour. Later these cells were washed and overlaid with carboxymethyl cellulose (CMC). About 48 hours of post infection, the cells were stained with crystal-violet 0.5%, and plaques were counted.

Results and Discussion

Preparation of polymer-peptide conjugates: High degree of maleimide conjugation was obtained with polymer-A with the optimized reaction conditions with a required degree of substitution (DS). The polymer-peptide conjugates were obtained using thiol-maleimide click chemistry with a very high efficiency of conjugation (more than 95%).

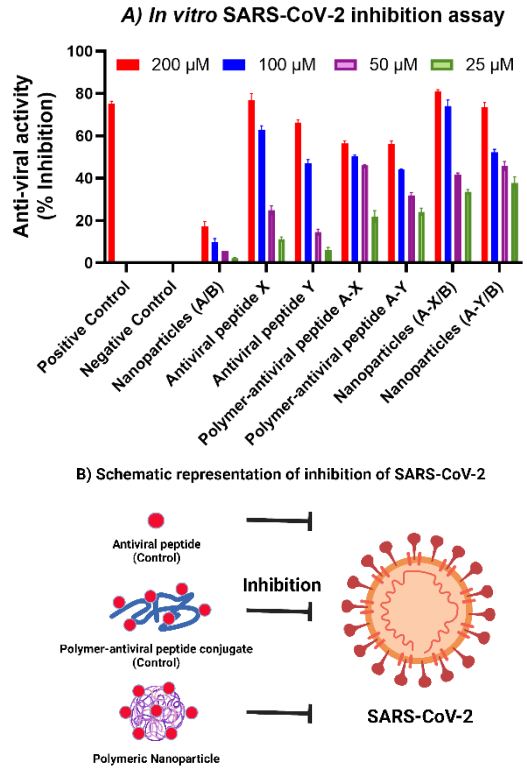

Figure:1 (A) The percent viral inhibition on Vero-76 cell line following pre-incubation of anti-viral compounds with SARS-CoV-2. Positive control was ivermectin while the negative control was water. (B) Schematic summary of results (Created with BioRender.com).

Nanoparticle preparation: Initial screening was performed with unmodified polymers (A and B). The optimized ratios were used to obtain polymeric nanoparticle with peptide-modified polymer-A (A-X or A-Y). All the formulations have an adequate physicochemical characteristic. Formulation A-X/B exhibited a size of 360±5 nm; PDI: 0.094; Zeta-potential: 21±2 mV whereas formulation A-Y/B exhibited a size of 480 ±5 nm; PDI: 0.187; Zeta-potential: 21±2 mV and formulation A-/B without antiviral peptide exhibited a size of 787±5 nm; PDI: 0.667; Zeta-potential: 25±2 respectively.

***In-vitro* SARS-CoV-2 inhibition Assay:** It is hypothesized that our antiviral peptides interact with the spike protein of the SARS-CoV-2 and inhibit the virus from infecting the target cells. Both polymer-peptide conjugates (A-X and A-Y) and polymeric nanoparticle (A-X/B and A-Y/B) were able to enhance the antiviral activity at lower concentrations compared to the free peptide (X and Y) as seen in the *in-vitro* virus pre-treatment assay (see in figure 1). Interestingly, the nanoparticle showed the highest anti-viral activity, while the control nanoparticle without anti-viral peptides did not show strong anti-viral effects. This indicates the need for both the anti-viral peptide and a suitable formulation to enhance the antiviral activity.

Conclusions

In this work, we are proposing new materials with a proof-of-concept *in-vitro* SARS-CoV-2 anti-viral activity. Next experiments include the *in-vivo* validation of these compounds. If proven effective, they are promising candidates for prophylactic and/or therapeutic nasal wash/ spray for human application.

Acknowledgments

This work was supported by Competitive Reference Groups, Consellería de Educación e Ordenación Universitaria, Xunta de Galicia, Ref: ED431C 2021/17.

References

[1] Kyriakidis, N.C., et al. SARS-CoV-2 vaccines strategies: a comprehensive review of phase 3 candidates. npj Vaccines 6, 28 (2021).

[2] Almanza-Reyes H, et al. (2021) Evaluation of silver nanoparticles for the prevention of SARS-CoV-2 infection in health workers: In vitro and in vivo. PLoS ONE 16(8): e0256401.

[3] T.G. Dacoba, et al. Polysaccharide Nanoparticles Can Efficiently Modulate the Immune Response against an HIV Peptide Antigen, ACS Nano. 13 (2019) 4947–4959.

[4] Cordeiro, A.S. et al. Carboxymethyl-β-glucan/chitosan nanoparticles: new thermostable and efficient carriers for antigen delivery. Drug Deliv. and Transl. Res. 11, 1689–1702 (2021).

P3.16: Novel Hybrid Nanosystem for Magnetically Targeted Antitumoral Activity Enhancement

N. Cruz[1,*], J.O. Pinho[2], G. Soveral[2], N. Matela[1], C. Pinto Reis[2], M.M. Gaspar[2]

[1]*IBEB, Faculty of Sciences, Universidade de Lisboa, Lisbon, Portugal*
[2]Research Institute for Medicines (iMed.ULisboa), Faculty of Pharmacy, Universidade de Lisboa, Lisbon, Portugal

*e-mail: nunocruz9009@gmail.com

Introduction

Cancer is a major health concern, and, in some cases, the prognosis is poor or limited due to late diagnose, advanced stage, and lack of efficacy of antitumoral agents or selectivity of conventional drugs. Nanomedicine as a field has been growing, one of its goals being to selectively deliver those drugs to tumour sites.
The goal of this study was to develop a novel hybrid nanosystem with magnetic properties and cytotoxic activity. Cuphen, a metal-based complex has shown high antiproliferative properties towards melanoma [1].

Materials and Methods

We designed long circulating and pH-sensitive liposomes loading both the metallodrug Cuphen and Dextran coated iron oxide nanoparticles (IONPs) as targeting modalities.
The IONPs were synthesized via one-step microwave assisted method, and then characterized by transmission electron microscopy and dynamic light scattering.
Lipid-based nanoformulations were prepared by the dehydration-rehydration method, followed by an extrusion step for reducing and homogenizing the mean size. Liposomes were characterized in terms of incorporation parameters and mean size.

Results and Discussion

High Cuphen loadings were obtained, and the presence of IONPs slightly reduced Cuphen incorporation parameters. Cuphen antiproliferative properties were preserved after association to liposomes and IONPs did not interfere on cellular proliferation of murine and human melanoma cell lines (Table 1).

Table 1. Cellular viability of B16F10 and MNT-1 cells after incubation with Cuphen, with or without IONPs.

	Cuphen 1 µM		Cuphen 5 µM	
	Without IONPs	**With IONPs**	**Without IONPs**	**With IONPs**
B16F10	104 ± 4	102 ± 2	65 ± 2	66 ± 2
MNT-1	106 ± 5	107 ± 5	59 ± 2	62 ± 2

Moreover, the developed nanoformulations displayed magnetic properties, being successfully captured by a magnetic field [2] (Fig 1). The formulations under study showed no haemolytic activity, demonstrating their safety for potential parenteral administration (Table 2).

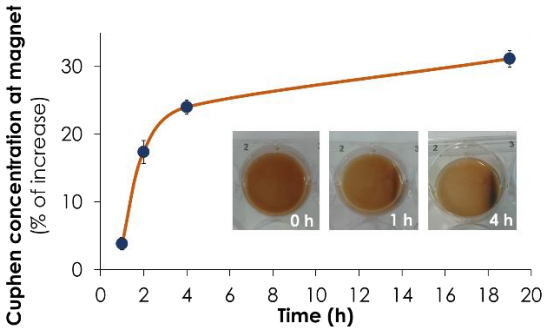

Fig 1. Graphical representation of the Cuphen concentration increase over time, in percentage. Liposomes were exposed to a magnetic field of 560.9 miliTesla for a total period of 19 h.

Table 2. Hemolytic activity of free FeO NPs, Cuphen liposomes and Cuphen liposomes co-loading FeO NPs. Tested concentrations ranged from 0.313 to 5 mg/mL and 3.125 to 200 uM for IONPs and Cuphen liposomes containing IONPs, respectively.

Formulation	Hemolytic activity in hRBC (%)
FeO NPs (2 mg/mL)	< 1
Cuphen Liposomes	< 4
Cuphen Magnetoliposomes	< 5

Conclusions

In conclusion, this lipid-based nanosystem loading the cytotoxic metallodrug, Cuphen, and displaying magnetic properties was successfully designed. As future strategies, in vivo tests can be conducted in an animal model to confirm whether the added targeting capabilities translate into an increase in treatment response.

Acknowledgments

Authors acknowledge the support by Fundação para a Ciência e Tecnologia (FCT) [projects PTDC/BTM-SAL/28977/2017, PTDC/MED-QUI/31721/2017, UIDB/04138/2020 and UIDP/04138/2020 and PhD fellowship SFRH/BD/117586/2016] and UI/BD/150754/2020.

References

1. Pinho, J.O.; Amaral, J.D.; Castro, R.E.; Rodrigues, C.M.P.; Casini, A.; Soveral, G.; Gaspar, M.M. Copper complex nanoformulations featuring highly promising therapeutic potential in murine melanoma models. *Nanomedicine* **2019**, *14*, 835–850, doi:10.2217/nnm-2018-0388.
2. Cruz, N.; Pinho, J.O.; Soveral, G.; Ascensão, L.; Matela, N.; Reis, C.; Gaspar, M.M. A novel hybrid nanosystem integrating cytotoxic and magnetic properties as a tool to potentiate melanoma therapy. *Nanomaterials* **2020**, *10*, doi:10.3390/nano10040693.

Abstracts for Poster Presentation

Session 4: Hydrogels and 3D Models for Drug Delivery Systems

P4.1: "*Carboxymethyl cellulose-based 3D scaffolds for wound healing* ". C. Alvarez-Lorenzo, L. Díaz-Gómez, I. González-Prada, R. Millán and A. Concheiro. Universidade de Santiago de Compostela. (p.175)

P4.2: " ***Gelatin hydrofilms with bioactive compounds Aloe vera and EGF for chronic wound healing applications*** ". I. Garcia-Orue, A. Etxabide, K. de la Caba, P. Guerrero, M. Igartua, E. Santos-Vizcaino, R. M. Hernandez. University of the Basque Country. (p.177)

P4.3: "***A novel sumecton enriched gelatin-based scaffold for bone regeneration***" I. Lukin, I. Erezuma, G. Orive. University of Basque Country. (p.179)

P4.4: "***Extracellular vesicle-loaded hydrogel for stimulating cardiac repair after myocardial infarction***" E. Garbayo, L. Saludas, P. Gil-Cabrerizo, G. Abizanda, F. Prosper, M.J Blanco-Prieto. University of Navarra. E. Garbayo, L. Saludas, P. Gil-Cabrerizo, G. Abizanda, F. Prosper, M.J Blanco-Prieto. University of Navarra. (p.181)

P4.5: "***Novel injectable thermosensitive hydrogel containing chitosan-dextran sulphate nanoparticles for antigen delivery***" E. Giuliano, S. Anthiya, C. Alvarez-Lorenzo, D. Cosco and M.J. Alonso. University of Santiago de Compostela. (p.183)

P4.6: "***Functionalized hyaluronic acid-based hydrogel for ophthalmic application. Preliminary studies***" A. Aragón-Navas, M. Johnson, Sigen A, I. Bravo-Osuna, V. Andrés-Guerrero, H. Tai, W. Wang, R. Herrero-Vanrell. Complutense University of Madrid. (p.185)

P4.7: "***Mucoadhesive nanoparticles for ocular delivery of ketorolac***" M. Oliva, F. Andrade, D. González, and D. Rafael. Universitat de Barcelona. (p.187)

P4.8: "***Licensing hydrogels maintain the immunomodulatory phenotype of human mesenchymal stromal cells in a murine colitis model***" A. Gonzalez-Pujana, A. Beloqui, J.J. Aguirre, M. Igartua, E. Santos-Vizcaino, R.M. Hernandez. University of the Basque Country. (p.189)

P4.1: Carboxymethyl cellulose-based 3D scaffolds for wound healing

C. Alvarez-Lorenzo[1]*, L. Díaz-Gómez[1], I. González-Prada[1], R. Millán[2] and A. Concheiro[2]

[1]*Departamento de Farmacología, Farmacia y Tecnología Farmacéutica, I+D Farma (GI-1645), Facultad de Farmacia and Health Research Institute of Santiago de Compostela (IDIS), Universidade de Santiago de Compostela, 15782-Santiago de Compostela, Spain*
[2]CEBEGA, Universidade de Santiago de Compostela, 15782 Santiago de Compostela, Spain

*e-mail: carmen.alvarez.lorenzo@usc.es

Introducction

Cellulose ethers have been reported as useful components of wound dressings due to their matrix-forming ability, cell compatibility, cross-linking versatility and exudate sorption capability. With the advent of 3D printing the interest in using polymers from natural, sustainable sources is increasing. Cellulose ethers can become green alternatives to the use of synthetic polymers in the preparation of scaffolds. Nevertheless, cellulose ethers, in particular carboxymethyl cellulose (CMC), have been considered to provide insufficient mechanical stability to printed structures. Therefore, so far CMC has been used in mixtures with diverse additives [1]. This shortcoming of CMC could be explained by the fact of that it has been used as low concentration dispersions.

In addition to the structure-forming capability, CMC has been suggested to act on specific cellular pathways. Cells may recognize the glucopyranose units of CMC through glucose receptors (GluT-1 receptor). Such a recognition may induce the chemotactic migration of a variety of cells and to facilitate cell movement in response to soluble factors [2].

The aim of this work was to elucidate whether inks made of CMC at sufficiently high concentration may provide 3D scaffolds for wound healing with the multi-fold functionalities of adequate exudate uptake, increased cell mobility for faster healing, and transparency for tissue monitoring. Porous scaffolds were prepared from steam-heat sterilized CMC dispersions applying semi-solid extrusion. Citric acid was chosen as a safe cross-linker to modulate the integrity of the scaffold. Some scaffolds were loaded with platelet rich plasma (PRP). Then, all scaffolds were characterized regarding mechanical properties, controlled release of growth factors, *in ovo* angiogenesis, cell migration, and *in vivo* wound healing properties using a diabetic rat wound defect model.

Materials and Methods

Materials

CMC (395 kDa, degree of substitution 0.9) from Ashland (Blanose® 9M31F PH; Wilmington, DE, USA); citric acid 1-hydrate (CA) from Panreac (Barcelona, Spain); DMEM, MEMα, fetal bovine serum (FBS), penicillin/streptomycin 100x solution, TryplE®, and phosphate buffer saline (PBS) from ThermoFisher Sci (Waltham, MA, USA); streptozotocin from Sigma-Aldrich (St. Louis, MO, USA); cell counting Kit-8 (CCK-8) from Dojindo (Kumamoto, Japan). Adipose-derived mesenchymal stem cells (MSCs; ATCC-PCS-500-011) were from the American Type Culture Collection (Manassas, VA, USA).

Scaffolds preparation

15% CMC dispersions were autoclaved and mixed with CA (20% w/wCMC). Self-healing properties were assessed by recording G' and G'' under cyclic shear strain in a MCR 302 rheometer [3]. The inks were extruded through a 22G conical needle at 2 mm/s feeding rate and 5 mm/s deposition speed. Scaffolds were printed as a cylinder (10 mm in diameter, 2 mm height, 1.2 mm on-center spacing) with a 90º crosshatch pattern using a Bio V1 3D printer (Regemat3D; Granada, Spain). The scaffolds were freeze-dried and then cured at 120 ºC for 7 min. Some CMC scaffolds were incubated with 1.5 mL of activated PRP for 2 h at 22 ºC.

Scaffolds characterization

Swelling was recorded as increase in weight after immersion in various solvents. Mechanical properties were recorded at crosshead speed of 1 mm/s and an activation force of 0.1 g using a TA.XTplus Texture Analyzer (Stable Micro Systems; Surrey, UK). Total protein (BCA Protein Assay Kit), TGF-β1 and VEGF (ELISA kits) release rates were monitored by placing the scaffolds in NaCl 0.9 %w/v at 37 ºC (n=5).

Cell infiltration and neo-vascularization in the scaffolds were evaluated in the chorioallantoic membrane (CAM) of fertilized eggs [4]. A scratch assay was carried out with MSCs incubated with scaffolds release medium (24 h).

In vivo procedures were approved by the University of Santiago de Compostela Bioethics Committee for Animal Studies (protocol No. 15007/16/001). Diabetes was induced in male Sprague Dawley rats using intraperitoneal injections of streptozotocin. At week 6, animals were anesthetized and four symmetrical, full-thickness wounds of 8 mm in diameter were created on the back of each animal. The wounds were randomly divided into 3 treatment groups: untreated controls, CMC scaffolds and CMC-PRP scaffolds. Wounds were monitored dialy and histopathological (hematoxylin and eosin staining) and immunohistochemical (CD31 and PCNA) analysis were done at various time points.

Results and Discussion

CMC (15 %w/v)-CA inks showed excellent self-healing rheological properties and stability during storage, and rendered 3D scaffolds with high design fidelity (Fig. 1).

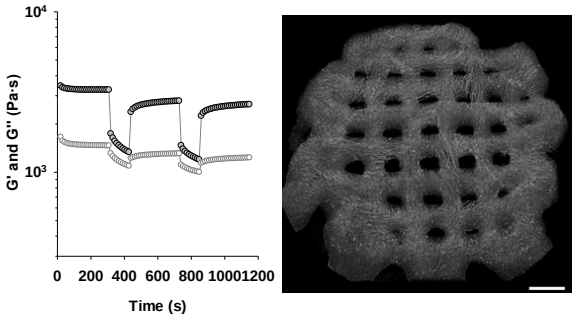

Fig 1. Rheological properties (G', black, and G'', grey symbols) of the CMC ink under cyclic changes in shear strain (0.5-100 %), and micro-CT images of the spongy scaffold.

CMC scaffolds sustained growth factors release for 3 days. At day 7, the scaffolds were completely disintegrated in the NaCl 0.9% medium.

The scaffolds showed excellent compatibility with CAM and facilitated neovascularization. Regarding the scratch assay, CMC and CMC-PRP release media reduced the gap significantly faster than the negative control.

At all time point, wounds treated with CMC and CMC-PRP scaffolds showed higher wound closure rate than the control group (Fig. 2).

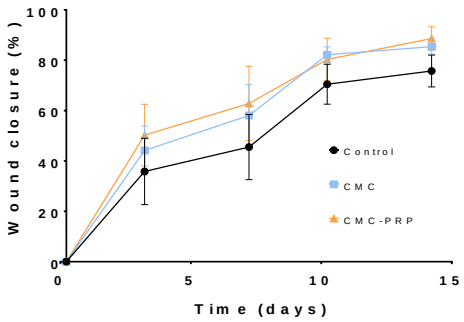

Fig 2. Contraction of wounds expressed as percent of initial area after 3, 7, 10 and 14 days since wound infliction.

Conclusions

Printable CMC inks can be prepared using 15 %w/v CMC dispersions with citric acid without other components. CMC scaffolds facilitated angiogenesis *in ovo* and favored MSCs migration *in vitro*; these performances being reinforced when the scaffolds contained PRP. In the diabetic wound model, a single application of the CMC scaffold promoted efficient dermis and epidermis healing facilitating wound contraction.

Acknowledgments

This work was supported by MCIN/ AEI/10.13039/501100011033 [PID2020-113881RB-I00], FEDER, and Xunta de Galicia [ED431C 2020/17, ED481D-2021-014].

References

[1] A. Zennifer, P. Senthilvelan, S. Sethuraman, D. Sundaramurthi, Key advances of carboxymethyl cellulose in tissue engineering and 3D bioprinting applications. Carbohydr. Polym. 256 (2021) 11756.

[2] Q. Garrett, P.A. Simmons, S. Xu, J. Vehige, Z. Zhao, K. Ehrmann, M. Willcox, Carboxymethylcellulose binds to human corneal epithelial cells and is a modulator of corneal epithelial wound healing. Invest. Opthalmol. Vis. Sci. 48 (2007) 1559.

[3] J. Conceição, X. Farto-Vaamonde, A. Goyanes, O. Adeoye, A. Concheiro, H. Cabral-Marques, J.M. Sousa Lobo, C. Alvarez-Lorenzo, Hydroxypropyl-β-cyclodextrin-based fast dissolving carbamazepine printlets prepared by semisolid extrusion 3D printing. Carbohydr. Polym. 221 (2019) 55.

[4] L. Diaz-Gomez, C. Alvarez-Lorenzo, A. Concheiro, M. Silva, F. Dominguez, F.A. Sheikh, T. Cantu, R. Desai, V.L. Garcia, J. Macossay, Biodegradable electrospun nanofibers coated with platelet-rich plasma for cell adhesion and proliferation. Mater. Sci. Eng. C 40 (2014) 180.

P4.2: Gelatin hydrofilms with bioactive compounds Aloe vera and EGF for chronic wound healing applications

I. Garcia-Orue[1,2,3], A Etxabide[4], K. de la Caba[4,5], P. Guerrero[4,5,6], M. Igartua[1,2,3], E. Santos-Vizcaino[1,2,3], R. M. Hernandez[1,2,3]

1NanoBioCel Research Group, Laboratory of Pharmaceutics, School of Pharmacy, University of the Basque Country (UPV-EHU), Vitoria-Gasteiz, Spain.
2 Biomedical Research Networking Centre in Bioengineering, Biomaterials and Nanomedicine (CIBER-BBN). Institute of Health Carlos III, Madrid, Spain.
3 Bioaraba, NanoBioCel Research Group, Vitoria-Gasteiz, Spain.
4 BIOMAT Research Group, University of the Basque Country (UPV/EHU), Escuela de Ingeniería de Gipuzkoa, Plaza de Europa 1, 20018 Donostia-San Sebastián, Spain.
5 BCMaterials, Basque Center for Materials, Applications and Nanostructures, UPV/EHU Science Park, 48940, Leioa, Spain.
6 Proteinmat materials SL, Avenida de Tolosa 72, 20018 Donostia-San Sebastian, Spain.

*e-mail: itxaso.garcia@ehu.eus

Introduction

Chronic wounds are wounds that fail to progress in the healing process, remaining open for long periods and worsening the patients' life quality. Chronic wounds are becoming a silent epidemic due to the rise of factors related to their onset, such as diabetes and obesity. In that regard, the aim of the current study was to develop a gelatin hydrofilm containing Aloe vera and EGF, since the extract of Aloe vera presents proliferative and anti-inflammatory properties [1] and EGF is a key molecule of wound healing [2].

Materials and Methods

2.1 Hydrofilm preparation

We prepared two different hydrofilms by solution casting. GA hydrofilm contained pork gelatin, agar, aloe vera powder, citric acid, and glycerol. G hydrofilm, which was used as a control, contained the same components except aloe vera powder. In addition, we prepared GAE hydrofilm, which contained EGF, pouring an EGF aqueous solution onto the GA hydrofilm.

2.2 Hydrofilm characterization

We characterized GA and G hdyrofilms in terms of swelling in PBS at 24 h; degradation in PBS at 48 h, water vapor transmission rate (WVTR) and mechacnical properties using tension-deformation tests. In addition, we analyzed the release profile of EGF from GAE hydrofilms using an EGF ELISA assay kit.

2.2. Hydrofilm biocompatibility

We assessed direct and indirect hydrofilm biocompatibility incubating Humand Dermal Fibroblasts (HDF cell line) directly with the hydrofilms or with their conditioned medium, and determining cell viability using a CCK8 colorimetric assay. Positive control was culture medium with 10 % (v/v) of DMSO, and the negative control fresh culture medium.

2.4. *In vitro* wound healing

We seeded HDF cells in culture inserts of 2-wells (Ibidi, Germany) and we incubated them to form a monolayer. Then, we removed culture inserts and added the hydrofilms to the cells. The closure of the gap was photographed using an inverted microscope at selected time points.

2.5 Anti-inflammatory activity

We seeded THP-1 human monocytes on 96 well culture plates and we differentiate them into macrophages with phorbol-miristate. Then, we added hydrofilm's conditioned medium and 100 ng/ml of lipopolysaccharide (LPS). As negative control, culture medium was used, and as positive control, culture medium with 100 ng/ml of LPS.24 later, we measured the levels of TNF-α and IL-8 in cell supernatants through an ELISA assay. Moreover, we conducted a CCK8 colorimetric assay to assess cell's viability.

Results and Discussion

Regarding the swelling ability of the hydrofilms, GA hydrofilms were able to absorb 883 ± 36 % of their dry weight and G hydrofilms 930 ± 67 %, showing no differences between them.

The degradation of GA and G hydrofilms reached similar values at 28 days: 28 ± 8 % and 24 ± 2 % of remaining weight, respectively. Nevertheless, their degradation profile was quite different, GA hydrofilms presented a quick degradation in the first 8 h, reaching a remaining weight of 37 ± 4 %, while the value for G hydrofilms was 61 ± 3 % at the same time point.

The hydrofilms presented the forllowing WVTR values, 1522± 55 g/m^{2}day for GA hydrofilms and 1479 ± 38 g/m^{2}day for GAE hydrofilms. Results obtained in the tension-deformation studies are summarized in table 1.

Table 1. Results obtained in tension-deformation studies. Being Mod. the moduli, Ten. the tension at breakage and def. the deformation at breakage.

Name	Mod. (MPa)	Ten. (MPa)	Def. (%)
GA	198.1 ± 16.2	27,7 ± 2	45,3 ± 4.4
GAE	361 ± 7.9	31.1 ± 2.1	36 ± 4.2

The release of EGF from GAE hydrofilms, showed a biphasic profile, with a fast release that achieved an 81 ± 3 % EGF release in the first 4 h, and a slower phase that achieved a total release in 48 h.

Viability studies revealed that the hydrofilms were biocompatible, since all of them showed a viability above 70 %, regarding to the negative control group.

We studied the wound healing effects of the hydrofilms using an *in vitro* wound closure assay (Fig. 1). Results showed that both GA and GAE hydrofilms were able to significantly promote wound closure in comparison to the untreated group. In addition, G hydrofilms did not show any differences with the control group, highlighting that the effect observed with GA and GAE was due to the Aloe vera and EGF present in the hydrofilms.

In addition, there were statiscally significant differences among G hydrofilms and GAE or GA hydrofilms at some time points. However, we did not found differences between GAE and GA hydrofilms.

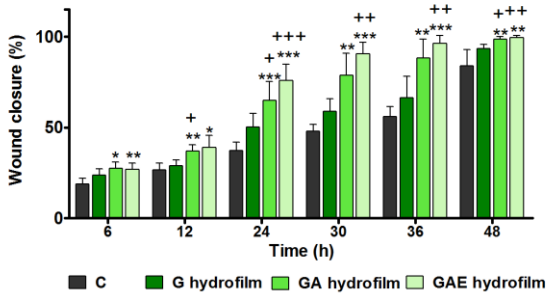

Fig 1. *In vitro* wound healing assay. Results show the percentage of wound closure in regard to the initial gap size at different time points. *, ** and *** represent p<0.5, p< 0.01 and p< 0.001 in comparison to control and +, ++ and +++ represent p<0.5, p< 0.01 and p< 0.001 in comparison to G hydrofilm.

Finally, we analized the anti-inflammatory effect of hydrofilms. Macrophages were incubated with the hydrofilm's conditioned medium and LPS, in order to determine if the conditioned medium was able to reduce the activation of macrophages due to LPS, and thus reduce the secretion of inflammatory mediators, such as IL-8 and TNF-α to the medium.

The results showed that all the formulations were able to reduce the inflammation caused by LPS, since the cytokine levels were significantly lower in the groups treated wth the hydrofilms (Fig. 2). It is noteworthy that there were no differences among the hydrofilms, indicating that the anti-inflammatory effect was not only exerted by the Aloe vera. Indeed, among the components of G hydrofilms, citric acid has been reported to present anti-inflammatory properties [3].

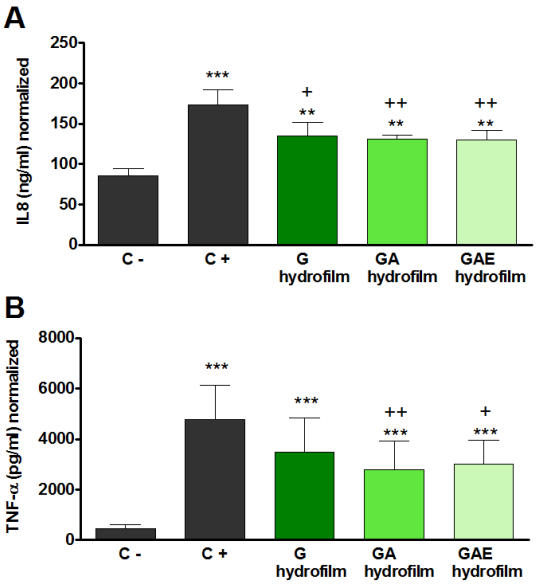

Fig 2. Anti-inflammatory assay. Results are expressed normalized by the viability of each group obtained in the CCK8 assay. (A) IL-8 secretion by each group. (B) TNF- α secretion by each group. ** and *** represent p< 0.01 and p< 0.001 in comparison to control negative and + and ++ represent p<0.5, and p< 0.01 in comparison to positive control.

Conclusions

The developed GAE and GA hydrofilms presented suitable characteristics for wound healing, with a proliferative and anti-inflammatory effect proven *in vitro.*

Acknowledgments

This work was supported by the dokberri grant conceded to I. Garcia-Orue by the UVP/EHU.

References

[1] E. Teplicki, Q. Ma, D.E. Castillo, M. Zarei, A.P. Hustad, J. Chen, et al., The Effects of Aloe vera on Wound Healing in Cell Proliferation, Migration, and Viability, Wounds. 30 (2018) 263-268.

[2] I. Garcia-Orue, J.L. Pedraz, R.M. Hernandez, M. Igartua, Nanotechnology-based delivery systems to release growth factors and other endogenous molecules for chronic wound healing, J. Drug Deliv. Sci. Technol. 42 (2017) 2-17.

[3] H.Y. Jeong, Y.S. Choi, J.K. Lee, B.J. Lee, W.K. Kim, H. Kang, Anti-Inflammatory Activity of Citric Acid-Treated Wheat Germ Extract in Lipopolysaccharide-Stimulated Macrophages, Nutrients. 9 (2017)

P4.3: A novel sumecton enriched gelatin-based scaffold for bone regeneration

I. Lukin[1;2*], I. Erezuma[1;2] and G. Orive[1;2]

[1]NanoBioCel Group, Laboratory of Pharmaceutics, School of Pharmacy, University of the Basque Country (UPV/EHU), Paseo de la Universidad 7, Vitoria-Gasteiz 01006, Spain.
[2]Bioaraba, NanoBioCel Research Group, Vitoria-Gasteiz 01009, Spain.

*e-mail: izeia.lukin@ehu.eus

Introduction

In the field of tissue engineering gelatin has emerged as a potential biomaterial to deal with the constant rise of bone fracture, which, indeed, has already been declared as an economic burden [1]. Although its biodegradability, biocompatibility and low toxicity make this biomaterial suitable for bone repair, its lack of mechanical stability makes a constant seek for blending with other materials capable of providing good mechanical properties [2]. In this line, there is a current trend of exploring nanoclays as an approach to improve mechanical stability. The multilayered sheets of nanoclays have demonstrated to generate multiple interactions with biologically active agents. In addition, these inorganic nanoparticles provide mechanical strength which turns out to better mimic bone tissue [3,4,5]. The aim of this work is to develop a novel nanoclay (sumecton) enriched gelatin scaffold for stimulating bone regeneration. Scaffolds were assessed in terms of microscopy, mechanical analysis and ability to absorb protein.

Materials and Methods

Enzymatically crosslinked gelatin-based three-dimensional (3D) scaffolds were prepared by freeze drying technique. Dissolved gelatin was reinforced with sumecton nanoclay, in different concentration: 0, 0.5, 1, 2% (w/v), sumecton content respectively (SUM0, SUM0.5, SUM1, SUM2), and freeze-dried.

Liophilized scaffolds were subjected to scanning electron microscopy along with mechanical tests and protein adsorption evaluation.

Results and Discussion

Different prototypes of scaffolds were enzymatically crosslinked as previously described by MC Echave et al [7]. Enzymatic crosslinking allows covalent binding of gelatin aminoacid sequences, and together with nanoreinforcement, results in stable hydrogels as for mechanical properties and thermosensibility [6,7].

Pore size plays a key role for cell nutrient diffusion; hence, regulating them is of paramount importance. SEM images showed that nanoclay addition diminished pore size. The latter is in consonance with previous studies that demonstrated that nanoclay addition is responsible for higher fiber arrangement and decrease pore size (Fig 1) [3,6].

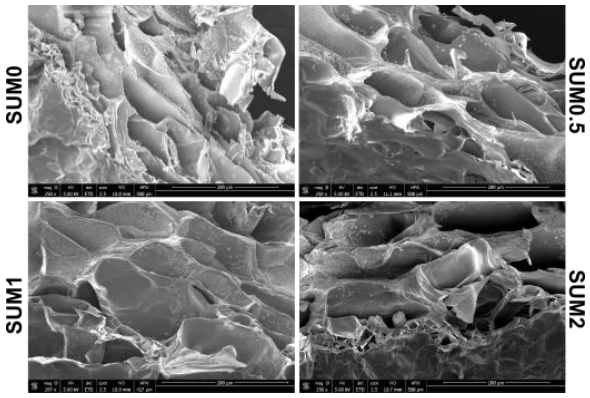

Fig 1. Scanning electron microscopy images. 0, 0.5, 1, 2% (w/v) sumecton-enriched dual gelatin scaffolds, respectively, scale bar = 200 µm.

The compressive stress-strain diagraman illustrated a higher total dissipated energy when the nanomaterial is incorporated into the scaffolds (Fig 2a). This phenomenon, in turn, leads to an upward tendency in terms of toughness, elastic modulus and ultimate stress. Data corresponding to SUM2 shows a statistically significant increase in the latter mentioned parameters, in fact, SUM2 values are three-fold higher in comparison to SUM0 (Fig 2b-d). The addition of these nanoparticles is attributed to be responsible for mechanical stability. Albeit the increase in mechanical parameters, all scaffolds remained in the scope of 25-60 kPa in terms of elatic modulus, which indicates that all prototypes developed are stiff enough to promote new bone formation [6,7,8].

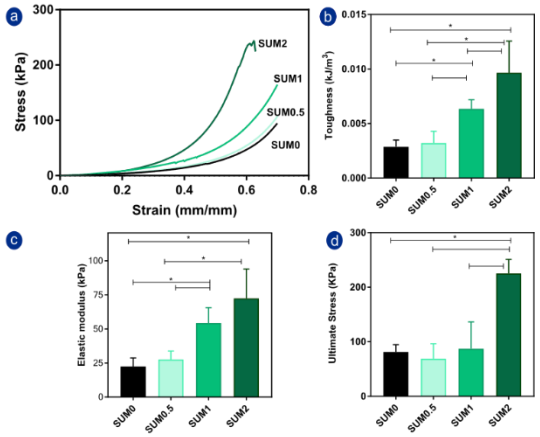

Fig 2. Biomechanical assessment. A) Stress-strain curve corresponding to the mechanical compression test. B-D) Data obtained from stress-strain curve: toughness, mechanical elasticity and ultimate stress respectively for each type of scaffold: 0, 0.5, 1, 2% (w/v), SUM0, SUM0.5, SUM1, SUM2. Differences were considered significant at *p < 0.05.

Nanoreinforcement modifies hydrogels' surface which may result in higher surface area and higher ability to absorb proteins, which leads to higher cell-adhesion and proliferation rates [9]. Protein adsorption assessment illustrates the statistically significant increased ability of SUM2 to absorb protein; indeed, it was two-fold larger than SUM0 (Fig 3), which may reveal the ability of scaffolds to use as drug delivery systems.

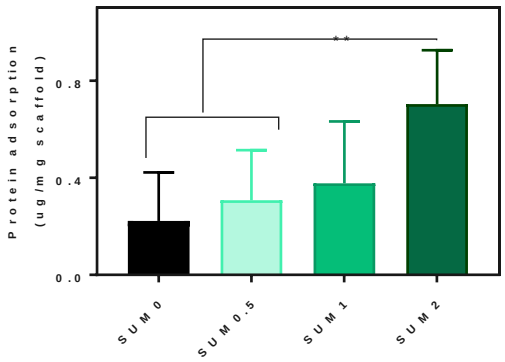

Fig 3. Protein adsorption ability of developed prototypes of scaffolds: SUM0, SUM0.5, SUM1, SUM2 (0, 0.5, 1, 2% (w/v) sumecton, respectively). Statistical significance between groups: **p < 0.01.

Conclusions

We have designed and developed mechanically stable sumecton-reinforced scaffolds. The latter showed adequate pore size to cell survival, as well as for delivery of biologically active agents. Therefore, we can conclude that these scaffolds might be suitable to undergo further tests as a means to be employed in tissue engineering.

Acknowledgments

This work was supported by the Spanish Ministry of Economy, Industry, and Competitiveness (PID2019- 106094RB- I00/AEI/10.13039/501100011033) and technical assistance from the ICTS NANBIOSIS (Drug Formulation Unit, U10) at the University of the Basque Country. We also appreciate the support from the Basque Country Government (Grupos Consolidados, No ref: IT907-16). I. Lukin and I. Erezuma would like to thank you the Basque Government for the Ph.D. grants (PRE_2020_2_0094 and PRE_2020_2_0042, respectively).

References

[1] A.M. Wu, *et al*. Global, regional, and national burden of bone fractures in 204 countries and territories, 1990–2019: a systematic analysis from the Global Burden of Disease Study 2019. *Lancet Healthy Longev*. 2 (2021) e580–592

[2] M. C. Echave, L. Saenz del Burgo, *et al.* Gelatin as Biomaterial for Tissue Engineering. *Curr. Pharm. Des.* 23 (2017) 3567–3584

[3] N. Khatoon, M.Q. Chu, C.H. Zhou, Nanoclay-based drug delivery systems and their therapeutic potentials. *J. Mater. Chem. B*. 8 (2020) 7335-7351

[4] S. G. Intasa-Ard, M. Ogawa, Layered Silicates as a Possible Drug Carrier. *Enzymes*. 44 (2018) 117–136

[5] J.I. Dawson, R.O.C. Oreffo, Clay: New Opportunities for Tissue Regeneration and Biomaterial Design. *Adv. Mater.* 25 (2013) 4069-4086

[6] M. Hasany, A. Thakur, *et al.* Combinatorial Screening of Nanoclay-Reinforced Hydrogels: A Glimpse of the "Holy Grail" in Orthopedic Stem Cell Therapy? *ACS Appl. Mater. Interfaces*. 10 (2018) 34924–34941

[7] M.C. Echave, C. Pimenta-Lopes, *et al*. Enzymatic crosslinked gelatin 3D scaffolds for bone tissue engineering. *Int. J. Pharm*. 562 (2019) 151–161

[8] A. Bharadwaz, A.C. Jayasuriya, Recent trends in the application of widely used natural and synthetic polymer nanocomposites in bone tissue regeneration. *Mater. Sci. Eng. C Mater. Biol. Appl*. 110 (2020) 110698

[9] A. Olad, H.B.K. Hagha, A. Mirmohsenia, F.F.Azhar. Graphene oxide and montmorillonite enriched natural polymeric scaffold for bone tissue engineering. *Ceram.* 45 (2019) 15609-15619

P4.4: Extracellular vesicle-loaded hydrogel for stimulating cardiac repair after myocardial infarction

E. Garbayo[1,2], L. Saludas[1,2], P. Gil-Cabrerizo[1], G. Abizanda[2,3], F. Prosper[2,3] and M.J Blanco-Prieto[1,2]*

[1]*Department of Pharmaceutical Technology and Chemistry, University of Navarra, 31008, Pamplona, Spain*
[2]*Instituto de Investigación Sanitaria de Navarra (IdiSNA), 31008, Pamplona, Spain*
[3]*Area of Cell Therapy, Clinic University of Navarra, 31008, Pamplona, Spain*

*e-mail: mjblanco@unav.es

Introduction

Extracellular vesicles (EVs) are nanosized membrane bodies secreted by all types of cells that mediate cell-cell communication [1,2]. Since the discovery of the beneficial therapeutical effects of EVs, these agents have been attracting great interest as next-generation therapies for cardiac repair. At present, different strategies are being investigated to prolong EV exposure to target myocardium and achieve optimal therapeutic effects. One promising approach is through EV-loaded in hydrogels (HGs). In this sense, HGs have demonstrated outstanding properties for the controlled delivery of several therapeutics to the heart [3]. Therefore, this study aimed to develop a biocompatible and injectable HG with the potential to stimulate cardiac repair and effectively deliver EVs derived from adipose stem cells (ADSCs) after myocardial infarction.

Materials and Methods

ADSC culture. ADSCs were cultured in α-MEM supplement with 10% of FBS, 1% of penicillin/streptomycin and 1 ng/mL of bFGF

EV isolation, fluorescent labelling and characterization. At 24 and 48h, conditioned medium was harvested and EVs were isolated by size-exclusion chromatography (SEC) using a qEV 10/35 mm column (Izon). For biodistribution studies, EVs were fluorescently labelled with DiR according to the manufacturer's instructions. Particle number and size distribution were measured by nanoparticle tracking analysis (NTA) using a Nanosight NS300 (Malvern Panalytical) with a camera level set at 13 and a detection threshold at 5.

HG preparation and characterization. A novel alginate-collagen HG consisting of 1% alginate and 1 mg/ml collagen crosslinked with 0.25% calcium gluconate was developed for the sustained local delivery of EVs to the ischemic heart. The injectability of the prepared alginate-collagen HG was assessed by their ability to flow through 25, 27 and 29-gauge needles, which are compatible with catheter-based intramyocardial delivery. Rheological experiments were performed to determine initial gelation kinetics and complex viscosity using a Discovery HR-2 hybrid rheometer (TA Instruments) with a parallel plate (40 mm diameter, 0º) set at the oscillatory mode.

HG retention in the heart Cardiac retention of the HG was analysed in infarcted rats. Myocardial infarction was induced by permanent occlusion of the left anterior descending coronary artery. 4 days later the HG was injected into the myocardium, where it was expected to undergo liquid-to-gel transition. At 2h, 7d, 1, 1.5 and 2 months post-administration animals were sacrificed and HG retention was analysed by immunohistochemistry.

EV release kinetics. For the *in vivo* biodistribution of EVs, DiR-labelled EVs were used. Treatments (EVs and HG-loaded EVs) were locally administered in 4 regions of the peri-infarcted myocardium 4 days after myocardial infarction. Animals were sacrificed 1-week post-injection to analyze EVs biodistribution by imaging the heart, kidneys, liver, spleen and lung.

Results and Discussion.

The size and the total number of particles isolated from the conditioned media of ADSCs by SEC were measured by NTA. We obtained a total number of 1.47×10^{11} particles with a mean particle size of 121.4 nm ± 59.6 nm.

Although the developed HG was designed to acquire its final mechanical properties *in situ* after heart delivery, rheological experiments were performed to determine initial gelation kinetics and complex viscosity. A few seconds after calcium gluconate incorporation in the alginate/collagen solution (< 10 sec, before measurement started), HG acquired an internal organized structure (G´ > G´´) indicating the crosslinking of the structure. Over time, storage modulus (G´) progressively increased but after 40

mins at 37ºC, it remained at a very low range (< 15 Pa). At the same time, G´´ was maintained constant (≈ 1 Pa) and tan delta decreased (< 0.1). This agrees with complex viscosity values, which barely exceeded 1.0 Pa·s after 5 mins at 22ºC.

Then, the injectability of the HG through 25, 27 and 29-gauge needles was analyzed. A tight adjustment of HG composition and calcium gluconate concentration allowed us to develop HGs that remained injectable for several hours. 1% alginate, 0.5 mg/ml collagen and 0.25% calcium gluconate HG, as well as 1% alginate, 0.75 mg/ml collagen and 0.20% calcium gluconate HG, proved their injectability with all tested needles. Alginate concentrations larger than 1% led to injectability difficulties, while an increase in collagen required a decrease in the crosslinking agent to assure injectability. On the other hand, 1% alginate, 0.5 mg/ml collagen and 0.3% calcium gluconate HG was only partially injectable, indicating that a 0.3% final concentration of the gelation agent compromised HG injectability. Therefore, an HG formulation consisting of 1% alginate and 0.5 mg/ml collagen pre-crosslinked with 0.25% calcium gluconate was selected for further studies.

Next, HG retention in the infarcted myocardium was investigated. We found that the HG was easily injected *in vivo*. The biomaterial undergoes liquid-to-gel transition upon administration in the infarcted myocardium, allowing gelation after administration. Immunohistochemistry studies reveal that the HG remained in the ischemic area for at least 2 months after administration (Fig 1).

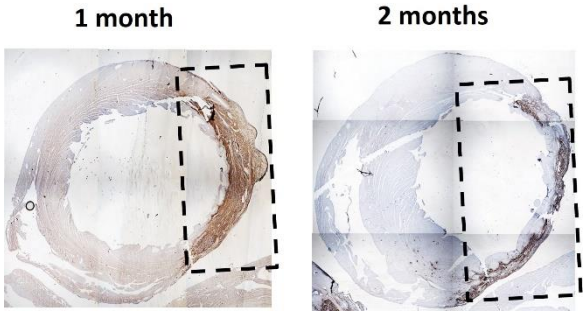

***Fig 1*. HG retention in the infarcted myocardium.** Cardiac retention of alginate-collagen HG (brown) in the infarcted area of rats after 1 and 2 months.

Finally, the biodistribution of the DiR-labelled EVs was *in vivo* investigated (Fig. 2). For a detailed examination of EV accumulation, different organs were harvested and subjected to *ex-vivo* imaging. The novel HG was able to release EVs in the infarcted myocardium in a sustained manner for at least 1 week prolonging the bioavailability of EVs in the target heart. No fluorescent signal was found in the liver or spleen. On the contrary, when EVs were free administered they accumulate in the liver and spleen. Current investigations are focused on evaluating the potential of the HG for EV sustained release and the therapeutic efficacy of the strategy.

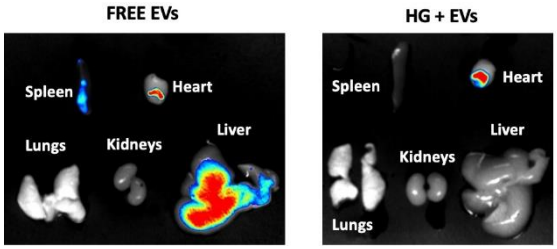

***Fig 2*. Biodistribution of DiR-labelled EVs.** Ex-vivo imaging of the harvested organs 7 days after treatment administration.

Conclusions

Here, we have developed a novel *in situ* forming HG constituted by alginate and collagen, two biocompatible materials with proven benefits for cardiac repair. Rheological properties as well as injectability studies suggested its easy intramyocardial administration using catheter-based technology. When *in vivo* administered, the biomaterial remained in the infarcted myocardium for at least 2 months. Upon intramyocardial injection, the HG release EVs in the heart in a sustained manner for at least 1 week, enhancing local EV retention *in vivo*. Together, these data contribute to establishing the basis for the combined use of EVs and HGs as therapeutic platforms, in particular in regenerative fields.

Acknowledgements

This work was supported by the Spanish Ministry of Economy and Competitiveness (SAF2017-83734-R). E.Garbayo is supported by a FSE/Ministry of Science and innovation-State Research Agency/ RYC2018-025897-I. L. Saludas thanks the “Asociación de Amigos de la Universidad de Navarra” and “La Caixa” banking foundation.

References

[1] L. Saludas, C.C. Oliveira, *et al*. Extracellular vesicle-based therapeutics for heart repair, *Nanomaterials* 11 (2021) 570

[2] S.G. Ong and J.C. Wu. Exosomes as potential alternatives to stem cell therapy in mediating cardiac regeneration, *Circ. Res.* 117 (2015) 7-9

[3] L. Saludas, S. Pascual-Gil, *et al*., Hydrogel-based approaches for cardiac tissue engineering, *Int. J. Pharm*. 523 (2017) 454–475

P4.5: Novel injectable thermosensitive hydrogel containing chitosan-dextran sulphate nanoparticles for antigen delivery

E. Giuliano[1]*, S. Anthiya[2], C. Alvarez-Lorenzo[3], D. Cosco[1] and M.J. Alonso[2;3]

[1]*Department of Health Sciences, University "Magna Græcia" of Catanzaro, I-88100 Catanzaro, Italy*
[2]*Center for Research in Molecular Medicine and Chronic Diseases (CiMUS), University of Santiago de Compostela, 15782 Santiago de Compostela, Spain*
[3]*Department of Pharmacy and Pharmaceutical Technology, University of Santiago de Compostela, 15782 Santiago de Compostela, Spain*

*e-mail: elena.giuliano@unicz.it

Introduction

Vaccines are the most cost-effective life-saving medications in history leading to the prevention of severe infectious diseases, and even in the eradication of some of them [1]. To elicit a durable and protective antibody response, vaccines must interact with the immune cells at the appropriate time and place. Various engineered nanocarriers (NCs) with different physicochemical characteristics and properties have been proposed as either delivery systems to enhance antigen presentation and/or as adjuvant to stimulate the immune response.

Chitosan (CS) is one of the most studied natural polymers in drug delivery because of its biocompatibility, biodegradability, low toxicity, and mucoadhesive properties. Our group has originally reported the feasibility of chitosan (CS)-based nanosystems to generate humoral responses against different antigens [1,2].

In the last decades, the association of different pharmaceutical technologies favoured the development of innovative formulations able to improve the therapeutic efficacy of various drugs. In particular, NCs-embedded hydrogels have shown promising preclinical results for medical applications and for the treatment of a large number of diseases [3].

In situ forming hydrogels can be easily administered in liquid form and undergo gelation in the body, allowing a prolonged and sustained drug release, reducing the frequency of the administrations, and improving the patient compliance [3]. We recently demonstrated the potential application of poloxamine 908 (P908)-based hydrogels as suitable delivery system for vaccination purposes [4]. Poloxamines are X-shaped amphiphilic block copolymers made up of an ethylenediamine central portion linked to four chains of polyoxypropylene-polyoxyethylene. This structure is characterized by peculiar thermo-responsive properties due to the capacity to self-assemble into micelles in aqueous solutions [4].

Taking all this into consideration, the aim of the proposed work was to combine the advantages of P908-based hydrogels and CS nanoparticles to design a novel multifunctional formulation. To evaluate the potential of the proposed nanocomposite-hydrogel for antigen delivery, ovalbumin (OVA), the most widely used protein for vaccine studies, was selected as a model compound.

Materials and Methods

Chitosan (CS) (hydrochloride salt, molecular weight (MW) 42.7 KDa and 88% deacetylation degree) was obtained from HMC+ (Halle, Germany). Dextran sulfate (DS), (sodium salt, MW 8 KDa) and ovalbumin (OVA, Grade V) were purchased from Sigma-Aldrich (St. Louis, USA). Poloxamine 908 (trademark Synperonic™ T/908) was a gift from Croda Italiana S.p.A (Pavia, Italy), and used without further purification.

OVA-loaded CS/DS NPs and nanocomposite hydrogels were prepared by ionic complexation [2] and the "cold method" [3], respectively. Mean sizes, size distribution and surface charges of the NPs were evaluated using photon correlation spectroscopy and laser Doppler anemometry (Zetasizer NanoZS®, Malvern Instruments; Malvern, UK).

The association efficiency of the model antigen was determined after isolation of NPs by ultracentrifugation (Optima L-90K Ultracentrifuge, Beckman Coulter, Brea, USA), and the amount of free OVA in the supernatant was determined using a microBCA™ Protein Assay Kit (Thermo Fisher Scientific, Massachusetts, USA).

Rheological analyses were performed using a Rheolyst AR-1000N rheomether equipped with an AR2500 data analyzer (TA Instruments, Newcaste, UK). *In vitro* dissolution profiles and *in vitro* release of OVA from thermosensitve hydrogels were studied at 37 °C in phosphate buffer solution (10 mM) using a membrane-less method [4]. The injectability/ syringeability of P908 nanocomposite hydrogels was investigated at room temperature. The proposed formulations

were loaded in liquid form into a syringe with a 25G needle and a 0.5 mm inner tube, then injected into a PBS solution pre-heated to 37 °C.

Results and Discussion

In this work, we selected chitosan and dextran sulphate as biomaterials for the development of the NPs designed to be included in the thermosensitive P908-hydrogel. A specific advantage associated to the use of CS/DS-based nanocarriers is related to the simple and mild techniques used to produce them, which minimize the use of solvents and high-energy sources, and therefore suitable for the association of labile biomolecules such as peptides and proteins. Three different theoretical loadings of the model antigen were tested with respect to the total amount of polymers in the formulation (4, 8, and 16% w/w).

The resulting OVA-loaded CS/DS NPs exhibited adequate physicochemical properties (~ 180 ±5 nm; PDI < 0.2), positive zeta-potential (+ 25.0 ± 0.7 mV), and an association efficiency close to 40% for the highest OVA theretical loading.

The incorporation of the NPs within the copolymeric matrix did not significantly affect the viscoelastic properties of P908 hydrogels. The sol-gel transition was below the body temperature for all the investigated formulations. The shear viscosity profiles of the systems were very similar, showing a useful non-Newtonian shear thinning behavior at 37 °C, which makes the formulations easily injectable (Figure 1A).

The syringeability of the proposed P908 nanocomposite hydrogel was also confirmed by a specific test (Figure 1B), demonstrating that it is suitable for an *in vivo* administration.

Membrane-free dissolution tests were carried out to simulate the contact between the P908-based hydrogels and the physiological environment subsequent to administration in the body. The dissolution of the hydrogels occurred in a constant and rapid manner up to 12 h, and it was not influenced by the presence of OVA and/or CS/DS NPs.

In vitro drug release studies demonstrated a constant and sustained release of the protein from the thermosensitive carriers. The incorporation of CS/DS NPs slowed down the OVA release rate, showing the advantage of the nanocomposite carrier compared with the hydrogel alone. In fact, the sustained antigen release could facilitate an increased interaction time between immune-stimulators and immune system, and subsequently increasing the possibility of an effective immune response.

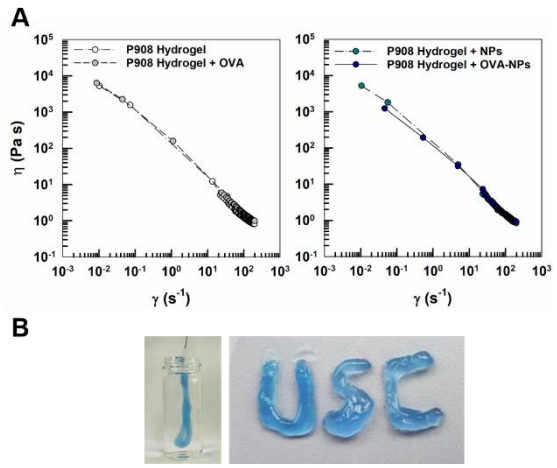

Fig 1. (A) Shear thinning behavior of P908 hydrogels at 37 °C. The inclusion of the nanoparticles (NPs) and/or ovalbumin (OVA) within the hydrogels did not affect the properties of the hydrogel. (B) Syringeability test of P908-based hydrogels (Bromphenol blue added for visualization).

Conclusions

Results demonstrate the potential application of P908-hydrogels containing CS/DS NPs as antigen delivery systems. The proposed formulations can be easily administered through a syringe needle in liquid form and undergo gelation in the body. The inclusion of the polymeric NPs allowed a prolonged protein release compared the hydrogel alone, which could improve the immune response of the antigens delivered. Further investigations are required in order to evaluate the real efficacy of the proposed formulation *in vivo*.

Acknowledgments

This work was supported by Competitive Reference Groups, Consellería de Educación e Ordenación Universitaria, Xunta de Galicia, Ref: ED431C 2021/17 and the Italian Ministry of University and Research (PRIN2017, prot. n. 20173ZECCM_003).

References

[1] A.S. Cordeiro, M.J. Alonso, M. de la Fuente, Nanoengineering of vaccines using natural polysaccharides, *Biotechnol. Adv.* 33 (2015) 1279–93

[2] T.G. Dacoba, L. Ruiz-Gatón, A. Benito, *et al.* Modulating the immune system through nanotechnology, *Drug Deliv. Transl. Res.* 10 (2020) 621-634

[3] E. Giuliano, D. Paolino, M. Fresta, *et al.* Mucosal Applications of Poloxamer 407-Based Hydrogels: An Overview, *Pharmaceutics* 10 (2018) 159

[4] E. Giuliano, M. Fresta, D. Cosco, Development and characterization of poloxamine 908-hydrogels for potential pharmaceutical applications, *J. Mol. Liq.* 337 (2021) 116588

P4.6: Functionalized hyaluronic acid-based hydrogel for ophthalmic application. Preliminary studies.

A. Aragón-Navas[1]*, M. Johnson[2], Sigen A[2], I. Bravo-Osuna[1], V. Andrés-Guerrero [1], H. Tai[3], W. Wang[2], R. Herrero-Vanrell[1].

[1]*Innovation, Therapy and Pharmaceutical Development in Ophthalmology (InnOftal) Research Group, UCM 920415, Department Pharmaceutics and Food Technology, School of Pharmacy, Complutense University of Madrid, 28040 Madrid, Spain.*
[2]*Charles Institute of Dermatology, School of Medicine, University College Dublin, Dublin 4, Ireland.*
[3]*Blafar Limited, NovaUCD, Belfield Innovation Park, Dublin 4, Ireland.*

*e-mail: albarago@ucm.es

Introduction

Hyaluronic acid (HA) is a natural ubiquitous polymer present in all vertebrates [1]. Among its remarkable properties, are biocompatibility, biodegradation and nonimmunogenity with wide potential applications for drug delivery [2].
In the ophthalmology field, HA has been used for diverse applications such as intravitreal injections, *in situ* forming hydrogels, artificial tears and eye drops, modified nanoparticles and tissue engineering [3].
Besides, it is possible to create tailored HA hydrogels that include functional groups. In addition, the interaction between these groups (covalent crosslinking) creates a matrix-like structure resulting in hydrogel formation [4, 5].
The aim of this work is the development of a crosslinked HA-functionalized hydrogel with suitable physicochemical properties for its application in drug delivery for diverse ophthalmic diseases. Also, preliminary studies of the addition of two anti-inflammatory drugs (dexamethasone and ketorolac) were performed.

Materials and Methods

1. *Hydrogels fabrication.*

Thiolated HA (HA-SH, 220 kDa) 20 % substitution degree and HA aldehyde (HA-CHO, 1000 kDa) with approximately a 20 % oxidation degree were dissolved in PBS (pH=7.4, isotonised with NaCl) at different concentrations. The crosslinked hydrogel was formed by mixing both solutions in a ratio of 1:1 at room temperature.

2. *Rheological properties analysis.*

Rheological properties were carried out by a Discovery HR-2 Rheometer (New Castle, DE, USA) at room temperature. The evolution of loss and storage modulus were evaluated at a constant frequency (1 Hz) and strain (1 %). For the oscillation strain steps, 2 cycles with low strain (1 %) for 1 minute and high strain (1000 %) other one minute were performed at a constant frequency (1 Hz).

3. *In vitro hydrogel degradation.*

Hydrogels were immersed in PBS or PBS containing 110 UI/mL of hyaluronidase. 200 µL of hydrogels were placed in a tube and 1 mL of the media were added. The tubes were placed in a shaker at 37 ºC and 100 rpm. At pre-set times, the PBS was removed, the remanent PBS was wiped off softly with a tissue and the tubes were weighed. The percentage of degradation was calculated by the deduction of the weight of the tube and hydrogel (Wht) and the initial weight of the tube (Wt) and dividing it to the weight of the hydrogel at time 0 (Wh) (Eq. 1):

$$\text{Degradation } (\%) = \frac{\text{Wht} - \text{Wt}}{\text{Wh}} \text{x } 100$$

Equation 1. Percentage of hydrogel degradation.

4. *Swelling studies.*

The swelling ratio was evaluated under the same conditions used in the *in vitro* degradation section. The swelling index was determined from the ratio between the final hydrogel weight and the initial hydrogel weight.

Results and Discussion

The functionalized-HA based hydrogels were formed by mixing both, HA-CHO and HA-SH solutions, in a ratio 1:1. Among the different concentrations tested, the chosen ones were 2 % of HA-CHO and 3 % of HA-SH, resulting in a pH between 6.4 and 6.7 with a viscous solution-soft gel formation in a few minutes (Table 1).

Table 1. Different HA concentrations tested.

HA-CHO (w/v) %	HA-SH (w/v) %	Aspect in 30 mins	pH
1.5	4	Gel	6.4
1.75	4	Gel	6.4
1.75	3	Gel	6.4
2	3	Gel	6.4-6.7
2	2	Liquid	6.4-6.7

Rheological tests were carried out to monitor the crosslinking process. The gelation process occurs fast with storage modulus (G') values above loss modulus (G'') ones due to the rapid interaction between the aldehyde groups of HA-CHO and thiol groups of HA-SH. The storage modulus continued increasing, reaching its maximum at 48 hours. The evolution with time could be explained by the interaction of the remaining free thiol groups between them. This reaction could be due to the oxidation of the thiol groups since the sulphur atom can be easily oxidized and form a disulphide bond (R-S-S-R).

The addition of anti-inflammatory drugs such as dexamethasone or ketorolac (each one at 0.25 %) did not affect the gel formation.

The self-healing capacity was assessed employing a 2-cycle of oscillation strain steps method in the blank hydrogel. The quick-change sol-to-gel indicates the suitability of this hydrogel to be administered through a needle since the gel can undergo from gel to a sol state when it is injected. When the shear force was removed, the gel was immediately restored (Fig 1).

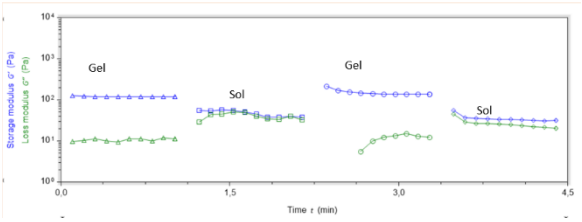

Fig 1. Self-healing capacity of the blank hydrogel.

The degradation studies compared the gel degradation only in PBS and in PBS with the addition of hyaluronidase (enzyme present in the posterior segment of the eye that cleaves this polymer). In presence of PBS the hydrogels degraded slowly, however, in the intraocular conditions, the hydrogel is completely degraded in 8 days (Fig 2).

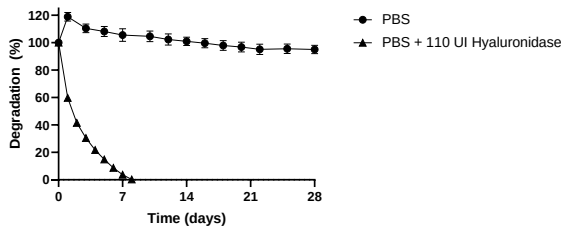

Fig 2. Degradation studies.

In the present work, the HA-based hydrogels achieved the maximum swelling ratio at 24 h (1.18 ± 0.05) decreasing this parameter slowly through time.

Conclusions

The functionalized HA hydrogel developed in this work presents good properties for its application in ophthalmic diseases in terms of pH, degradation and injectability. The addition of dexamethasone and ketorolac does not affect its gelation properties indicating good properties for drug loading.

Acknowledgements

MSCA-RISE-3DNEONET/734907.Research Group UCM 920415 (InnOftal). ISCII-FEDER RETICS (OFTARED) (RD16/0008/0009). MINECO (MAT2017-83858-C2-1 and PID2020-113281RB-C21). AAN thanks MICIU for her fellowship granted (PRE2018-083951).

References

[1] G. Abatangelo, V. Vindigni, G. Avruscio, L. Pandis, P. Brun, Hyaluronic Acid: Redefining Its Role, *Cells*. 9 (2020).

[2] J.A. Burdick, G.D. Prestwich, Hyaluronic Acid Hydrogels for Biomedical Applications, *Adv. Mater*. 23 (2011) H41-56.

[3] W.-H. Chang, P.-Y. Liu, M.-H. Lin, C.-J. Lu, H.-Y. Chou, C.-Y. Nian, Y.-T. Jiang, Y.-H.H. Hsu, Applications of Hyaluronic Acid in Ophthalmology and Contact Lenses, *Molecules*. 26 (2021).

[4] M.M. Pérez-Madrigal, J.E. Shaw, M.C. Arno, J.A. Hoyland, S.M. Richardson, A.P. Dove, Robust alginate/hyaluronic acid thiol–yne click-hydrogel scaffolds with superior mechanical performance and stability for load-bearing soft tissue engineering, *Biomater. Sci.* 8 (2019) 405–412.

[5] S A, J. Lyu, M. Johnson, J. Creagh-Flynn, D. Zhou, I Lara-Sáez,Q Xu, H Tai, W Wang. Instant Gelation System as Self-Healable and Printable 3D Cell Culture Bioink Based on Dynamic Covalent Chemistry. *ACS Appl Mater Interfaces*. 2020;12(35):38918-38924.

P4.7: Mucoadhesive nanoparticles for ocular delivery of ketorolac

M. Oliva[1,2,3]*, F. Andrade[1;4], D. González[1], and D. Rafael[3,4]

[1] Department of Pharmacy and Pharmaceutical Technology, and Physicochemistry, Faculty of Pharmacy and Food Sciences, Universitat de Barcelona (UB), 08028 Barcelona.
[2] Nanoprobes and Nanoswitches Group, Institute for Bioengineering of Catalonia (IBEC), 08028 Barcelona.
[3] Networking Research Centre for Bioengineering, Biomaterials, and Nanomedicine (CIBER-BBN), Instituto de Salud Carlos III, 28029, Madrid.
[4] Drug Delivery and Targeting Group, Vall d'Hebron Institut de Recerca (VHIR), Universitat Autònoma de Barcelona (UAB), 08035, Barcelona

*e-mail: mireia_oliva@ub.edu

Introduction

Ketorolac is a Non-Steroidal Anti-Inflammatory Drug (NSAID) commonly used in the treatment of ocular pain and inflammation diseases. Lately it has also been employed in the treatment of post—surgical pain and inflammation associated to cataract removal. However, currently available formulations generally have a short ocular residence time, requiring repeated daily administration.

A desired ophthalmic drug delivery system must be able to maintain the drug release and to remain in the proximity of the eye for a long time. For these reasons, much effort has been put in expanding nanotechnology-based DDS to improve ocular availability of drugs by increasing the pre-corneal residence time.

But formulation of ophthalmic pharmaceutical dosage forms is a complex, delicate process, since requirements to these medicines are very strict. Thus, eye drops should be non-irritable to the ocular mucosa, sterile, isosmotic (296 ± 9,8 mOsm/L), buffered to a pH around 7,4 (which is considered the normal physiological pH of tear fluid), and present particle diameters better than 250 nm (in order to avoid blurred vision). [1,2]

This work aims to develop ketorolac nanoparticles using lambda-carrageenan, a well-known hydrophilic biopolymer for controlled drug release, that is capable to self-assemble with Lewis basic drug in aqueous medium. [3]

Materials and Methods

Materials

Here we use ketorolac tromethamine salt (Merck Life Science) in order to increase water solubility and promote self-assembling with λ-carrageenan (Viscarin® PC 209, FMC Corp.). Moreover, poly-L-lisine (PLL) 0,1% aqueous solution (Sigma-Aldrich) was used to undergo ionotropic gelation. All formulations were prepared in 10 mM HEPES medium buffered at pH 7,4.

Nanoparticles formulation

Preliminary studies were performed by means of a factorial design, taking into account different variables such as drug-polymer ratio, PLL concentration and total solid concentration.

The final drug:polymer ratio proposed in this work was 65:35, and two different concentrations were studied, 0,4 and 1 mg/mL.

Formulation composition is described in table 1.

	NP1	NP2
Keto. sol. conc.	0,4 mg/mL	1 mg/mL
Carr. sol. conc.	0,4 mg/mL	1 mg/mL
Keto:Carr ratio	6,5:3,5	6,5:3,5
PLL solution conc.	1mg/ml	1mg/ml
PLL final conc.	75 µl/ml	75 µl/mL

Table 1: NPs composition

PLL solution was passed through a 0,22 µm filter, and then carefully added to the Ketorolac solution, under magnetic stirring, followed by 20" vortex stirring. Carrageenan dispersion was prepared by magnetic stirring at 40ºC, followed by 10 min sonication.

To prepare NPs dispersions, carrageenan dispersion was slowly added to ketorolac/PLL solution under magnetic stirring at room temperature (15 min), followed by vortex stirring during 30". Finally, NPs dispersions were left at room temperature for an hour and stored in fridge at 4ºC until characterization.

NPs characterization

Initially, non-irritability of NPs was tested by the Hen Embryo Test – Corioalantoic Membrane method (HET-CAM), using positive and negative controls. Particle size and polidispersion index (PdI) were characterized by means of Dynamic Light Scattering, and Zeta potential (ζ) by means of Electrophoretic Light Scattering, both using a Zetasizer Nano ZS (Malvern Instruments, UK).

Results and Discussion

HET-CAM

All formulations were non irritable for the ocular mucosa, and no vasoconstriction/dilatation was observed when applied to the CAM of hen embryos, as shown in Figure1, which reports an image of the experiment with the most concentrated formulation.

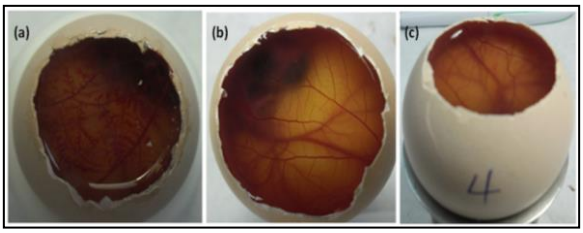

Figure 1. Observation of HET-CAM test of NP2: positive control (a), negative control (b), and NP2 formulation (c).

Particle size and Zeta potential

In Table 2 mean values of particle diameter (ϕ), polydispersity index (PdI) and Zeta potential (ζ) are reported. Taking into account that acceptability limits are <250 nm (ϕ), <0,3 (PdI) and -10 mV>ζ>+10 mV, both formulations match the requirements for ocular delivery.

	ϕ(nm)	PDI	ζ(mV)
NP1	158,5	0,190	-28,6±12,7
NP2	229,0	0,290	-31,7±7,5

Table 2: Diameter, polidispersity index and Zeta potential for NPs formulations.

In Figures 2 and 3 the frequency histograms expressing the particle size distribution based on the intensity of dispersed light obtained by DLS are exhibited. However, it should be considered that bigger particles disperse higher amounts of light, so that the mean size cannot be considered as an absolute value.

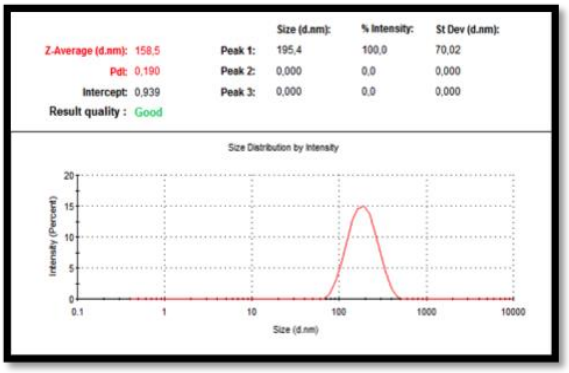

Figure 2. Particle size distribution of NP1

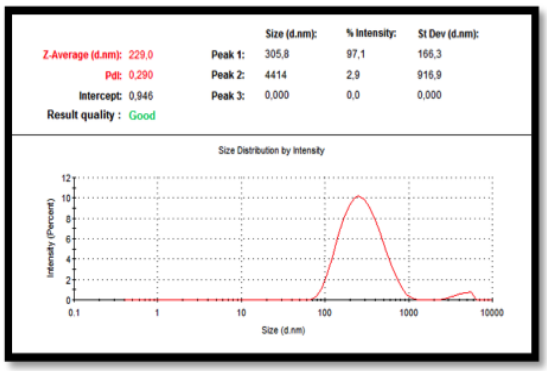

Figure 3. Particle size distribution of NP2

Conclusions

This work is the first step in the development of a mucoadhesive formulation for the ocular delivery of the anti-inflammatory drug ketorolac based on polymeric nanoparticles.

The results here reported demonstrate that the proposed formulations are non-irritable for the ocular mucosa, since no undesirable effect was observed in the HET-CAM experiments, which is probably caused by the fact that no synthetic polymer, nor organic solvent have been used for their preparation.

Moreover, the regular, small size of the NPs, along with the physiological pH of the system, ensures a safe and comfortable administration that stands for the therapeutic compliance from the patient.

Ongoing experiments with tis systems are considering the freeze-drying of the formulation, in order to increase stability, as well as recovering NPs with a positive-charged biopolymer, in order to achieve an electrostatic interaction with the outer mucine layer of the eye.

References

[1] Y. Ali, K. Lehmussaari, Industrial perspective in ocular drug delivery, *Adv. Drug. Deliv. Rev.* 58 (2006) 1258–68

[2] P. Versura, V. Profazio, E. Campos, Performance of tear osmolarity compared to previous diagnostic tests for dry eye diseases, *Curr. Eyes. Res.* 35 (2010) 553–64

[3] M. Oliva, I. Díez-Pérez, P. Gorostiza *et al*., Self-assembly of drug-polymer complexes: a spontaneous nanoencapsulation process monitored by atomic force microscopy, *J. Pharm. Sci. 92 (2003) 77-83*

[4] M. Bin-Jumah, S. J. Gilani, M. A. Jahangir *et al.,* Clarithromycin-Loaded Ocular Chitosan Nanoparticle: Formulation, Optimization, Characterization, Ocular Irritation, and Antimicrobial Activity, *Int. J. Nanomedicine,* 15 (2020) 7861-7875

P4.8: Licensing hydrogels maintain the immunomodulatory phenotype of human mesenchymal stromal cells in a murine colitis model

Ainhoa Gonzalez-Pujana[1,2,3]*, Ana Beloqui[4], José Javier Aguirre[1,5,6], Manoli Igartua[1,2,3], Edorta Santos-Vizcaino[1,2,3], Rosa Maria Hernandez[1,2,3]

1 NanoBioCel Research Group, Laboratory of Pharmaceutics, School of Pharmacy, University of the Basque Country (UPV/EHU), Paseo de la Universidad 7, 01006 Vitoria Gasteiz, Spain.
2 Biomedical Research Networking Centre in Bioengineering, Biomaterials and Nanomedicine (CIBER-BBN), Institute of Health Carlos III, Madrid, Spain.
3 Bioaraba, NanoBioCel Research Group, Vitoria Gasteiz, Spain.
4 Advanced Drug Delivery and Biomaterials, Louvain Drug Research Institute, Université Catholique de Louvain, Avenue Mounier 73, B1.73.12, 1200 Brussels, Belgium.
5 Biokeralty Reseach Institute. Alava Technology Park, Miñano, 01510, Spain.
6 Bioaraba, Osakidetza, Pathological Anatomy clinical management, Hospital Universitario de Álava (HUA) Txagorritxu, Vitoria-Gasteiz 01009, Spain.
*e-mail: ainhoa.gonzalez@ehu.eus

Introduction

Inflammatory bowel diseases (IBD) – comprising Ulcerative Colitis and Crohn's Disease – are immune-mediated disorders that lead to gastrointestinal inflammation. The use of mesenchymal stromal cells (MSCs) emerges as a promising alternative for the management of IBD for being able to modulate cells from both, innate and adaptive immunity [1].

Nevertheless, nude MSC administration still faces important issues, including low persistence once implanted and the impossibility to retrieve the cells in case of adverse events. Furthermore, MSCs have to present a MSC2 anti-inflammatory phenotype to release the immunomodulatory factors responsible for their therapeutic effect. Despite multiple studies have proposed strategies to induce this MSC2 phenotype prior to MSC administration – including exposure to inflammatory cytokines such as interferon γ (IFNγ) or hypoxia – the effect of these pre-treatments is only transient [2]. To overcome these issues, in the present work, and based on our previous studies [3], we developed an injectable licensing hydrogel system with intrinsic characteristics to continuously promote the MSC2 phenotype, ensure cell retention and enable implant recovery. In particular, human MSCs (hMSCs) were encapsulated in *in situ* crosslinking alginate hydrogels (iSCA) in which IFNγ loaded heparin-coated agarose beads were included to continuously promote MSC2 activation. The resulting IFNγ-iSCA encapsulated hMSCs were subcutaneously (SC) xenotransplanted in a mouse model of ulcerative colitis. At the end of the *in vivo* study, IBD severity was assessed and hydrogels were retrieved to evaluate MSC viability and immunomodulatory capacity.

Materials and Methods

In vivo studies were performed in 6 week-old male C57BL/6 mice (Janvier Laboratories) in accordance with the University of the Basque Country (UPV/EHU) animal committee (approved protocol M20/2018/004). The following study groups (n = 5) were included in the experimental design: healthy group (no DSS exposition), untreated group (DSS exposure), nude hMSCs group (DSS + $2x10^6$ nude hMSCs), isCA-hMSCs (DSS + $2x10^6$ isCA-hydrogel encapsulated hMSCs – with no inclusion of IFNγ–) and IFNγ-isCA-hMSCs (DSS + $2x10^6$ IFNγ isCA-hydrogel encapsulated hMSCs). At day 0, the corresponding treatment was administered and acute colitis was induced by including 3% (w/v) dextran sodium sulfate (DSS) in the drinking water. DSS was withdrew at day 5 and replaced by regular water. To evaluate the severity of colitis, the disease activity index (DAI) of each mouse was calculated according to weight loss, stool consistency and rectal bleeding (Hemoccult, Sensa) as described by Wirtz et al. [4]. After animal sacrifice at day 7, hydrogels were retrieved to assess hMSC viability – via Live/Dead staining – and immunomodulatory capacity – via ELISA of the immunomodulatory factors galectin-9 (GAL-9) and prostaglandin-E2 (PGE2) –. Statistical analyses were conducted by means of IBM SPSS Statistics 26.

Results and Discussion

Regarding DAI at day 7, the groups treated with hydrogel-encapsulated hMSCs did not present statistically significant differences to healthy mice, whereas the nude hMSC and untreated groups did (Fig. 1). Specifically, whereas an 80 % of the mice in the nude hMSCs group showed a DAI of 3 or higher, an 80% of the mice treated with isCA

hMSCs and a 60% of the mice treated with IFNγ-isCA presented a DAI of 2.

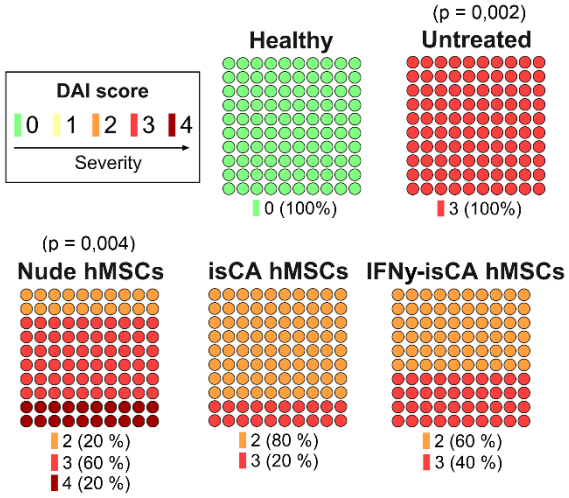

Fig 1. Disease activity index (DAI) evaluation in murine acute colitis upong IFNy-iSCA hydrogel-encapsulated hMSC administration. Statistical significance: p values in comparison to Healthy control

At day 7, animals were sacrificed. Whereas nude-administered hMSCs could not be recovered, hydrogel-encapsulation allowed implant retrieval. The recovered hMSCs presented a high viability (Fig. 2) and maintained the capacity to produce the immunomodulatory factors PGE2 and Gal-9 (Fig. 3).

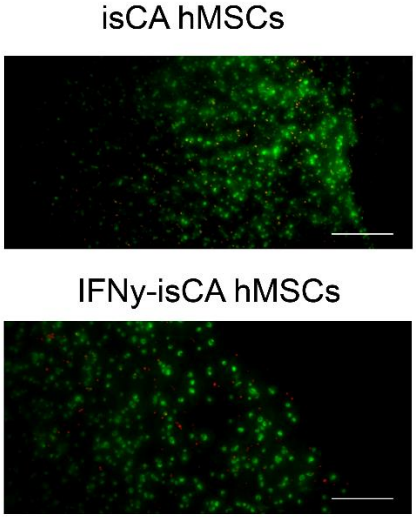

Fig 2. Viability of explanted xenogeneic hMSCs. Recovered hMSCs were microscopically analyzed under Live/Dead staining. Calcein in green for live cells, propidium iodide in red for dead cells (scale bars 200 µm).

Importantly, IFN-γ-iSCA hMSCs showed a significantly higher initial PGE2 release and a prolonged Gal-9 secretion in comparison to hydrogels without IFN-γ inclusion.

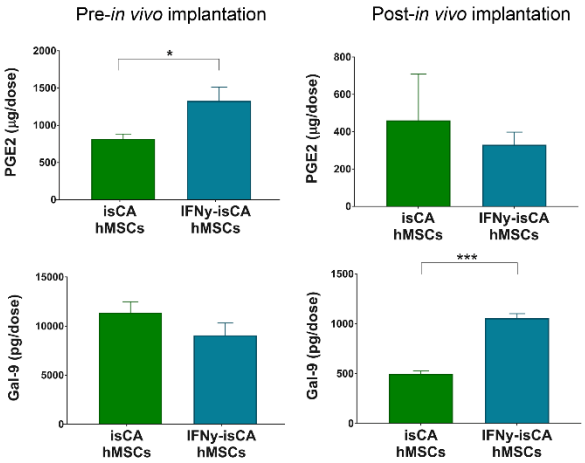

Fig 3. Immunomodulatory capacity of explanted hMSCs. PGE2 and Gal-9 secretion was determined prior to or after *in vivo* implantation. Statistical significance: *p < 0.05, ***p < 0.001.

Conclusions

IFNy-iSCA hydrogel-encapsulated hMSCs were able to limit the progression of IBD not showing significant differences with the healthy controls in the disease activity index. Moreover, hydrogels were easily retrieved after 7 days of xenogeneic implantation and the recovered cells were viable and presented an enhanced capacity to produce immunomodulatory factors including PGE2 and Gal-9.

Acknowledgments

This work was supported by MINECO SAF2017-82290-R, University of the Basque Country (A. Gonzalez-Pujana ESPDOC20/119).

References

[1] A. Ceruso, A. Gonzalez-Pujana, M. Igartua, E. Santos-Vizcaino, R.M. Hernandez, Latest advances to enhance the therapeutic potential of mesenchymal stromal cells for the treatment of immune‑mediated diseases, *Drug Deliv. Transl. Res.* 11 (2021) 498–514.

[2] J.R. Ferreira, G.Q. Teixeira, S.G. Santos, M.A. Barbosa, G. Almeida-Porada, R. M. Gonçalves, Mesenchymal stromal cell secretome: influencing therapeutic potential by cellular pre-conditioning, *Front. Immunol.* 9 (2018) 2837.

[3] A. Gonzalez-Pujana, K.H. Vining, D.K.Y. Zhang, E. Santos-Vizcaino, M. Igartua, R.M. Hernandez, D.J. Mooney, Multifunctional biomimetic hydrogel systems to boost the immunomodulatory potential of mesenchymal stromal cells, *Biomaterials* 257 (2020) 120266.

[4] S. Wirtz, V. Popp, M. Kindermann, K. Gerlach, B. Weigmann, S. Fichtner-Feigl, M.F Neurath, Chemically induced mouse models of acute and chronic intestinal inflammation, *Nat. Protoc*. 12 (2017) 1295–1309.